Department of Civil and Environmental Engineering

University of Strathclyde

The use of the high-capacity tensiometer as part of an integrated system to monitor the soil-plant continuum for geotechnical applications

A thesis presented for the Degree of Doctor of Philosophy

By

Roberta Dainese

2019

THÈSE POUR OBTENIR LE GRADE DE DOCTEUR DE L'UNIVERSITÉ DE MONTPELLIER

En Ecologie fonctionnelle

École doctorale GAIA

Unité de recherche AMAP

En partenariat international avec University of Strathclyde, UK

L'utilisation du tensiomètre de grande capacité dans le cadre d'un système intégré de surveillance du continuum sol-plante pour les applications géotechniques

Présentée par Roberta DAINESE

Le 4 Octobre 2019

Sous la direction de Alessandro TARANTINO et Thierry FOURCAUD

Devant le jury composé de

Enrique ROMERO, PhD, Universidad Politecnica Catalunya	Examinateur
Grainne EL MOUNTASSIR, PhD, University of Strathclyde	Examinatrice
Glyn BENGOUGH, PhD, University of Dundee	Examinateur
Jean-Yves DELENNE, PhD, INRA-CIRAD	Président du jury
Frederic GERARD, PhD, INRA	Examinateur
Matteo PEDROTTI, PhD, University of Strathclyde	Examinateur

UNIVERSITÉ DE MONTPELLIER

Declaration

This thesis is the result of the author's original research. It has been composed by the author and has not been previously submitted for examination which has led to the award of a degree.

Signed: 

Date: 29/10/2019

Abstract

The presence of vegetation at the interface between the soil and the atmosphere is the situation most commonly found in nature. The hydrological regime in the vadose zone is therefore influenced by the presence of plants and by the mutual interaction between the different components of the soil-plant-atmosphere continuum. A better understanding of the hydrological response of a vegetated ground is key in several fields, from agriculture and the study of ecosystems to the use of vegetation as a remedial measure for a number of geotechnical problems (e.g. slope instability).

The study undertaken in this dissertation aimed at improving the understanding of the hydraulic process of water removal from a vegetated system with the long term objective of 'engineering' vegetation to stabilise natural and man-made slopes. The initial focus was on the development of an integrated system for the monitoring of the hydraulic behaviour of the coupled soil-plant system in a coherent and consistent way. The work has then investigated the different mechanisms of water extraction occurring in a vegetated and a bare ground.

A novel technique was developed to monitor the xylem water pressure. The High-Capacity Tensiometer (HCT), developed by geotechnical researchers, was tested on plants to measure the xylem water pressure. The instrument showed it to be consistent with techniques routinely used in plant science, both in the field and laboratory conditions, for discontinuous and continuous monitoring of xylem water pressure. The novel procedure for the measurement of negative xylem water pressure is a step change in the study of continuous flow along the soil-plant system, especially in the geotechnical field. This allows the use of a single instrument to monitor the entire soil-plant continuum.

The effectiveness of vegetation in removing soil water by transpiration was then investigated. The overall methodology consisted in comparing the soil water regime generated by transpiration (from vegetated soil) with the one generated by evaporation (from bare soil), both in the laboratory and in the field.

Two soil columns were developed, one vegetated and one left bare to compare the transpiration and evaporation respectively under the same laboratory atmospheric conditions. The experiments showed that differences in water extraction between bare and vegetated soils depend on whether transpiration/evaporation occurs in the water limited or energy limited regimes, with plants showing better efficiency in generating suction only in the case of water limited regime. For the case of bare ground, the concentration of water extraction at the soil-atmosphere interface generated high hydraulic gradients that, in turn, reduced the hydraulic conductivity of the soil at such an interface with the effect of reducing the outward flow. The outcome of the experiments was confirmed by numerical simulations. In these simulations, the water flow was modelled on the basis of the water pressure in the soil-plant system monitored using High-Capacity Tensiometers. The interpretation of the results allowed a more robust experimentally-based approach to be developed for the estimation of the coefficients of the Feddes function.

The experimental setup validated at the laboratory was 'scaled up' to the field by monitoring a plantation of Poplar trees in Southern France for four months. The water content profile was monitored throughout the dry season and the following rainy period in a poplar vegetated area as well as in the adjacent ploughed (virtually bare) field. The results were interpreted based on the conceptual framework developed during the experiments undertaken under controlled conditions in the laboratory. The field test allowed the hydraulic behaviour of the SPAC to be monitored identifying potential and current limitations.

In summary, this dissertation has developed a specific experimental procedure and tested the use of High-Capacity Tensiometers for the measurement of water pressure along the soil-plant system. Furthermore, it has configured an experimental setup to be implemented in the field for the study of the water extraction efficiency of vegetation considering the interplay between soil, plant, and atmosphere.

Résumé

La stabilité des pentes, des berges et des structures de terre est déterminée par la force de cisaillement que le sol peut mobiliser. La portion supérieure du profil du sol (zone vadose) ainsi que les structures de terre sont généralement partiellement saturées et la force de cisaillement est affectée par la pression de l'eau interstitielle (négative) et le degré de saturation. Quand la quantité d'eau dans le sol est réduite, la pression d'eau interstitielle est épuisée, ce qui augmente la force de cisaillement. L'extraction d'eau du sol peut ainsi être vue comme une technique permettant de renforcer le sol et d'en améliorer sa stabilité.

Une approche naturelle pour extraire l'eau du sol, consiste à exploiter la demande évaporative de l'atmosphère. Le problème de la transpiration des plantes est complexe, car il dépend d'un couplage entre le sol, les plantes et l'atmosphère. Cependant, il présente une opportunitée de contrôler activement le procédé d'extraction d'eau par la sélection adéquate d'espèces couvrant la surface du sol. Il en résulte que la végétation peut potentiellement être 'conçue' pour stabiliser les structures géotechniques.

Ce travail propose un cadre expérimental pour l'étude de l'efficacité de la végétation à extraire l'eau du sol par transpiration, dont la méthodologie générale se base sur la comparaison entre la transpiration (depuis un sol végétal) et l'évaporation (depuis un sol nu), tant en laboratoire que dans le milieu naturel. L'étude expérimentale du processus de transpiration requiert ainsi le suivi continu des flux d'eau sol-plante-atmosphère. Une nouvelle méthode a été développée pour suivre la pression d'eau du xylème : Le tensiomètre à haute-capacité (HCT) a été appliquée sur le xylème végétal pour mesurer la pression d'eau du xylème. Cette méthode a été validée en comparaison avec les méthodes usuelles utilisées en science des plantes. La nouvelle procédure est une évolution majeure dans l'étude des flux parce que il permet l'utilisation d'un seul instrument pour suivre la totalité de la continuité sol-plante.

Le processus de transpiration a tout d'abord été étudié en laboratoire où deux colonnes de sol ont été développées, une avec végétation et l'autre laissée avec un sol nu pour comparaison de la transpiration et évaporation sous conditions atmosphérique équivalentes. Les colonnes étaient instrumentées pour suivre la quantité d'eau et la pression négative d'eau interstitielle et le taux de transpiration.

Le résultat direct de ces tests en laboratoire est que la végétation n'a pas toujours un effet bénéfique. Dans le régime énergie-limitée, la combinaison de la résistance aérodynamique et de la résistance du canopée peut avoir une influence en faveur du sol nu ou végétal en fonction du type de végétation. Ceci a été démontré par les expériences en laboratoire. Dans le régime eau-limitée, l'effet de la végétation est toujours bénéfique car le mode d'extraction d'eau est différent. Ceci est apparent dans le temps que met le processus de transpiration à entrer en régime d'eau-limitée, qui est plus long dans un sol végétal que dans un sol nu.

Les effets hydrauliques de la végétation ont finalement été étudiés en milieu naturel dans une plantation de peupliers à Montpellier, France. Le profil de contenu en eau a été suivi pendant toute la saison sèche et la période de pluie suivante dans une zone peuplée de peuplier ainsi que dans le champ voisin labouré (virtuellement nu). Le cadre conceptuel développé sur la base d'expériences en laboratoire a été ainsi fondamental pour permettre l'interprétation des résultats obtenus en milieu naturel, et montrer dans quel régime la végétation a un effet bénéfique dans ce cas précis.

Pour conclure, cette dissertation a permis de démontrer les effets de la transpiration des plantes dans l'extraction d'eau du sol, grâce à quoi l'amélioration la stabilité des pentes et des structures terrestres peut désormais être évaluée sur la base de mesures quantitatives.

Acknowledgements

First of all, I would like to thank my first supervisor, Prof. A. Tarantino. He has been a role model in terms of scientific rigour and passion for knowledge I am very grateful for the deep technical knowledge he shared with me and for the opportunities he gave me throughout the PhD of enhancing my technical skills through collaborations with other scientific centers.

I would like to thank my second supervisor, Dr. T. Fourcaud, for introducing me to the incredible field of plant science, and for the support he gave to my research during my time in Montpellier.

I would like to thank Bruna for the collaboration during the years of my PhD, the sharing experiments and scientific discussion has been part of the experience I am really grateful for. For the same reason I would like to thank Raniero, Matteo, Lorena, Sara, and all the laboratory partners at Strathclyde.

I am thankful to the bachelor and master students that accompanied me in the laboratory and field experimentation, in particular Yan, Francesco, Alice, Eve and Giuseppe. All them made me improve the communication skills and acquire more in-depth and confidence in theoretical concepts. Indeed, the best way to learn is to teach. I think a very small amount of the work produced for my thesis would have been possible without the help of the technicians, they have been an extremely precious help, in terms of logistic, problem solving and as 'tutors' for my English and French skills. I would like to thank Derek, Darren, Mara, Gavin, and Maggy at Strathclyde; and Stephane and Merlin in Montpellier.

I have been extremely lucky to be part of the TERRE project and to be able to collaborate and exchange ideas in such a multi-disciplinary and stimulating group. I would like to thank all the supervisors, for their insightful comments on my research,

and all the ESRs, for proving me how fun science can be, and for all the conversations about soil, plants and maximum systems.

Last but not least, I would like to thank my family, the one I was born in and the one I chose for myself along my life. I'll never be able to explain you how much your support has meant to me. Thank you.

Publications

1. R. Dainese, N. Weddell, A.Tarantino (2016). Measurement of stem water tension to monitor the "hydraulic boundary condition" of geotechnical system. *Book of Abstracts, ICEM17 17th International Conference on Experimental Mechanics, Rhodes, Greece, July 3-7, 2016.*

2. R.Dainese, A.Belli, T.Fourcaud, A.Tarantino (2018). An infiltration column to investigate experimentally the response of the Soil-Plant-Atmosphere Continuum. *Proceedings of the 7th International Conference on Unsaturated Soils (UNSAT), Hong-Kong, August 3-5, 2018.*

3. R. Dainese, A. Tarantino (2019). Measurement of plant xylem water pressure using the High-Capacity Tensiometer and implications on the modelling of soil-atmosphere interaction. Accepted by *Geotechnique* in February 2020.

4. High-Capacity Tensiometers: a novel technique for the continuous measurement of xylem water pressure. A cross-validation with the Thermocouple Psychrometer. Written up for submission to *Journal of Experimental Botany* or *Tree physiology* journal. Authors: R.Dainese, G. Tedeschi, T. Fourcaud, A.Tarantino

5. An experimental and numerical investigation into the mechanisms of water removal through plants (transpiration) via benchmarking against evaporation from bare soil. Written up for submission to *Geotechnique* journal. Authors: R.Dainese, A.Tarantino.

6. Accessible approach for the selection of candidate vegetation species for hydraulic groundwater remediation. Written up for submission as conference paper. Authors: R.Dainese, E. Roberts-Self, A.Tarantino.

7. Field monitoring of water content in ground vegetated with poplars and grass: lessons learned to design transpiration boundary condition in geotechnical applications. Written up for submission to the Special Issue of *Geomechanics for Energy and the Environment* journal.

Contents

List of Figures

List of Tables

Chapter 1 Introduction

The presence of vegetation at the interface between soil and atmosphere is the situation most commonly found in nature. The hydrological regime of the ground is therefore influenced by the presence of plants and by the mutual interaction between the different components of the soil-plant-atmosphere continuum. The water removal from the soil occurs through the plant, driven by the evaporative demand of the atmosphere. Water flows from the soil into the roots and upwards through the xylem, until it reaches the *stomata* –small apertures on the leaf surface– where it evaporates. The Soil, Plant, and Atmosphere form a Continuum that is referred to as SPAC (Philip, 1966). The upward movement of water is driven by the drop in water potential at the stomata, i.e. the site of evaporation. This mechanism is similar to the water extracted by evaporation in bare ground, which is driven by the drop in water potential at the evaporation site, i.e. the interface between the soil and the atmosphere.

Therefore, the processes of water removal from vegetated ground by plant transpiration and from bare ground by evaporation are both driven by the solar energy supplied and the difference in vapour pressure between the evaporative surface (the surface of bare soil or the surface of the leaf) and the air in the surroundings (Monteith, 1965). In fact, root water uptake is mainly due to the replacement of the water lost by transpiration at the leaves with less than 10 % of the extracted water is required for physiological purposes (Sinha, 2004)

The process of water extraction from the soil through vegetation involves the interaction between soil, plant and atmosphere and coupled processes between these three components are difficult to fully understand and disentangle one from each other. The hydraulic interaction may be affected by phenomena like change in soil properties due to the presence of vegetation (Bowman, et al., 1990) (Evrendilek, et al., 2004), biological effects (i.e. presence of fungi (Salifu & Mountassir., 2020)), change in the interaction with the atmosphere (e.g. shading, changed turbulence, etc.).

The understanding of the hydraulic process of bio-mediated water removal from the soil by the atmosphere, is key in several fields, e.g. knowledge of the plant life-related processes, optimization of irrigation methods, and prediction of ecosystem dynamics. Furthermore, a better understanding of the soil-plant-atmosphere interaction is the first step in use of plants as a remedial measure for slope instability. Vegetation represents indeed an ideal low carbon 'technology' and a viable remedial measure for diffuse hazards, as is the case of rainfall-induced diffuse shallow landslides.

The influence of vegetation on slope stability has been observed repeatedly, e.g. there is evidence that deforestation caused increased frequency of landslides (Guthrie, 2002) (Saito, et al., 2017). Vegetation can have several beneficial and adverse effects on the stability of a slope, and such effects are usually divided into mechanical, hydraulic and hydrological. Roots can enhance the mechanical properties of the soil by creating a 'fibre-reinforced' material or can act as anchors whenever they penetrate beyond the failure surface (Greenway, 1987) (Coppin & Richards, 1990).The effect of vegetation on hydraulic soil properties is due to the plant-soil interaction and the different biochemical activities occurring within the upper soil layers (rhizosphere) (Angers & Caron, 1998).The higher porosity of the rhizosphere, enhanced by the gaps at the root interface generated by soil shrinkage and possible cracking (Morris, et al., 1992), often promotes higher hydraulic conductivity (Leung, et al., 2015) that may lead to preferential water flow (Beven & Germann, 1982) (Aubertin, 1971). In sloping ground, this preferential water flow may have beneficial effects on slope stability.

The hydrological effect of the vegetation on slope stability is related to the water content depletion resulting from root water uptake. The water depletion in the vadose zone is associated with an increase of the shear strength of the soil –as widely documented experimentally (Tarantino & El Mountassir, 2013). Water depletion may therefore enhance stability (e.g. slopes, river dam) by reinforcing the ground in the zone below the rooting system.

An increase in suction is generally beneficial to stability. On the other hand, it should be recognised that the effect of water removal and suction increase is not always beneficial. This can generate subsidence and consecutive damage to buildings and

infrastructures (Skempton, 1954); furthermore, in the case of cracking in horizontal ground, the surface permeability may alter, leading to a faster infiltration of water into the deeper layers after rainfall events (Zhan, et al., 2007).

In the case of shallow landslides, the mechanical effect of the roots is concentrated only within the rooting depth, the contribution to the shear strength is dependent on the root distribution (Ziemer, 1981) (Gray & Leiser, 1982) and becomes negligible in the bottom part of the rooting zone (De Baets, et al., 2008). The anchoring effect of the roots on slope stability is related to the amount of roots crossing the failure surface and by the force mobilised by the root during the sliding process (Chiaradia, et al., 2016). For the case of shallow landslides, typically characterised by 1- 2m thick cover over a bedrock formation, roots rarely penetrate the bedrock. As a result, root anchoring plays little or no role and the failure surface simply tends to develop in between the rooting zone and the underlying bedrock (Balzano, Tarantino, Ridley (2019); Balzano, et al. (2018); Tsukamoto and Kusakabe(1984)).

On the other hand, the effect of water removal on vegetated soil was observed to extend beyond the rooting zone (where failure surface tends to develop) and to be persistent during the year. Measurements by Ziemer (1978) showed that the a the tree can affect soil moisture regime in layers much deeper than the rooting zone. The case study reported showed the greatest moisture depletion occurring at 2-4 m beneath ground level and extending up to 6 m from the single tree. Biddle (1998) observed in clay persistent differences in the soil moisture between the volume affected by the presence of a tree and the control volume where tree was not present. The increased water depletion did not disappear during the wet season and was concentrated between 2 and 3.2 m depth and between 1.5 and 3.6 m depth, respectively at a distance of 2.8 m and 4.5 m from the tree.

The shear strength of the soil under partially saturated conditions is influenced by both the (negative) pore-water pressure and the degree of saturation (Toll, 1990) and (Vanapalli, et al., 1996):

$$\tau = \sigma \cdot \tan \phi' + \Delta\tau(u_w, S_r) \qquad [1]$$

where τ is the shear strength, σ is the total normal stress, ϕ' is the angle of shearing resistance measured under saturated conditions, and $\Delta\tau$ is the additional contribution of partial saturation to the shear strength, in turn controlled by the (negative) pore-water pressure, u_w, and the degree of saturation, S_r. It is generally observed that a drop in degree of saturation due to water removal is accompanied by an increase in suction and an overall increase in shear strength.

Pollen-Bankhead & Simon (2010) evaluated the contribution to slope stability of the different effects related to the presence of riparian vegetation on streambank. The outcome was that the change in pore-water pressure within the soil due to the presence of vegetation provided the greatest potential benefit to the factor of safety, whenever the hydrological effect was appreciable during the year (the negative pore-water pressure tended to disappear during the wet season, in contrast to what observed by Biddle (1983). Similar observations were made by Kim, et al.(2017), who reported the effects of pore-water pressure depletion due to transpiration on slope stability. Boldrin, et al.(2017) studied quantitatively the effect of plant transpiration on the hydrological reinforcement of soil and related statistically the hydrological reinforcement to specific plant traits. Transpiration was studied mainly in conditions of relatively low plant water stress (possibly in the energy-limited regime) and there appears to be a clear correlation between water uptake and specific leaf area. In these series of tests, transpiration was not compared to a fallow soil (control). Vegetated and bare (control) soil were indeed compared in a subsequent work (Boldrin et al., 2018) and transpiration appeared to be more efficient than evaporation from bare soil in removing water. However, differences between species did not appear to correlate well with root biomass and root length density.

The development of remedial measures based on the hydrological effects of vegetation on soil moisture regime requires an understanding of the mechanisms of water extraction by the plant and the formulation of physically-based models for quantitative prediction of root water uptake.

A better understanding of the hydraulic interaction between soil, plant and vegetation is fundamental for the definition of the hydrological contribution of plants to slope

stability, because this is key to characterise the outward water flow due to transpiration. It is worth highlighting that the focus here is on the long-term goal of 'engineering' vegetation as a remedial measure for (shallow) landslides, where the effect of suction increase on soil deformation is generally not relevant. In other words, hydrological effects are beneficial when ultimate limit states are relevant and serviceability limit states are not of concern. The suction-induced fissuring and cracking generally occurring in the rhizosphere, which can promote detrimental downward infiltration in horizontal ground, does not always have adverse effects on the stability of the slope. In sloping ground, the rhizosphere acts as a lateral drainage, i.e. it promotes subsurface parallel flow of infiltrating rainwater and preserves suction in the deeper layers (Balzano, Tarantino, and Ridley 2019).

Since the atmosphere removes water from the ground also in the absence of vegetation, any potential beneficial effect of the vegetation in depleting soil moisture should be assessed in comparison with water extracted from bare soil by evaporation.

The work presented has the aim of studying the hydraulic process of water extraction from soil through vegetation. Two main objectives were pursued:

- *Develop suitable measurement techniques to characterise the flow of water within the soil-plant continuum.*

  In the transpiration process, water flows from regions at high water potential to regions at low water potential, i.e. from the soil into the roots along the stem to the leaves. Water flow is driven by the water potential generated at the leaves by the interaction with the atmosphere. The first objective of the work presented was to define suitable monitoring techniques to characterise water flow in both the soil and the plant.
- *Develop a conceptual framework to assess quantitatively the water extraction capability of a vegetated ground in comparison to bare soil.*

  The mechanisms of water extraction from the ground may occur via evaporation or transpiration, both processes driven by the evaporative demand of the atmosphere. However, the presence of the plant at the interface between soil and atmosphere changes the mechanisms of water extraction and the consequent water

depletion within the soil. In order to assess the beneficial hydrological effect of vegetation in comparison to bare soil, it is therefore essential to understand the different mechanisms of water extraction and characterise the flow of water at the macroscale.

The first objective is discussed in Chapter 3 and Chapter 4 and presents the validation of the use of High-Capacity Tensiometers (HCT) as a novel technique for the monitoring of xylem water pressure.

A conceptual framework for the mechanism of soil water depletion via transpiration and evaporation is explored in Chapter 5 based on laboratory experiments. Based on this conceptual framework, Chapter 6 presented an accessible approach for rapid selection of candidate species to be used as vegetation-based remedial measure. The development a field case study was aimed to scale up the monitoring system to the field and investigate more realistic conditions than the ones addressed at the laboratory scale (i.e. shallow vegetation, limited root development within the soil, absence of water recharge from the water table, etc). The interpretation of the field data, based on the conceptual model previously defined, is presented in Chapter 7.

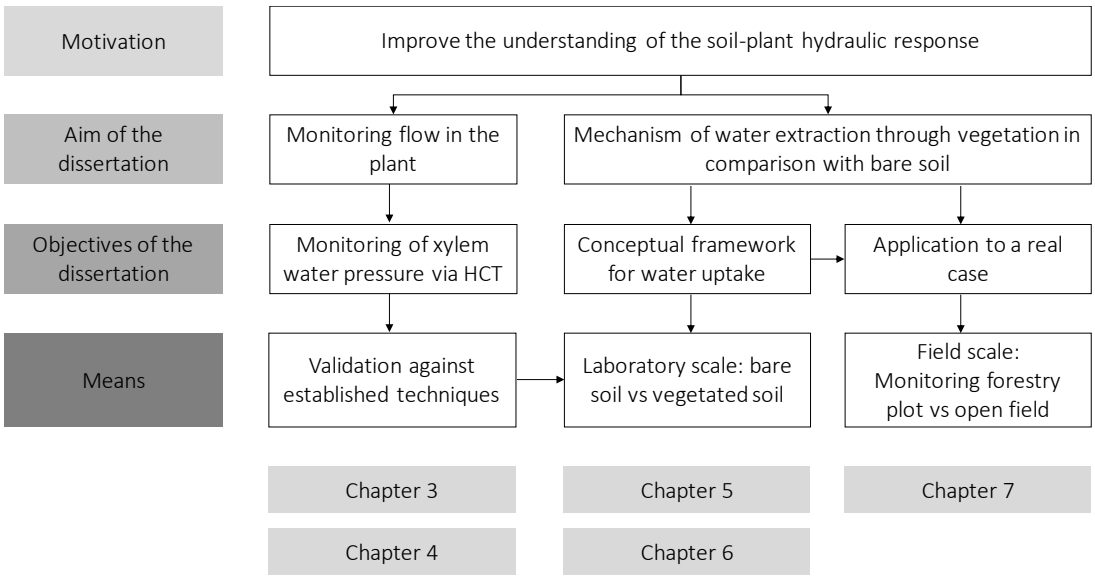

Figure 1.1: Conceptual organisation of the work

Organisation of the work

The work is divided into 8 chapters. Chapter 3 and chapter 4 focus on the problem of monitoring water flow through the soil-plant system. Chapter 5 and chapter 6 explore the different mechanisms of water uptake in vegetated and bare soils via laboratory experiments. Chapter7 applies the conceptual framework developed on the basis of laboratory experiments to a real case in the field. The content of each chapter can be summarises as follows:

Chapter 1: This Introduction presents the general framework of the dissertation, the objectives and the organisation of the work.

Chapter 2 'Literature Review' presents the background about the effect of vegetation on slope stability, with a major focus on transpiration-driven water content depletion and the role unsaturated soil mechanics and hydraulics. The processes of evaporation and transpiration are described, with reference to the energy-limited regime or water-limited regime.

Chapter 3 describes the development of a technique to monitor xylem water pressure. The High-Capacity Tensiometer (HCT) is an instrument used in geotechnical engineering to measure the negative pore-water pressure in soil. The working principle is based on the equilibrium established via liquid phase between the water in the instrument and the water in the specimen. A high-entry porous ceramic interface allows this equilibrium to establish and monitoring the water pressure down to -1.5/-2 MPa. A novel procedure was developed for the to measure the (negative) xylem water pressure of plants. The technique was preliminary validated via comparison with the Pressure Chamber, an instrument used in plant science for measurements of leaf and xylem water pressure. Validation has involved field and laboratory measurements. An immediate geotechnical application of the HCT measurement is the determination of the parameters characterising the transpiration reduction function used to model transpiration in geotechnical applications (e.g. the Feddes function). It is shown that HCT xylem water pressure measurement, in conjunction with the soil pore-water

pressure measurement, allows characterising the parameters of the reduction function that identify the water-limited regime.

Chapter 4 presents a comparison of the HCT with the thermocouple psychrometer, a continuous non-destructive technique. This instrument reads the relative humidity of the air in equilibrium with the water in the xylem, which is then related to the xylem water pressure via the psychrometric law. The HCT and the thermocouple psychrometer were installed on the same tree. Discontinuous readings by the Pressure chamber were taken as a further comparison. The experiment was carried out only in the laboratory at controlled temperature, to avoid the psychrometer measurement to be effected by thermal gradients.

Chapter 5 presents the comparison between the of water uptake from bare soil and vegetated soil. Two instrumented columns of soil were implemented, one column was vegetated while the second one was left bare. The two samples were subjected to the same atmospheric boundary conditions. The columns were instrumented with i) TDR probes and HCTs to monitor the water content and (negative) pore-water pressure in the soil respectively, ii) HCTs to monitor the xylem water pressure, and iii) balances to monitor soil water loss and hence the transpiration rate. The comparison between the hydraulic responses of the two columns allowed gaining an insight into the mechanisms of water uptake by evaporation and transpiration and to understand whether and how plants can be effective in generating suction, i.e. reinforcing the soil hydrologically.

Chapter 6 describes an accessible approach for the preliminary selection of candidate vegetation species to be implemented as vegetation-based remedial measures. The approach is designed to allow testing multiple species in a cost- and time-efficient manner.

Chapter 7 presents the field monitoring in a poplar plantation near Montpellier, France. Soil water content profiles were monitored during the summer months and part of the autumn period in a forest-vegetated area and in the adjacent ploughed field

(virtually bare). Undisturbed samples of soil were used for the characterization of the properties of the soil and the root distribution. It is shown how the field measurements can be potentially used to inform the modelling of the transpiration-driven water uptake.

Chapter 8 'Conclusions and future works' summarises the major outcomes of this work. The section 'future works' discusses possible future development and the steps to be undertaken towards the design of vegetation-based remedial measures.

Rationale of plants selection

The plant used for the studies presented in this thesis are reported in Table 1.1. Woody angiosperms plants have been selected for experiments involving High-Capacity Tensiometers. The reason was to avoid possible clogging of the tensiometer porous ceramic filter due to the frequent presence of resin in gymnosperms. The other requirement for the use of High-Capacity Tensiometers is the diameter of the stem that should be wide enough (diameter > 2÷3 cm) to allow the application of the instrument and ensure an adequate contact between the ceramic and the xylem.

The selection of the young trees/shrubs for the laboratory experiments was dictated by the availability of plants in the nurseries at the time of the experiments. The additional requirement was the presence of a number of leaves sufficiently high to allow measurements of plant water tension by the Pressure Chamber. The selection of the species for field tests was based on similar criteria and also the site made available for the experiments.

The herbaceous species were selected because typically used as riparian vegetation (Coppin & Richards, 1990) and to have a variety of root systems.

Table 1.1:Summary of the plant species used during the studies reported in this thesis.

Chapter 3	Chestnut tree	*Castanea sativa mill.*	Tree, angiosperm	Field test
	Pear tree	*Pyrus communis*	Shrub, angiosperm	Laboratory experiment
	Salix tree	*Salix cinerea*	Shrub, angiosperm	
Chapter 4	Cherry tree	*Bigarreau burlat*	Shrub, angiosperm	Laboratory experiment
	Oak tree	*Quercus rubra*	Shrub, angiosperm	
Chapter 5		*Lollium perenne*	Herbaceous species	Laboratory experiment
	Willow tree	*Salix cinerea*	Shrub, angiosperm	
Chapter 6		*Lollium perenne*	Herbaceous species	Laboratory experiment
		Medicago sativa	Herbaceous species	
Chapter 7	Poplar tree		Tree, angiosperm	Field test

References

Angers, D. & Caron, J., 1998. Plant induced changes in soil structures: processes and feedbacks. *Biogeochemistry,* Volume 42, pp. 55-72.

Anon., 2018. *2016 UK greenhouse gas emissions, final figures,* s.l.: Department for businness, energy & industrial strategy.

Anon., n.d. *https://www.legislation.gov.uk/ukpga/2008/27/contents.* [Online].

Aubertin, G., 1971. Nature and extent of macropores on forest soils and their influence on subfarce water movement. *U.S.D.A. FOREST SERVICE RESEARCH PAPER* .

Balzano, B. et al., 2018. Building physically based models for assessing rainfall-induced shallow landslide hazard at catchment scale: case study of the Sorrento Peninsula (Italy). *Canadian Geotechnical journal,* Volume 999, pp. 1-13.

Balzano, B., Tarantino, A. & Ridley, A., 2016. *Analysis of a rainfall-triggered landslide at rest and be thankful in Scotland.* s.l., E3S Web of Conferences .

Baum, R. & Godt, J., 2010. Early warning systems of rainfall-induced shallow landslides and debris flow in the USA. *Landslides,* Volume 7, pp. 259-272.

Beven, K. & Germann, P., 1982. Macropores and water flow in soils. *Water resources research,* Volume 18, pp. 1311-1325.

Biddle, P., 1983. Patterns of soil drying and and moisture deficit in the vicinity of trees on clay soils. *Geotechnique,* Volume 33, pp. 107-126.

Biddle, P., 1998. *Patterns of Soil Drying in the proximity of trees on clay soils.* Wantage (UK): Willowmead Publishing Ltd..

Boldrin, D., Leung, A. & Bengough, A., 2017. Correlating hydrologic reinforcement of vegetated soil with plant traits during establishment of woody perennials. *Plant soil,* Volume 416, pp. 437-451.

Boldrin, D., Leung, A. & Bengough, A., 2018. Hydrologic reinforcement induced by contrasting woody. *Plant soil,* Volume 427, pp. 369-390.

Boldrin, D., Leung, A. & Bengough, A., 2018. Hydrologic reinforcement induced by contrasting woody species during summer and winter. *Plant soil,* Volume 427, pp. 369-390.

Bowman, R., Reeder, J. & Lober, R., 1990. Changes in soil properties in a central plains rangeland soil after 3, 20, and 60 years of cultivation1.. *Soil Science,* 150(6), pp. 851-857.

Burt, C., Mutziger, A., Allen, R. & Howell, T., 2005. Evaporation Research: Review and Interpretation. *Journal of irrigation and drainage engineering,* Volume 131, pp. 37-58.

Calcaterra, D. & Santo, A., 2004. The January 10, 1997 pozzano landslide, Sorrento Peinsula, Italy. *Engineering Geology,* Volume 75, pp. 181-200.

Canny, M., 1977. Flow and transport in Plants. *Annual Review of Fluid Mechanics,* pp. 275-296.

Chiaradia, E., Vergani, C. & G.B., B., 2016. Evaluation of the effects of three European forest types on slope stability by field and probabilistic analyses and their implications for forest management. *Forest ecology and management,* pp. 114-129.

Coppin, N. & Richards, I., 1990. *Use of Vegetation in Civil Engineering.* s.l.:CIRIA.

De Baets, S. et al., 2008. *Root tensile strength and root distribution of typical Mediterranean plant species and their contribution to soil shear strength.* s.l., Springer.

Dekić, L., Mihailović, D. T. & Rajković, B., 1995. A study of the sensitivity of bare soil evaporation schemes to soil surface wetness, using the coupled soil moisture and surface temperature prediction model, BARESOIL.. *Meteorology and Atmospheric Physics,* pp. 101-112.

Endo, T. & Tsuruta, T., 1969. On the effect of roots upon the shearing strength of soil.. *Annual report of Hokkaido Branch,* pp. 167-183.

Evrendilek, F., Celik, I. & Kilic, S., 2004. Changes in soil organic carbon and other physical soil properties along adjacent Mediterranean forest, grassland, and cropland ecosystems in Turkey.. *Journal of arid environments,* 59(4), pp. 743-752.

Fredlund, D. & Raharjo, H., 1993. *Soil Mechanics for unsaturated soils.* s.l.:John Wiley & Sons.

Garg, A., Coo, J. & Ng, C., 2015. *Field study of indluence of root characteristics on soil suction distribution in slopes vegetated with Cynodon dactylon and Schefflera heptaphylla,* s.l.: Earth surface process and landforms.

Gray, D. & Leiser, A., 1982. *Biotechnical slope protection and erosion control.* New York: Van Nostrand Reinhold.

Greenway, D., 1987. Vegetation and slope stability. In: M. Anderson & K. Richards, eds. *Slope stability.* s.l.:John Wiley & Sons Ltd., pp. 187-230.

Guthrie, R., 2002. The efefcts of logging on frequency and distribution of landslides in three watersheds of Vancouvver Island, British Columbia.. *Geomorphology,* Volume 43, pp. 273-292.

Jackson, R. et al., 1996. A global analysis of rot distributions for terrestrial biomes. *Oecologia,* Volume 108, pp. 389-411.

Jarvis, P. & McNaughton, K., 1986. Stomatal control of transpiration: scaling up from leaf to region. *Advances in Ecological research,* Volume 15.

Kim, J. et al., 2017. Vegetation as a driver of temporal variations in slope stability: The impact of hydrological processes. *Geophysical research letters,* Volume 44, pp. 4897-4907.

Leung, A., Garg, A. & Ng, C., 2015. Effect of plant roots on soil-water retention and induced suction in vegetated soil. *Engineering geology.*

Li, A. et al., 2005. Field-monitoring variations of soil moisture and matric suction in a saprolite slope. *Canadian Geotechnical Journal,* Volume 42, pp. 13-26.

Monteith, J., 1965. *Evaporation and environment. The state and movement of water in living organisms.*. s.l., Cambridge University Press.

Morris, P. H., Graham, J. & Williams, D. J., 1992. Cracking in drying soils.. *Canadian Geotechnical Journal,* 29(2), pp. 263-277.

Or, D., Lehmann, P., Shahraeeni, E. & Shokri, N., 2013. Advances in Soil Evaporation. *Vadose Zone Journal.*

Penman, H., 1948. Natural evaporation from open water, bare soil and grass. *Proceedings of the Royal Society of London. Series A. Mathematical and Physical Sciences,* pp. 120-145.

Philip, J., 1966. Plant water relations: some physical aspects. *Annual Review in Plant Physiology,* pp. 245-268.

Pollen-Bankhead, N. & Simon, A., 2010. Hydrologic and hydraulic effects of riparian root networks on streambank stability:Is mechanical root reinforcement the whole story?. *Geomorphology,* Volume 116, pp. 353-362.

Romero, E., Gens, A. & Lloret, A., 1999. Water permeability, water retention and microstructure of unsaturated compacted Boom clay. *Engineering geology,* Volume 54, pp. 117-127.

Saito, H., Murakami, W., Daimaru, H. & Oguchi, T., 2017. Effect of clear-cutting on landslides occurrences: Analysis of rainfall thresholds at Mt. Ichifusa, Japan.. *Geomorphology,* Volume 276, pp. 1-7.

Salifu, E. & Mountassir., G. E., 2020. Fungal-induced water repellency in sand. *Géotechnique,* pp. 1-22.

Shao, J. et al., 2015. Biotic and climatic controls on interannual variability in carbon fluxes across terrestrial ecosystems.. *Agricultural and forest meteorology,* Volume 205, pp. 11-22.

Sinha, R., 2004. *Modern Plant Physiology.* s.l.:CRC Press.

Skempton, A. W., 1954. A foundation failure due to clay shrinkage caused by poplar trees.. *Proceedings of the Institution of Civil Engineers,* pp. 66-86.

Tarantino, A. & El Mountassir, G., 2013. Tarantino, Alessandro, and Gráinne El Mountassir. "Making unsaturated soil mechanics accessible for engineers: Preliminary hydraulic–mechanical characterisation & stability assessment.. *Engineering geology,* Volume 165, pp. 89-104.

Tarantino, A. & Tombolato, S., 2005. Coupling of hydraulic and mechanical behaviour in unsaturated compacted clays. *Geotechnique,* Volume 55, pp. 307-317.

Toll, D., 1990. A framework for unsaturated soil behaviour. *Geotechnique,* Volume 132, pp. 31-44.

Tsukamoto, Y. & Kusakabe, O., 1984. *Vegetative influences on debris slide occurrences on steep slopes in Japan*. Honolulu, Hawaii, Environment and Policy Institute.

Vanapalli, S., Fredlund, D., Pufahl, D. & Clifton, A., 1996. Model for teh prediction of shear strength with respect to soil suction. *Canadian geotechnical journal,* Volume 33, pp. 379-392.

Zhan, T. L., Ng, C. W. & Fredlund, D. G., 2007. Field study of rainfall infiltration into a grassed unsaturated expansive soil slope.. *Canadian Geotechnical Journal,* 44(4), pp. 392-408.

Ziemer, R., 1978. *Logging effects on soil moisture losses,* s.l.: Colorado State University.

Ziemer, R., 1981. *The role of vegetation in the stability of forested slopes.* Kyoto, s.n.

Chapter 2 Literature review

2.1. Unsaturated soils

Unsaturated soils are a tri-phase media, characterized by a solid phase (grains of soil), a wetting phase (usually water) and a gas solution, a mixture of air and water vapour usually referred to as *air*. The interaction between the three phases and the natural surface tension of water may allow, under the right conditions, the formation of inter-grain water *menisci*, able to support negative pore-water pressure.

The mechanism of water under tension is well explained by (Marinho, et al., 2008). The surface tension of water is due to an imbalance of the intermolecular attraction at the surface, that brings the surface of the liquid to behave like a membrane under tension. In the case of water and soil, the *meniscus* that forms at the interface liquid-solid is able to support a negative pressure inversely proportional to the radius of the *meniscus* itself. The distribution of water pressure along a capillary tube with constant diameter is shown in Figure 2.1.

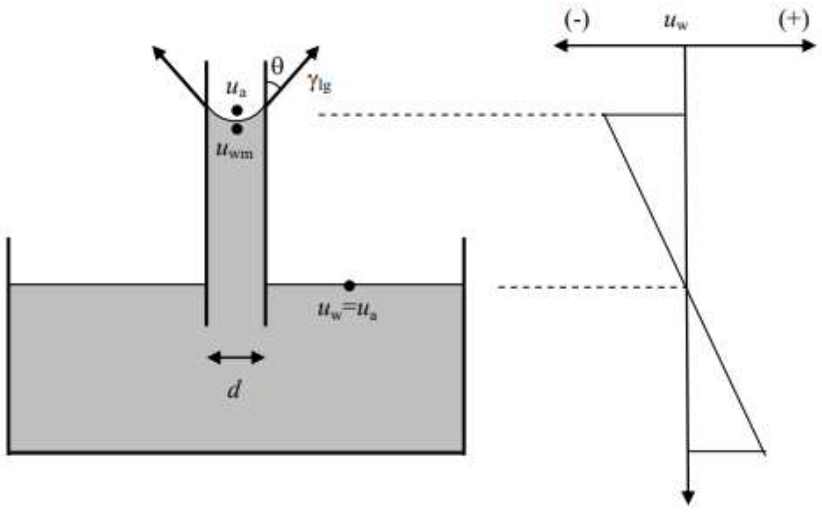

Figure 2.1:Capillary rise of wetting fluid, from (Marinho, et al., 2008)

The minimum water pressure in the system u_{wm} can be calculated considering the vertical force equilibrium at the air-water interface:

$$u_{wm} = u_a - \frac{4T\cos\theta}{d} \quad [1]$$

Where u_a is the pressure of the air, T is the surface tension of the liquid considered, θ is the contact angle and d is the diameter of the capillary tube. The water tension the soil is able to support is therefore related to the size the pores within the grains, and therefore to the size of the grains too, and it is in the order of magnitude of few kPa for sands and thousands of kPa for fine clays.

The presence of additional capillary forces within the grains has a mechanical effect on the behavior of the soil. Testing on shear strength of unsaturated soils was commenced under the supervision of Bishop at Imperial college (Bishop, et al., 1960). It was the first attempt to separately observe the air pressure and the pore-water pressure as the soil was deformed to failure. In a later work Fredlund and Morgenstern extended the Mohr-Coulomb failure criterion to unsaturated soil, using (σ-u_a) and (u_a-u_w) as stress state variables (Fredlund, et al., 1978).

In the case of saturated soils, the failure envelope of the Mohr-Coulomb is a straight line define by the effective cohesion c' and by the tangent of the effective angle of internal friction, ϕ' (respectively the intercept and the slope of the failure envelope). The extension of the Mohr-Coulomb failure criterion for unsaturated soils is described by Fredlund (1987), who extend the two-dimensional failure line to a three-dimensional failure surface, to take into account the contribution of the stress state variable (u_a-u_w) (Figure 2.2).

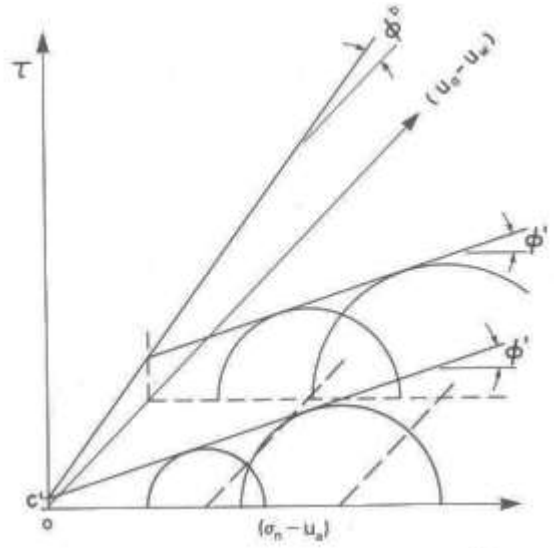

Figure 2.2: by (Fredlund, 1987). Mohr circles at failure for an unsaturated soil.

However, experimental results on a wide range of soil negative pore-water pressure showed a non-linear dependency between the suction in the specimen and the observed increase in shear strength (Gan & Fredlund, 1988), suggesting a dependency of the additional shear strength to the degree of saturation of the soil (Figure 2.3) (Vanapalli, et al., 1996):

$$\tau = c' + (\sigma_n - u_a) \tan \phi' + \Delta\tau(s, Sr) \qquad [2]$$

Where τ is the unsaturated shear strength, c' is the effective cohesion, σ_n is the normal stress, u_a is the air pressure and ϕ' is the effective angle of internal friction. The increment of shear strength ($\Delta\tau$) arising from the status of partial saturation of the soil is dependent to the suction in the soil s and the degree of saturation S_r.

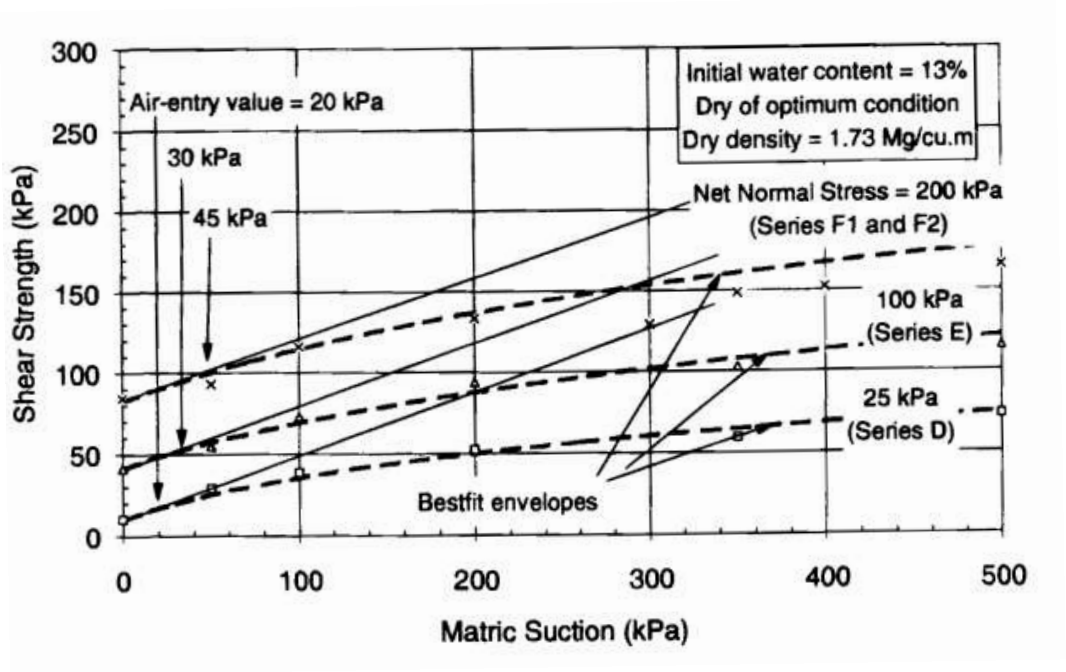

Figure 2.3: variation of shear strength with matric suction under different net normal stresses with initial water content at dry of optimum conditions. From (Vanapalli, et al., 1996)

The graphs reported in Figure 2.4, called water retention curve, express the relation between the degree of saturation and the negative pore-water pressure in the soil. When the soil is fully saturated and menisci among soil grains are flat, suction is nil. When water is removed, usually by evaporation, menisci start to form at the interface between the soil and the atmosphere: the suction increases, but the change in the degree of saturation is negligible. When the suction increases, the air breaks through the surface, to create a discontinuous phase within the continuous water phase (quasi-saturated soil). When the degree of saturation decreases and the suction increases accordingly, water menisci retract within the matrix of soil, until water becomes a discontinuous phase and the majority of the pores is occupied by air (Tarantino, 2010).

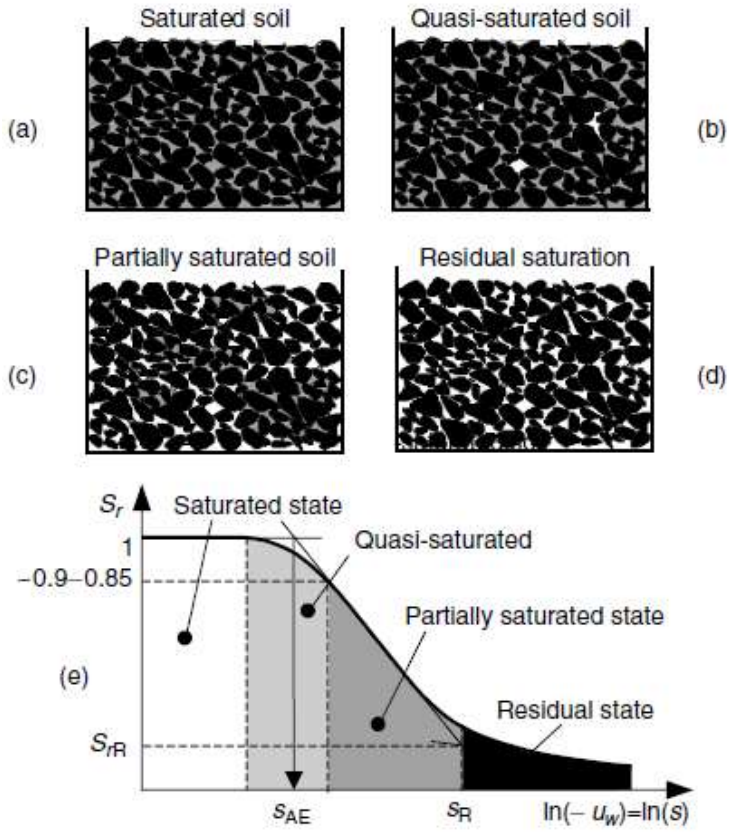

Figure 2.4:states of saturation. From (Tarantino, 2010)

The water retention curve gives essential information both for problems of unsaturated flow and for analysis of the stress-strain behavior, given the hydro-mechanical coupling determining the behavior of unsaturated soils (Wheeler, et al., 2003).

The water retention curve is usually defined through the separate measurement of the degree of saturation (from measurements of gravimetric water content and the void ratio) and suction of water in the soil. The water retention curve can be both in terms of total suction or matric suction, depending on the instrumentation used to assess it. The matric suction is related to the sole capillary forces in the soil, while the total suction has an additional osmotic component. A graphic representation pf the concept of matric and total suction is reported in Figure 2.5 (Tarantino, 2010). Instruments measuring the matric suction are based on water-equilibrium and are usually characterized by the absence of semipermeable membrane that can lead to a gradient

in ions concentration. Instruments measuring the total suction are usually based on vapor equilibrium, and are affected by the presence of solutes in the specimen. The first class of instruments includes tensiometers, electrical/thermal conductivity sensors and contact filter paper technique. The second class includes humidity measurement techniques, thermocouple psychrometers, chilled mirror hygrometers and the non-contact filter paper method (Masrouri, et al., 2008).

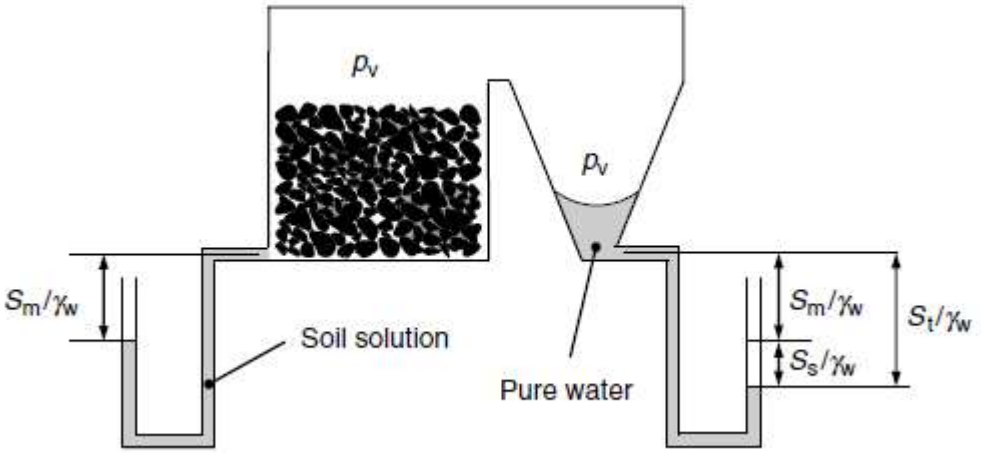

Figure 2.5: Definition of total and matric suction. From (Tarantino, 2010)

In saturated soil the hydraulic conductivity is defined as the constant of proportionality between the flow rate and the hydraulic gradient, referring to Darcy's law. When the soil starts desaturating and water is not a continuous phase anymore, the hydraulic conductivity starts decreasing. Richards (1931) and Childs and Collis-George (1950) validated Darcy's law for the case of unsaturated soils, defining the hydraulic conductivity as a dependent on the degree of saturation and void ratio of the soil, as lately observed experimentally (Peroni, 2002)(Figure 2.6).

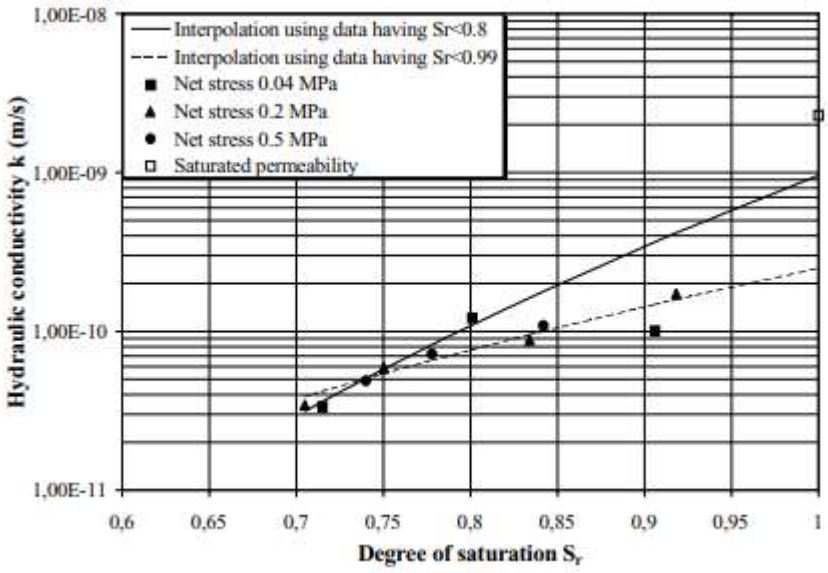

Figure 2.6:Variation of water permeability with the degree of saturation with different vertical stresses. From (Peroni, 2002)

The definition of the hydraulic conductivity as a function of the degree of saturation or of the water suction within the sample can be assessed though direct methods (Klute, 1972) , or via empirical, macroscopic (Gardner, 1958; Richards, 1931) and statistical models (Fredlund, Xing, & Huang, 1994; Mualem, 1976). A common method is the definition of the hydraulic function by inverse analysis, based on data of infiltration and evaporation processes (Bitterlich, Durner, Iden, & Knabner, 2004; Yeh, 1986).

Several models have been suggested throughout the years to describe the water retention curve and the hydraulic conductivity function in terms of both the degree of saturation or suction (Leij, et al., 1997).

2.1.2. Slope stability in Unsaturated conditions

The slope stability analysis is usually based on the theoretical model of the slope and the soil and it defines a failure criterion is introduced, taking into account the loadings effecting the slope and the boundary conditions. The limit equilibrium method hypothesises that the slope should fail by a mass of soil sliding along a failure surface,

assuming that all the shear strength the soil can developed is mobilised along the surface of failure (Nash, 1987). In saturated conditions the shear strength of the soil is normally given by the Mohr-Coulomb failure criterion:

$$\begin{aligned} s &= c_u && (for\ total\ stress\ analysis) \\ s &= c' + \sigma' \tan \phi' && (for\ effective\ stress\ analysis) \end{aligned} \qquad [5]$$

In conditions of equilibrium the shear strength mobilised is less than the available shear strength, resulting in a factor of safety F >1. In other words, F is defined as:

$$F = \frac{Shear\ strength\ available}{Shear\ strength\ required\ for\ stability} \qquad [6]$$

When the stability of a slope is taken into account, several slip surface are studied and the most critical one, hence the slip surface with the smallest factor of safety, is assumed to be the failure surface. The factor of safety referred to the adopted failure surface is then taken to be the factor of safety of the slope.

Classic slope stability analysis usually considers fully saturated conditions of the soil. However, for deep water tables the failure can occur within the shallow vadose zone under partially saturated conditions (de Campos, et al., 1991; Wolle & Hachich, 1989), invalidating the model adopted. An example of slope stability analysis for an infinite slope in the case of partially saturated conditions is presented by (Lu & Godt, 2008) with the conceptual model presented in Figure 2.7.a. The factor of safety of the slope in respect with the distance from the water table is reported in Figure 2.7.b: the continuous line refers to unsaturated conditions while the dotted line refers to saturated conditions.

The implementation of the conditions of partially saturation in the evaluation of slope stability can be addressed, but the following aspects need to be fulfilled (Fredlund, 1987): i) it must be possible to appropriately define the shear strength parameters for the soil in unsaturated conditions, possibly allowing a smooth transition between saturated and unsaturated conditions; ii) a monitoring system for the observation or

estimation of the negative pore-water pressure should be put in place in the slope under study; iii) the conventional methods for slope analysis should be adapted to the study of unsaturated conditions.

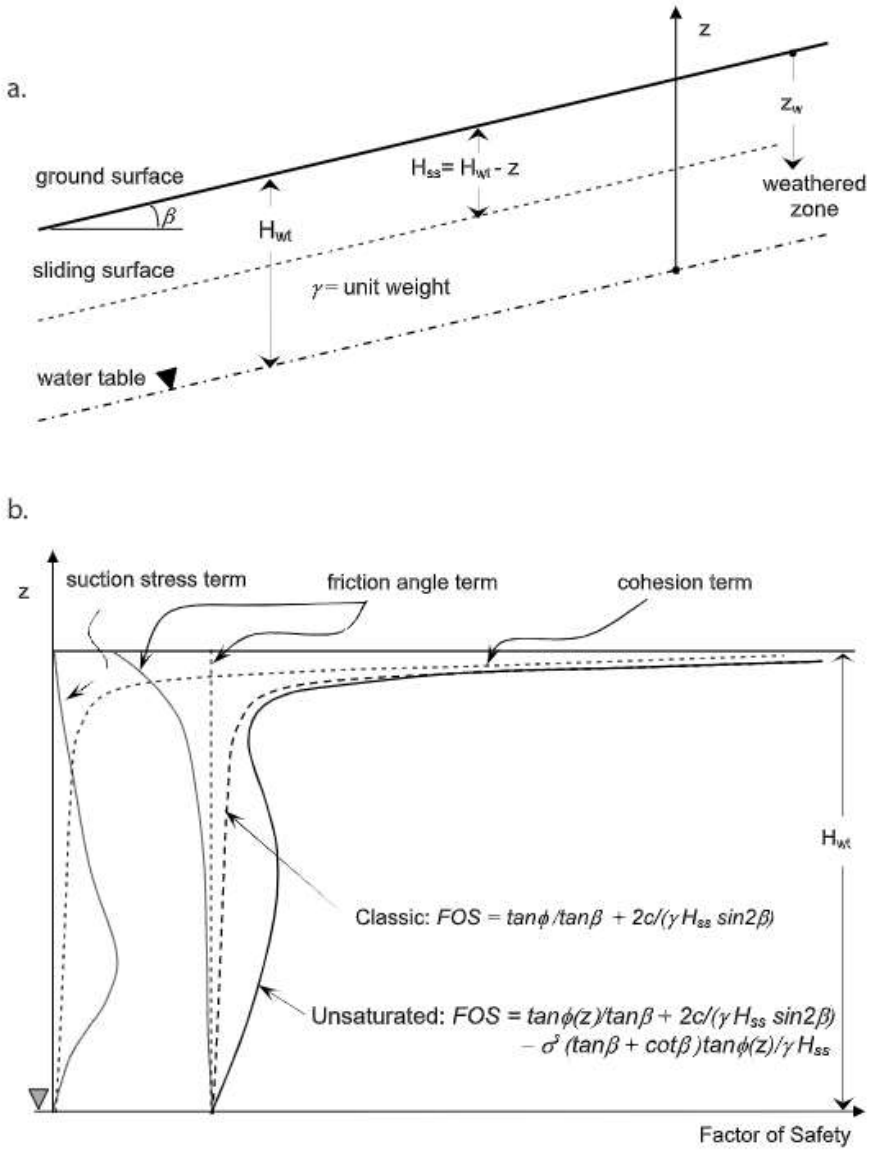

Figure 2.7: Infinite slope model for a variably-saturated infinite slope with a weathered mantle. (a) Basic definitions. (b) Conceptual illustration of differences between the factor of safety profiles for the classical and unsaturated models. From (Lu & Godt, 2008).

2.2. Plants and slope stability

The presence of the vegetation has an influence on the behaviour of a slope, as demonstrated by the increase in soil erosion and landslides usually found following forest clearance (Guthrie, 2002; Saito, Murakami, Daimaru, & Oguchi, 2017). The presence of trees, shrubs and grasses can add a protection to the shallow soil layers and modify the hydraulic boundary condition between the soil and the atmosphere. The main effects of vegetation can be bundled into two main categories, mechanical and hydrological (Figure 2.8), and can both enhance or worsen slope stability, their effectiveness always related to the specific context. A summary of the effects on slope stability related to the presence of vegetation is presented by Greenway (1987), discriminating between factors having a Beneficial (B) or Adverse (A) influence on slope stability.

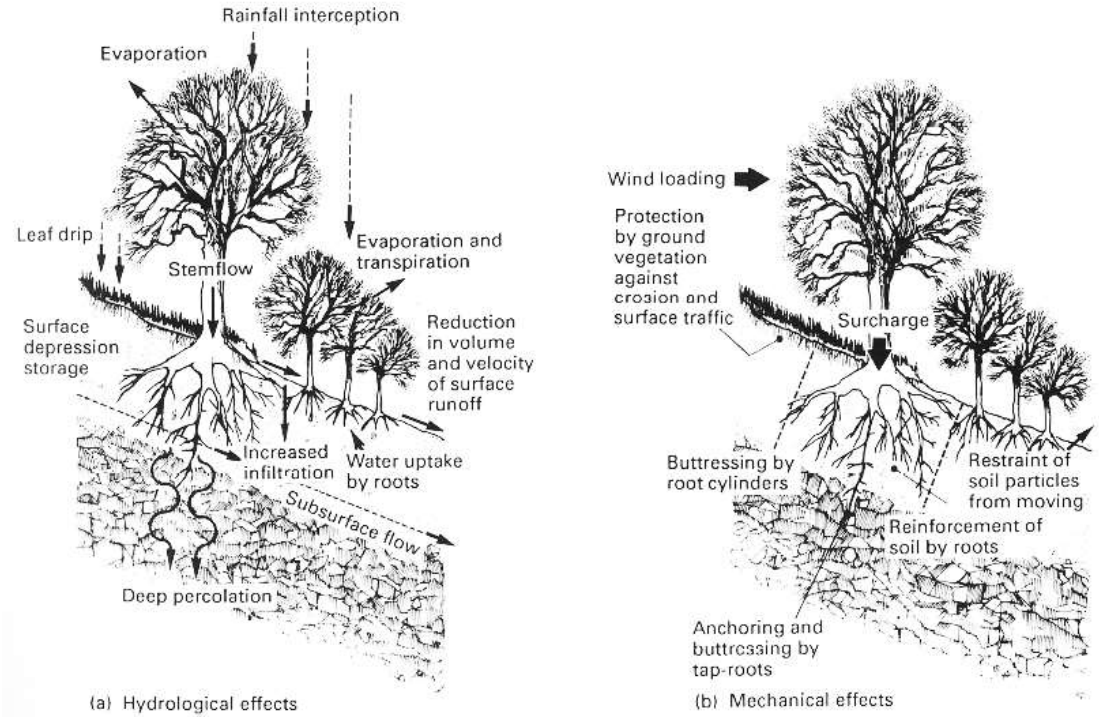

Figure 2.8: Physical effects of vegetation (Coppin & Richards, 1990)

Table 2.1: Effects of vegetation on slope stability. From (Greenway, 1987)

Hydrological Mechanisms	**Effect**	**Influence**
Foliage interception of rainfall	Reduces the rainfall available for infiltration	B
Increased roughness of the ground surface and permeability of the soil	Increased infiltration capacity	A
Roots water uptake (transpiration)	Soil moisture depletion, leading to a lower pore water pressure in the ground	B
Depletion of soil moisture may result in desiccation cracking in the soil	Higher infiltration capacity	A
Mechanical Mechanisms		
Roots reinforcement	Increased shear strength of the soil	B
Anchoring effect by roots crossing the failure surface	Support to the upslope soil mantle	B
Weight of trees surcharges the slope	Increasing normal and downhill force components	A/B
Exposition to the wind	Transmission of dynamic forces to into the slope	A
Roots binding of soil particles	Reduced susceptibility to erosion	B

A- Adverse to Stability

B- Beneficial to Stability

2.2.1. Mechanical effects

The roots can enhance the mechanical properties of the soil (fine roots, Ø≤15÷20 mm), work as an anchoring element (medium-big roots, Ø>20 mm), or add a loading factor to the slope (Greenway, 1987).

The roots act as a fibre-reinforcement of the low tensile strength matrix of the soil, that can be described as an increase of the soil cohesion c_R(Figure 2.9) (Coppin & Richards, 1990). The contribution of the matrix of roots to the shear strength of the soil was measured by direct shear test on alder in loamy soil, who measured a c_R in the range of 2÷12 kN/m^2 (Endo & Tsuruta, 1969).

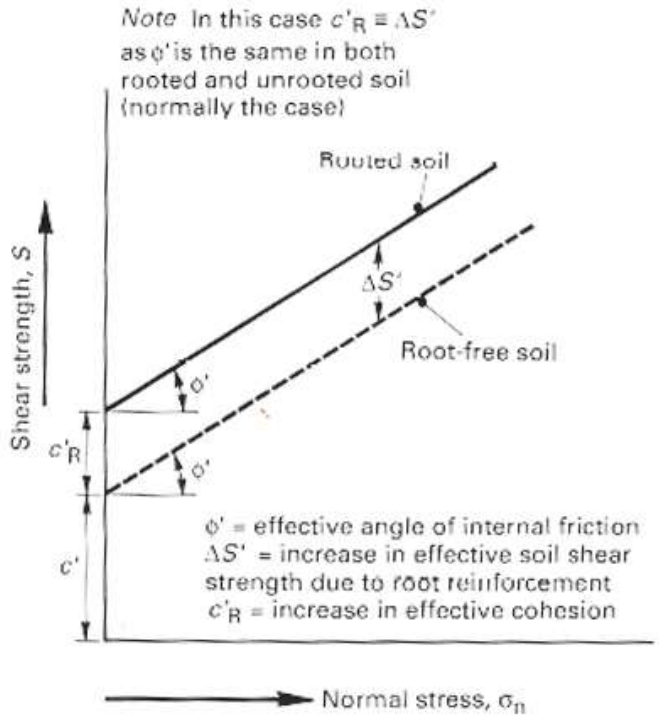

Figure 2.9: Effect of root reinforcement on the shear strength of soil. From (Coppin & Richards, 1990)

However, although the fibre-reinforcement effect may be significant in comparison to the natural strength of the soil, the contribution to the shear strength is dependent to the root distribution (D. H. Gray, Leiser, & others, 1982; Ziemer & Service, 1981). The additional contribution to soil shear strength given by the presence of vegetation is related to the root density (Figure 2.10), and therefore becomes negligible in the deeper layer of the ground (De Baets, et al., 2008), given that over 90% of the root biomass is usually found within the first meter of soil (Jackson, et al., 1996).

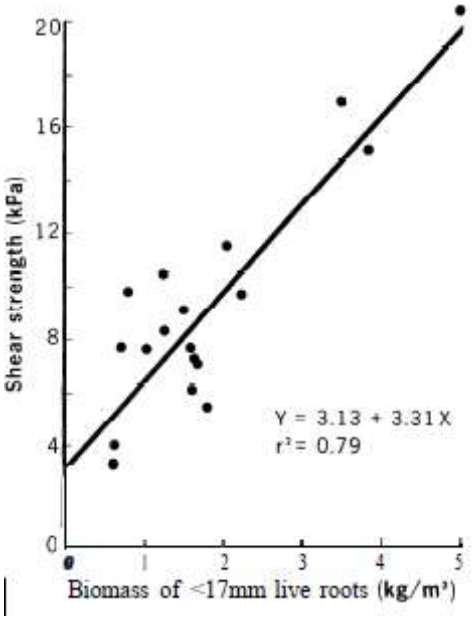

Figure 2.10: Shear strength of root permeated sand as a function of root density. From (Ziemer, 1981)

In the case of shallow landslides, or thin layers of superficial soil, if the roots can penetrate into the ground beyond the failure surface, or if they can attach themselves to the bedrock underneath, they act as tie-rods, avoiding soil down-slope movements (Coppin & Richards, 1990). Riestenberg (1994) calculated that the presence of roots penetrating into the bedrock increased the Factor of Safety of a hypothetic 30° slope of 30% for the Sugar Maple and 120% for the White Ash, for a displacement of 3 cm, with a dependency of the root tensile strength on the root size and type.

The presence of high trees, though beneficial for the presence of an extended rooted zone, may add a surcharge to the slope, increasing the down-slope forces and can implicate a destabilizing effect especially if the trees are concentrated in the upper part of the slope, while it can help the stability if the trees are at the bottom. The surcharge of a single tree, acting on the area within the root spread, can go from the 5 kPa for a 6m tall spruce tree (Wu, et al., 1979) to 70 kPa for a 60 m tall Douglas-fir (Gray, 1978).

Recurring to the conceptual model introduced by Tsukamoto & Kusakabe (1984) (Figure 2.11) for the case of vegetative covers in Japan, it appears clear that the stabilizing mechanical effect due to the presence of the vegetation may be not

sufficient to stabilize the slope. The trees may have a major beneficial effect for the stability of the slope when it is possible for the roots to behave as anchors, such as in the case of relatively thin layers of soil and a bedrock that can be penetrated by the roots, or for soil mantles in which the soil shear strength and density increase with depth (respectively Type C and Type B in Figure 2.11). When this is not the case, i.e. if the massive bedrock that underlays the soil layer cannot be penetrated by the roots (Type A), or if the trees are 'floating' on a thick soil layer and cannot hold on more resistant layers underneath (Type D), the mechanical effect of the roots on the overall stability of the slope becomes negligible.

While the mechanical effects of roots can be very beneficial in the case of shallow landslides in the case of roots penetrating in the bedrock, their effect beyond the rooting zone is quite negligible (De Baets, et al., 2008).

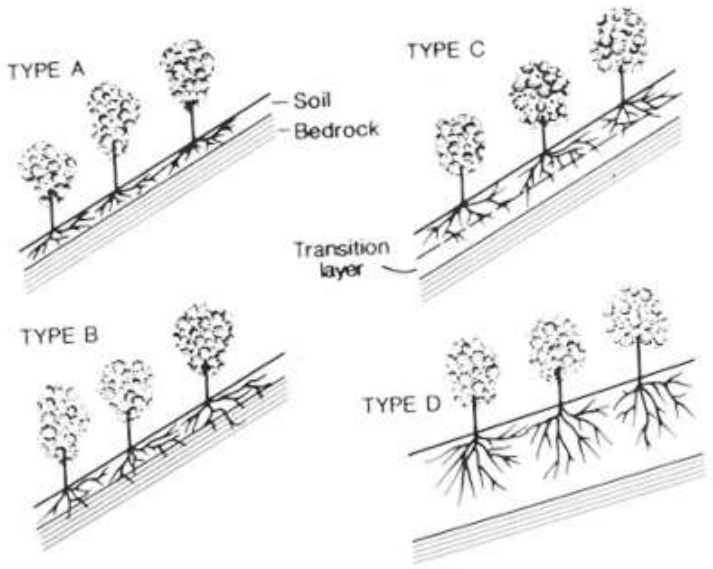

Figure 2.11: by (Tsukamoto & Kusakabe, 1984).Slope classification scheme based on root reinforcement and anchoring.

2.2.2. Hydrological effects

The presence of the vegetation on a slope can have a double effect on the hydrology of a system: modifying the infiltration or enhancing the soil water removal.

The first aspect is due to changes in the surface water regime caused by the presence of vegetation, i.e. reducing the amount of water that actually reaches the soil (i.e. rainfall interception) and modifying the runoff and creating preferential water path within the soil (Braud, Vich, Zuluaga, Fornero, & Pedrani, 2001; Hendrickx, 2017).

Furthermore, the presence of bio-chemical activity within the first layers of the ground can change the structure of the soil and its water retention properties (Czarnes, Hallett, Bengough, & Young, 2000; Hallett, Gordon, & Bengough, 2003).

The second aspect is related to the capability of vegetation in enhancing the water depletion from the deeper layers of the soil, improving the soil strength by adding to it an unsaturated component. Measurements by (Ziemer, 1978) showed how the influence of the tree can reach layers deeper than the rooting zone, with the greatest moisture depletion occurring at 2-4 m beneath ground level and extending up to 6 m from the single tree; Biddle (1998) observed persistent differences in the soil moisture between the volume effected by the presence of the tree and the control: the increased water depletion did not disappeared during the wet season and was concentrated between 2 and 3.2 m depth and between 1.5 and 3.6 m depth, respectively at a distance of 2.8 m and 4.5 m from the tree.

As previously see for the case of unsaturated soils and for the case of slope stability in unsaturated conditions, the water depletion in the soil via the root water uptake may lead to an increase of the negative-pore water pressure and hence to an associated increase of the shear strength of the soil (Garg, et al., 2015). If the effect of trees can reach the failure surface within the vadose zone, the root water uptake may lead to an improvement of the conditions of stability of the slope.

Pollen-Bankhead and Simon (2010) evaluated the contribution to slope stability of the different effects related to the presence of riparian vegetation on streambank.The outcome was that the change in pore-water pressure within the soil due to the presence of vegetation provided the greatest potential benefit to the factor of safety, whenever the hydrological effect was appreciable during the year. The same result was obtained by Kim, et al. (2017), with a considerable contribution to slope stability related to the enhance negative soil pore-water pressure during the summer months. The studies reported are characterized by the soil characteristics, location and climate summarized in Table 2.2.

Table 2.2: Details for soil and climate for the studies presented on the hydraulic effect of plants

Reference	**Type of soil**	**Location and typical climate**
(Biddle, 1998)	clay	England (UK), temperate
(Pollen-Bankhead & Simon, 2010)	Silt-loam	Oxford, USA, temperate
(Kim, et al., 2017)	clay	Laos, Subtropical
	clay	Costa Rica, tropical
	sandy loam	France, temperate

The possible increase in shear strength in the soil is not the only possible consequence of water depletion related to plant water uptake. The volume reduction often associated with water removal may (Morris, et al., 1992) be associated to subsidence and consecutive damage to buildings and infrastructures (Skempton, 1954); furthermore, in the case of cracking, the surface permeability may alter, leading to a faster infiltration of water into the deeper layers after rainfall events (Zhan, et al., 2007). Studies done with different kind of clays and for several tree species identified the damage to buildings due to the tree water uptake and related soil shrinkage (Biddle, 1983), noticing that the most consistent effect was given by poplar trees. The study highlighted how the presence of most of the plant species lead to problems related to

soil shrinkage in the first 1,5 m of soil, with few species effecting the system to deeper layers.

The problem of fissuring and cracking is due to the suction levels reached in the soil due to water removal (Williams, 1992). The relation between soil cracking and the presence of vegetation has been explored in several studies, showing how the presence of plants tends to reduce the water suction reached near the surface, but can at the same time favour cracks formations (Bordoloi et al., 2018; Ravina, 2009). The creation of cracks and fissures among the soil can have a great influence in the hydrology of a slope (Stirk, 1954); however, the final effect is not always adverse to the stability of the slope: it was observed that water may create a sub-surface flow within the more permeable shallow layer rather than infiltrate in depth (Balzano, et al., 2016).

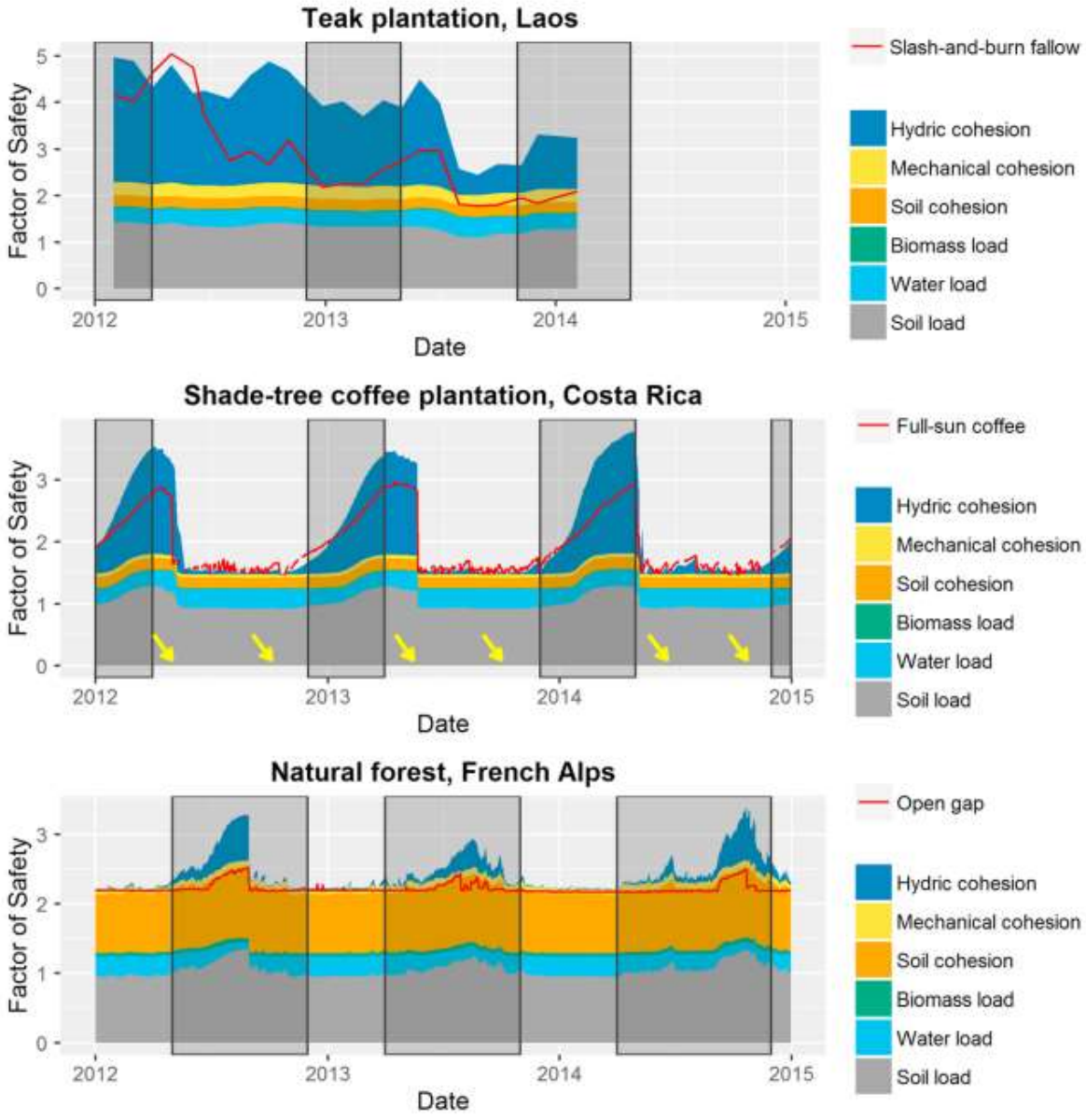

Figure 2.12: Factor of safety (FoS) at the most vulnerable depths under contrasting land uses for Laos (1.8 m), Costa Rica (1.5 m) and France (1.2 m) during the monitoring period (2012-2015). From (Kim, et al., 2017)

2.2.3. Engineering vegetation for slope stabilization

Coppin and Richards (1990) described the use of vegetation in civil engineering, defining a useful guide for the use of vegetation in different applications. The main applications found were related to slope stabilization and water erosion control. Although a useful tool for the use of vegetation by to face specific engineering situations, the experience-based observations cannot be quantified nor applied to different scenarios.

Stokes, et al.(2009) has reviewed the functional traits of vegetation related to the mechanical stabilization of slopes, defining the specific beneficial or adverse effect. Whereas several studies have assessed the mechanical contribution of vegetation to slope stability (Norris et al., 2008; Pollen & Simon, 2005), less studies have faced the hydrological reinforcement. Boldrin, et al. (2017) explored statistically the plant traits related to the maximum hydrological reinforcement. 10 different species were monitored, registering the daily rate of transpiration, the suction in the soil and the soil resistance. The latter was assessed by means of a penetrometer, testing the soil next to the surface. The results assessed the correlation between the maximum water uptake and the leaf conductance characterizing the specie in absence of water stress. Plant traits considered to be more correlated to the transpiration-induced suction were the specific leaf area, the root length density and the root-shoot ratio. In a further study, Boldrin, et al. (2018) evaluated the hydrological reinforcement of plants subjected to summer and winter conditions, concluding that evergreens may give a contribution to slope stability during the winter months.

2.3.Evapo-transpiration

The process of evaporation from a wet surface is driven by the energy given by the atmosphere, via heat exchange and solar radiation, that leads to the vaporization of water within the first layers next to the surface (Monteith, 1965). Penman (1948) defined the evaporation as a function of the irradiance and the vapor pressure deficit of the environment. However, the equation suggested was valid only in the case of

saturated water pressure at the evaporative surface. This is not the case for a soil in partially saturated conditions not in the case of transpiration from the leaves.

When the water table is near the ground surface and the evaporative demand of the atmosphere is modest, the hydraulic system is usually able to accommodate the latter; in this case, the system is in the *Energy Limited Regime* (Figure 2.13.a), and the amount of water loss depends mainly on the atmospheric conditions (potential evapo-transpiration PET). When the water availability reduces and the system is not able to accommodate the evaporative demand of the atmosphere anymore, the system enters a condition of *Water Limited Regime*, where the Actual Evapo-Transpiration will me a portion of the outward water flux induced by the interaction with the atmosphere (AET<PET).

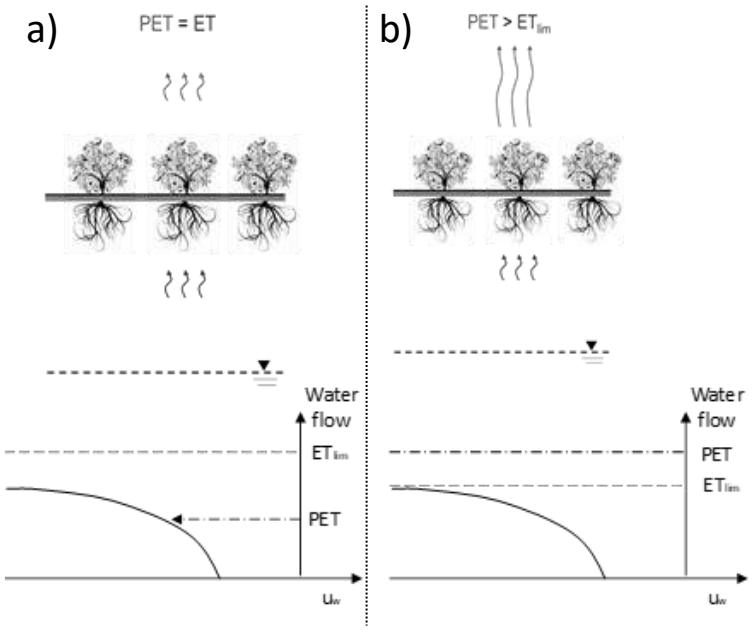

Figure 2.13:energy limited (a) and water limited (b) regime

Transpiration is the process of evaporation from the wet cells (Mesophyl) within the leaf and consequent stream of water from the roots to replace the water lost. The exchange of water vapour between the mesophyll cells and the atmosphere is located within the *stomata* (Figure 2.14), small apertures at the surface of the leaves that

regulate the water and CO2 exchange (Canny, 1977). The potential transpiration from the plant is dependent on the evaporative demand of the atmosphere: only a relatively small percentage of the water absorbed by the roots is used for physiological processes (photosynthesis and growth), while more than 90% is lost in transpiration (Sinha, 2004). The water loss from the plant is the unavoidable consequence of the vapour pressure gradient between the wet leaf mesophyll and the often quite dry atmosphere. In fact, plants can thrive in a saturated or nearly-saturated atmosphere with very little transpiration (Hillel, 1980).

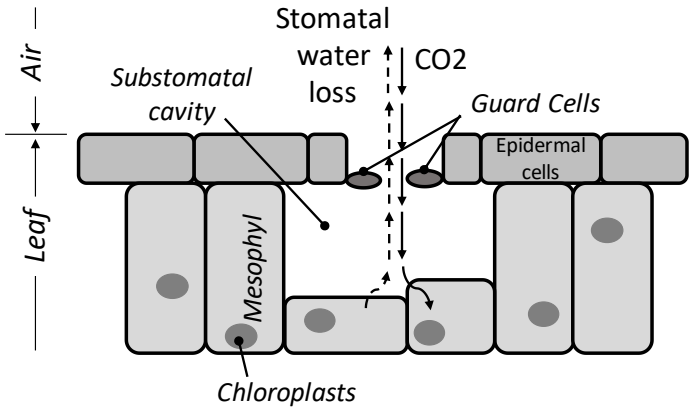

Figure 2.14: Simplified representation of the Stomata

2.3.1. Energy limited regime

The most commonly used model to calculate potential evapo-transpiration was suggested by Penman and lately modified by (Monteith, 1965). The method is based on the physical process of evapo-transpiration and requires detailed information about the weather conditions and an exhaustive characterization of the site. A review and comparison of other methods is presented by Xu and Chen (2005), who divides the methods for the calculation of the Potential evapo-transpiration between the temperature-based approach and the radiation-based approach.

The potential evapo-transpiration described using the Penman-Monteith equation (Monteith, 1965) is as follow:

$$PET = \frac{1}{\lambda}\frac{\Delta \cdot R_n + \rho_a \cdot c_p \cdot p_{v0}(z) \cdot [1 - RH(z)]/r_a}{\Delta + \gamma \cdot [(r_a + r_c)/r_a]} \quad [7]$$

where λ is the latent heat of vaporisation of water at the air temperature T(z), Δ is the slope of the saturation vapour pressure curve at the air temperature T(z), γ is the psychrometric constant at the air temperature T(z), R_n is the net solar radiation, ρ_a is the density of the air, c_p is the specific heat of air, p_{v0} is the saturation vapour pressure at the air temperature T at the elevation z, p_v is the actual air vapour pressure at the elevation z, RH is the relative humidity at the elevation z, r_a is the aerodynamic resistance and r_c is the surface resistance of the transpiring crop.

The solar net radiation Rn is dependent on the albedo α of the reflecting surface, $R_n = R_s(1 - \alpha)$, where Rs is the short-wave incident radiation. Typical values of albedo per different surfaces are reported in Table 2.3 (Ahrens, 2012; Oke, 2002).

Table 2.3Albedo values of various surfaces. From (Ahrens, 2012; Oke, 2002)

Surface	**Details**	**Albedo**
Soil	Dark & wet versus Light & dry	0.05-0.40
Sand		0.15-0.45
Grass	Long versus short	0.16-0.26
Agricultural crops		0.18-0.25
Tundra		0.18-0.25
Forest	Deciduous	0.15-0.20
	Coniferous	0.05-0.15

The aerodynamic resistance r_a takes into account the progressive saturation of the air layers next to the evaporative surface. When water evaporates, the molecules tend to accumulate within air layer next to the surface, reducing the vapour pressure gradient and ultimately leading to a nil evapo-transpiration (ideal case). The aerodynamic resistance takes into account the phenomena, and it is a function of the wind speed and the roughness of the evaporating speed. The equation reported of r_a is the simplified version suggested by

Brutsaert (1982), where the roughness length governing momentum, heat and vapour transfer are identical:

$$r_a = \frac{\left[\ln\left(\frac{z-d_0}{z_{0m}}\right)\right]}{k^2 \cdot u(z)} \quad [8]$$

where z is the height of wind measurements, $u(z)$ is the wind speed at height z, d_0 is zero plane displacement height, k is the von Karman's constant (k=0.41), and z_{0m} is the roughness length [m].

The canopy resistance is the resistance of the crop to vapour transfer, and it is determined by the leaf area, leaf age and condition. The canopy resistance is usually taken with reference to well-watered conditions (Allen, et al., n.d.). Experimental values of aerodynamic resistance and canopy resistance are reported by Monteith (1965).

Table 2.4: Values of height, canopy resistance, surface roughness and aerodynamic resistance. From experimental data reported by Monteith (1965)

Surface	$\boldsymbol{h}$ (m)	$\boldsymbol{r_{cm}}$ (sm^{-1})	$\boldsymbol{z_{0m}}$ (m)	$\boldsymbol{r_a}$ (sm^{-1})
Bare surface	0	0.001	170	0.35
Lawn	0.01	410	0.006	100
Rough pasture	0.05-0.1	50	0.02	63
Timothy	0.6-0.7	50	0.05	36
Pine forest	5.5	90	0.4	8

2.3.2. Water limited regime

When the water recharge from the water table is not enough anymore to allow the outward water flow required by the atmosphere, the system enters a condition of drought, referred to as *Water Limited Regime (*Figure 2.13). In this condition the actual evapo-transpiration rate is smaller than the PET and it depends on the characteristics of the whole hydraulic system. In the latter case it is a hard task to forecast the water

loss from the evaporative/transpiration surface, because it requires a detailed knowledge of all the hydraulic resistances of each element in the hydraulic system.

For the case of soils, the decrease in the evaporation rate following the increasing desaturation was modelled by Wilson, et al. (1993). A typical trend of the actual evaporation with respect to the maximum evaporation is reported in Figure 2.14, for decreasing water availability. The actual evaporation begins to decline when the surface becomes unsaturated and the amount of water at the surface becomes limited (D. M. Gray, 1970; Morton, 1975). Wilson (1990) modified the Penman equation to include a condition of unsaturated soil surfaces, to include the actual vapor pressure at the soil surface.

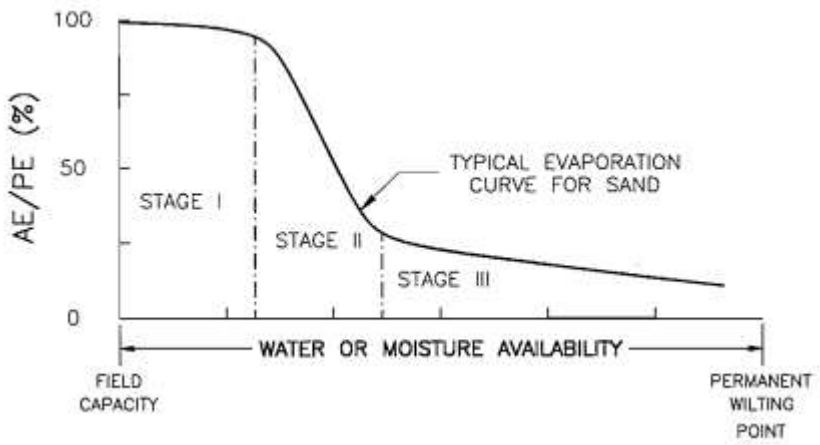

Figure 2.15: The relationship between the rate of actual evaporation and potential evaporation (AE/PE) and water availability. From Wilson, et al (1993).

In the case of vegetated soil, the description of the outward water flow in the Water limited regime is more complex, due to the coupling of soil and plant behaviour. An example of the complexity of the soil-plants interaction is given by the inner mechanism plants use to protect themselves from drought, through a mechanism of 'root to shoot' communication able to trigger stomata closure when roots perceive a

water deficit in soil (Blackman & Davies, 1985). The partial closure of stomata reduces the water loss from leaves and prevent an excessive water stress in the plant.

Philip (1966) described the system mutual interaction with the term 'Soil-Plant-Atmosphere continuum', or SPAC. In this conceptual model, the system act as a whole and the water flows from the soil into the roots, along the stem, until it evaporates in the atmosphere. The flow of water is driven by the pressure gradient generated at the level of the leaves (Pickard, 1981).

Several physical based model have described the process of root water uptake through analogies to the Ohm's law (Hillel, Talpaz, & Van Keulen, 1976; Whisler, Klute, & Millington, n.d.).

The most adopted method to take into account the reduction of transpiration for geotechnical applications is through the Feddes function (Feddes, 1982), relating the plant water uptake to the water pressure in the soil, . An exhaustive discussion of the Feddes function and its use if reported in Chapter 3.

References

Ahrens, C., 2006. *Meteorology today. An introduction to weather, cimate, and the environment.* Rome, Italy: Thompson, Brooks/Cole.

Allen, R., Pereira, L., Raes, D. & Smith, M., n.d. *FAO irrigation and drainage paper No.56 Crop EvapoTranspiration,* s.l.: s.n.

Anon., 2018. *2016 UK greenhouse gas emissions, final figures,* s.l.: Department for businness, energy & industrial strategy.

Anon., n.d. *http://www.ictinternational.com/casestudies/physiology-of-water-absorption-and-transpiration/.* [Online].

Balzano, B., Amabile, A., Caruso, M. & Tarantino, A., 2014. *A numerical study of hydrological effects of vegetation on slope stability.* s.l., s.n.

Balzano, B., Tarantino, A. & Ridley, A., 2016. *Analysis of a rainfall-triggered landslide at rest and be thankful in Scotland.* s.l., E3S Web of Conferences .

Biddle, P., 1983. Patterns of soil drying and and moisture deficit in the vicinity of trees on clay soils. *Geotechnique,* Volume 33, pp. 107-126.

Biddle, P., 1998. *Patterns of Soil Drying in the proximity of trees on clay soils.* Wantage (UK): Willowmead Publishing Ltd..

Bishop, A., Alpan, I., Blight, G. & Donald, I., 1960. *Factors controlling the shear strength of partly saturated cohesive soils.* Boulder, Colorado, University of Colorado, pp. 503-532.

Bitterlich, S., Durner, W., Iden, S. & Knabner, P., 2004. Inverse estimation of the unsaturated soil hydraulic properties from column outflow experiments using free-form parametrizations. *Vadose zone journal,* pp. 971-981.

Boldrin, D., Leung, A. & Bengough, A., 2017. Correlating hydrologic reinforcement of vegetated soil with plant traits during establishment of woody perennials. *Plant soil,* Volume 416, pp. 437-451.

Boldrin, D., Leung, A. & Bengough, A., 2018. Hydrologic reinforcement induced by contrasting woody species during sumemr and winter. *Plant soil,* Volume 427, pp. 369-390.

Braud, I. et al., 2001. Vegetation influence on runoff and sediment yield in the Andes region: observation and modelling.. *Journal of hydrology,* Volume 254, pp. 124-144.

Brutsaert, W., 1982. *Evaporation into teh atmosphere.* Dordrecht: Kluwer academic publisher.

Canny, M., 1977. Flow and transport in plants. *Annual review of fluid mechanics,* Volume 9, pp. 275-296.

Childs, E. & Collis-George, N., 1950. The permeability of porous materials. *Proceedings of teh Royal Society,* pp. 392-405.

Coppin, N. & Richards, I., 1990. *Use of Vegetation in Civil Engineering.* s.l.:CIRIA.

Czarnes, S., Hallett, P., Bengough, A. & Young, I., 2000. Root- and microbial-derived mucilages affect soil structure and water transport. *European Journal of soil science,* Volume 51, pp. 435-443.

De Baets, S. et al., 2008. *Root tensile strength and root distribution of typical Mediterranean plant species and their contribution to soil shear strength.* s.l., Springer.

de Campos, T., Andrade, M. & Vargas, E., 1991. *Unsaturated colluvium over rock slide in a forested site in Rio de Janeiro,Brazil.* Rotterdam, the Netherlands, s.n.

Endo, T. & Tsuruta, T., 1969. On the effect of roots upon the shearing strength of soil.. *Annual report of Hokkaido Branch,* pp. 167-183.

Escario, V., 1980. *Suction controlled penetration and shear tests.* Denver, Colorado, s.n.

Feddes, R., 1982. Simulation of field water use and crop yield. In: *Simulation of Plant growth and crop production.* Wageningen: Pudoc, pp. 194-209.

Fredlund, D., 1987. Slope stability analysis incorporating the efefct of soil suction. In: M. Anderson & K. Richards, eds. *Slope Stability, Geotechnical Engineering and Geomorphology.* s.l.:John Wiley & Sons Ltd., pp. 113-144.

Fredlund, D., Morgenstern, N. & Widger, R., 1978. Shear strength of unsaturated soils. *Canadian geotechnical journal,* Volume 15, pp. 313-321.

Fredlund, D. & Raharjo, H., 1993. *Soil Mechanics for unsaturated soils.* s.l.:John Wiley & Sons.

Fredlund, D., Xing, A. & Huang, S., 1994. Predicting of the permeability function of for unsaturated soil using the soil-water characteristic curve. *canadian geotechnical journal,* 31(4), pp. 533-546.

Gan, K. & Fredlund, D., 1988. Multistage direct shear testing in unsaturated soils. *Geotechnical testing journal, GTJODJ,* Volume 11, pp. 132-138.

Gardner, W., 1958. Some steady-state solutions of the unsaturated moisture flow equation with application to evaporation from a water table. *Soil science,* 85(4), pp. 228-232.

Garg, A., Coo, J. & Ng, C., 2015. Field study on the influence of root characteristics on soil suction distributionin slopes vegetated with Cynodon dactylon and Schefflera heptaphylla. *Earth surface process and landforms,* 40(12), pp. 1631-1643.

Gray, D., 1970. *Handbook of the principals of hydrology,* Ottawa, Canada: National research council of Canada.

Gray, D., 1978. *Role of woody vegetation in reinforcing soils and stabilising slopes..* Sidney, Australia, s.n.

Gray, D. & Leiser, A., 1982. *Biotechnical slope protection and erosion control.* New York: Van Nostrand Reinhold.

Greenway, D., 1987. Vegetation and slope stability. In: M. Anderson & K. Richards, eds. *Slope stability.* s.l.:John Wiley & Sons Ltd., pp. 187-230.

Guthrie, R., 2002. The efefcts of logging on frequency and distribution of landslides in three watersheds of Vancouvver Island, British Columbia.. *Geomorphology,* Volume 43, pp. 273-292.

Hallett, P., Gordon, D. & Bengough, A., 2003. Plant influence on rhizosphere hydraulic properties: direct measurements using a miniaturizes infiltrometer. *New physiologist,* Volume 157, pp. 597-603.

Hendrickx, J. & Flury, M., 2001. Hendrickx, J. M., & Flury, M. (2001). Uniform and preferential flow mechanisms in the vadose zone.. *Conceptual models of flow and transport in the fractured vadose zone,* pp. 149-1887.

Hillel, D., 1980. *Applications of soil physics.* London: Academic press.

Hillell, D., Talpaz, H. & Van Keulen, H., 1976. A macroscopic scale model of ewater uptakeby a non-uniform root system and of water and salt movement in soil profiles. *Soil science,* pp. 242-255.

Husken, D., Steudle, E. & Zimmermann, U., 1978. Pressure probe technique for measuring water relations of cells in higher plants. *plant physiology,* Volume 61, pp. 158-163.

Jackson, R. et al., 1996. A global analysis of rot distributions for terrestrial biomes. *Oecologia,* Volume 108, pp. 389-411.

Jarvis, P. & McNaughton, K., 1986. Stomatal control of transpiration: scaling up from leaf to region. *Advances in Ecological research,* Volume 15.

Kim, J. et al., 2017. Vegetation as a driver of temporal variations in slope stability: The impact of hydrological processes. *Geophysical research letters,* Volume 44, pp. 4897-4907.

Kim, J. et al., 2017. Vegetation as a driver of temporal variations in slope stability: The impact of hydrological processes.. *Geophysical research letters,* Volume 44, pp. 4897-4907.

Klute, A., 1972. The determinationof teh hydraulic conductivity and diffusivity of unsaturated soils. *Soil science,* 113(4).

Leij, F., Russell, W. & Lesch, S., 1997. Closed-form expressions for water retention and conductivity data. *Ground water,* pp. 848-858.

Leung, A. & Ng, C., 2013. Analyses of groundwater flow and plant evapotranspiration in a vegetated soil slope. *Canadian Geotechnical Journal,* p. 1204:1218.

Lu, N. & Godt, J., 2008. Infinite slope stability under steady unsaturated seepage conditions. *Water resources research,* Volume 44, pp. 1-13.

Marinho, F. A. M., Take, W. A. & Tarantino, A., 2008. Measurement of matric suction using tensiometric and axis translation techniques. *Geotechnical and Geological Engineering,* Volume 26(6), pp. 615-631.

Masrouri, F., Bicalho, K. & Kawai, K., 2008. Laboratory hydraulic testing in unsaturated soils. *Geotechnical and geological engineering,* 26(6), pp. 691-704.

Monteith, J., 1965. *Evaporation and environment. The state and movement of water in living organisms.*. s.l., Cambridge University Press.

Morris, P. H., Graham, J. & Williams, D. J., 1992. Cracking in drying soils.. *Canadian Geotechnical Journal,* 29(2), pp. 263-277.

Morton, F., 1975. Estimating evaporation and transpiration from climatological observations. *Journal of applied meteorology,* pp. 477-497.

Mualem, Y., 1976. A new model for predicting the hydraulic conductivity of unsaturated porous media. *Water resources research,* 12(3), pp. 513-522.

Nash, D., 1987. A comparative reviewof limit equilibrium methods of stability analysis. In: *Slope stability. Geotechnical Engineering and Geomorphology.* s.l.:John Wiley & Sons Ltd., pp. 11-75.

Norris, J. et al., 2008. *Slope stability and erosion control:ecotechnological solutions.* s.l.:Springer science and businness media.

Oke, T., 1992. *Boundary Layers climates.* New York: Routledge.

Or, D., Wraith, J. & Warrick, A., 2002. Soil water content and water potential relationships.. In: *Soil physics companion.* s.l.:s.n., pp. 49-84.

Penman, H., 1948. Natural evaporation from open water, bare soil and grass. *Proceedings of the Royal Society of London. ,* Series A. Mathematical and Physical Sciences 193(1032), pp. 120-145.

Peroni, N., 2002. *Contributo allo studio delle proprietà idrauliche e della deformabilità di un terreno insaturo.* Ancona: universita' degli studi di Ancona, Italy.

Philip, J., 1966. Plant water relations: physical aspects. *Annual review in plant phisiology,* Volume 17, pp. 245-268.

Pickard, W., 1981. The ascent of sap in plants. *Progress in biophysics and molecular biology,* Volume 37, pp. 181-229.

Pollen-Bankhead, N. & Simon, A., 2010. Hydrologic and hydraulic effects of riparian root networks on streambank stability:Is mechanical root reinforcement the whole story?. *Geomorphology,* Volume 116, pp. 353-362.

Pollen, N., Simon, A. & Collison, A., 2004. Advances in assessing the mechanical and hydrogeologic effects of riparian vegetation on streambank stability. *Riparian veegetation and fluvial geomorphology,* Volume 8, pp. 125-139.

Richards, L., 1931. Capillary conduction of liquids through porous medium. *Journal of Physics,* pp. 318-333.

Riestenberg, M., 1994. *Anchoring of thin colluvium by roots of Sugar Maple and White Ash on hillslopes in Cincinnati,* s.l.: U.S. Geological Survey Bulletin.

Saito, H., Murakami, W., Daimaru, H. & Oguchi, T., 2017. Effect of clear-cutting on landslides occurrences: Analysis of rainfall thresholds at Mt. Ichifusa, Japan.. *Geomorphology,* Volume 276, pp. 1-7.

Saito, H., Murakami, W., Daimaru, H. & Oguchi, T., 2017. Effect of forest clear-cutting on landslide occurrences: Analysis of rainfall. *Geomorphology,* Volume 276, pp. 1-7.

Sinha, R., 2004. *Modern Plant Physiology.* s.l.:CRC Press.

Skempton, A. W., 1954. A foundation failure due to clay shrinkage caused by poplar trees.. *Proceedings of the Institution of Civil Engineers,* pp. 66-86.

Stirk, G., 1954. Some aspects of soil shrinkage and the effect of cracking upon water entry into the soil.. *Australian Journal of Agricultural Research,* 5(2), pp. 279-296.

Stokes, A. et al., 2009. Desiderable plant root traits for protecting natural and engineered slopes against landslides. *Plant soil,* Volume 324, pp. 1-30.

Tarantino, A., 2010. Basic concepts in the mechanics and hydraulics of unsaturated geomaterials.

Tarantino, A. & El Mountassir, G., 2013. Tarantino, Alessandro, and Gráinne El Mountassir. "Making unsaturated soil mechanics accessible for engineers: Preliminary hydraulic–mechanical characterisation & stability assessment.. *Engineering geology,* Volume 165, pp. 89-104.

Toll, D., 1990. A framework for unsaturated soil behaviour. *Geotechnique,* Volume 132, pp. 31-44.

Tsukamoto, Y. & Kusakabe, O., 1984. *Vegetative influences on debris slide occurrences on steep slopes in Japan.* Honolulu, Hawaii, Environment and Policy Institute.

Van Asch, W., Buma, J. & Van Beek, L., 1999. A view on some hydrological triggering systems in landslides. *Geomorphology,* 30(1-2), pp. 25-32.

Vanapalli, S., Fredlund, D. & Pufahl, D., 1996. The relationship between the soil-water characteristic curve and the unsaturated shear strength of a compacted glacial till. *Geotechnical testing journal, GTJODJ,* 19(3), pp. 259-268.

Vanapalli, S., Fredlund, D., Pufahl, D. & Clifton, A., 1996. Model for teh prediction of shear strength with respect to soil suction. *Canadian geotechnical journal,* Volume 33, pp. 379-392.

Veylon, G., Ghestem, M., Stokes, A. & Bernard, A., 2015. Quantification of mechanical and hydric components of soil reinforcement by plant roots. *Canadian geotechnical journal,* pp. 1839-1849.

Wheeler, S., Sharma, R. & Buisson, M., 2003. Coupling of hydraulic hysterisis and stress-strain behaviour in unsaturated soil. *Geotechnique,* 53(1), pp. 41-54.

Whisler, F., Klute, A. & Millington, R., 1970. *Analysis of radial, steady state solution and solute flow.* s.l., s.n.

Wilson, G., 1990. *Soil evaporative fluxes for geotechnical engineering problems.* Saskatoon: University of Saskatchewan.

Wilson, G., Fredlund, D. & Barbour, S., 1993. Coupled soil-atmosphere modelling for soil evaporation. *Canadian geotechnical journal,* pp. 151-161.

Wolle, C. M. & Hachich, W., 1989. *Rain-induced landslides in south-eastern Brazil.* Rotterdam, the Netherlands, s.n.

Wu, T., McKinnell, W. & Swanston, D., 1979. strength of tree roots and landslides on Prince of Wales island, Alaska. *Canadian Geotechnical Journal,* Volume 16, pp. 19-33.

Xu, C.-Y. & Chen, D., 2005. Comparison of seven models for estimation of evapotranspiration and groundwater recharge using lysimeter measurement data in Germany. *Hydrological processes,* Volume 19, pp. 3717-3734.

Yeh, W.-G., 1986. Review of parameter identification procedures in ground water hydrology: the inverse problem. *Water resources research,* 22(2), pp. 95-108.

Zhan, T. L., Ng, C. W. & Fredlund, D. G., 2007. Field study of rainfall infiltration into a grassed unsaturated expansive soil slope.. *Canadian Geotechnical Journal,* 44(4), pp. 392-408.

Ziemer, R., 1978. *Logging effects on soil moisture losses,* s.l.: Colorado State University.

Ziemer, R., 1981. *The role of vegetation in the stability of forested slopes.* Kyoto, s.n.

Chapter 3 Measurement of plant xylem water pressure using the High-Capacity Tensiometer and implications on the modelling of soil-atmosphere interaction.

Abstract

The response of shallow geotechnical structures is affected by the interaction with the atmosphere. Since the ground surface is very often vegetated, plant transpiration plays a major role in the removal of soil water by the atmosphere. Transpiration in geotechnical applications is generally modelled macroscopically via the Feddes reduction function. However, its parameters are often borrowed from the agricultural literature, where the focus is on crop species and often loosely compacted organic agricultural soils. For non-crop species in denser soils typically encountered in geotechnical applications, monitoring of the flow taking place in the soil through the xylem up to the leaves can potentially be exploited to characterise the Feddes reduction function. In this respect, the main challenge faced by geotechnical researchers and practitioners is the measurement of the water pressure in the xylem. Techniques currently used include the Pressure Chamber and Thermocouple Psychrometer. The Pressure Chamber is destructive and thus not suitable for continuous monitoring and/or where a relatively small number of leaves is available for measurement (as often occurs in laboratory experiments). The Thermocouple Psychrometer is not accurate at low suction, is affected by the presence of solutes in the xylem water, and is significantly sensitive to temperature. This paper explores a novel application of the High-Capacity Tensiometer (HCT), initially developed for soil pore-water pressure-measurement. The HCT was installed on the stem or branch of different trees and its measurement validated against Pressure Chamber measurements over a range xylem water pressure down to -1300 kPa via laboratory and field experiments. Results show that the HCT is a viable and convenient instrument to use for xylem water pressure measurement and can provide field-based data for the modelling of the transpiration

rate. Installing HCTs on stems and branches is quite straightforward and this will help achieve a step-change in testing and modelling the effect of plant transpiration on soil water regime in the vadose zone.

3.1. Introduction

The response of the shallow portion of the ground (vadose zone) and of earth structures is affected by the interaction with the atmosphere. Rainwater infiltration and evapotranspiration cause settlement and heave in shallow foundations and embankments, and control the stability of man-made and natural slopes.

The ground surface is often covered by vegetation and, as a result, transpiration plays a major role in the mechanisms of water removal by the atmosphere. Transpiration is the process of water movement taking place from the soil through the plant up to the leaves, where water eventually evaporates through the stomata.

A very common approach to model water uptake by vegetation macroscopically is to consider actual transpiration T as the product of the potential (energy-limited) transpiration T_P times a reduction factor α, assumed to be a function of the pore-water pressure, u_w, in the root zone:

$$T = \alpha(u_w) \cdot T_P \qquad [1]$$

Under optimal soil water conditions, root water extraction rate is equal to the maximum transpiration rate, T_P (α=1). Under non-optimal conditions, i.e. the soil is either too dry or too wet, transpiration is reduced by means of the factor α (α <1).

Feddes (1976) first assumed the reduction factor as a function of soil water content θ, and improved this later as a function of soil pore-water pressure (Feddes et al. 1978) as presented in Figure 3.1. The transpiration is assumed to be equal to zero for a u_w higher than u_{w1}, the 'anaerobiosis point', and below the wilting point u_{w4}; the transpiration is maximum (α=1) between u_{w2} and u_{w3}, with the latter corresponding to the pore-water pressure in the soil below which plant growth starts to be limited. The pore-water pressure u_{w3} marks the transition from the energy-limited (potential) transpiration to the water-limited transpiration and is the most critical parameter of the Feddes function (Nyambayo and Potts, 2010).

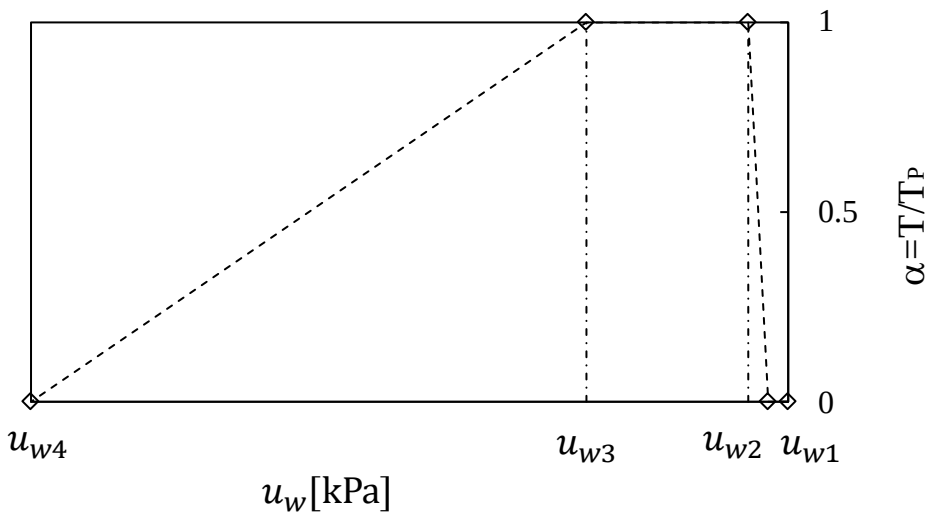

Figure 3.1: Feddes reduction function (Feddes, et al., 1982)

The approach proposed by Feddes, et al. (1978) to model the reduction factor is widely used in geotechnical applications (Briggs, 2016; Cui, Vincent, & Paristech, 2010; Greco et al., 2013; Nyambayo & Potts, 2010; Pagano, Reder, & Rianna, 2019; Tsiampousi, Zdravkovic, & Potts, 2017; Zhu & Zhang, 2019).This approach is convenient because only requires information about the pore-water pressure in the root zone without the need to address the complex interaction between the soil, the plant, and the atmosphere.

However, this simplicity is only apparent because the complexity of such an interaction is hidden in the choice of the Feddes parameters. These parameters should take into account the physiological reaction of the plant. The transpiration rate is controlled by the stomata conductance, which is in turn regulated by the leaf water pressure (Lu, et al., 1995). When the (negative) leaf water pressure falls below a certain threshold, the stomata begin to close to prevent excessive water loss and excessive decrease in leaf water pressure (Gollan, et al., 1985). It is actually the water pressure in the leaf and not the pore-water pressure u_{w3} in the soil that dictates the transition from the energy-limited to the water-limited regime.

The problem of the choice of the Feddes parameters is reflected in the very wide range of parameters adopted in the literature for u_{w3} as reported in Table 3.1. Feddes et al. (1978) proposed u_{w3}=-40 kPa but a wide range of values for u_{w3} have been derived by Wesseling (1991) and Utset et al. (2000) depending on the nature of the crop and the level of potential transpiration rate. When the Feddes function is used in geotechnical applications, the parameter u_{w3} is generally borrowed from the agricultural literature (Table 3.1). This approach may be questionable as the parameters derived for crop species and often loosely compacted organic agricultural soils may significantly differ from non-crop species in often densely-compacted soils that are typically encountered in geotechnical applications (Garg et al., 2015).

Table 3.1: Values of the Feddes function, suggested by Feddes et al. (1978) and adopted in agricultural and geotechnical applications.

			u_{w1} [kPa]	u_{w2} [kPa]	u_{w3} [kPa]	u_{w4} [kPa]
Feddes model	Feddes (1978)		-5	-5	-40	-1500
Agricultural crop models	(Wesseling 1991)	Potatoes	-1	-2.5	-32/-60	-1600
		Sugar beet	-1	-2.5	-32/-60	-1600
		Wheat	0	-0.1	-50/-90	-1600
		Pasture	-1	-2.5	-20/-80	-800
		Corn	-1.5	-3	-32.5/-60	-800
	Utset et al. 2000	Potatoes	-1	-3.5	-32/-60	-800
Geotechnical models	Indraratna et al. (2006)		-5	-5	-40	-1500
	(Nyambayo and Potts, 2010)		0	-5	-100/-400	-1500
	(Hemmati, et al., 2010)		-4.9	-4.9	-40	-1500

	Greco et al., 2013		0	-5	-150	-1500
	Briggs et al. (2016)		0	0	-100	-1500
	Tsiampousi et al. (2017)		0	-5	-50	-1500
	Garg et al. (2015) Zhu and Zhang (2019)		-0.1	-5	-52/ -90	-1500

To cope with this uncertainty, Nyambayo and Potts (2010) have analysed the sensitivity of the transpiration model to the parameter u_{w3} and concluded that this parameter had little effect on the simulated pore-water pressure distribution. However, as acknowledged by the same authors, this finding may be specific to the climate and soil conditions they have investigated and should not be generalised. Garg et al. (2015) designed a laboratory programme on S. Heptaphylla vegetated in compacted silty sand to derive experimentally the Feddes parameters for non-crop species. However, their method is applicable to laboratory condition and would be difficult to implement in the field.

The reduction function under field conditions can be investigated by monitoring the Soil-Plant-Atmosphere Continuum (SPAC) as illustrated later in the paper and this includes the measurement of the (negative) xylem water pressure in the plant. The most common techniques to measure xylem water potential are the Pressure Chamber (PC) (Scholander, et al., 1965) and the Thermocouple Psychrometer (TP) (Martinez, et al., 2011). The working principle of the Pressure Chamber is the same as the axis-translation technique used to measure matric suction in soils (Marinho, et al., 2008). Air pressure is increased around the xylem/leaf until water pressure is 'translated' from negative values to zero. This is a destructive technique as it requires the trunk or branch to be cut or leaves to be excised. As a result, the PC is not suitable for continuous

measurement and/or for monitoring leaf water pressure when a relatively small number of leaves is available, which is generally the case in laboratory experiments. Furthermore, the design of the pressure chamber makes very difficult the measurement in locations other than leaves and small twigs.

The Thermocouple Psychrometer is similar in concept to the instruments used to measure total suction in soils via vapour-phase equilibrium (Bulut and Leong, 2008). It is widely used in the field for continuous monitoring of xylem/leaf water potential, but its measurement is affected by the presence of solutes in the xylem water (osmotic suction). The common assumption that solutes have negligible effects (Jones, 2006) does not always hold as demonstrated by Goode and Higgs(1973) and Campbell and Gardner,(1971) and this can make the Thermocouple Psychrometer measurement difficult to interpret. Another limitation of the Thermocouple Psychrometer is the poor accuracy at values of (negative) xylem water pressure close to zero (high relative humidity) and its sensitivity to temperature, which is a critical issue in field measurements (Martinez, et al., 2011).

A direct measurement of xylem water pressure was attempted by (Balling and Zimmermann, 1990), using a pressure probe made of a capillary tube filled with water and silicon oil. When the tip of the probe was inserted into a vessel, the vessel water pressure was transmitted through the liquid in the probe and measured by a pressure transducer. However, this pressure probe has never registered vessel water pressures below -0.65 MPa (Wei, et al., 2001) and for no more than a few hours due to cavitation occurring in the probe (Balling and Zimmermann, 1990). This was probably due to the absence of a high-air-entry porous interface, which is actually incorporated into high-capacity tensiometer used to measure uw in soil (Marinho, et al., 2008).

This paper presents a novel use of High-Capacity Tensiometer (HCT) to monitor the negative xylem water pressure in plants. The measurement of the HCT was validated against the measurement of xylem water pressure via the Pressure Chamber over a relatively wide range of xylem water pressures via field and laboratory experiments.

It is then demonstrated how the measurement of the xylem water pressure in conjunction with the measurement of soil matric suction can be potentially used to characterise the transition from energy-limited to water limited regime and, hence, the most critical parameter of the Feddes reduction function.

3.2. Plant Hydraulics

3.2.1. Hydraulic architecture of plants

Water flows from the soil through the plant up to the leaves, where it evaporates into the atmosphere. Water flowing from the soil crosses the outer layers of root living cells and moves radially towards the xylem at the centre of the root itself. Water may flow through the apoplastic or symplastic routes (Figure 3.2). Apoplast refers to the "dead" part of the plant, the xylem and the cell walls, while the symplast represents the "living" part, i.e. the internal part of the cells. When water reaches the xylem of the roots, it flows upwards through the xylem (apoplast) along the stem up to the leaves.

The stem of a plant is composed of different tissues, each one having its own specific role and structure (Figure 3.2.b). The phloem and the xylem are the main pathways for solutes and water within the stem. The phloem is the tissue of the plant that redistributes downward the sugars synthetized in the leaves. The xylem (part of the apoplast) is dedicated to the transport of water from the roots to the leaves and it is characterized by a porous structure made of *vessels* (diameter Ø~300 μm) and *tracheids* (diameter Ø~40 μm). These are similar to capillary tubes (Canny, 1977) and act as conduits for the transport of water. The water flows mainly vertically through the xylem, driven by the water pressure gradients between the xylem and the leaves. Under normal conditions, the water in vessels and tracheids is continuous and under tension and this allows the ascent of water to considerable heights. If the water tension becomes too high, embolism (cavitation) may occur in some of the transporting channels, preventing the flow of water to occur any further in the channel itself.

The water moves from the xylem in the stem into the leaves. Photosynthesis occurs in the leaf, where CO_2, water, and solar energy are converted into sugars and oxygen in the chloroplasts. The CO_2 enters the leaf through the *stomata*, apertures on the surface of the leaf (Figure 3.2.c). The guard cells can close or open the stomata, in response to the environmental conditions (i.e. irradiance) and water availability, to regulate the CO_2 exchange and water loss from the mesophyl, i.e. the *transpiration*. For most plants, stomata close during night-time, when no photosynthetic process and transpiration occur (Salisbury, 1992).

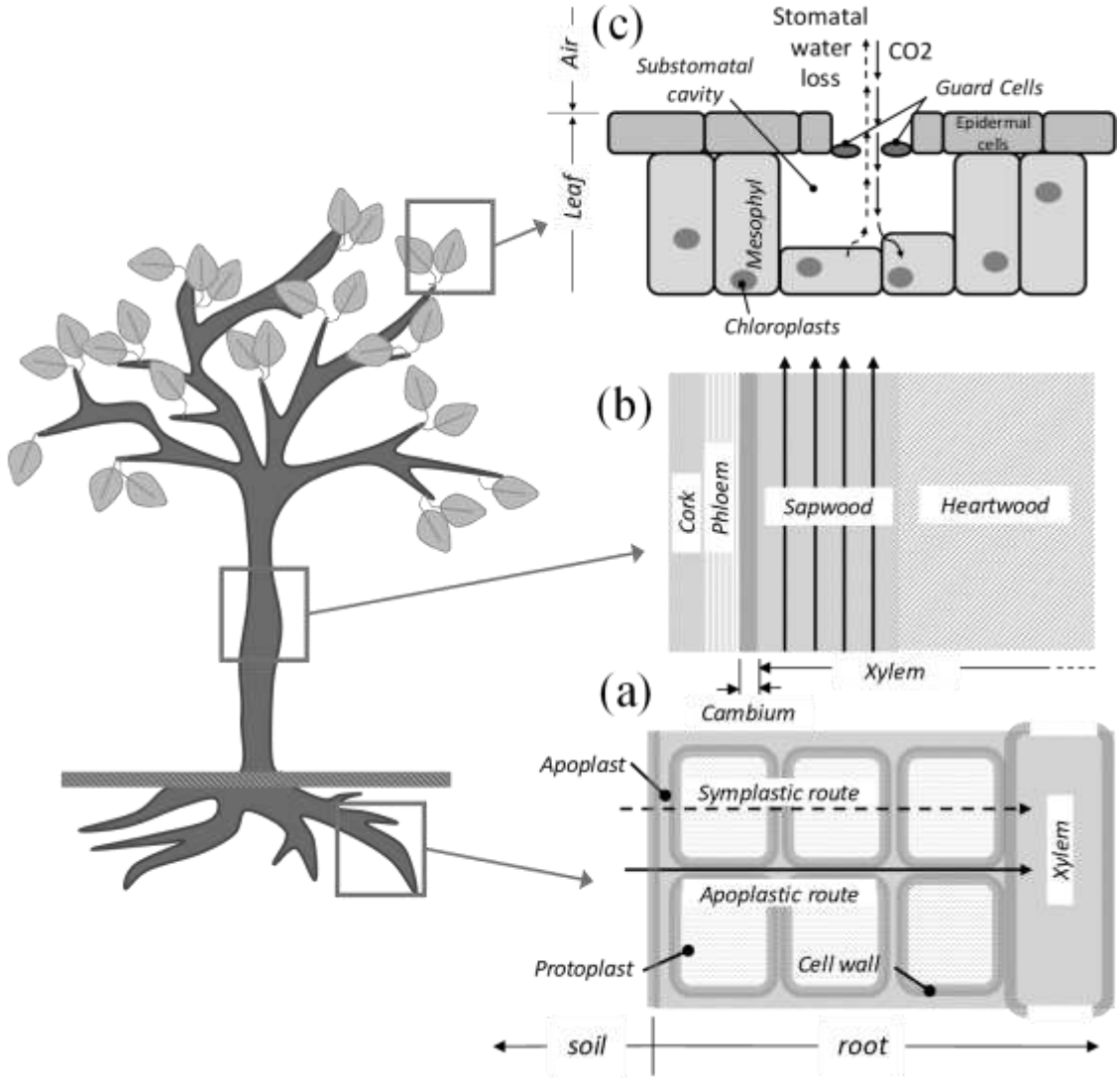

Figure 3.2: (a) radial flow from the soil to the root; (b) structure of the stem and flow through the xylem; (c) leaf structure: stomata and gas exchange

3.2.2. Water potential and principles of measurement

Only a relatively small percentage of the water absorbed by the roots is used for physiological processes (photosynthesis and growth), while more than 90% is lost in transpiration (Sinha, 2004). The water loss from the plant is the unavoidable consequence of the vapour pressure gradient between the wet leaf mesophyll and the often quite dry atmosphere. In fact, plants can thrive in a saturated or nearly-saturated atmosphere with very little transpiration (Hillel 1980).

Transpiration is therefore the main water flow process occurring in the plant. According to the Cohesion-Tension theory (Pickard, 1981), the ascent of water is driven by the (negative) water pressure generated in the leaf by the evaporation taking place through the leaf stomata and the consequent reduction of the menisci curvature in the cell walls of the mesophyll. Similar to soils, water potential is formed by a gravitational and pressure term. As a result, characterisation of the water flow of water within the plant requires the measurement of the (negative) water pressure in the xylem.

The systems used in plant science for the measurement of xylem water pressure are essentially the same used in soil science. An equilibrium is established between the sensor and the xylem water via either liquid or vapour phase.

Liquid equilibrium is associated with a homogeneous concentration of ions between the sensor and the xylem water (because ions diffuse freely towards the sensor). As a result, equilibrium indicates that water pressures in the sensor and the xylem are the same. Sensors involving equilibrium via liquid phase include the pressure chamber, the high-capacity tensiometers, and the Zimmermann's pressure probe (Husken, et al., 1978). It is worth noticing that measurement involves equilibrium between the water in the sensor and the xylem. As a result, measurement is not affected by the presence of any porous tissue interposed between the sensor and the xylem, i.e. the apoplast cells.

When equilibrium is established via the vapour phase, the vapour pressure in the sensors is not only affected by the liquid pressure in the xylem but also by the concentration of solutes in the xylem water. The measurement cannot therefore be directly correlated to the (liquid) water pressure in the xylem unless the effect of the solutes concentration is other assumed to be negligible or assessed independently. The thermocouple psychrometer falls in this class of sensors.

3.3. Equipment

3.3.1. High-Capacity Tensiometer

The High-capacity Tensiometers (HCT) used in this experimental work are home-made and are based on the design of Tarantino and Mongiovi (2002), which is in turn similar in concept to design introduced by Ridley (1993). The HCT is showed in Figure 3.3 and is composed of an integral strain gauge diaphragm 0.4mm thick and a ceramic filter. A rosette strain gauge is bonded to one side of the diaphragm to measure water pressure in the water reservoir in the positive and negative range. A ceramic filter with a nominal air-entry value of 1.5 MPa is the interface interposed between the water in the reservoir and the xylem water. When the instrument is put in contact with the xylem, the tension of the xylem water is transferred to the water reservoir, deflecting the diaphragm and deforming the strain gauge. HCT measures the 'matric' water pressure in soil. There is in fact no difference in ion concentration between the sample water and the water reservoir of the instrument, giving that the porous ceramic allows free diffusion of ions (Tarantino, 2004).

The challenge of direct measurement of (negative) water pressure by HCT is associated with the metastable state of water under tension. Water under tension is subject to cavitation, i.e. water tend to move from metastable states, where the liquid is under tension, to stable states where liquid and vapour phases coexist under positive absolute pressure. The presence of imperfections within the sensor increases the probability of instability (cavitation). These imperfections can arise in principle from

homogeneous nucleation or heterogeneous nucleation. In the first case, temporary microscopic voids are created by the thermal motion within the liquid, constituting the origin nuclei for the growth and rupture of macroscopic bubbles. The tension necessary to activate homogeneous nucleation has been estimated to be of the order of 800 MPa (Brenner, 1995). As a result, instability observed at much lower water tensions is attributed to heterogeneous nucleation. In this case, the cavitation nuclei originate from air pockets 'invisible at naked eye' that remain entrapped at the boundary between the liquid and the surface of the water container or impurities dispersed in the water. The slow diffusion of gas through the porous ceramic of the HCT increases progressively the concentration of imperfections and therefore the probability of cavitation. This transition cannot be prevented but it can be delayed long enough to allow for long-term measurement of negative water pressure. This is achieved by utilizing only de-aerated water and by pre-pressurising water in the measuring instrument to dissolve the majority of cavitation nuclei (Marinho, et al., 2008).

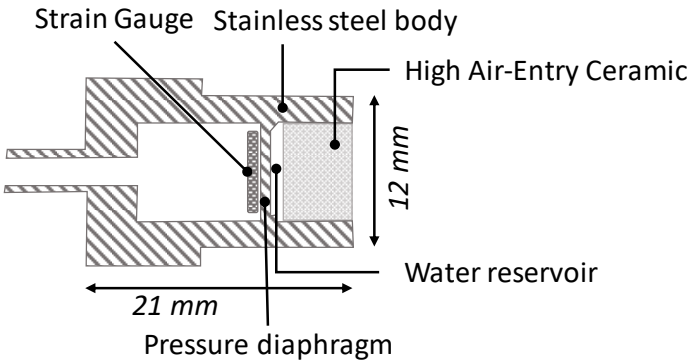

Figure 3.3: High-Capacity Tensiometer (after Tarantino and Mongiovi'(2002))

3.3.2. Pressure Chamber

The working principle of the Pressure Chamber is similar to the axis-translation technique used to measure matric suction in soils (Marinho, et al., 2008). On the plant, water in the leaf is under tension whereas the air surrounding the leaf is at atmospheric pressure (Figure 3.4a). When the leaf is excised, the water retracts into the petiole and

menisci form at the interface between the cut end of the petiole and the atmosphere (Figure 3.4b). In the Pressure Chamber, only the last part of the petiole is left outside in direct contact with the atmosphere (Figure 3.4c). The air pressure in the chamber is then gradually incremented until water can be observed to form a flat meniscus on the excised end of the petiole (Figure 3.4c). The air pressure is then taken numerically equal to the water tension in the leaf before excision (Boyer, 1967). This technique is based on the assumption that the difference between the leaf water pressure and the surrounding air pressure is kept constant throughout the whole procedure (Figure 3.4d,e) (Scholander, et al., 1965).

The (negative) water pressure of the leaf measured by the pressure chamber may be used to assess the xylem water pressure on the stem at the base of the petiole. To this end, the leaf is wrapped with aluminium foil for some time prior to excision in order to stop transpiration. The water potential in the leaf then reaches an equilibrium with the xylem at the junction with the stem (Lang and Barrs, 1965; Riceter, 1973).

The PC is a commonly used and trusted technique in plant science to measure the leaf and xylem water pressureand has often been used as a benchmark to validate several other measurement techniques (Balling & Zimmermann, 1990; Boyer, 1995; Brown & Tanner, 1981; Scholander, Bradstreet, Hemmingsen, & Hammel, 1965; Turner, Spurway, & Schulze, 1984).Typical values of leaf water pressure taken at pre-dawn with a soil pore-water pressure at around -150 kPa are in the range -100 to -1000 kPa and -250 to -1250 kPa depending on the broadleaf species considered (Kocher, et al., 2009).

It is very difficult, if not impossible, to quantify the accuracy of the Pressure Chamber because there is no independent reference measurement that can be used to benchmark the Pressure Chamber measurements. It is only possible to assess the precision of the measurement when multiple leaves are tested. Clearly, it is difficult to establish whether precision is associated with the Pressure Chamber measurement (including the operator-dependent detection of the flat meniscus appearing at the petiole cut end)

or the possible local variation of xylem water pressure at the base of the petiole of the different leaves excised.

The PC used in this experimental programme is commercialised by PMS Instrument Company (Model 1515D). It consists of a nitrogen cylinder with 20.7 MPa pressure connected via internal piping and a control valve to the measurement chamber. The chamber lid is fitted with sealing gasket that can seal stems/petioles that are no larger than 6.3 mm in diameter down to a completely closed position. The instrument is equipped with a 10 MPa digital gauge to record the air pressure in the measurement chamber.

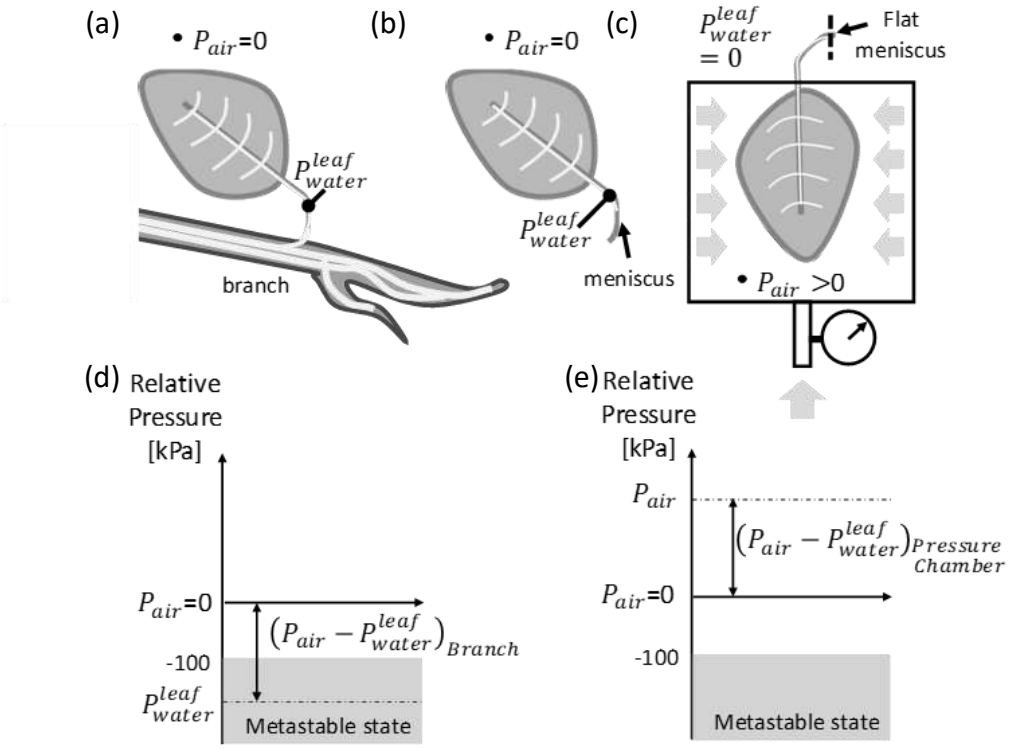

Figure 3.4:Figure 4. Working principle of the Pressure Chamber (PC) technique for measurement of leaf water pressure. (a) leaf on the tree (water pressure is negative); (b) leaf excised (curved meniscus forming at the end of petiole); (c) air pressure increased around leaf (meniscus becomes flat). (d) Air and leaf water pressure on the branch. (e) Air and leaf water pressure in the PC at equilibrium when the reading is taken.

3.4.Materials

The results presented in this paper include one test in the field on a chestnut tree and two tests in the laboratory, on a pear tree and on a willow tree respectively. The three selected plants are angiorsperms, whose xylem is characterized by broad (150 μm) continuous *vessels* in a matrix of fibres. Vessel connectivity reduces potential local variability of xylem water potential.

The chestnut (*Castanea sativa mill*.) belongs to the family of Fagaceae and is part of a chestnut plantation located in Penisola Sorrentina, Naples, Italy, at about 850 m above sea level. The age of the plant is approximately 15 years, the diameter of the trunk at breast height is around 20 cm and the total height of the plant is around 8÷10 m. The soil is a pyroclastic soil, presenting a shallow layer of organic matter, a layer of cinerite and angular pumices with a thickness varying from a few millimetres to a few centimetres and an underlying layer of 3÷4 cm angular pumices at least 1 m thick (Rodrigues Afonso Dias, 2019)

The two plants tested in the laboratory came from a nursery. The pear tree (P*yrus communis*) was tested in its original pot, which contained highly organic and lose soil (92 % organic matter, 8% sandy silt (68% silt, 32% sand)). Prior to the experiment, the tree was kept in the laboratory under a growth lamp at controlled temperature of 20°C to mimic spring weather conditions and allow the leaves to sprout up. At the time of the experiment, the plant was approximately 2.30 m high, the diameter of the stem at 100 mm from the soil was around 17 mm. The shrub of willow (*Salix cinerea*) was transplanted into a pot of silty sand (73% sand, 23% silt, 4% clay). In the new container, the willow grew 2 main branches, reaching a height of about 150 cm. The diameter of the stem at 100 mm from the soil was around 16 mm.

3.5. Xylem water pressure measurement: experimental procedures

3.5.1. High-Capacity Tensiometer

3.5.1.1. Conditioning

Adequate saturation of the high-capacity tensiometer is the key to successful measurement (Marinho, et al., 2008). Conditioning is carried out before each test, which includes cavitation induced by evaporation from the ceramic porous filter and the following saturation at 4 MPa for at least 48h in a saturation chamber (Tarantino, 2004). After removal from the saturation chamber, HCTs are then placed in water at atmospheric pressure until equilibrium is reached. Tensiometer are then subjected to two cycles of imposed suction, where negative water pressure is first generated up to about 1MPa by wiping the porous ceramic and allowing for some evaporation by exposing the filter surface to air and then placing again the tensiometer in free water to relieve the negative water pressure. This is aimed at relieving some residual stresses in the diaphragm when it is deformed in the negative range of water pressure, after long exposure to high positive water pressures (Tarantino and Mongioví, 2003). The tensiometer is zeroed at the end of the second cycle.

3.5.1.2. Application to the stem

HCTs can be installed on trunks or branches provided their diameter is greater than about 15mm. The bark and the living tissues of the plant (phloem and cambium) are removed to expose the xylem underneath (Figure 3.5a). The surface is then cleaned with some drops of distilled water. The surface is usually kept moist during the installation to avoid excessive dehydration of the tissues. HCTs are applied to the stem using a paste of kaolin clay at approximately the liquid limit interposed between the porous ceramic filter and the xylem (Figure 3.5b). The paste tends to extrude slightly through the lateral gap between the tensiometer and the recessed installation site. A latex membrane is then used to cover the paste to avoid evaporation from the paste (Figure 3.5c). The paste is required to ensure hydraulic continuity between the porous

ceramic filter and the plant xylem. The water content of the paste is a compromise between two conflicting requirements. Water content should be sufficiently high to give enough plasticity to the paste and ensure good adherence between the HCT and the xylem. On the other hand, excessive water content would increase considerably the equilibration time due to the amount of water that needs to be sucked out by the xylem to reach equilibrium.

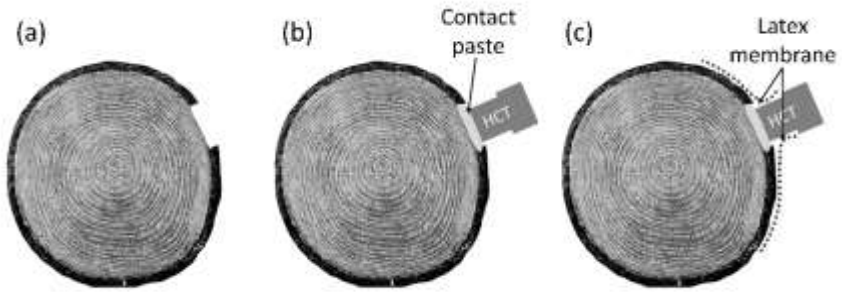

Figure 3.5: HCT installation on stem. (a) exposure of xylem tissues. (b) HCT application. (c) sealing with latex membrane

3.5.1.3. Post-measurement checks

During measurement, air cavities may form into the ceramic filter. These air cavities may not trigger cavitation but can alter the measurement by generating a differential between the pressure in the xylem and the pressure in the tensiometer water reservoir (Tarantino, 2004). The presence of air cavities generating possible spurious readings is checked in two ways at the end of the test. If cavitation does not occur during measurement, it is checked that the tensiometer recovers zero pressure after placement in free water (a residual water pressure of 10-20 kPa is considered acceptable according to Tarantino and Mongioví(2001). If cavitation occurs during measurement, it is checked that cavitation occurs at a gauge pressure of around -100 kPa.

3.5.2. Pressure Chamber

Leaves are initially wrapped in aluminium foil for at least 10 min, as suggested by the manufacturer (Anon., n.d.). Leaf wrapping prevents any light to reach the leaf and causes the stomata to close. This stops transpiration from the leaf and allows for the

water in the leaf to equilibrate with the water in the branch. As a result, the water pressure recorded in the leaf is assumed to coincide with the water pressure in the branch at the base of the petiole (Richter, 1973).

The leaf is then excised with a sharp blade and promptly inserted into the pressure chamber, apart from the end of the excised petiole that is kept outside the chamber at atmospheric pressure. The air in the chamber is gradually pressurised and the end of the petiole is continuously inspected using a magnifying glass. When water forms a flat meniscus at the end of the excised petiole, the air pressure increase is stopped (Meron, et al., 1985). The air pressure in the chamber recorded when the flat meniscus appears is assumed to be equal to the negative water pressure in the leaf before excision. A pressure chamber reading is an average of the water pressure recorded on a number of leaves excised in rapid succession at time intervals of about ~5min, which is the time usually required to excise a leaf, insert it in the pressure chamber, and take the measurement.

The number of leaves excised for each measurement is reported in Table 3.2. Six leaves where taken for the measurement on the chestnut tree on the same branch where HCTs were installed. The leaf wrapping time was set to 10 minutes. Leaves taken before dawn, in darkness, were not covered before excision as the stomata were assumed to be close overnight and the leaf not transpiring (Deloire and Heyns, 2011).

Readings on the pear tree were based on sets of 3 leaves taken all over the foliage with leaf wrapping time of 10 min. Readings on the willow were based on sets of 3 leaves with leaf wrapping time of at least 2 hours according to Patakas, et al.(2005) who suggested a wrapping time greater than 1h for plants under stress (i.e. subjected to very low xylem water pressure).

Table 3.2: Procedure for leaf water pressure measurement using the PC.

Type of test	**Plant**	**# leaves for each set**	**Wrapping time**

Field	Chestnut	6	≥10 min
Lab	Pear tree	3	>10 min
	Willow	3	>2 h

3.6. Field test: Chestnut in Monte Faito

3.6.1. Setup

The experiment was carried out on a chestnut grove in Monte Faito, Naples, Italy. Two HCTs were applied 10 cm apart on the branch of a chestnut at around 1.5 m from the soil (Figure 3.6). The HCTs were kept in place for approximately 80 hours uninterruptedly to monitor the evolution of xylem water pressure at different times of the day. Measurements were recorded along four time intervals as shown in the timeline in Figure 3.7 (the data acquisition system was connected to the HCTs only at these times). Measurements were taken at night before dawn (Figure 3.7c), after dawn before sunrise (Figure 3.7b), and during the day (Figure 3.7.a to Figure 3.7d). The measurements of the HCT were compared with sets of readings from the PC.

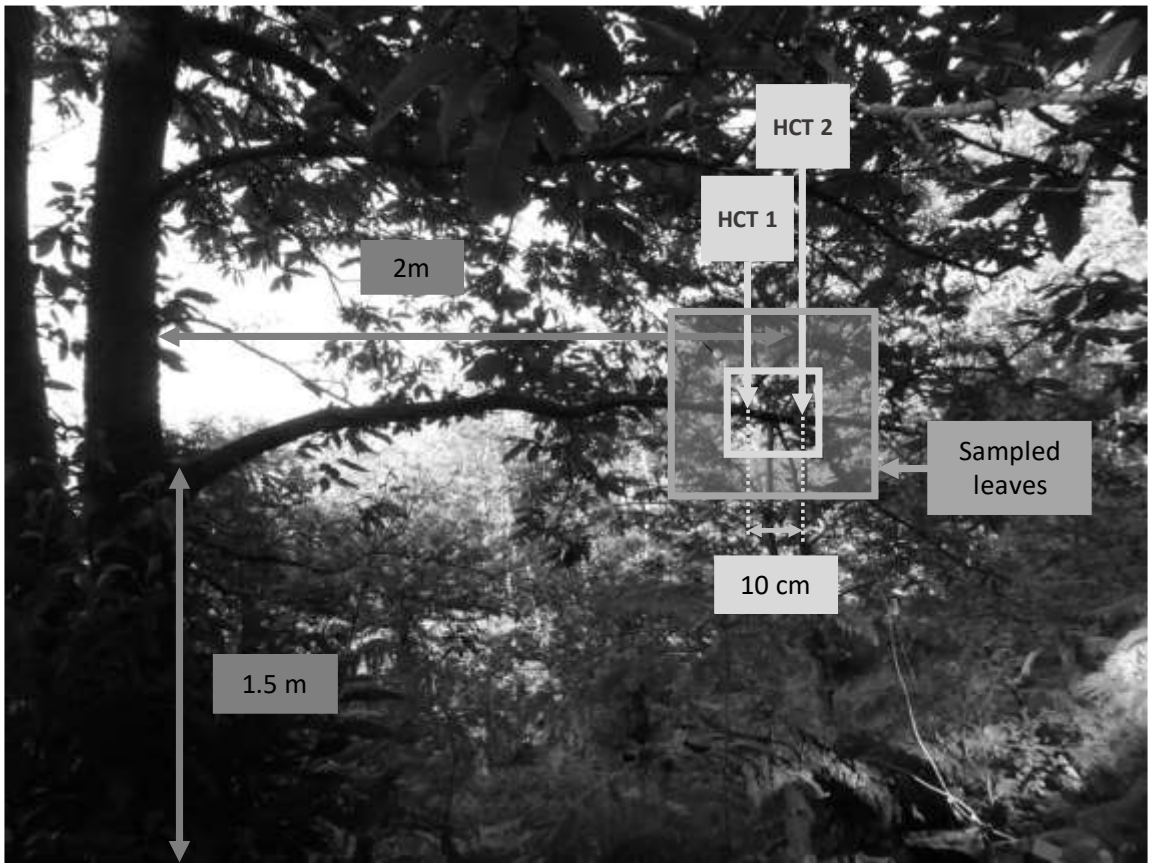

Figure 3.6: Location of the HCTs installed on chestnut tree measuring site and of the area where the set of leaves were sampled for PC measurements.

3.6.2. Results

Figure 3.7 shows the measurement of two HCTs together with the PC (the average of each set of leaves is indicated by a cross) . Figure 3.7a shows the initial installation of the HCTs. The initial decrease in pressure from 13:00 to 16:30 is associated with the process of hydraulic equilibration between the saturated paste and the branch xylem. During equilibration, the kaolin paste lost water in order to generate pore-water pressure in the paste until equilibrium was eventually reached with the xylem water pressure. The increase in pressure recorded by the HCTs after 16:30 is an indicator of the achieved hydraulic equilibrium between the water pressure in the xylem and in the paste and, hence, the HCT. The increase in xylem water pressure after 16:30 is associated with the decrease of solar radiation occurring in the afternoon. It is worth

noticing that the first measurement with the PC (Figure 3.7a) was taken when the hydraulic equilibrium between the branch and the instrument was not achieved yet.

Figure 3.7b shows the measurement at dawn, with an almost stable reading of approximately -200 kPa between 5:15 (start of the measurement) and 5:36 (sunrise). As soon as the sun rose, the xylem pressure started to decrease at a faster rate because of the exposure of the leaves to sunlight and the consequent stomata opening. The xylem water pressure stabilised at around -400 kPa between 8:00 and 13:30. The slight increase in xylem pressure between 9:30 and 11:00 was associated with clouds that partially shadowed the canopy. It is remarkable to note that the HCT can reveal fine adjustments of stromata aperture. In the presence of clouds, sunlight reduces and so does the CO_2 exchange. Stomata close partially and transpiration reduces with the xylem water pressure increasing accordingly. The PC measurements were taken at 5:40, before sunrise, and at 8:35 and 13:00 during the period where the xylem pressure adjusted to 'day' conditions.

Figure 3.7c shows the measurement starting at 4:30 (night-time before dawn). The pattern is similar to Figure 3.7b with the xylem water pressure decreasing significantly after sunrise. Figure 3.7d shows the last time interval including the post-measurement check. After removal from the branch and placement in free water the measurement recorded to the HCTs returned values close to 0 (-18kPa for HCT1 and -6 kPa for HCT2).

Overall, the two HCTs measured approximately the same xylem pressure. This was not surprising as the two HCTs were placed at a distance of only 10 cm on a branch segment with no twigs or secondary branches. The slight difference (~25 kPa) measured during daytime when transpiration was taking place is consistent with the direction of water flow that goes from the trunk towards the leaves (HCT1 closer to the trunk recorded higher water pressures than HCT2 closer to the leaves). During night-time, dawn, and after a short period after sunrise, the two HCTs recorded very

close values, which is again consistent with no or little transpiration taking place through the leaves over these periods.

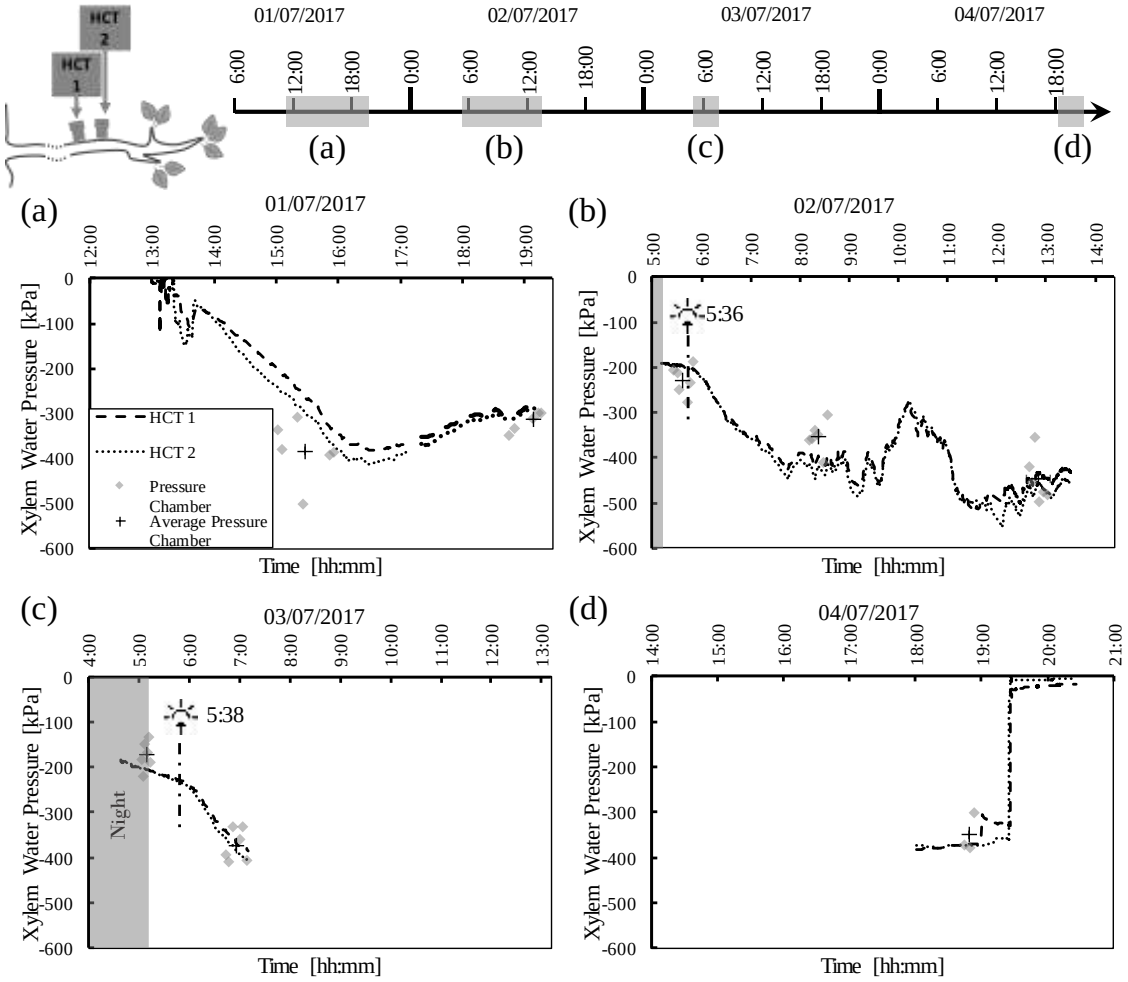

Figure 3.7: Measurements of xylem water pressure using HCT and leaf water pressure using PC on chestnut tree. Pressure chamber measurements are reported individually and average pressure chamber measurement is indicated by a cross.

3.6.3. HCT versus PC

Figure 3.8 shows the measurements from the PC plotted against the measurement of water pressure by the HCTs recorded at the time of PC measurement (the average of each set of leaves is indicated by a cross). The first measurement by the PC was excluded because it was taken when HCTs where not yet in equilibrium with the xylem water pressure. The measurements fairly align along a 1:1 line. The discrepancy between the HCT and PC measurements has a maximum value of ±0.06 MPa.. Figure

3.8 therefore appears to demonstrate the capability of the HCT to measure xylem water pressure.

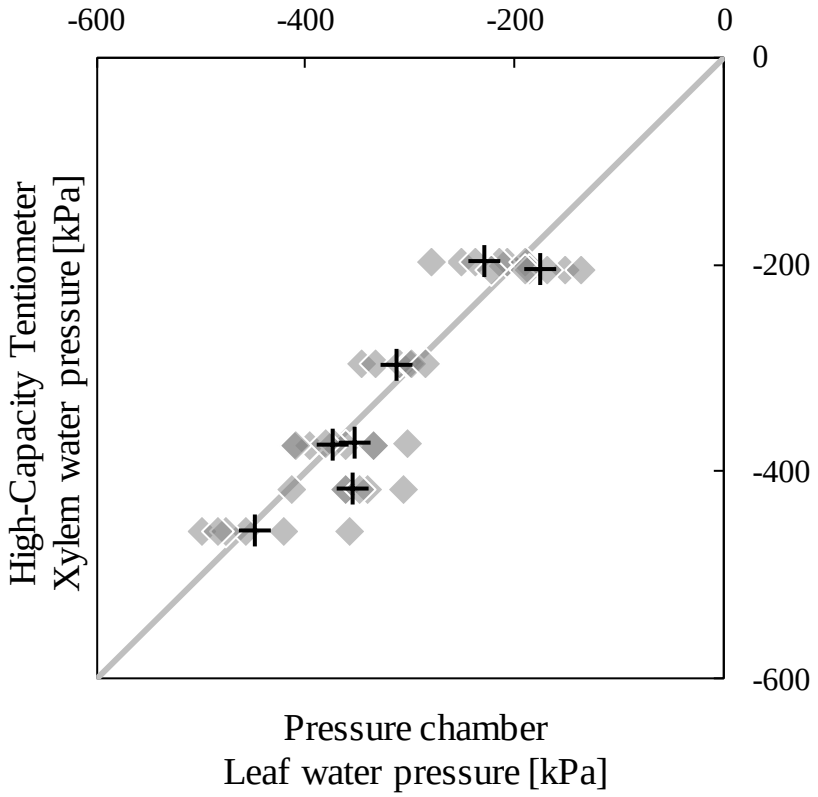

Figure 3.8: Comparison of PC and HCT measurements on Chestnut tree in the field. Pressure chamber measurements are reported against the average measurement of HCT and average pressure chamber measurement is indicated by a cross.

3.7.Laboratory tests

As shown in Figure 3.8, the comparison between HCT and PC was explored over a limited range of xylem water pressure, i.e. down to -500 kPa only. The laboratory experiments were aimed at widening the range of measurements by purposely creating drought conditions.

Experiments were carried out in a temperature-controlled room, a growth lamp to mimic solar radiation; transpiration was accelerated by exposing the tree to ventilation generated by a fan (Table 3.3). Each test started with the soil in fully saturated

conditions. A condition of drought was then let develop by preventing any watering of the soil for the whole duration of the test.

Table 3.3: 'Atmospheric' Boundary Conditions imposed in the laboratory test

Stage	BC2
First test: *Pear tree*	
Time interval (days)	0-7
Forced ventilation (fan)	Yes
Second test: Willow tree	
Time interval (days)	0-89
Forced ventilation (fan)	Yes
Daily cycle:	
Growth lamp (h)	14
Darkness (h)	10
Environmental conditions:	
Temperature (°C)	20°C
Relative humidity (%)	~45 %

3.7.1. Pear tree

3.7.1.1. Setup

Two HCTs were installed on the stem of a pear tree and the measurement of xylem water pressure was compared with the measurement of leaf water pressure using the PC. The leaves used for PC measurements were excised from branches above the HCTs (Figure 3.9). The elevation of the selected leaves with respect to the location of the HCTs was between 70 cm and 180 cm. Measurement of leaf water pressure was carried out using two different procedures. The first procedure is the ‘standard’ one described in the experimental procedures, where leaves are wrapped with aluminium foil for 10 min before measurements (these leaves are referred to as PC_10min). The

second procedure is associated with a different test run in parallel on the same setup, which is not discussed in this paper. The procedure consisted in wrapping the leaves with aluminium foil and Parafilm® for several days, unwrapping the leaf and let it exposed to air for few minutes, and then excising the leaf for the measurement with the PC (these leaves are referred to as PC_>1 day).

The experiment lasted for 8 days, with continuous monitoring of xylem water pressure by HCTs and discontinuous periodic monitoring of leaf water pressure using the PC. The tree was subjected to daily cycles of 14 hours of light and 10 hours of darkness.

Table 3.4:Location of HCTs and of leaves sampled for PC measurements in Pear tree experiment

Measurement	Distance	
HCT	h1	40 cm
	h2	50 cm
Leaves	h_{leaf}^{min}	120 cm
	h_{leaf}^{max}	190 cm

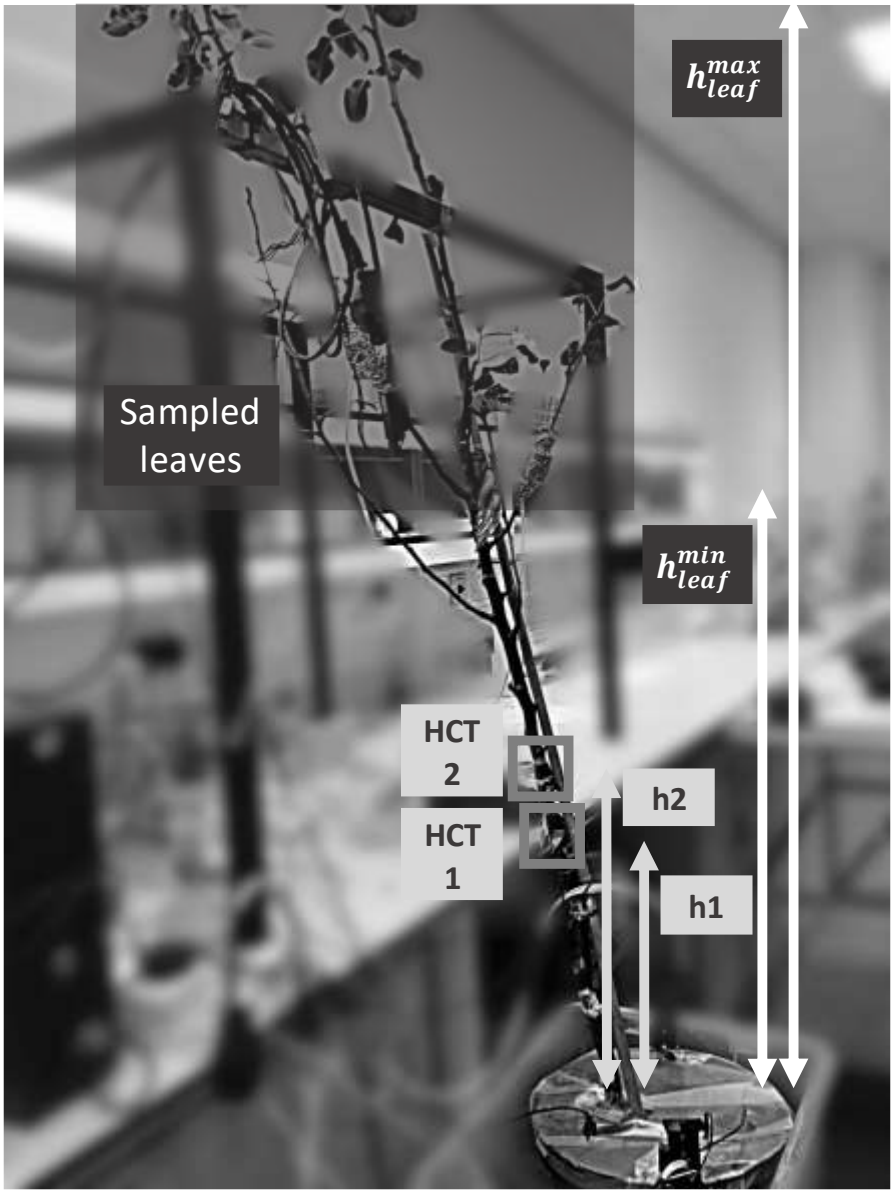

Figure 3.9: Pear tree setup and location of HCTs and leaves sampled for PC measurement

3.7.1.2. Results

Figure 3.10 shows the measurements of the HCTs installed on the stem and the measurement of leaf water pressure by the PC. The maximum pressure recorded by the HCT was ~-300 kPa while the minimum was ~-800 kPa.

The non-shadowed areas represent the daytime from 6AM to 8PM where solar radiation was mimicked using a growth lamp, whereas the shadowed areas in the graph

represent the ‘night time’ from 8PM to 6AM when the growth lamp was switched off. The daily cycles of xylem water pressure are consistent with the day/night cycles imposed by the growth lamp and consistent with similar experiments reported in the literature (Jones, 2006). When the lamp was switched on at 6AM, leaf stomata opened and the daily transpiration commenced. Accordingly, the xylem water pressure recorded by the HCTs started to decrease. At the beginning of the afternoon, the water pressure started increasing and kept increasing during night-time.

The values recorded by the two HCTs were very similar during night-time whereas a pressure differential established during daytime, coherently with experimental results from literature (Begg & Turner, 1970). The difference measured during daytime (~100 kPa) when transpiration was taking place is consistent with the direction of water flow that goes from the trunk towards the leaves (HCT1 closer to the soil recorded higher water pressures than HCT2 closer to the leaves). During night-time there was no or little transpiration and the xylem water pressure measured by the two HCTs reflects the hydrostatic conditions establishing in the stem.

The measurements of xylem water pressure using the PC on non-transpiring leaves were consistent regardless of the wrapping procedure used, 10min or >1day wrapping time respectively. The measurement on the leaf, which is assumed to coincide with the xylem pressure in the branch at the base of the excised petiole, was lower than the xylem pressure recorded by the HCTs. Again, the PC values are consistent with the direction of flow that goes from the soil towards the leaves during ‘daytime’.

The relatively high standard deviation of PC measurement on 26 January is likely due to leaves sampled from two different branches. PC measurements were similar for leaves excised from the same branch but different from one branch to another. This may not be surprising if one considers the variability of xylem conductivity that may exist between different branches. In any case, the leaf water pressure measured by the PC was significantly greater the water pressure measured on the stem by the HCTs.

The xylem pressure measured by the two HCTs and the PC showed significant hydraulic gradients during daytime. This is likely due to a low xylem hydraulic conductance of the pear tree, which results in high hydraulic gradients that need to be established along the stem to accommodate the daily transpiration rate. As result, HCT measurements could not be validated by comparison with PC measurements.

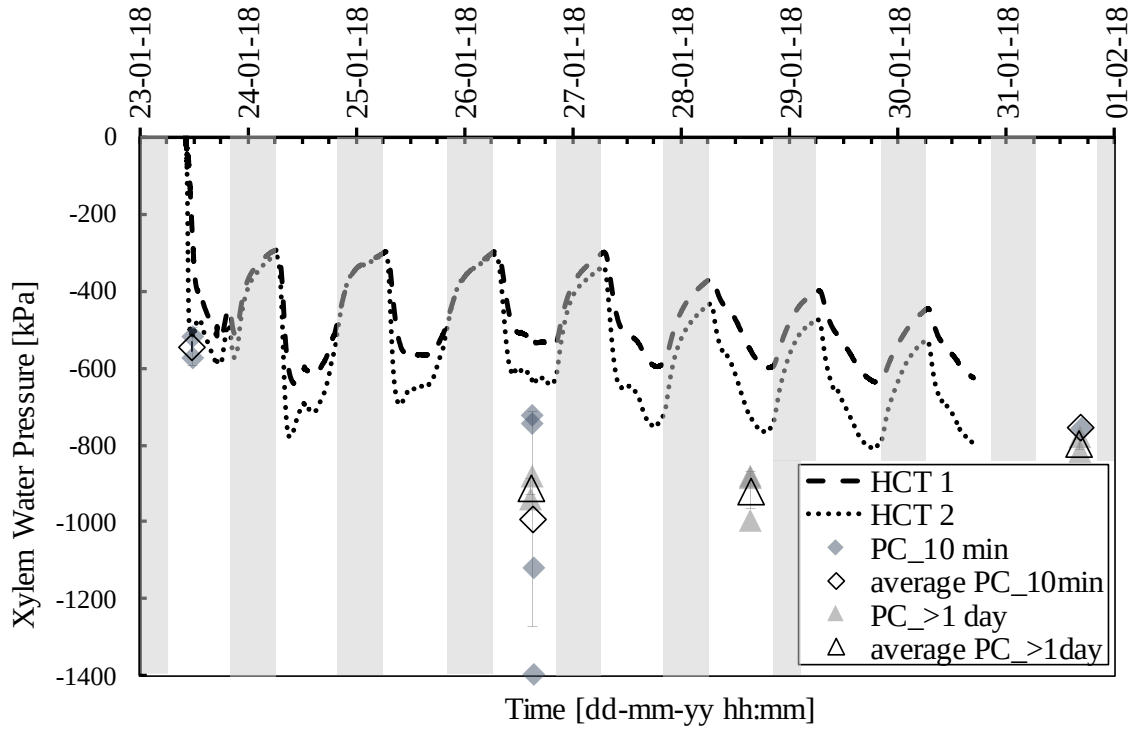

Figure 3.10: HCT and PC measurements on Pear tree (shadowed areas represent the 'night time' when the growth lamp is switched off). Pressure chamber measurements are reported individually and average pressure chamber measurement is indicated by void symbols.

3.7.2. Willow Tree

3.7.2.1. Setup

A small shrub of willow tree was transplanted into a pot silty sand. The plant was let grow in the new container before starting the test. Two HCTs were installed on the stem and periodical readings of leaf water pressure were taken using the PC (the position of the instruments is shown in Figure 3.11). Day/night cycles were controlled by a growth lamp and forced ventilation was imposed using a fan. The system started

with the soil in fully saturated conditions and was let dry out avoiding any irrigation during the whole duration of the test.

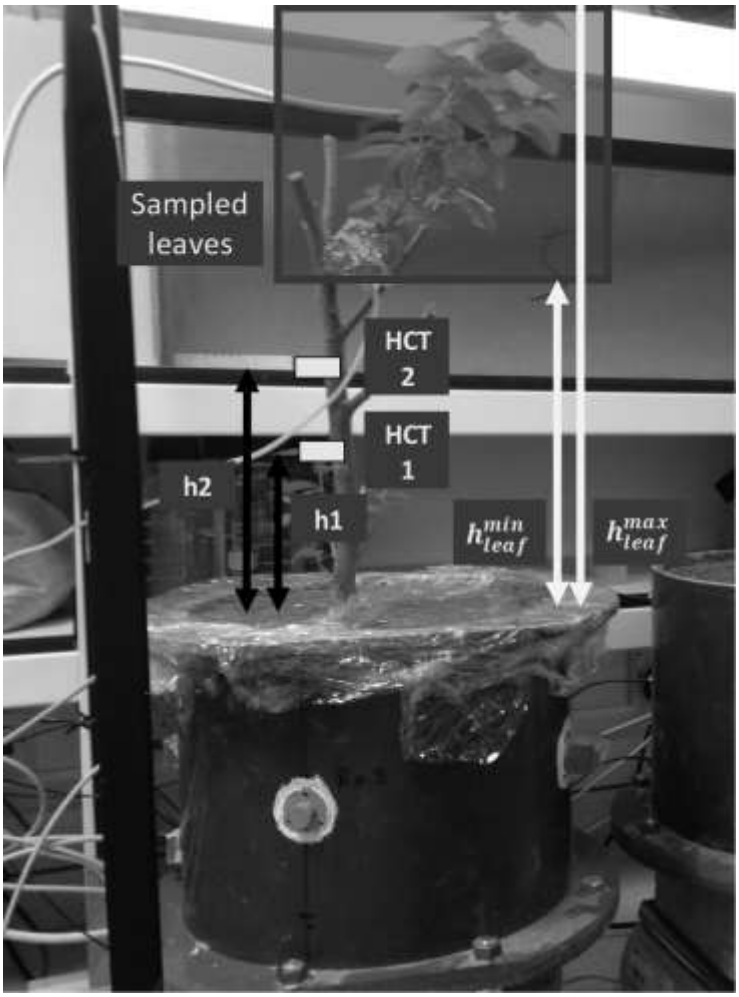

Figure 3.11: Willow tree setup and location of HCTs and leaves sampled for PC measurement.

Table 3.5:Location of HCTs and of leaves sampled for PC measurements in Willow tree experiment

Measurement	Distance	
HCT	h1	12 cm
	h2	25 cm
Leaves	h_{leaf}^{min}	35 cm
	h_{leaf}^{max}	150 cm

3.7.2.2. Results

Figure 3.12 shows the water pressure recorded by HCTs installed on stem and by the PC on the leaves. The measurement lasted over two and a half months and high transpiration rate caused by the fan allowed generating relatively high xylem water pressure in the tree.

The HCT readings show daily cycles similar to the ones observed in the pear tree. The two HCTs fluctuate in phase and read almost the same value of negative water pressure with discrepancies generally lower than 10kPa. In the period from 04/06/2018 to 18/06/2018, differences in HCT reading are higher, reaching 40 kPa during daytime. The lower tensiometer (HCT1) records lower xylem water pressure than the upper tensiometer (HCT2). This would indicate a downward flux which does not make physical sense. A possible explanation is the change of computer connected via a USB port to the data acquisition/DC power supply unit. The change of computer might have changed the power supply to the unit and, hence, to the individual tensiometers, causing a slight change in offset of the instrument

The variation of the HCT readings over a period of a week is shown in Figure 3.13. The pattern is similar to the one observed in the Pear tree. Xylem water pressure decreased during daytime and increases again as night-time was approaching. The HCT readings are very close, suggesting a relatively high hydraulic conductance of the xylem. One would therefore expect small gradients in xylem water pressure through the plant, from the stem up to the branches and leaves. Measurements of xylem water pressure at the base of the leaf petiole using the PC are indeed close to the measurements of xylem water pressure on the stem using the HCTs. As a result, HCT and PC measurements can be compared.

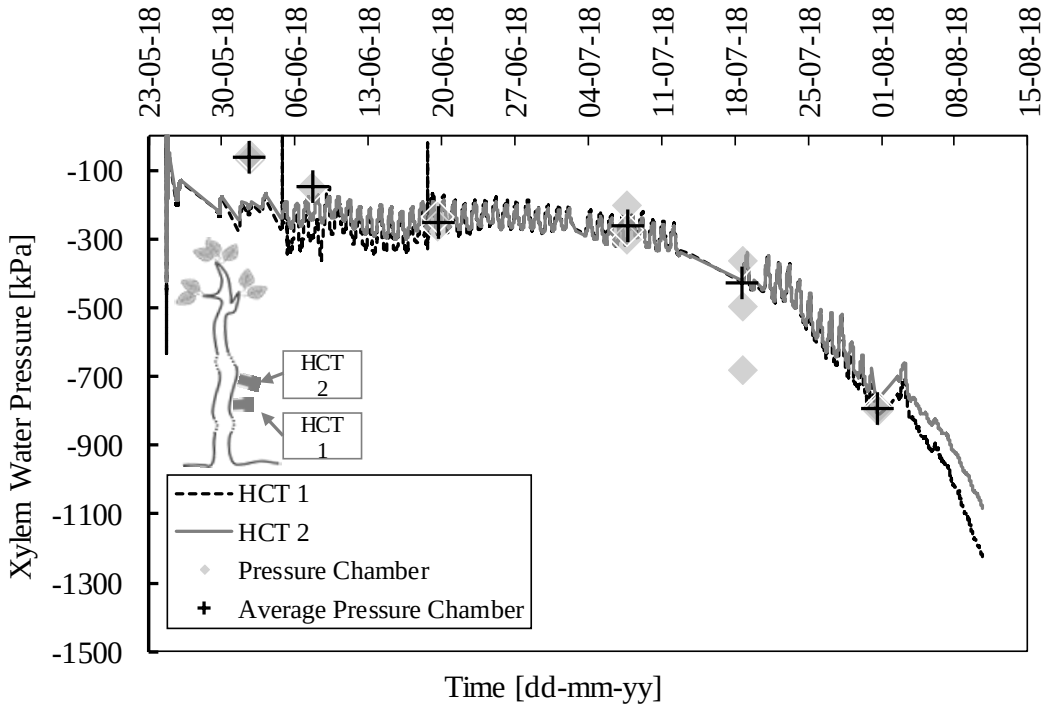

Figure 3.12: HCT and PC measurements on Willow tree. Pressure chamber measurements are reported individually and average pressure chamber measurement is indicated by a cross.

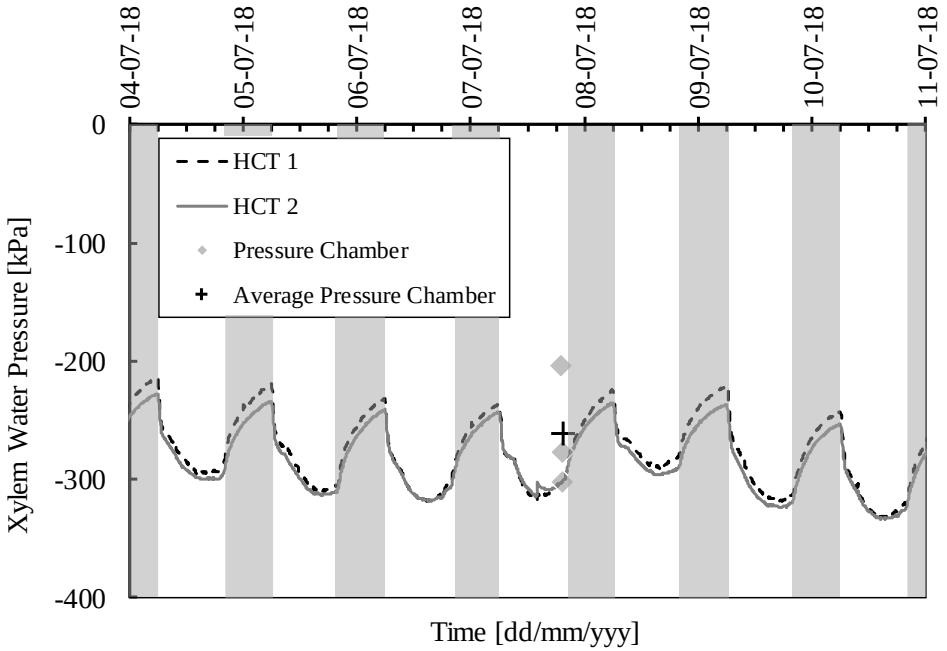

Figure 3.13: Zoom of HCT and PC measurements on Willow tree (shadowed areas represent the 'night time' when the growth lamp is switched off)

3.7.2.3. HCT versus PC

The xylem water pressure measured by the HCT is plotted against the xylem water pressure measured by the PC in Figure 3.14. The data points are aligned along the 1:1 line with the only exception of the data point at the lowest value of suction, where the PC measurement tends to overestimate the value recorded by the HCTs. The reason is not clear and may be associated with the reaction of the plant to the extremely wet conditions (stomata may tend to close under very wet conditions) and/or to local variability of xylem water pressure.

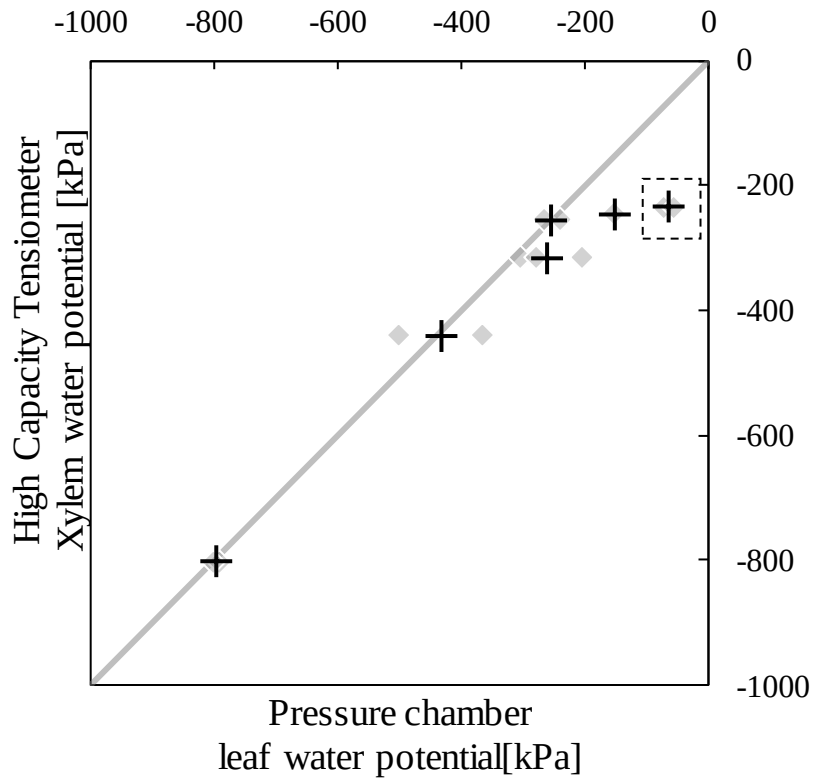

Figure 3.14: Comparison of PC and HCT measurements on Willow tree in the laboratory. Pressure chamber measurements are reported against the average measurement of HCT and average pressure chamber measurement is indicated by a cross.

3.8. The use of High-Capacity Tensiometers to inform the transpiration reduction function

The measurement of the xylem water pressure via the High-Capacity Tensiometers in conjunction with the measurement of pore-water pressure in the soil can be potentially used to model the Feddes reduction function and, in particular, the parameters u_{w3} and u_{w4} (Figure 3.1). In turn, this can be used to represent transpiration as hydraulic boundary conditions in geotechnical models where interaction with the atmosphere is taken into account.

The test on the willow tree presented in the previous sections included, in addition to the monitoring of the xylem water pressure in the tree, the monitoring of the pore-water pressure in the soil and the transpiration rate. The willow was initially transplanted into a column holding a silty sand sample 295 mm diameter and 230 mm height and let grow into it for 2 months. Afterwards, the tree was subjected to a condition of induced drought (no irrigation) and the evolution of the water pressure in the xylem was monitored continuously for more than 2 months. Additional HCTs were applied to the sides of the column at different depths (40 mm, 125 mm, 210 mm from the top of the column) to monitor the evolution of the negative pore-water pressure in the soil. The whole system was placed on a balance to monitor the water loss over time and hence the transpiration rate (Figure 3.15). The soil surface was covered with a plastic film, to prevent evaporation from the bare soil and allow the sole transpiration from the leaves. A growth lamp was used to simulate diurnal (6:00 am-8:00 pm) and nocturnal (8:00 pm-6:00 am) cycles. The experimental setup and the full dataset are presented in detail Chapter 5.

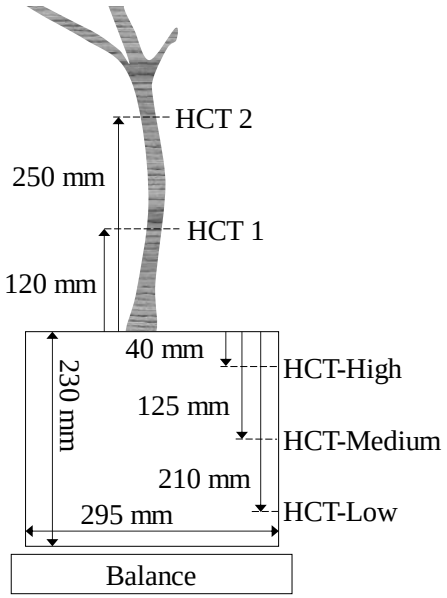

Figure 3.15: Experimental setup to investigate the transpiration reduction function.

The water pressure in the soil and the tree is reported in Figure 3.16. The solid symbols on the curves mark the water pressure at 6am, when the water pressure in the xylem

reaches its daily maximum, at least in the period 0-40 days. The pressure at 6am can considered a pre-dawn value as the growth lamp used to mimic solar light was off overnight. The difference between the (average) water pressure in the xylem and the water pressure measured by the three HCTs in the soil, all recorded at 6am, is plotted in Figure 3.16.b. Figure 3.16.c shows the transpiration rate over time derived from the water loss measured by the balance. The reference area is the total leaf surface before the beginning of the test, in date 04/06/2018, equal to approximately 680 cm2.

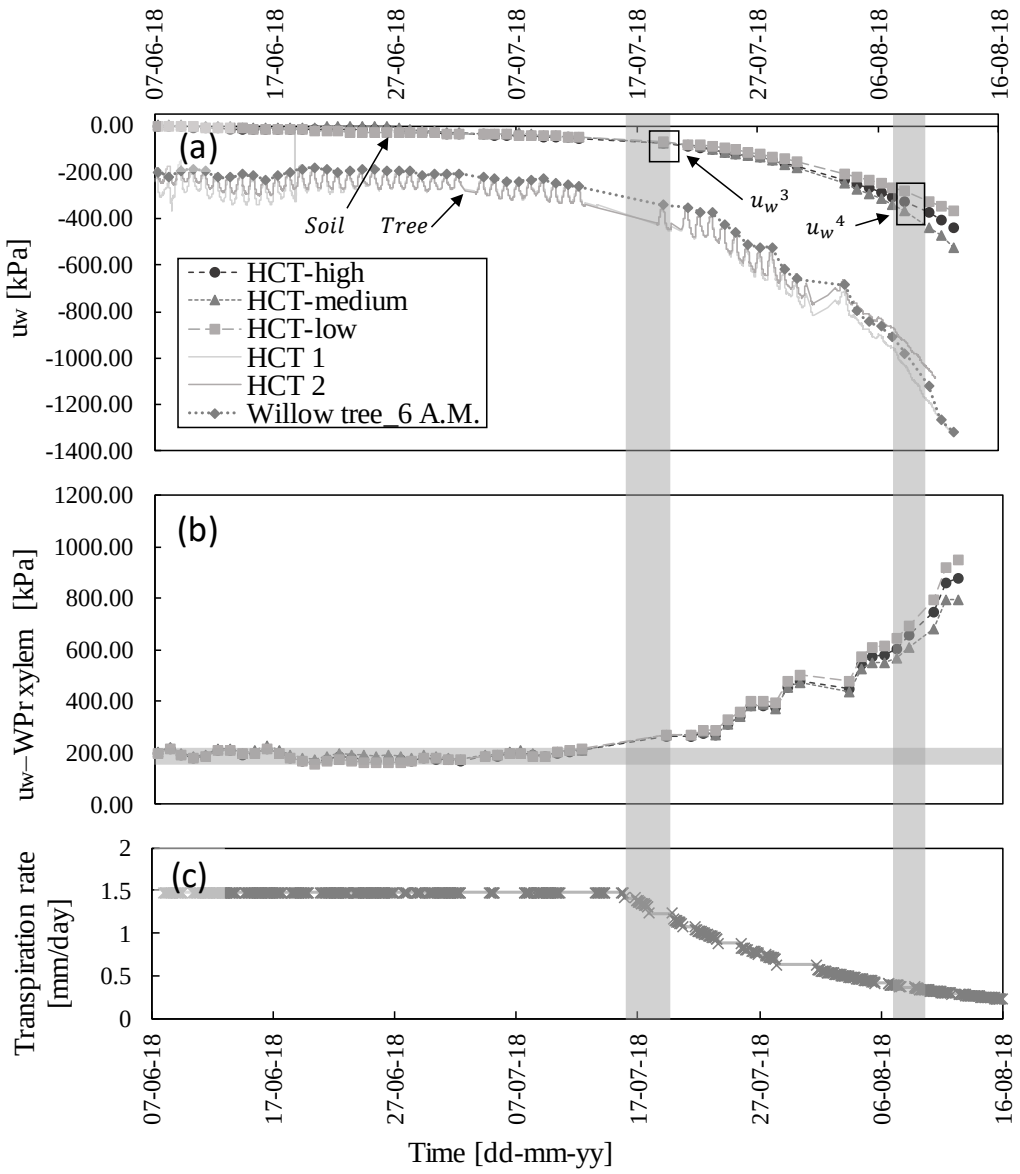

Figure 3.16: (a) Water pressure in soil and tree xylem under induced drought conditions. (b) Difference between the water pressure in the soil at 3 different depths and the average water pressure measured by two HCTs on the xylem. (c) transpiration rate.

Three stages can be identified. In the first stage (days 0 to 38 days, from 07/06/18 to 15/07/18), the pressure differential between the xylem and the soil remains essentially constant. This is associated with a transpiration rate that also remains fairly constant at its maximum value. At the same time, xylem water pressure shows daily fluctuations, associated with the growth lamp that is switched on during the day and switched off at night. In this stage, the leaves are actively transpiring, the maximum

(potential) transpiration is accommodated by the same pressure differential over the 38 days indicating that the hydraulic conductivity of the soil remains relatively high. The constant pressure differential between soil and xylem can therefore be taken as an indicator of the energy-limited (potential) regime for the case where the direct measurement of transpiration rate is not available, as is often the case in the field.

In the second stage (days 38 to 62, from 15/07/18 to 08/08/18), the water pressure differential between soil and xylem significantly increases while the transpiration rate starts to decay. This is associated with the more rapid decrease in soil pore-water pressure in turn associated with the soil degree of saturation approaching its residual state. As the degree of saturation decreases, the soil hydraulic conductivity reduces and the plant increases the pressure differential in the attempt to sustain (unsuccessfully) the maximum transpiration. At this stage, daily fluctuations in xylem water pressure are noticeable indicating that transpiration is still active. As a conclusion, the increase in the pressure differential can be taken as an indicator of the transition from the energy-limited to the water-limited regime if direct measurement of transpiration rate is not available.

In the last stage (days 62 to 70, from 08/08/18 to 16/08/18), the daily fluctuations disappear while the pressure differential keeps increasing and the transpiration rate decreases to very low values, almost reaching a plateau of residual transpiration. A zoom of this last stage is shown in Figure 3.17. Between 03/08/18 and 08/08/18 (starting from the vertical dotted line), daily cycles in the xylem water pressure are still visible although the xylem pressure increases only slightly overnight. After 08/08/18 (highlighted by the vertical grey band), daily fluctuations are not detectable indicating that leaves are no longer transpiring. This can be interpreted as an indicator of the attainment of wilting conditions.

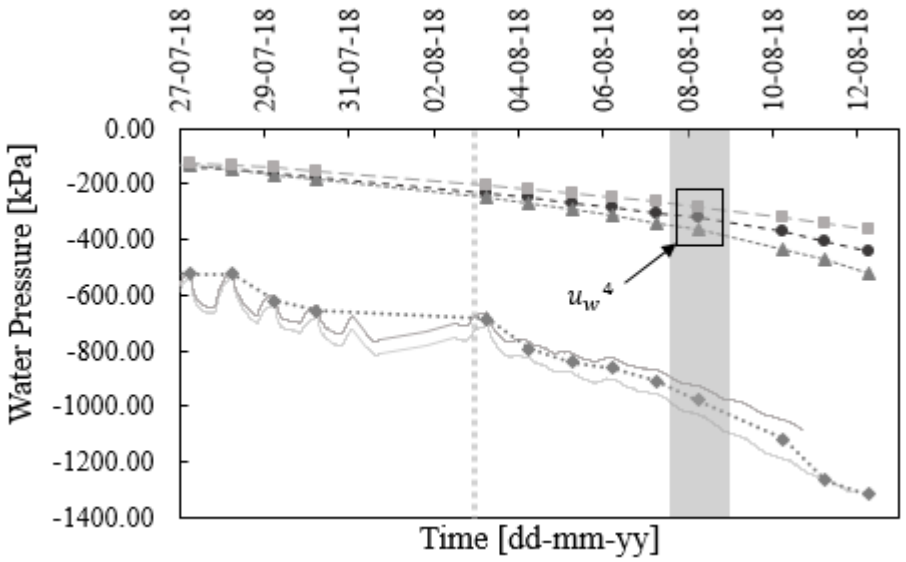

Figure 3.17: Evolution of water pressure in soil and xylem under plant stress conditions (from 27/07/18 to 13/08/18).

The results presented in Figure 3.16 and Figure 3.17 suggest an approach to derive the two critical parameters of the Feddes reduction function, i.e. the parameters $\underline{u}_{w3}$ and $u_{w4,}$ via the measurement water pressure in the xylem and the soil.

The soil pore-water pressure in the period 15/07/18 to 18/07/18 (first grey band in Figure 3.16) is associated with the transition from the energy-limited to the water-limited regime and therefore matches the parameter $\underline{u}_{w3}$ ($\underline{u}_{w3}$=-50 to -75 kPa). The soil pore water pressure in the period 08/08/18 to 09/08/18 when fluctuations disappear and transpiration rate reduces by ~75% (second grey band in Figure 3.16) can be tentatively assumed to represent u_{w4} (u_{w4}=-280 to -370 kPa). In order to evaluate the reliability of such an assumption, the reduction function derived experimentally, based on the measured values of transpiration rate and soil pore-water pressure, is compared with the Feddes function based on the average values of u_{w3} and u_{w4} inferred from HCT measurements (Table 3.6). The HCT-derived Feddes parameters approximate quite satisfactorily the experimental data. Figure 3.17.a also shows the Feddes function based on the parameters commonly adopted in geotechnical applications (u_{w3}=-100 kPa, u_{w4}=-1500 kPa (Briggs, 2016; Nyambayo & Potts, 2010). The discrepancy with the experimental data is remarkable, which highlights the relevance of the

experimental determination of the Feddes parameters via the simultaneous HCT measurement of soil and xylem water pressure.

The results presented in Figure 3.18.a are recast in terms of transpiration rate in Figure 3.18.b, where the experimentally determined transpiration rate is compared with the transpiration rate one would predict using the parameters suggested by Feddes et al.(1978) and the HCT experimentally-derived parameters. Again the traditionally-adopted Feddes parameters significantly overestimate the transpiration rate whereas the transpiration rate based on the parameters derived from HCT measurements shows a much better approximation of the experimental data.

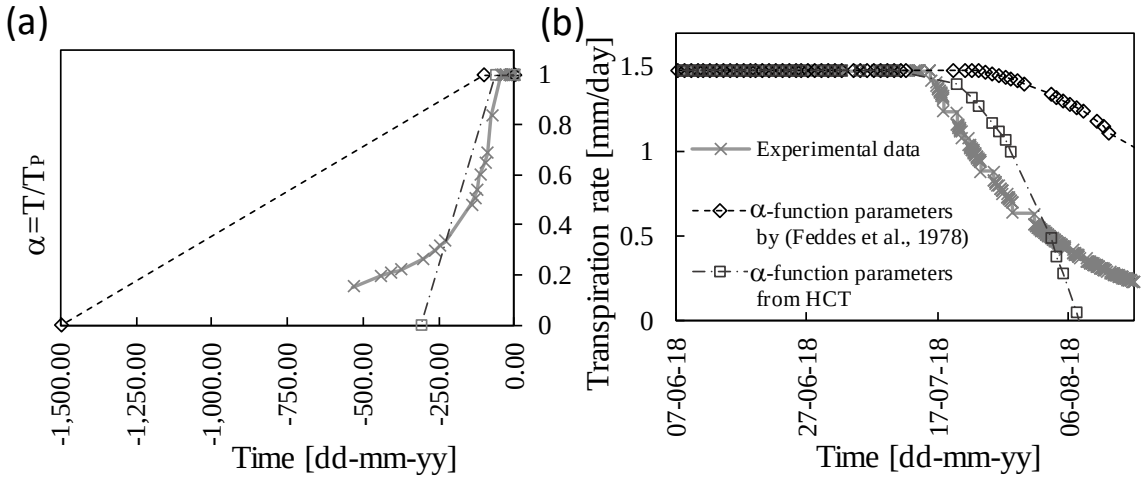

Figure 3.18: Reduction factor and transpiration rate from experimental data, estimated using the parameters proposed by Feddes et al. (1978), and estimated using the parameters derived from HCT measurements in plant and soil. (a) Reduction factor (b) Transpiration.

Table 3.6: Feddes function parameters used in geotechnical applications and estimated using the HCT measurements in plant and soil

Measurement	Feddes reduction function parameters			
	Typically adopted in geotechnical applications	Experimentally derived from HCT measurement		
		Lower limit	Upper limit	Average
u_{w3}	−100 kPa	−75 kPa	−50 kPa	−62.5 kPa

u_{w4}	-1500 kPa	-340 kPa	-285 kPa	-312.5 kPa

3.9. Conclusions

The paper has demonstrated for the first time the use of High-Capacity Tensiometer (HCT) for measuring xylem water pressure in plants. HCTs were installed on branch of a Chestnut in the field and on the trunk of a Pear tree and a Willow tree in the laboratory. The HCT measurement was compared to the measurement of xylem water pressure at the base of leaf petioles using the Pressure Chamber (PC) for validation.

The HCTs were placed at closer distance (~10cm) on the branch or stem and their measurement always showed to be very consistent. In the field, xylem water pressure was stable overnight, decreased during daytime when transpiration was taking place, and tended to increase again at the end of the afternoon when transpiration slows down and eventually stops overnight. Overall, the measurements of the two HCTs on the Chestnut branch remained very close over the entire period of measurement. When HCT measurements were plotted against PC measurements, data points fairly aligned on a 1:1 line. This was taken as a validation of the HCT against the well-established PC technique.

In the laboratory, day and night cycles were simulated by switching on and off a growth lamp. Similar pattern in day/night cycles were observed as in the field. The xylem pressure differential between the two HCTs was significant in the Pear tree during daytime when transpiration was taking place (whereas the xylem pressure differential was nil over night when transpiration was not occurring and hydrostatic conditions established in the plant). This diurnal xylem pressure differential was probably associated with a relatively low xylem hydraulic conductance, which resulted in relatively high xylem pressure gradients to be generated in the plant to accommodate the diurnal transpiration rate. The significant gradients in xylem pressure through the plant were confirmed by the measurements of xylem water pressure at the base of leaf petioles using the Pressure Chamber, which were much lower than the ones measured

on the stem using the HCTs. As a result of these significant xylem water pressure gradients, the measurement by the HCT could not be validated by comparison with the measurement by the PC for the case of the Pear tree.

On the contrary, xylem water pressure gradients in the Willow tree were very small and this made it possible to compare HCT and PC measurements. Again, when HCT measurements were plotted against PC measurements, data points fairly aligned on a 1:1 line further validating HCT against the PC technique.

The HCT therefore proved to be a viable and convenient instrument for xylem water pressure measurement. Further studies will be necessary to investigate the response of the instrument for different species and environmental conditions, and to compare the use of HCTs to other techniques for continuous non-destructive measurement of xylem water potential on the stem (i.e. thermocouple psychrometer).

The use of HCT on plants is a step change in the understanding and modelling the effect of plant transpiration on suction and moisture regime in a vegetated ground. HTCs have been used for more than 20 years in geotechnical engineering and this instrument is available in many research laboratories. Installing HCTs on stems and branches is quite straightforward and this will allow analysing the soil and the plant as a continuum in the same experimental setup rather than borrowing transpiration models developed by plant scientists for their specific applications.

A straightforward geotechnical application of the xylem water pressure measurement is the derivation of the parameters characterising the reduction function used to model transpiration as hydraulic boundary condition. The interpretation of the simultaneous measurement of water pressure in the soil and xylem allowed for an experimental determination the Feddes reduction function parameters, at least for the laboratory test presented in the paper. Further studies are required to validate the HCT-based experimental method suggested here. However, this preliminary study shows the relevance of the experimental determination of the reduction function parameters

compared to the approach based on borrowing values from the agricultural literature, which can lead to misleading prediction of the transpiration rate.

Acknowledgement
The authors wish to acknowledge the support of the European Commission via the Marie Skłodowska-Curie Innovative Training Networks (ITN-ETN) project TERRE 'Training Engineers and Researchers to Rethink geotechnical Engineering for a low carbon future' (H2020-MSCA-ITN-2015-675762).

References

Anon., n.d. *https://www.pmsinstrument.co.* [Online].

Balling, A. and Zimmermann, U., 1990. Comparative measurements of xylem pressure of Nicotiana plants by means of the pressure bomb ad pressure probe. Planta, pp. 325-338.

Begg, J. & Turner, N., 1970. Water potential gradients in field tobacco. *Plant Physiology*, Volume 46, pp. 343-346.

Boyer, J. S., 1967. Leaf water potentials measured with a pressure chamber. Plant Physiology.

Boyer, J. S., 1995. *Measuring the Water status of Plants and Soils.* s.l.:Academic Press.

Briggs K.M., Smethurst J.A., Powrie W., O'Brien A.S. (2016). The influence of tree root water uptake on the long term hydrology of a clay fill railway embankment. Transportation Geotechnics 9: 31–48

Brown, P. and Tanner, C., 1981. Alfalfa water potential measurement: a comparison of pressure chamber and leaf dew-point hygrometers. Crop Science, pp. 240-244.

Bulut, R. and Leong, E., 2008. Indirect measurement of suction. In: *Laboratory and field testing of unsaturated soils.* s.l.:Springer, pp. 21-32.

Campbell, G. and Gardner, W., 1971. Psychrometric measurement of soil water potential: temperature and bulk density effect. Soil Science Society of America Journal, pp. 8-12.

Canny, 1977. *Flow and Transport in Plants.* s.l.:s.n.

Deloire, A. and Heyns, D., 2011. The leaf water potentials: principles, method and thresholds. Wynboer, pp. 119-121.

Salisbury, F.B. and C. R., 1992. *Plant Physiology.* s.l.:Wadsworth.

Feddes, R., 1971. Water, heat and crop growth. Wageningen: H.Veenman & Zonen N.V.

Feddes, R.A., Kowalik, P., Kolinska-Malinka, K., et al., 1976. Simulation of field water uptake by plants using a soil water dependent root extraction function. Journal of Hydrology, 31 (12), 13-26.

Feddes, R.A., Kowalik, P.J. and Zaradny, H., 1978. *Simulation of field water use and crop yield*. Pudoc, Wageningen. Simulation Monographs

Feddes, R., 1982. Simulation of field water use and crop yield. In: Simulation of Plant growth and crop production. Wageningen: Pudoc, pp. 194-209.

Garg, A., A. K. Leung, and C. W. W. Ng. 2015. Transpiration Reduction and Root Distribution Functions for a Non-Crop Species Schefflera Heptaphylla. Catena 135: 78–82.

Gollan, T., Turner, N. & Schulze, E.-D., 1985. The responses of stomata and leaf gas exchange to vapour pressure deficits and soil water content. III. In the sclerophyllous woody species Nerium oleander. Oecologia, Volume 65, pp. 356-362.

Goode, J. and Higgs, K., 1973. Water, osmotic and pressure potential relationships in apple leaves. Journal of Horticultural Science, pp. 203-215.

Greco R, Comegna L, Damiano E, Guida A, Olivares L, and Picarelli L (2013). Hydrological modelling of a slope covered with shallow pyroclastic deposits from field monitoring data. Hydrol. Earth Syst. Sci., 17, 4001–4013. DOI: 10.5194/hess-17-4001-2013

Hemmati, S., Gatmiri, B., Y.-J., C. & Vincent, M., 2010. Soil-vegetation-atmosphere interaction by a multiphysics approach. Journal of multiscale modelling, Volume 2, pp. 163-184.

Hillel, D., 1980. *Fundamentals of soil physics*. Academic press.

Husken, D., Steudle, E. & Zimmermann, U., 1978. Pressure probe technique for measuring water relations of cells in higher plants. Plant physiology, Volume 61, pp. 158-163.

Indraratna B, Fatahi B, Khabbaz H. (2006). Numerical analysis of matric suction effects of tree roots. *Proceedings of the institution of civil engineers –geotechnical engineering*,159:77–90.

Jones, H., 2006. Monitoring Plant and Soil water status: established and novel methods revisited and their relevance to studies of drought tolerance. Journal of Experimental Botany.

Kocher, P., Gebauer, T., Horna, V. & Leuschner, C., 2009. Leaf water status and stem xylem flux in reltion to soil drought in five temperate broad-leaved tree species with contrasting water use strategies. Annals of forest science.

Lang, A. & Barrs, H., 1965. An apparatus for measuring water potential in the xylem of intact plants. Australian Journal of biological sciences, Volume 18, pp. 487-497.

Lu, P., Biron, P., Breda, N. & Granier, A., 1995. Water relations of adult Norway spruce (Picea abies (L) Karst) under soil drought in the Vosges mountains: water potential, stomatal conductance and transpiration. Annales Des Sciences Forestieres, Volume 52, pp. 117-129.

Marinho, F.A.M., Take, W.A. and Tarantino, A., 2008. Measurement of matric suction using tensiometric and axis translation techniques. In *Laboratory and field testing of unsaturated soils* (pp. 3-19). Springer, Dordrecht.

Martinez, E., Cancela, J., Cuesta, T. and Neira, X., 2011. Review. Use of Psychrometers in field measurements of plant material: accuracy and handling difficulties. Spanish Journal of Agricultural Research, pp. 313-328.

Meron, M., Grimes, D., Phene, C. and Davis, K., 1985. Pressure chamber procedures for leaf water potential measurements in cotton. Irrigation Science, pp. 215-222.

Nyambayo, V. & Potts, D., 2010. Numerical simulation of evapotranspiration using a root water uptake model. Computers and geotechnics, Volume 37, pp. 175-186.

Pagano l, Reder A, and Rianna G (2018). Effects of vegetation on hydrological response of silty volcanic covers. Can. Geotech. J., DOI: 10.1139/cgj-2017-0625.

Patakas, A., Noitsakis, B. and Chouzouri, A., 2005. Optimization of irrigation water use in grapewines using the relationship between transpiration and plant water status. Agricolture, Ecosystems and Environment, pp. 253-259.

Philip, J., 1966. Plant water relations: some physical aspects. *Annual Review in Plant Physiology*, pp. 245-268.

Pickard, W., 1981. The ascent of sap in plants. Progress in biophysics and molecular biology, Volume 37, pp. 181-229.

Richter, H., 1973. Frictional potential losses and total water potential in plants: a re-evaluation. Journal in experimenatl bothany, Volume 24, pp. 983-994.

Ridley, B., 1993. A new instrument for the measurement of soil moisture. *Geotechnique,* pp. 321-324.

Rodrigues Afonso Dias, A., 2019. *The effect of vegetation on slope stability of shallow pyrooclastic soil covers.* Naples: s.n.

Scholander, P., Hammel, H. and Breadstreet, E. H. E., 1965. Sap pressure in vascular plants: negative hydrostatic pressure can be measured in plants.. Science, pp. 339-346.

Sinha, R., 2004. *Modern Plant Physiology.* s.l.:CRC Press.

Take, W. and Bolton, M., 2003. Tensiometer saturation and the reliable measurement of soil suction. Geotechnique, pp. 159-172.

Tarantino, A., 2004. *Panel lecture: direct measurement of soil water tension.* Recife, Brasil, s.n., pp. 1005-1017.

Tarantino, A. and Mongiovi', L., 2001. Experimental procedures and cavitation mechanisms in tensiometer measurements. In: *Unsaturated Soil Concepts and Their Application in Geotechnical Practice.* s.l.:Springer, pp. 189-210.

Tarantino, A. and Mongiovi', L., 2002. Design and construction of a tensiometer for direct measurement of matric suction. s.l., Recife, pp. 319-324.

Tarantino, A. and Mongiovi, L., 2003. Calibration of tensiometer for direct measurement of matric suction. Géotechnique, *53*(1).

Tsiampousi A, Zdravkovic L, and Potts D.M. (2017). Numerical study of the effect of soil–atmosphere interaction on the stability and serviceability of cut slopes in London clay. Can. Geotech. J. 54: 405–418. DOI: 10.1139/cgj-2016-0319

Turner, N., Spurway, R. and Schulze, E.-D., 1983. Comparison of water potentials measured by in Situ psychrometry and pressure chamber in morphologically different species. Plant Physiology, pp. 316-319.

Utset, A., Ruiz, M. E., Garcia, J., Feddes, R. A., 2000. A SWACROP-based potato root water uptake function as determined under tropical conditions. Potato research, 43(1), 19-29.

Wei, C., Steudle, E., Tyree, M. and Lintilhac, P., 2001. The essentials of direct xylem pressure measurement. Plant, cell and environment, pp. 459-555.

Wesseling, J.G., 1991. Meerjarige simulatie van grondwaterstroming voor verschillende bodemprofielen, grondwatertrappen en gewassen met het model SWATRE. DLO-Staring Centrum, Wageningen. Rapport / DLO-Staring Centrum no. 152.

Zhu H and Zhang L (2019): Root-soil-water hydrological interaction and its impact on slope stability, Georisk: Assessment and Management of Risk for Engineered Systems and Geohazards, DOI: 10.1080/17499518.2019.16160

Chapter 4 High-Capacity Tensiometer as a novel technique for continuous monitoring of xylem water pressure: cross-validation with Thermocouple Psychrometer

Abstract

Continuous non-destructive monitoring of xylem water pressure can currently be achieved only via the thermocouple psychrometer. The pressure chamber, which is generally considered as a reference for the of xylem 'matric' water pressure measurement, is a discontinuous and destructive technique and therefore not suitable for prolonged and automated monitoring. This paper presents a novel application of the High-Capacity Tensiometer (HCT), an instrument developed in geotechnical engineering to measure soil water matric potential, for the continuous non-destructive measurement of 'matric' xylem water pressure in the range from 0 to -2 MPa. The potential advantage of the HCT against the thermocouple psychrometer is that its measurement is not affected by the presence of solutes in the xylem water ('osmotic' component of xylem water potential) and its working principle makes it significantly less sensitive to temperature effects. In addition, the HCT can be used to measure the (negative) pore-water pressure in the soil, making it a very convenient instrument to monitor water flow in the soil-plant continuum. In this laboratory study, HCTs were installed on the stem of two trees and HCT measurement of xylem water pressure was compared to measurements via the thermocouple psycrometer (and some discontinuous pressure chamber measurements). The trees were subjected to day/night cycles and were tested under both well irrigated and drought conditions. The HCTs were installed in pairs to detect any faulty response associated with ongoing heterogeneous cavitation. The HCT and the thermocouple psychrometer showed excellent agreement for xylem water pressures <-700 kPa. Their response to night/ and day cycles was remarkably in phase indicating an excellent response time of both

instruments. The thermocouple psychrometer appeared to be less reliable for xylem water pressures > -700 kPa.

4.1. Introduction

The thermocouple psychrometer and the pressure chamber are most common instruments to measure xylem water potential. The pressure chamber is an established technique and is considered as a reference for the measurement of xylem the water pressure. However, this technique cannot be automated and the number of measures is limited by the number of leaves available, i.e. the pressure chamber is a destructive technique. On the other hand, the thermocouple psychrometer is the only technique available for long-term monitoring, being a continuous and non-destructive technique.

Measurement of (negative) water pressure in the xylem/soil requires equilibrium to be established between water in xylem/soil and water in the measuring device. Such equilibrium can be achieved through vapour or liquid phase. The thermocouple psychrometer is based on vapour phase equilibrium. The air in contact with the xylem/soil water adapts its relative humidity to the water potential of the xylem/soil water. The relative humidity measured by the thermocouple is converted to xylem/soil water pressure via the psychrometric law. Since the air acts as a semipermeable membrane, the presence of solutes in the xylem/soil water affects the relative humidity in the air surrounding the xylem/soil water and, hence, the measurement by the thermocouple psychrometer (Marinho, et al., 2008). In addition, any instrument based on the vapour equilibrium is sensitive to temperature fluctuations lose accuracy for air relative humidity close to saturation (Boyer, 1995). Instruments based on liquid equilibrium, as is the case of the Pressure Chamber, measure the ‘matric’ pressure of xylem/soil water. Since there is no semipermeable barrier, solute concentration equalises between the xylem/soil water and the water in the measuring instrument and the measurement is therefore associated with the ‘matric’ pressure of xylem/soil water. Balling and Zimmermann (1990) have attempted to measure directly ‘matric’ xylem

water pressure using a pressure probe made of a capillary tube filled with water and silicon oil was inserted into a xylem vessel. The pressure of the xylem water was transmitted through the liquid and measured by a pressure transducer. However, they could not record xylem water pressures below -0.65 MPa (Wei, et al., 2001) and were not able to prolong measurement for more than a few hours due to the cavitation occurring in the instrument.

This paper presents the use of High-Capacity Tensiometers (HCT) as a novel technique for the direct continuous measurement of 'matric' water pressure in the xylem, in the range from 0 to -2MPa. This instrument has long been used in geotechnical engineering to monitor the (negative) water pressure of the soil water. It is based on the liquid equilibrium, it has accuracy typically below 1-2 kPa over the entire measurement range and the effect of ambient temperature is negligible. The study compares the measurements of xylem water pressure by HCT and the Thermocouple Psycrometer installed on two small trees in the laboratory. These measurements were complemented by some discontinuous measurements by the Pressure Chamber. The trees were subjected to day/night cycles and were tested under both well irrigated and drought conditions. The HCTs were installed in pairs to detect any faulty response associated with ongoing heterogeneous cavitation. The work focused on the cross-validation of the HCT and Thermocouple Psychrometer techniques in terms of xylem water pressure measurement and instrument response time.

4.2.Background

4.2.1. Water under tension (absolute negative pressures)

The phase diagram of water (Figure 4.1) reports the conditions of temperature and absolute pressure characterising the solid (ice), liquid and vapour phases of water. Since vapour pressure cannot be negative, this diagram seems to suggest that water cannot exist in liquid phase under tension (negative absolute water pressure).

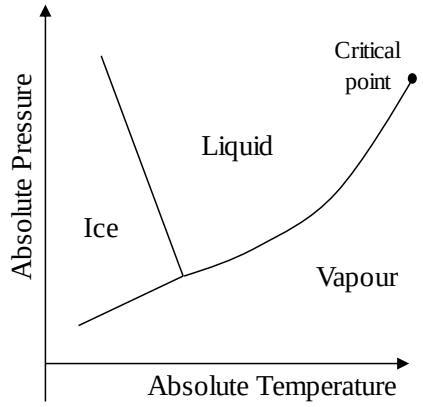

Figure 4.1: Water phase diagram

However, the phase diagram represents only the *stable* states of water, while other *metastable* states are possible without violating the principles of classic thermodynamics. The existence of a status of liquid water under tension may be considered through the van der Waals' equation of state of fluids (De Benedetti, 1996):

$$\left(p + \frac{a}{v^2}\right)(v - b) = RT \qquad [1]$$

where p is the pressure, v the molar volume, R the universal gas constant, T the absolute temperature, a and b the van der Waals' constant, depending on the kind of fluid. With respect to eq. [1], which takes into account the contribution of intermolecular attractive and repulsive forces, the maximum water tension liquid water at 20°C can sustain is of the order of 100 MPa (Marinho, et al., 2008). However, the values of water tension experimentally measured are usually two orders of magnitude smaller. The difficulty for water to reach the theoretical value is related to the presence of imperfections that lead to instability. These imperfections can arise in principle from homogeneous nucleation or heterogeneous nucleation. In the first case, temporary microscopic voids are created by the thermal motion within the liquid, constituting the origin nuclei for the growth and rupture of macroscopic bubbles. The tension necessary to activate homogeneous nucleation has been estimated to be of the order of 800 MPa (Brenner, 1995). As a result, instability observed at much lower water tensions is attributed to heterogeneous nucleation. In this case, the cavitation nuclei originate from

air pockets ‘invisible at naked eye’ that remain entrapped at the boundary between the liquid and the surface of the water container or impurities dispersed in the water.

The challenge of direct measurement of (negative) water pressure is associated with the metastable state of water under tension. Water under tension is subject to cavitation, i.e. water tend to move from metastable states, where the liquid is under tension, to stable states where liquid and vapour phases coexist under positive absolute pressure. This transition cannot be prevented but it can be delayed long enough to allow for long-term measurement of negative water pressure. This is achieved by pre-pressurising water in the measuring instrument to dissolve the majority of cavitation nuclei (Marinho, et al., 2008). This is the working principle behind the HCT measurement as first developed by Ridley (2003).

4.2.2. Equilibrium via liquid and vapour phase

Measurement devices are based on the equilibrium between the water in the xylem/soil and the water in the measuring instrument. For the case of vapour equilibrium (i.e. thermocouple psychrometer), the probe measures the relative humidity of the air surrounding the xylem/soil water. The (negative) pressure of *pure* liquid water required to equilibrate the air relative humidity is then inferred theoretically via the psychrometric law (Tarantino 2010):

$$p_w - p_w^0 = \frac{RT}{v_w} \ln \frac{p_v}{p_v^0} = \frac{RT}{v_w} \ln RH \qquad [2]$$

where p_v is the vapour pressure in equilibrium with the liquid, ${p_v}^0$ is the vapour pressure at saturation in equilibrium with the reference liquid pressure, p_w is the pressure of the liquid, p_w^0 is the reference liquid pressure, v_w is the molar volume of liquid water, RH is the relative humidity, R is the universal gas constant, and T is the absolute pressure. The measurement of liquid water pressure as inferred from relative humidity is intrinsically not very accurate at water pressure close to zero. For example, liquid pressures higher than -700 kPa requires measurements of RH > 99.5% and such

high values of relative humidity are not easy to measure because temperature fluctuation in proximity of vapour saturation causes water condensation in the instrument. In addition, air acts as a semipermeable membrane and the presence of solutes in the xylem/soil water contributes to deplete the vapour pressure p_v similarly to the negative pressure of the liquid water in the xylem/soil. As a result, it is impossible to discriminate between the contribution of (negative) xylem/soil liquid pressure and the solutes in the xylem/soil water to the vapour pressure, i.e. the measurement of the psychrometer is affected by the osmotic effects of the solutes in the xylem/soil (Figure 4.2). The common assumption is that solutes in the sap have a low concentration (Boyer, 1995) and a negligible effect on the xylem water potential (Jones, 2006). However, the hypothesis does not always hold, as observed during certain studies on plants under drought (Goode & Higgs, 2015), and it neither can be assumed that the osmotic component is constant over time (Campbell and Gardner, 1971). The difficult discrimination of the osmotic pressure in the xylem may lead to a misleading interpretation of the Thermocouple Psychrometer measurement.

For the case of equilibrium via liquid phase, solutes in the xylem/sol water diffuse into the measuring instrument. since there is no concentration differential between the xylem/sol water and the water in the instrument, the measurement can be directly associated with the water pressure in the xylem/soil (Figure 4.2).

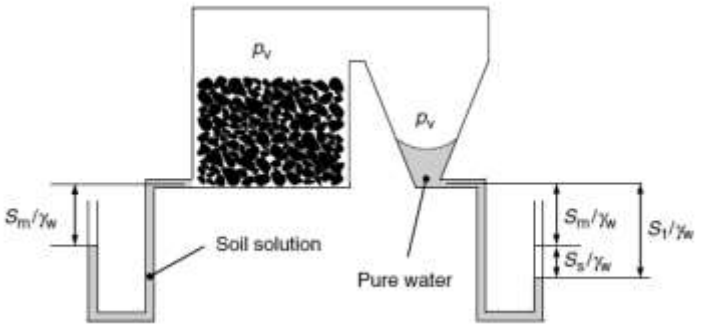

Figure 4.2:Definition of total and matric pressure for soil (Marinho, et al., 2008).

4.3.Materials

4.3.1. Equipment

4.3.1.1. High-capacity Tensiometers

The first high-capacity Tensiometer was designed by Ridley (1993); later designs improved the instrument, aiming to reduce the sources of heterogeneous cavitation within the device, minimizing volume and surface of the water reservoir and selecting materials less prone to be a good source of nucleation sites (Marinho, et al., 2008). The HCT used for this study was developed at University of Trento by Tarantino & Mongiovi' (2002).

High-capacity Tensiometers are formed by a porous ceramic, a water reservoir and a device to correlate the water pressure to an electrical signal (a strain-gauged diaphragm)(Figure 4.3). When the instrument is applied to a specimen with a negative pore-water pressure, the water is drawn out of the water reservoir and the metallic diaphragm bends in accordance to the negative pressure, changing the electrical resistance of the strain gauge. The water in the reservoir and in the porous ceramic can sustain the tension thanks to the menisci forming within of the porous filter. The nominal maximum water tension sustainable by the HCT depends on the air-entry value of the ceramic and it is inversely proportional to the diameter of the pores. The instrument used for this study has a nominal air-entry value of 1.5 MPa.

The HCT is susceptible of heterogeneous nucleation. Imperfections within the water reservoir may accommodate micro-bubbles of air, particularly difficult to dissolve into water because of the meniscus formed at the interface air-water. When the instrument is subjected to descending negative water pressure, the pressure in the bubble will have to decrease as well, increasing its volume. A critical contact angle will eventually be reached, the stability of the growing bubble will be compromised and a part of the gas will be detached in form of free cavity. The unstable free cavity will expand, occupying a large part of the water reservoir. As the gas pressure in the cavity is initially very close to the water vapour pressure, the HCT will read an absolute pressure close to

zero, and a gauge pressure of about -100 kPa. The process of nucleation and expansion of the free cavity with the HCT is referred to as cavitation.

The delay of cavitation in the instrument can be improved by a suitable design, but experience showed how critical an adequate saturation and pre-conditioning of the instrument are on the reliability of the measurement (Take & Bolton, 2003). When the HCT is saturated for the first time, the water needs to enter pores previously occupied by air. If a pressure ΔP is applied to the water, the air in the pores will compress (according to Boyle's law) and part of it will dissolve into the pore water (Henry's law). The pressure necessary to saturate the instrument depends on the initial saturation of the porous ceramic and on the pressure of the air in the voids, therefore ΔP can be minimized bringing the pressure of the air near to zero. Tarantino and Mongiovi' (2002) and Take and Bolton (2003) suggested a two-stages saturation procedure, where a completely dry porous ceramic is first subjected to vacuum and then flushed with water under pressure. The application of ΔP for the initial saturation is sufficient to dissolve most but not all the air in the ceramic and in the reservoir. A minor part of the air retracts in the smaller pores and it will not dissolve into the water because of the curvature of the menisci forming at the air-water interface. The application of an additional pressure should increase the amount of air dissolved into water; when the pressure of the system returns to atmospheric pressure, a significant quantity of the recently dissolved air will diffuse in free air instead than returning to the cavity (Ridley & Wray, 1996). Coherently to this principle, Tarantino and Mongiovi' (2001) suggested cycles of cavitation and re-saturation at high water pressure to "extract" cavitation nuclei remained undissolved upon pressurization.

The measurement of negative water pressure by the HCT is a consequence of the hydraulic equilibrium between the water in the sample and the one in the instrument. The porous ceramic does not prevent the diffusion of ions into the water reservoir; the instrument is therefore not liable of differences in concentration between the specimen and the measuring site that would result in an additional component of osmotic pressure. This was proved by Tarantino (2004): a HCT was alternatively placed in

water and in NaCl solutions at increasing osmotic pressure. The pressure recorded by the instrument did not changed during the test, indicating that the porous ceramic in the instrument does not act as a semipermeable membrane.

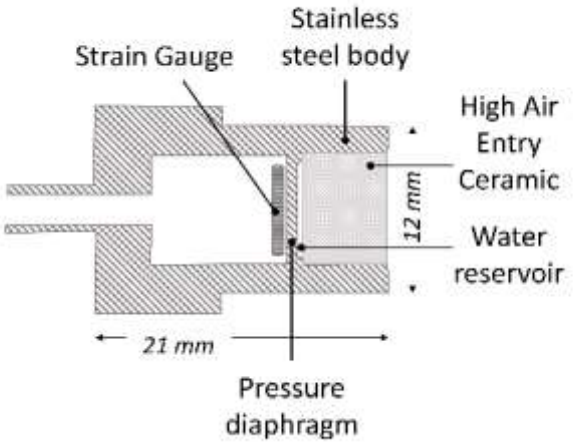

Figure 4.3: High-capacity Tensiometer. Design by Tarantino and Mongiovi' (2002)

4.3.1.2. Thermocouple psychrometer

A thermocouple psychrometer (TCP), consists of three separate thermocouple junctions attached to lead wires connected to a microvoltmeter. The sensing junction is usually formed by welding the ends of chromel and constantan wires together to form a bead; The wires of chromel and constantan, behind the welded junction, are attached to two copper lead wires of much larger diameter to form two reference junctions (Figure 4.1)(Brown & Oosterhuis, 1992). The psychrometer used for this study is produced by ICT international (PSY1 Stem Psychrometer).

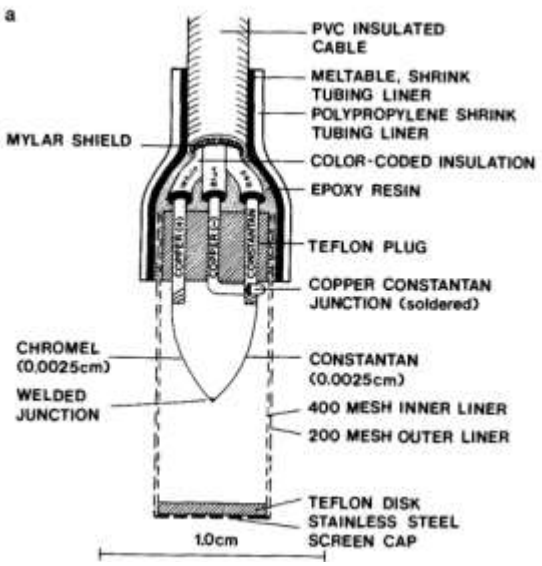

Figure 4.5:Thermocouple Psychrometer design (Brown & Oosterhuis, 1992)

The sensing junction, enclosed in a ceramic or stainless steel case to avoid any damage, is placed in contact with the sample. During the test, the air surrounding the thermocouple achieves an equilibrium with the water within the sample. Before the measurement, a small electrical current (usually 5 mA) is induced through the sensing junction from the constantan to the chromel side of the junction, in order to lower the temperature below the dew point of the air at the given temperature. The liberation of heat from the sensing junction during the flow of current is known as the "Peltier effect".

As consequence of the Peltier cooling, the water vapour in the air condenses on the surface of the sensing junction, in the form of water film or beads (Salisbury & Ross, 1992). The model used for this study allows to set a "cooling time" as input, to be selected in order to ensure condensation on the sensing junction.

When the cooling stops, the droplets of water on the sensing junction commence heating by conduction and convection from air in the enclosed chamber. The difference in temperature between the sensing junction and the reference junction generates an electric potential, registered by the microvoltmeter of the instrument. A

typical trend of the electric potential is reported in Figure 4.6 (Bristow & De Jager, 1980). The initial cooling of the sensing junction is represented by a sharp increase in electric potential ('cooling trace') and the following peak shows the transition between the induced cooling and the following heating of the water condensed on the junction. As visible in Figure 4.6, the liquid water, in contact with the enclosed air, rapidly increases its temperature towards ambient temperature, reducing the electric potential of the junction ('heating trace I'). When the sensing junction reaches the *wet bulb depression temperature*, the energy absorbed for water evaporation counterbalances the heat absorbed from the air in the surroundings. The consequence is a decline of the heating speed of the junction, resulting in a 'plateau' of the registered voltage. This corresponds to the *voltage endpoint.* When the water on the thermocouple is completely evaporated, the temperature of the sensing junction starts increasing again ('heating trace II'), until the sensing junction is at the same temperature as the reference junction, returning to a stable pre-cooling condition ('zero offset'), referred to as *dry bulb temperature.*

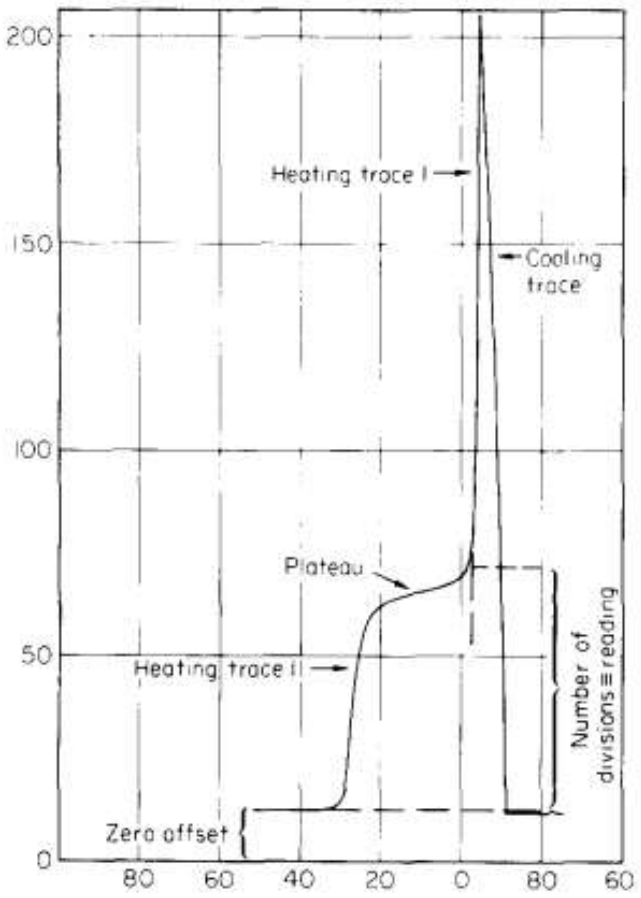

Figure 4.6: Thermocouple psychrometer typical voltage output (Bristow & De Jager, 1980).

The magnitude of the voltage endpoint and the length of the plateau are related to the water potential of the sample (Boyer, 1967): a high microvolt output with a short plateau is generated for a low water potential (or high suction), while a low voltage with a long plateau is registered for high water potential (or low suctions)Figure 4.7 (Brown & Oosterhuis, 1992). The response of the psychrometer must be calibrated against solution of known vapour pressure in order to be able to assess the water potential of each sample.

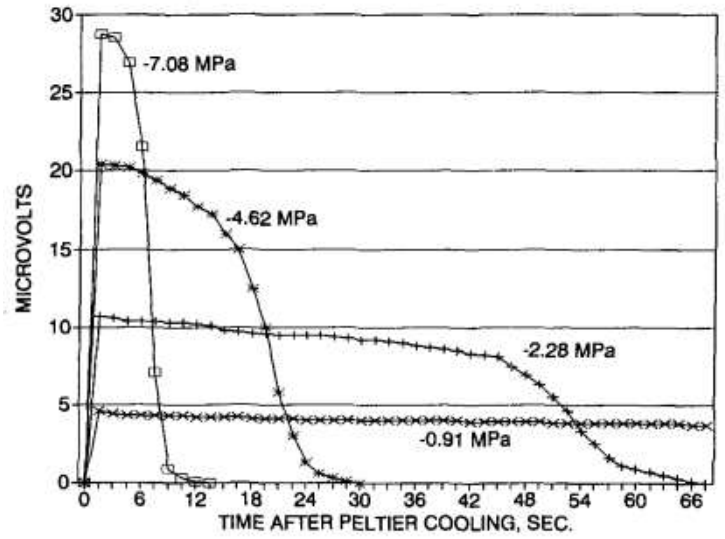

Figure 4.7:TCP voltage output for different molal NaCl solutions at 25°C using a 5mA cooling current for 15 s, (Brown-Oosterhuis 1992)

The instrument was calibrated using the procedure suggested by the manufacturer (Anon., n.d.), for the waiting time (6 sec) and cooling time (8 sec) used lately during the test. The psychrometer was kept in a desiccator overnight, in order to start from a known condition of 0% relative humidity. Solutions of NaCl at different concentrations, in the range of 0.1÷1 molality, were used to impose known water potentials. Those concentrations were selected in order to capture a typical range of water potential for plants, respectively 0.454÷4.550 MPa at 20 °C (Lang, 1967). A filter paper disk was soaked with the first solution and placed in the disk holder of the psychrometer. The psycrometer was put in contact with the filter paper and sealed with silicon grease, to avoid any interference with air outside the chamber. The disk holder is produced by the manufacturer of the psychrometer and act as lid of the instrument. The reduced dimension of the inner chamber makes the use of this lid advisable to reduce the equilibration time and minimize the evaporation from the filter paper necessary to reach an equilibrium with the air in the chamber.

Table 4.1: Relative Humidity, salt concentration and water potential of 6 solutions of NaCl used for the calibration of the thermocouple psychrometer.

RH	Molality (salt=NaCl)	Water potential at 20 ° [MPa]
0.996	0.1	0.454
0.993	0.2	0.900
0.990	0.3	1.344
0.987	0.4	1.791
0.983	0.5	2.241
0.967	1	4.550

4.3.1.3. Pressure chamber

The PC used in this experimental programme is commercialised by PMS Instrument Company (Model 1515D). It can be used to measure the negative water pressure in the range 0÷ -10 MPa.

4.3.2. The plant material

Two broad-leaves young trees were selected for the tests, a cherry tree (*Bigarreau burlat*) and an oak tree (*Quercus rubra*). Gymnosperms were avoided because of possible clogging of the porous ceramic due to the presence of resin. The trees (Table 4.2 and Figure 4.8), provided by an external nursery, were approximately 1 year old and came in pots of lose highly-organic soil. They were tested in their original soil (very lose and high in organic content). Prior to the experiment, both trees were kept in the laboratory at controlled temperature (20 °C) and relative humidity (40%) (See Appendix A for further information about the laboratory environment). They were irrigated regularly and kept under a growth lamp.

Table 4.2: characteristics of the trees selected for the test.

	Cherry tree	Oak tree
Total height [cm]	190	230
Diameter at 10 cm from the soil [cm]	2.4	2.1

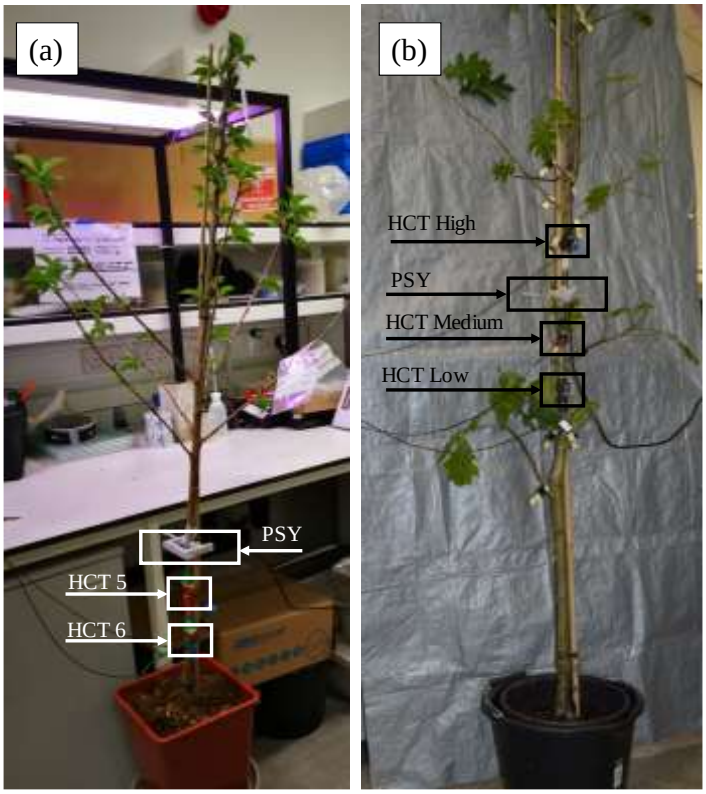

Figure 4.8:instruments installed on the a) cherry tree and on the b) oak tree

4.4.Experimental procedure

4.4.1. High-Capacity Tensiometer

4.4.1.1. Conditioning

As previously discussed, an adequate saturation of the HCT is essential for a successful measurement of negative water pressure. HCTs were briefly exposed to the atmosphere, in order to induce cavitation in the porous ceramic, and sequentially saturated at 4 MPa for at least 48 h in a saturation chamber (Tarantino, 2004). Before the application, the pressure applied was reduced to zero and each instrument was placed in water at atmospheric pressure. The porous ceramic was then exposed to the atmosphere and the pressure was let drop to around -1 MPa, when the HCT was placed back in free water to release the negative water pressure generated. This procedure was

repeated at least a couple of time for each instrument, in order to release any residual stresses in the diaphragm caused by the high positive pressure applied during saturation (Tarantino & Mongiovi, 2003). The final value measured at equilibrium in free water was used as a reference point for the zeroing of the instrument.

4.4.1.2. Application to the stem

The diameter of the HCT is 12 mm, in order to ensure a good installation it would then be advisable to use it on stem or branches with a diameter greater than 15 mm. The goal of the installation is to make the water in the xylem accessible to the instrument and avoid any disturbance due to localized evaporation or wetting. The bark and the living tissue underneath (phloem and cambium) were removed, to expose an area of xylem of approximately the same dimension of the HCT (Figure 4.9.a).The surface was then cleaned with few drops of distilled water, in order to remove any remaining living cells. The scratching procedure is the same used for the Psychrometer installation (Anon., n.d.), but the exposed surface was kept wet before the installation, in order to avoid desiccation of the xylem tissues. HCTs were installed on the stem using a saturated paste of kaolin, in order to ensure the hydraulic contact between the xylem and the porous ceramic (Figure 4.9.b). A latex membrane was used to wrap tightly the interested area to avoid any evaporation from the paste (Figure 4.9.c). The kaolin is an inert very fine clay, ideal to avoid any spurious effect due to choice of the material used for the paste. The paste is prepared at approximately the liquid limit, in order to reduce the delay required for the equilibration and to guarantee enough elasticity and limited shrinkage for perfect contact.

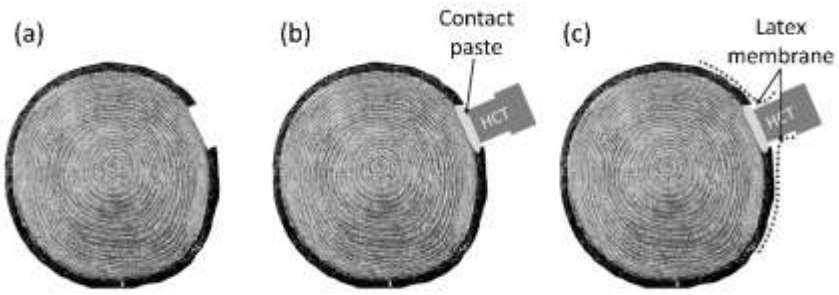

Figure 4.9: HCT installation on stem. (a) exposure of xylem tissues. (b) HCT application. (c) sealing with latex membrane

4.4.1.3. Post-measurement checks

The presence of air cavities in the porous ceramic may affect the measurement of the HCT, generating a differential between the pressure in the xylem and the pressure in the water reservoir of the instrument (Tarantino, 2004). The presence of anomalous air cavities is checked at the end of each measurement: if the HCT didn't cavitate during the test, it is placed in free water: the instrument is supposed to recover the initial value of zero pressure (a residual water pressure of 10-20 kPa is considered acceptable according to (Tarantino & Mongioví, 2001)). An additional indicator of reliable measurement is the value reached by the HCT immediately after cavitation: if there are no anomalous air cavities in the instrument, the gauge pressure should indicate ~-100 kPa.

4.4.2. Thermocouple Psychrometer

Before each installation, the psychrometer was observed under the microscope to assess the integrity of the thermocouple. The installation site on the stem of the tree was prepared removing the bark and the living tissues underneath. The exposed xylem was cleaned with few drops of distilled water and wiped dry. The psychrometer was then applied on the area, making sure one junction of the thermocouple was in contact with the xylem. Particular care was paid to insulate the measuring site with parafilm and silicon grease, avoiding the source of error coming from possible contact with the atmosphere and the resulting impossibility of reaching a condition of equilibrium in

the chamber. The cooling time imposed was 8 seconds and the waiting time was 6 seconds.

4.4.3. Pressure chamber

Three samples of non-transpiring leaves were taken for each measurement. Each leaf was wrapped in aluminium foil and inserted in a plastic bag at least 2 hours before the measurement was taken. When the leaf stops transpiring, the water in the leaf equilibrates with the water in the xylem at the junction with in the stem (Lang & Barrs, 1965). As a result, the water pressure measured in the leaf is assumed to coincide with the water pressure in the branch at the base of the petiole (Richter, 1973). Leaves were selected especially on the lower branches of the tree, to be as near as possible to the installation site of the instruments.

4.4.4. Instrumentation of the specimens

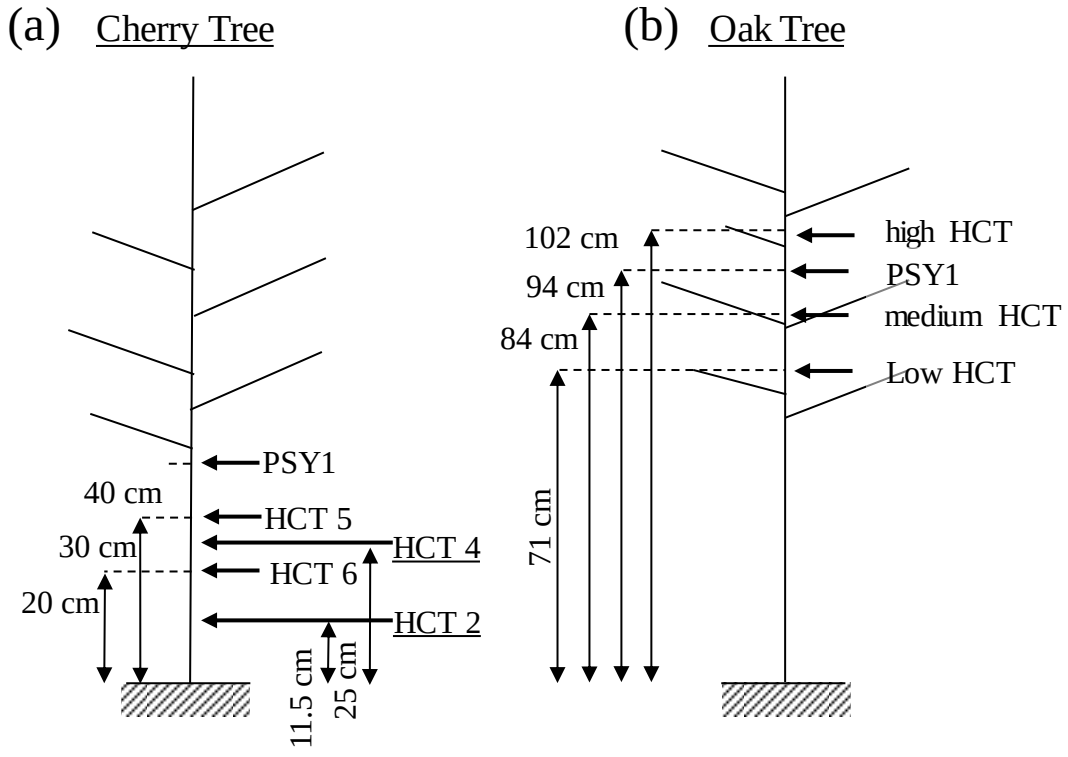

Figure 4.10: Instruments position a) on the cherry tree and b) on the oak tree

4.4.4.1. Cherry tree

The position of the instrument is shown in Figure 4.10.a. HCTs and the psychrometer were installed at a short distance, around 10 cm one from each other. The site was selected in order to have a stem diameter wide enough to allow the installation of the instruments and to have the 3 of them in an interval with no junctions of secondary branches. HCT 5 and HCT 6 were installed at the beginning of the test with the psychrometer. When the HCTs cavitated, it was necessary to substitute them with HCT 2 and HCT 4. The installation area of the first two instruments was sealed with parafilm to avoid localized evaporation, and the xylem was exposed at two different locations, as showed in Figure 4.10.a.

Pressure chambers readings were taken during the whole test, at day-time on non-transpiring leaves.

The tree had been kept in well irrigated conditions before the test. During the test, the tree was kept in a laboratory at constant temperature and relative humidity, in proximity of a growth lamp to mimic the solar radiation (lamp on 6 am- 8 pm, lamp off 8 pm- 6 am). The tree was let enter a condition of drought in the first 18 days, preventing any irrigation. Water was added on day 18 and on day 27. The different conditions were imposed in order to explore different ranges of xylem water pressure in the tree.

4.4.4.2. Oak tree

The instruments (Figure 4.10.b) were installed close together, approximately 10 cm one from each other. The psychrometer was placed between two of the HCTs. At the beginning of the test two HCTs were installed, respectively at 84 cm (medium HCT) and 102 cm (high HCT) from the level of the soil. At day 13, a new HCT was installed at 71 cm (low HCT). The system was entering a condition of drought and consequent low water pressure, increasing the chances of cavitation of the HCTs. A third instrument was added in order to enhance the probability of having at least two active instruments on the stem at all time. When a HCT cavitated, it was removed for re-saturation, and substituted with a fully saturated HCT. The new HCT was placed in

the same application spot, taking care of removing any healing tissue that may have developed during the time the previous instrument had been kept and exposing a part of active xylem underneath the damaged one.

Pressure chamber readings were taken approximately every 3 days during the first two weeks and once a day for the rest of the test (twice a day when the water pressure was at its minimum).

Before the test the tree was kept in the lab and watered regularly. The environmental conditions during the experiment were the same described for the cherry tree. Irrigation was prevented during the first part of the test, in order to reach a condition of increasing drought. At day 19 the soil was completely flooded and it was kept fully saturated until day 25.

4.5. Results

4.5.1. Cherry tree

The measurement of xylem water pressure by the HCTs applied on the stem of the cherry tree is represented in Figure 4.11. The measurement lasted 30 days and two different sets of HCTs were used. HCT 5 and HCT 6 were applied for the first 15 days: HCT 6 cavitated at day 11 (post-cavitation measurement -111 kPa), HCT 5 cavitated at day 15 (post-cavitation measurement -118 kPa). Cavitation in Figure 4.11 appears as a vertical straight line interrupting abruptly the measurement (day 11 and day 15). HCT 2 and HCT 4 were installed on day 16 and were kept in place for the following 13 days. The very steep lines at day 0 and at day 16 represents the hydraulic equilibration between the instrument and the xylem: the saturated paste needs to lose water in favour of the xylem until an equilibrium of the negative water pressure in the porous ceramic and in the water reservoir of the HCT and in the xylem is reached. The reading during the equilibration is not representative of the water status of the plant. The measurement of HCT 5 and HCT 6 is considered to be not valid after day 5, when the readings diverge more than 50 kPa, indicating an anomalous measurement. The

readings of the two instruments are in fact overlapping during the first three daily cycles, sign that the stem hydraulic resistance is low and does not rise gradients of pressure within the short distance between the two HCTs. The divergence between the two readings could be attributed to a drift in the reading of the instrument (the post-cavitation readings tend to exclude this hypothesis) or a change at the level of the measuring site.

The valid measurement of xylem water pressure via HCTs are reported in Figure 4.11 with thick lines, while the reading to be considered not valid are represented by thin lines.

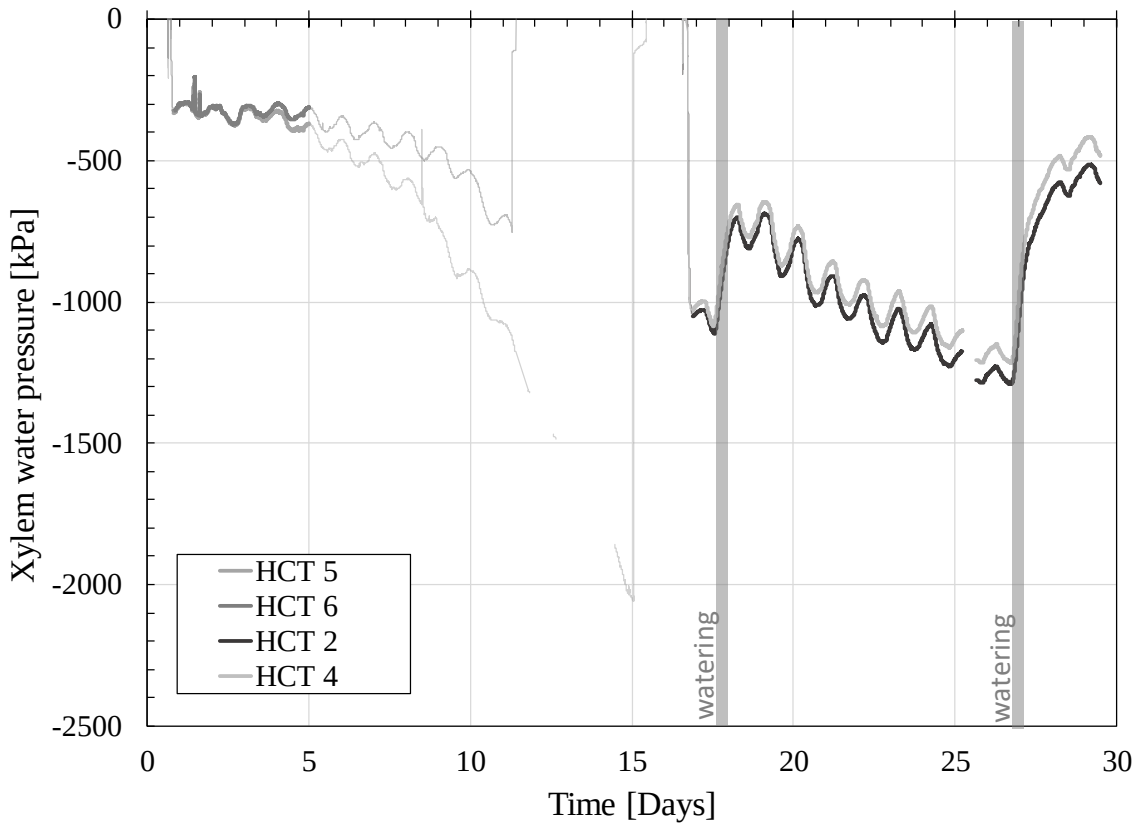

Figure 4.11: Measurement of HCT on the cherry tree. The thick lines represent the measurement in hydraulic equilibrium with the xylem, the fine lines represent the non-valid measurement of xylem water pressure.

The valid measurement of xylem water pressure via HCTs and the readings by thermocouple psychrometer and pressure chamber are represented in Figure 4.12. The continuous thick grey lines represent the HCTs, the fine dotted black line is the measurement of the thermocouple psychrometer; the grey dots are measurements of pressure chamber: each data set is represented by the average value and the standard deviation of the three sampled leaves.

Daily cycles are clearly visible in the trend of all the instruments measuring in continuous, coherently with the imposed time of activity of the growth lamp. The higher water pressure was registered daily between 12 pm and 6 am, when the lamp was switched on. The daily oscillation is quite limited in the first 10 days of the test (~80 kPa), while it amplifies in the second part (~150 kPa). The psychrometer shows high reading of xylem water pressure in the first 10 days, if compared with the first reading of water pressure by the pressure chamber (day 8, water pressure by pressure chamber= -680 kPa, by thermocouple psychrometer= -200 kPa). After day 10 the pschrometer starts reacting to the decreasing water pressure in the system due to prolonged drought. At day 17 and day 26 the system was watered and the water pressure in the plant consequently increased. The reaction of the HCTs and the psychrometer was almost immediate and synchronous along the whole recovery to higher values of xylem water pressure.

The HCTs are in good accordance with each other and the comparison between the HCTs and the thermocouple psychrometer shows a coherent measurement by the two instruments: the readings are perfectly in phase and consistent with the boundary conditions imposed. The reaction to the daily cycles of light and darkness is clearly identified, as the increase in xylem water pressure consequent to the watering of the system. After day 16, for a xylem water pressure lower than-700 kPa (identified in the graph by the horizontal grey band), the error between the readings of the three instruments is reduced to an offset of approximately 80 kPa. For a xylem water pressure nearer to 0, the thermocouple psychrometer tends to overestimate the value in respect with the readings by the HCTs (day 0-day 5). Both the continuous non-

destructive techniques measured a higher xylem water pressure than the pressure chamber.

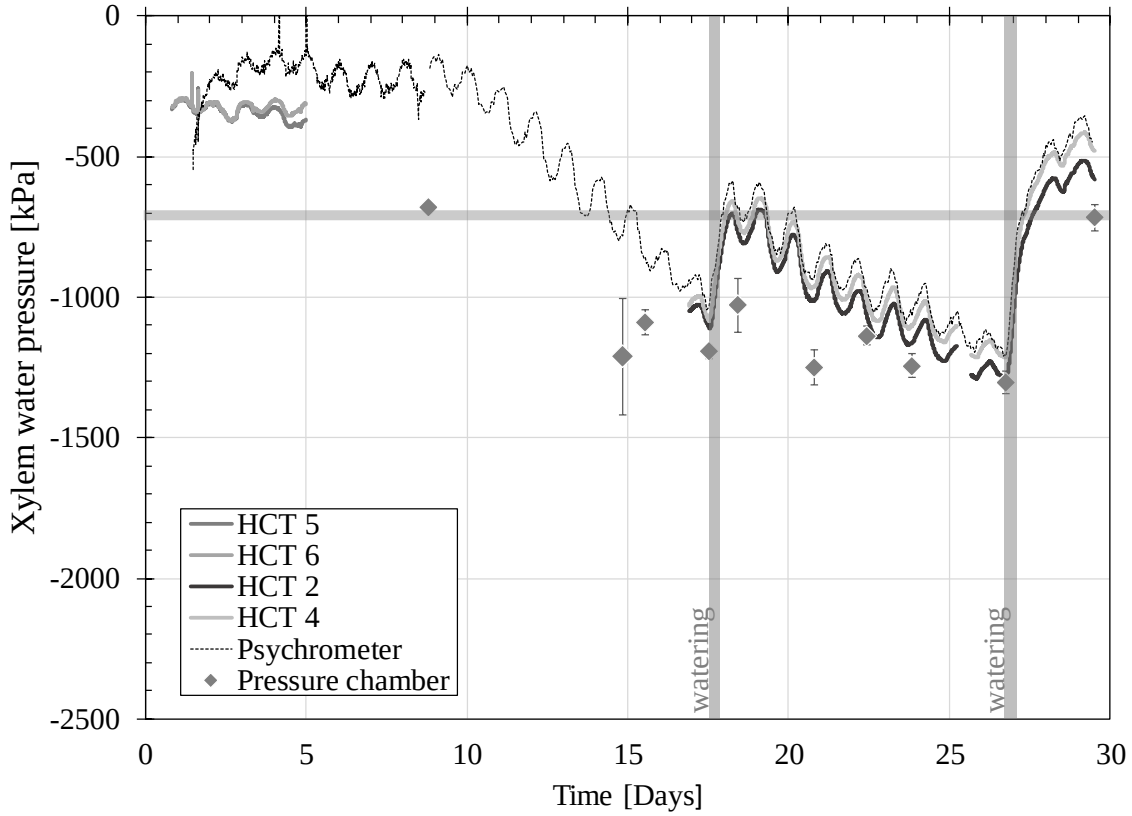

Figure 4.12:Cherry tree, measurement of xylem water pressure via the HCT, the PSY1 and the Pressure chamber on non-transpiring leaves. The vertical grey bands indicate the watering of the system. The horizontal grey line highlights the value of -700 kPa.

The comparison of xylem water pressure measured via the three instruments is reported in Figure 4.13. The reading taken by HCTs (horizontal axis) are compared to the thermocouple psychrometer (open circles◯) and the pressure chamber (solid diamonds♦). Each point refers to a moment in which a measurement of pressure chamber was taken. The readings of HCT and pressure chamber are reported as average value; readings taken in a condition of non-equilibrium have been omitted.

Readings of xylem water pressure on the stem by HCT and Psychrometer are higher than the readings done on leaves by the Pressure chamber, coherently with the gradient induced by transpiration. The direct comparison of the two instruments shows a very good agreement for xylem water pressures below -700 kPa. The difference is more relevant between 0 and -500 kPa, as clearly visible in Figure 4.12 during the first 5 days; unfortunately there is no

contemporary measurement by the three techniques in the first 15 days, for a xylem water pressure above -700 kPa.

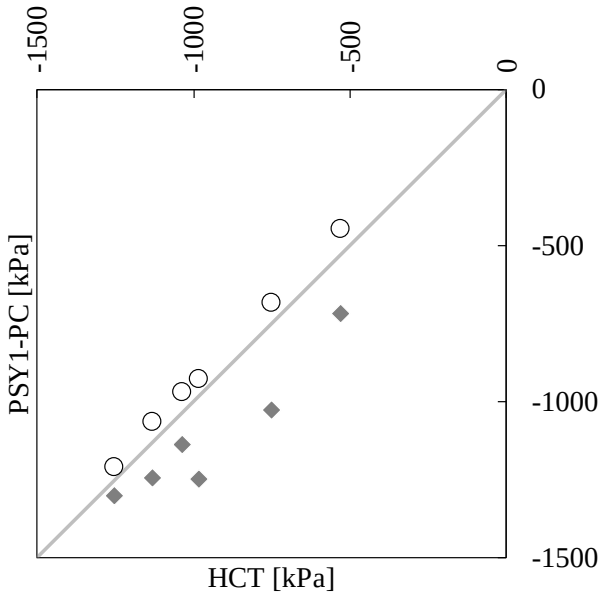

Figure 4.13:comparison of xylem water pressure on the cherry tree measured by the HCT (horizontal axis) and the thermocouple psychrometer (empty dots◯) and the Pressure chamber (full squares♦).

4.5.2. Oak tree

The measurement of xylem water pressure by the HCTs applied on the stem on the oak tree is represented in Figure 4.14. Different instruments were installed on the stem throughout the test, due to the replacement of the cavitated HCTs. The position of the instruments throughout the test is reported on top of Figure 4.14. The instruments were installed at three different positions along the stem (High-Medium-Low): for the sake of clarity, the measurement will be discussed in respect with the position of the measuring site.

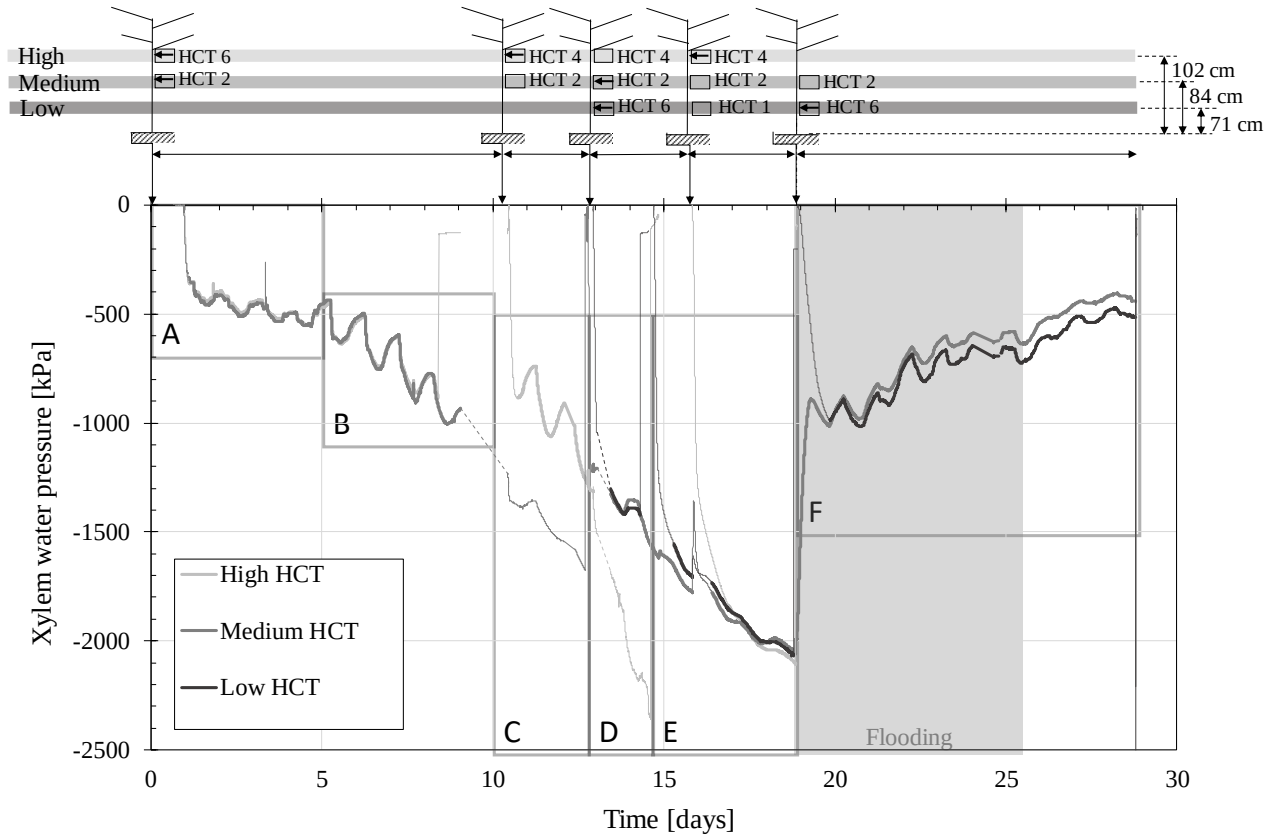

Figure 4.14:Measurement of HCT on the oak tree. The thick lines represent the measurement in hydraulic equilibrium with the xylem, the fine lines represent the non-valid measurement of xylem water pressure. Each instrument is represented by a square □; if the instrument is newly installed, it is represented by an additional arrow ←.

The different intervals of the measurement identified in Figure 4.14 are reported in a different scale in Figure 4.15. The valid measurement of xylem water pressure via HCTs are represented by thick lines, while the reading to be considered not valid are represented by fine lines.

The almost vertical line in Figure 4.14.A represents the hydraulic equilibration of the instrument with the xylem, through the process previously described. The same process occurs at the beginning of every new installation (Figure 4.15.C-D-E-F). The sudden vertical lines that interrupt abruptly some of the measurements indicate cavitation occurring in the instrument (Figure 4.15.B-C-D-E). During the initial equilibration and after cavitation the reading is not representative of the water status of the plant. The measurement of the two HCTs installed almost coincide for the first

10 days (Figure 4.15.A-B); from day 12, Medium HCT shows an anomalous behaviour in comparison with the newly re-installed High HCT: there is a relevant difference between the readings of the two, but while the latter shows evident daily cycles, the first has very reduced differences between day and night readings, probably caused by a loss in hydraulic contact with the xylem: the reading cannot be considered reliable after day 10. Between day 12 and 14, two HCTs are installed in the medium and low position along the stem (Figure 4.15.D). The HCT in the high position has evidently been disturbed during the procedure of installation, losing contact with the xylem (as revealed by the sharp change in the measurement trend, in the black square). The anomalous peak around day 15.75 in Figure 4.15.E is due to a physical pressure applied by the operator on the back of the HCTs to ensure the contact between the paste placed on top of the instrument and the exposed stem; the disturbance effected the measurement for approximately 9 hours. This kind of effects usually disappear within minutes, but the low water exchange between the instrument and the stem due to the condition of water stress of the plant has probably prolonged it.

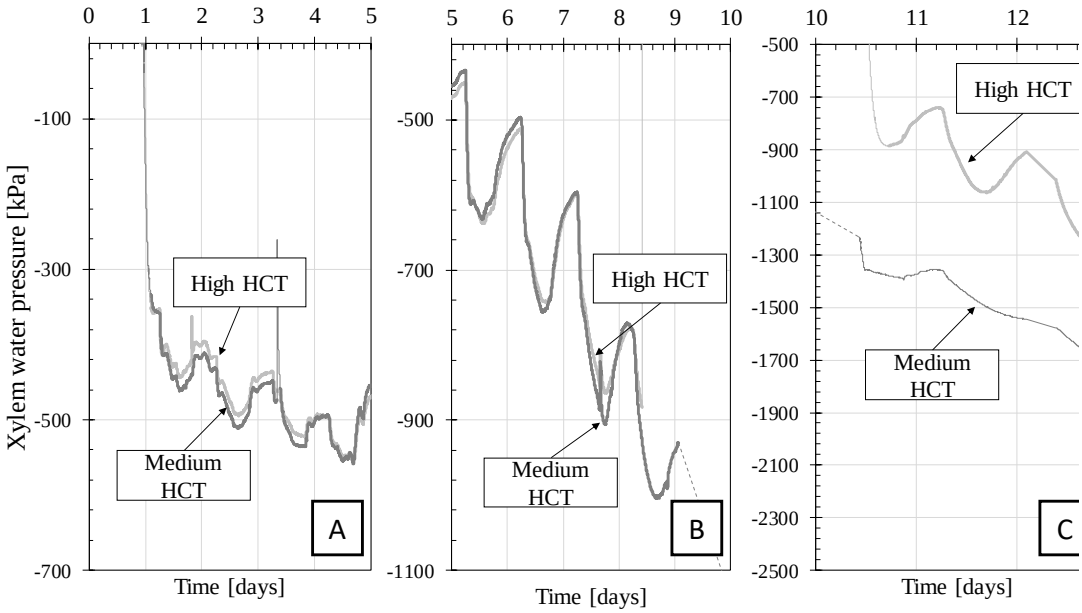

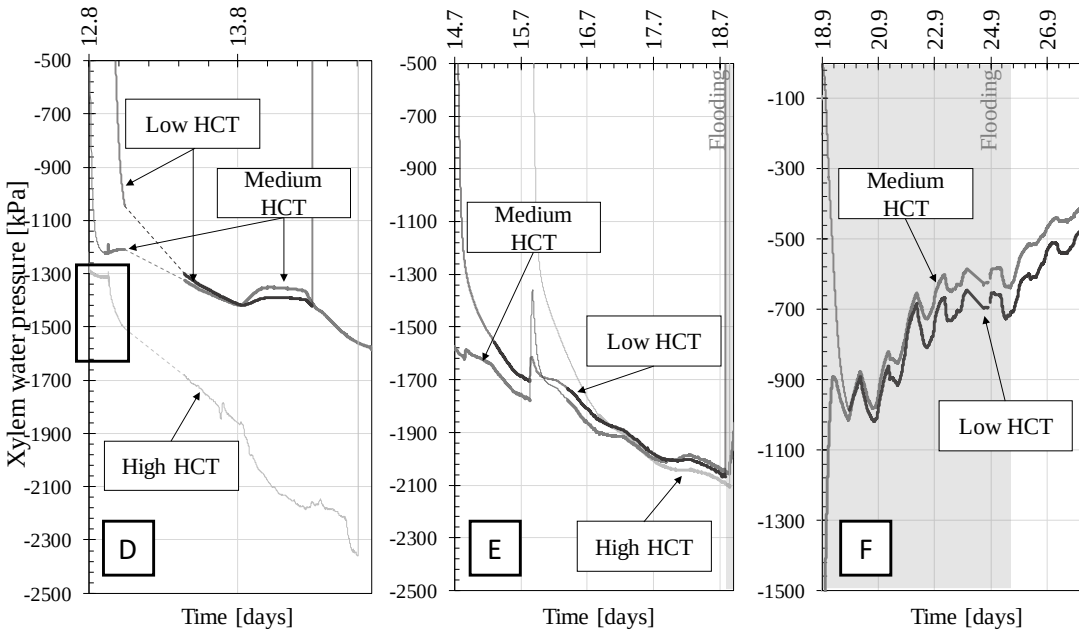

Figure 4.15: Zoom of measurement of xylem water pressure by HCTs.

The valid measurement of xylem water pressure on the oak tree via HCTs and the readings by thermocouple psychrometer and pressure chamber are represented in Figure 4.16. The continuous thick grey lines represent the HCTs, the fine dotted black line is the measurement of the thermocouple psychrometer; the grey dots are measurements of pressure chamber: each data set is represented by the average value and the standard deviation of the three sampled leaves. The system started in well-watered conditions and it was let entering a condition of drought for the first 18 days, preventing any irrigation. From day 18 to day 25 the system was flooded, in order to release the negative water tension in the xylem (large grey area in the graph).

Daily cycles are clearly visible in both measurements by HCTs and psycrometer. The daily fluctuation is very reduced during the first five days, in well-watered conditions, and between day 15 and 18, when the water pressure dropped below -1500 kPa. Daily cycles are coherent with the time of activity of the growth lamp, with maximum values of xylem water pressure recorded around 6 am (the growth lamp was switched on from 6am to 8pm every day). The xylem water pressure oscillation associated with the daily cycles is reduced during the first 5-6 days, when the soil is very wet, and starts

increasing when the average xylem water pressure of the system shows a declining trend. The minimum point of xylem water pressure is reached at day 18, immediately before the flooding of the system. The instruments responded accordingly, showing a sudden increase of water pressure in the 10 hours following the flooding. From day 19 to the end of the test the measurement kept increasing at a slower rate. The HCTs and the psychrometer shown a perfectly synchronous behaviour, both in terms of readiness of reaction in detecting changes in the boundary conditions and in the intensity of the phenomena registered. The measurement of the psychrometer always shows a higher water pressure than the one recorded by the HCTs.

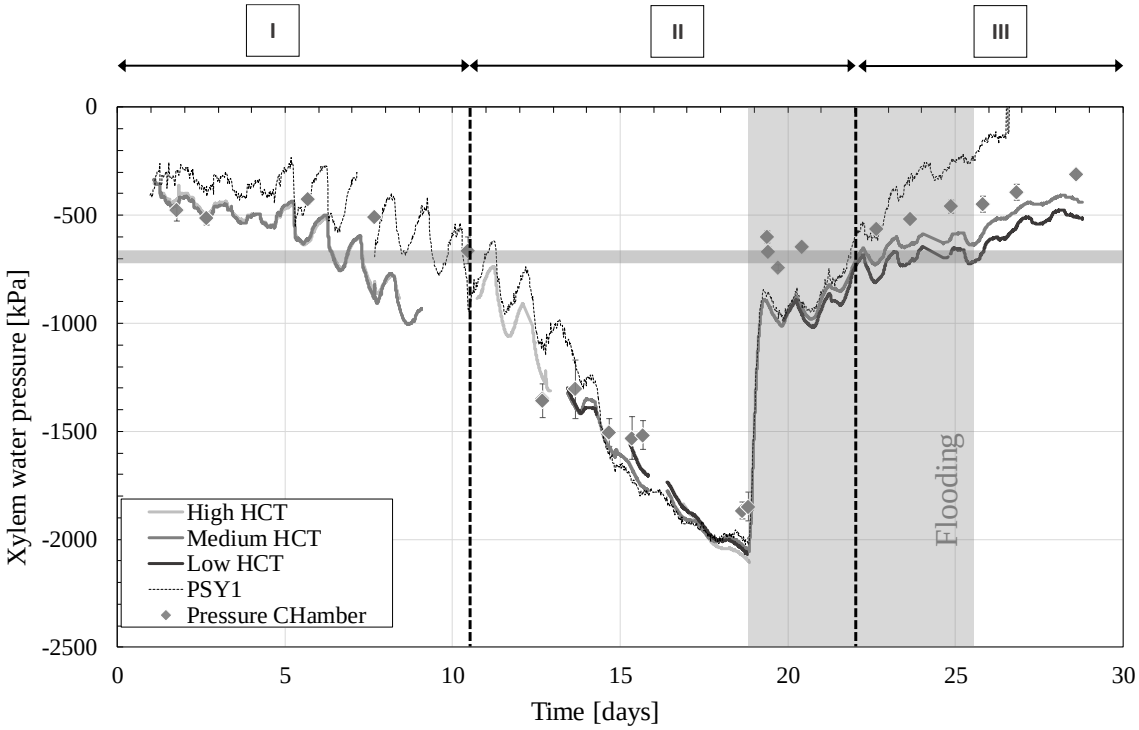

Figure 4.16:Oak tree, measurement of xylem water pressure via the HCT, the PSY1 and the Pressure chamber on non-transpiring leaves. The grey area indicates the flooding of the system. The horizontal grey line highlights the value of -700 kPa while the vertical dotted line separate the interval of xylem water pressure measurement above (I-III) or below (II) -700 kPa.

Three phases are clearly identified in Figure 4.16: the intervals in which the measurement of xylem water pressure is above -700 kPa (I-III) and the intervals where it is below it (II). Figure 4.17 reports the comparison of xylem water pressure measured via the three instruments for the three identified intervals; interval II is further split

into the condition of drought and flooded system. The reading taken by HCTs (horizontal axis) are compared to the thermocouple psychrometer and the pressure chamber. Each point refers to a moment in which a measurement of pressure chamber was taken. The readings of HCT and pressure chamber are reported as average value; readings taken in a condition of non-equilibrium have been omitted.

Below -700 kPa the HCTs and the thermocouple psychrometer have a very good agreement, as shown by Figure 4.16 and Figure 4.17 with respect to data concerning Interval II. The measurement of the pressure chamber is in line with the other two instruments during the dry period, while it tends to be lower than the other two during the flooding.

For xylem water pressure above -700 kPa, the difference between the readings by HCTs and the thermocouple psychrometer increases, with the latter constantly reporting higher readings of water pressure. In respect with the first 10 days of the test, the readings by the thermocouple psychrometer compared with the HCTs do not fall on the 1:1 line (Figure 4.17_Interval I), but on a higher parallel line. The measurements by the pressure chamber do not support neither one technique or the other: of the 4 points taken during Interval I, two coincide with the measurement by HCT and two with the thermocouple psychrometer.

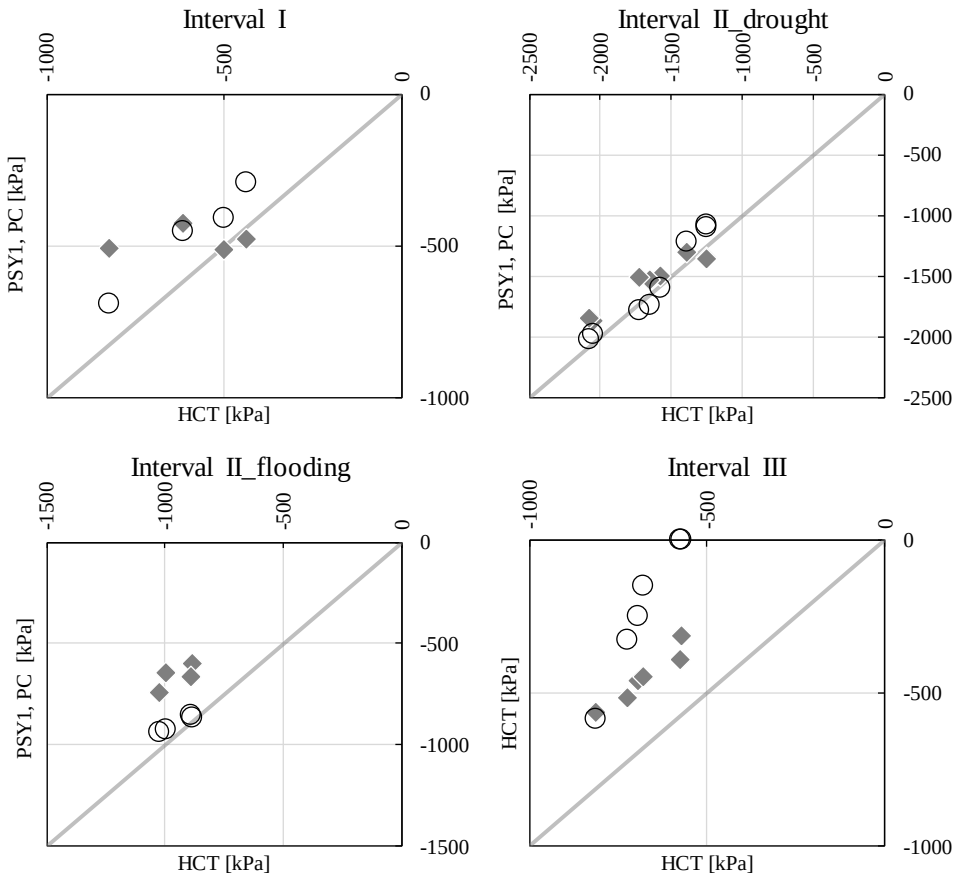

Figure 4.17: comparison of xylem water pressure on the cherry tree measured by the HCT (horizontal axis) and the thermocouple psychrometer (empty dots ○) and the pressure chamber (full squares ♦).

During flooding, the three instruments register accordingly the release of water tension in the xylem, with synchronous and almost coinciding measurements. When the xylem water pressure rises above -700 kPa, the pressure registered by the thermocouple psychrometer keeps on increasing, until it reaches the positive range of pressure. The instrument is outside its range of measurement and readings cannot be considered to be reliable. On the other hand, readings by the pressure chamber are constantly higher than the measurements by the HCTs from the beginning of the flooding, and show a higher pressure than the one registered by the thermocouple psychrometer within the range of validity of the readings of the latter, as shown in detail in Figure 4.18.

The measurement by the psychrometer is evidently anomalous, with a continuous increase in registered pressure. On the other hand, the trend of HCTs and the pressure

chamber are consistent and behave accordingly. The xylem pressure on the non-transpiring leaves is lower than the xylem pressure measured on the stem, with a difference read by the two techniques that is reducing over time.

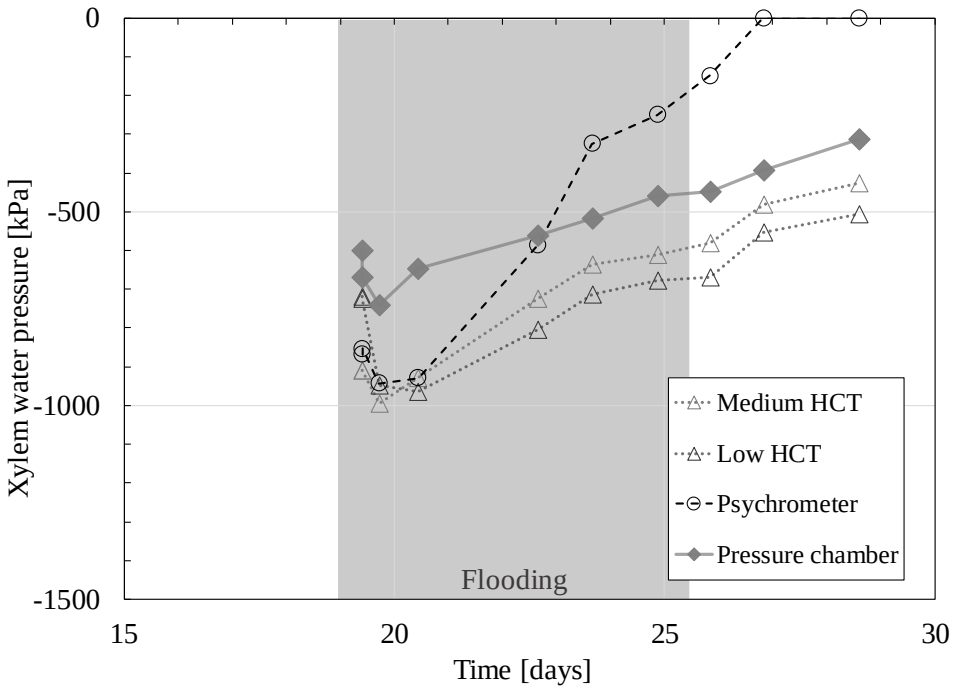

Figure 4.18: zoom of the measurement for day 19-29. Only the readings of HCT and thermocouple psychrometer taken at the same time as the pressure chamber are shown.

4.6. Discussion

The measurement by the HCTs and the thermocouple psychrometer are perfectly synchronous and coherent to the changes in boundary condition for xylem water pressures lower than -700 kPa. The response of the two instruments is in phase, i.e. record comparable day/night oscillations of xylem water pressure. The response of the HCTs and in the psychrometer upon watering was also consistent. The equilibration of the plant against the low soil water pressure imposed by the watering lasted ~11h on day 17 and ~14h on day 26 for the cherry tree and ~9h for the oak tree; the HCTs and the thermocouple psychrometer registered accordingly the transition process. In order to measure the pore-water pressure, both instruments need to equilibrate with the

specimen: when a change in pore-water pressure occurs within the sample, water needs to flow from the HCT to the sample (drying of the sample) or *vice versa* (wetting of the sample), according to the pressure gradient. In the case of the psychrometer, the change in water pressure is associated to the evaporation at the surface, or condensation, until an equilibrium is achieved between the water in the sample and in the surrounding air. Both processes of liquid and vapour equilibrium usually require some time to reach a stable condition. Furthermore, the time acquisition of the psychrometer was set at an interval of 30 minutes. Nevertheless, no time delay was appreciated between the monitoring of the two instruments. It can be assumed that possible delays due to the working principle of the instruments were, if present, not relevant at the time scale of the phenomena investigated.

For the cherry tree, the measurement of the pressure chamber is consistently lower than the values observed on the stem. Instead, for the case of the oak tree the water pressure measured by the pressure chamber on non-transpiring leaves often results higher than the water pressure measured on the stem, especially after the flooding. This is in contrast with the pressure gradient one would expect for upward flow, from the soil through the stem and up to the leaves. This non-intuitive discrepancy may be due to either errors in the measurements or a flow in the plant that does not take place from the roots through the stem to the leaves.

The very similar independent measurements of HCT and psychrometer from day 18 to day 21 (Figure 4.18) seems to suggest that there is no error in the measurement of xylem water pressure. At the same time, pressure chamber measurements have been consistent in the cherry tree experiments and measurement procedures did not change for the case of the oak tree experiment. If the measurement of the pressure chamber is also correct, the discrepancy between pressure chamber and HCT/psychrometer measurement can be explained by a flow in the plant that is not directed upward.

A possible explanation is discussed hereafter and is illustrated by the simplified model in Figure 4.19. The process of hydraulic equilibration of the soil-plant can be described as an ongoing process of propagation of water potential along the plant in response to

the boundary condition imposed by the soil and the boundary condition imposed by the leaves.

Let us assume that

i) The water pressure in the leaf is related to the stomata behaviour (Klein, 2014).
ii) When the plant is in a condition of anaerobiosis, the stomata tend to close, even when no water deficit is present in the leaves (Bradford & Hsiao, 1982; Jackson, Gales, & Joan, 1978; Kozlowski, 1977).Studies on tomato plants have shown that the stomata closure started around 4 h after flooding and could persist for several days after the end of the flooding (Else, et al., 1996) .
iii) The stem is a deformable porous medium and deforms in relation to the xylem water pressure (Simonneau, et al., 1993). The deformation of the stem can be delayed with respect to the change of xylem water pressure at the boudaries (Klepper, Browning, & Taylor, 1971; Parlange, Turner, & Waggoner, 1975)

The evolution of xylem water pressures during the entire test on the oak tree can therefore be described as follows. In the first part of the test, the soil had very high water content (Day 0 in Figure 4.19_Interval I), the leaves were close to a condition of anaerobiosis, and the stomata resistance was probably considerably high, as substantiated by the very small daily oscillation of the xylem water pressure. The surface of the pot was not covered, and evaporation occurred from the bare soil during the whole test, with consequent decrease of soil pore-water pressure. The pressure in the xylem measured by both HCT and the psychrometer was then driven by the decrease in soil pore-water pressure after day 5. The readings of pressure chamber between day 5 and day 10 remains essentially constant as if there was a delay in the stomata aperture following the end of the anaerobiosis conditions (Else, et al., 1996).

Between day 10 and day 18 the stomata were initially open, as shown by the amplitude of the daily oscillations, and the water pressure in the stem was driven by water pressure in the leaf. When the water pressure in the leaf increases too much, stomata

start closing in order to reduce the water loss from the leaves (daily cycles reduced accordingly) (Figure 4.19_Interval II).

When the system was flooded, the pore water pressure in the soil suddenly reduced to zero (Day 19 in Figure 4.19_Interval III). The measurements by the pressure chamber showed a sudden increase in the xylem water pressure on the non-transpiring leaves. A consistent increase was recorded simultaneously by the HCT and the psychrometer, although the xylem water pressure measured on the stem was lower than the one measured on the non-transpiring leaves. It can be specuated that the leaves had a rapid response to the watering of the system, entered state of anaerobiosis, and stomata closed. The xylem water pressure was then driven by the change in water pressure in the soil with the plant upper boundary condition equivalent to an impermeable boundary.

The pressure imposed at the base of the plant did not propagate instantaneously through the stem up to the leaves because of the deformability of the stem. This delay and the reduced flow due to the stomata closure have probably generated a water pressure in the transpiring leaves temporarily higher than the water pressure in the stem (Figure 4.19_Interval II-III). The reaction of plants to condition of anaerobiosis and the intra-plant signals behind several of the actions activated by the plant itself to face conditions of water stress are a matter of study for plant physiologist, but even now there are several aspects that are not completely clear about the mysteries behind the life of the vegetable kingdom.

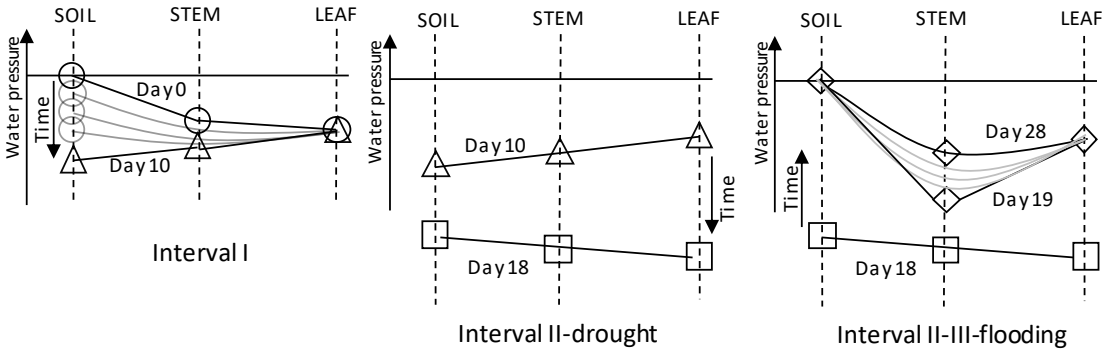

Figure 4.19: conceptual model of water flow within the soil-stem-leaf. The arrow appointed as 'Time' identify the element of the soil-stem-leaf regulating the stem xylem water pressure during the time interval.

4.7. Conclusions

This paper has presented the use of HTs to monitor xylem water pressure and cross-validated the HCT against the thermocouple psychrometer.

Tensiometers were installed in pairs to detect anomalous behaviours due to the presence of air cavities in the instruments or the loss in hydraulic contact between the instrument and the measuring site. The need of using HCTs in pairs is consistent with the suggestion by Tarantino & Mongiovi' (2001) when discussing measurement in soil. The comparative study allowed to investigate the response time of the HCT and of the thermocouple psychrometer. The response time of the HCT is related to the flow of water necessary for the instrument plus contact paste to equilibrate with the sample. The response time of the thermocouple psychrometer is related to the time necessary for the water particles to evaporate into the measurement chamber, until an equilibrium between the air and the evaporative surface is reached. The response time of the two instruments is based on completely different processes, therefore it can be concluded that there is no delay in the response time of both.

The psychrometer tended to considerably overestimate the values of xylem water pressure in the range from -700 to 0 kPa. As the xylem water pressure approaches zero, the psychrometer seems to respond inconsistently when compared to HCT and

pressure chamber. In the testes presented in this paper, the possible presence of solutes in the sap appeared to have negligible effects on psychrometer readings (HCT and psychrometer returned very similar reading foe pressure <-700 kPa).

References

Anon., n.d. *http://ictinternational.com/content/uploads/2014/03/PSY-Calibration.pdf.* [Online].

Anon., n.d. *http://ictinternational.com/products/psy1/psy1-stem-psychrometer/.* [Online].

Anon., n.d. *www.pmsinstrument.com.* [Online].

Balling, A. & Zimmermann, U., 1990. Comparative measurements of xylem pressure of Nicotiana plants by means of the pressure bomb ad pressure probe. *Planta,* pp. 325-338.

Boyer, J. S., 1967. Leaf water potentials measured with a pressure chamber. *Plant Physiology.*

Boyer, J. S., 1995. *Measuring the Water status of Plants and Soils.* s.l.:Academic Press.

Bradford, K. & Hsiao, T., 1982. Stomatal behavior and water reations of waterlogged tomato plants. *Plant physiology,* Volume 70, pp. 1508-1513.

Brenner, C., 1995. *Cavitation and bubble dynamics.* s.l.:Oxford university press.

Bulut, R. & Leong, E., 2008. Indirect measurement of suction. In: *Laboratory and field testing of unsaturated soils.* s.l.:Springer, pp. 21-32.

Campbell, G. & Gardner, W., 1971. Psychrometric measurement of soil water potential:temperature and bulk density effect. *Soil Science Society of America Journal,* pp. 8-12.

Dainese, R. & Tarantino, A., 2019. Measurement of plant xylem water pressure using High-Capacity Tensiometers. *Geotechnique.*

De Benedetti, P., 1996. *Metastable liquids.* s.l.:Princeton university press .

Else, M. et al., 1996. Stomatal closure in flooded tomato plants involves abscisic acid and a chemically unidentified anti-transpirant in xylem sap. *Plant physiology,* Volume 112, pp. 239-247.

Jackson, B., Gales, K. & Campbell, D., 1978. Effect of waterlogged soil conditions on the production of ethylene and on the water relationships in tomato plants. *Journal of experimental botany,* 29(108), pp. 183-193.

Klein, T., 2014. The variability of stomata sensitivity to leaf water potential across tree species indicates a continuum between isohydric and anisohydric behaviours. *Functional ecology,* Volume 28, pp. 1313-1320.

Klepper, B., Browning, V. & Taylor, H., 1971. Stem diameter in relation to plant water status. *Plant physiology,* Volume 48, pp. 683-685.

Lang, A., 1967. Osmotic coefficients and water potentials of sodium chloride solutions from 0 to 40 C. *Australian Journal of Chemistry.*

Lang, A. & Barrs, H., 1965. An apparatus for measuring water potential in the xylem of intact plants. *Australian Journal of biological sciences,* Volume 18, pp. 487-497.

Marinho, F. A. M., Take, W. A. & Tarantino, A., 2008. Measurement of matric suction using tensiometric and axis translation techniques. *Geotechnical and Geological Engineering,* Volume 26(6), pp. 615-631.

Parlange, J.-Y., Turner, N. & Waggoner, P., 1975. Water uptake, diameter change, and nonlinear diffusion in tree stems. *Plant physiology,* Volume 55, pp. 247-250.

Pereira, J. & Kozlowski, T., 1977. Variations among woody angiosperms in response to flooding. *Physiologia plantarum,* Volume 41, pp. 184-192.

Richter, H., 1973. Frictional potential losses and total water potential in plants: a re-evaluation. *Journal in experimenatl bothany,* Volume 24, pp. 983-994.

Ridley, A., 1993. A new instrument for the measurement of soil moisture suction.. *Geotechnique,* Volume 43, pp. 321-324.

Ridley, A. & Wray, W., 1996. Suction measurement: a review of current theory and practices. In: A. E.E. & P. Delage, eds. *Unsaturated soils.* s.l.:s.n., pp. 1293-1322.

Simonneau, T., Habib, R., Goutouly, J.-P. & Huguet, J., 1993. Diurnal changes in stem diameter dependent upon variations in water content: direct evidence in peach trees. *Journal of experimental botany,* 44(260), pp. 615-621.

Take, W. & Bolton, M., 2003. Tensiometer saturation and the reliable mesurement of soil suction. *Geotechnique,* pp. 159-172.

Tarantino, A., 2004. Panel lecture: direct measurement of soil water tension. pp. 1005-1017.

Tarantino, A. & Mongiovi', L., 2001. Experimental procedures and cavitation mechanisms in tensiometer measurements. *Geotech Geol Eng,* pp. 189-210.

Tarantino, A. & Mongiovi', L., 2002. *Design and construction of a tentiometer for direct measurement of matric suction.* s.l., Recife, pp. 319-324.

Tarantino, A. & Mongiovi, L., 2003. Calibration of tensiometer for direct measurement of matric suction. *Geotechnique,* Volume 53.

Wei, C., Steudle, E., Tyree, M. & Lintilhac, P., 2001. The essentials of direct xylem pressure measurement. *Plant, cell and environment,* pp. 459-555.

Chapter 5 An experimental and numerical investigation into the mechanisms of water removal through plants (transpiration) via benchmarking against evaporation from bare soil

Abstract

The atmosphere removes water from the ground resulting in an increase in suction and, hence, shear strength. Atmosphere-generated suction can therefore be regarded as a low-cost and low-carbon soil reinforcement technique. Water is removed either through the ground surface (evaporation) or by plant roots through evaporation at the leaf stomata (transpiration). These two processes are driven by the same atmospheric demand but may lead to different amount of water removed from the ground. This paper investigates these two different mechanisms of water extraction with the aim of understanding whether and how vegetation is beneficial in reinforcing the ground hydrologically. A vegetated column and a bare column were equipped with High-Capacity Tensiometers (HCTs) and TDR probes to monitor (negative) pore-water pressure and volumetric water content respectively and placed on balances to monitor evaporation/transpiration. An herbaceous species and willow shrub were tested in two different series of tests respectively. Xylem water pressure was monitored via a second set of HCTs. The experiments were designed to compare evaporation and transpiration in both energy-limited and water-limited regime. Experimental results show that vegetation does not necessarily enhance water uptake by the atmosphere if compared with water removal occurring in absence of vegetation (bare soil). In the energy limited regime, the performance of transpiration (through the plant) with respect to evaporation (from base soil) depends on the competition between aerodynamic resistance and canopy resistance. In the water-limited regime, vegetation always outperforms because it is capable of extracting water from the deeper layers which are not accessed from the ground surface for the case of bare soil. Numerical simulations of 2D water flow in the bare and vegetated column corroborated these findings. It is

also suggested that transpiration be modelled by imposing suction rather than water outflow via a sink term in the water flow equation.

5.1 Introduction

Traditional techniques for stabilisation of natural and man-made slopes (cut slopes and earth embankments) are not designed to be carbon-efficient and the worldwide ambition to reduce carbon emissions in the next decades calls for new approaches to be developed. In this context, vegetation represents an ideal 'technology' because its 'installation' has limited carbon footprint and has the benefit of acting as carbon sink, with 'operational' carbon fixed in vegetation or soil via CO_2 absorption due to photosynthesis (e.g. Shao et al 2015). In addition, vegetation is potentially the only viable 'diffuse' remedial measure for rainfall-induced diffuse shallow landslides, which are one of the most critical natural hazards as they often evolve into highly destructive flow slides and debris flows.

The interplay between vegetation and slope stability has long been recognised, for example there is evidence that deforestation can lead to an increase in landslide frequency(Guthrie, 2002; Saito et al., 2017). The first step towards 'engineering' vegetation (trees, shrubs and grass), i.e. design vegetation-based remedial measures based on quantitative analysis, is to understand and model the mechanisms by which vegetation can reinforce the ground.

Vegetation can enhance stability via root mechanical reinforcement, i.e. roots can act as anchors and/or improve mechanical properties by enmeshment similarly to fibre reinforced materials . However, the mechanical effect of roots is limited to the rooting zone and there is no benefit for the case where the failure surface develops below the rooting zone. This is often the case of shallow landslides as the failure surface tends to develop between the rooting zone and the underlying bedrock (Balzano et al. 2018; Balzano et al. 2019).

On the other hand, hydrological effects due to water content depletion can extend beyond the rooting zone (Greenway, 1987). Measurements by Ziemer(1978) showed that the hydrological influence of a tree could reach layers much deeper than the rooting zone, with the greatest moisture depletion occurring at 2-4 m beneath ground level and extending laterally up to 6 m from a single tree. Biddle(1983) and Biddle (1998) observed persistent differences in soil moisture within and below the rooting zone in clay ground vegetated with poplar trees compared with the non-forested control ground. The increased water depletion in the ground vegetated with poplar trees extended up to a depth of 3.5 m and did not disappear during the wet season.

Soil moisture depletion in the (unsaturated) vadose zone is accompanied by an increase in shear strength as widely demonstrated experimentally (Tarantino and El Mountassir 2013). As a result, hydrological effects of vegetation have direct impact on slope stability.

Understanding and modelling water uptake by roots is key to quantify the effect of transpiration on soil moisture regime. Water sucked up by plants is mainly related to the replacement of water lost in the leaf by evaporation when stomata open up to allow the ingress of CO_2 for photosynthesis. Less than 10 % of the water extracted from the soil is used for physiological purposes (Sinha, 2004). Transpiration is essentially driven by the evaporative demand of the atmosphere similarly to evaporation occurring at the surface of bare ground. Both these processes are regulated by the solar energy supplied and the difference in vapour pressure between the evaporative surface (the surface of bare soil or the surface of the leaf) and the air in the surroundings (Monteith, 1965).

Since the atmosphere removes water from the ground also in the absence of vegetation, any potential beneficial effect of the vegetation in soil moisture depletion should be assessed in comparison with water extracted from bare soil by evaporation.

The aim of the paper is to investigate experimentally the differences in the two mechanisms of water removal, transpiration and evaporation, and to provide a

conceptual framework for assessing whether and how vegetation is beneficial in reinforcing the ground hydrologically.

The experimental study consisted in comparing the response of a column of bare soil and column of vegetated soils subjected to the same atmospheric boundary conditions. One column test involved a sample vegetated with an herbaceous species and one test where a shrub of willow was transplanted into the column. The evaporation and transpiration rates were monitored using balances and the evolution of suction and water content profiles in the soil were monitored by means of High-Capacity Tensiometers (HCT) and Time Domain Reflectometry (TDR) probes.

For test on the shrub of willow, the plant xylem water pressure was also monitored via an additional pair of HCTs.

5.2 Material and Methods

5.2.1 Experimental Setup

Two cylindrical columns were implemented, one to accommodate a vegetated soil sample and the second one to accommodate a bare soil sample. The first column was vegetated with grass for the first test (Figure 5.1.a) or with transplanted shrub for the second test (Figure 5.1.b). The two columns were placed on balances to monitor the evaporation rate (bare soil), the evapo-transpiration rate (soil vegetated with grass), and transpiration rate (soil vegetated with shrub). The terms evapo-transpiration is adopted here for the soil vegetated with grass as the processes of evaporation from the ground surface and transpiration through the grass occur concurrently. Holes were created on the sides of the columns to accommodate Time Domain Reflectometry (TDR) probes and the High-Capacity Tensiometers (HCT), in order to monitor water content and suction profiles respectively. Column dimensions and instrument positions are reported in (Table 5.1). The bottom of each column was provided with a filter made of a layer of coarse sand and gravel sandwiched between to geotextile sheets. The columns were connected at their bottom to an external water reservoir via a valve. To

impose an initial hydrostatic pressure in the column, the water reservoir was positioned level with the top surface of the sample and the valve was maintained opened. When transpiration/evaporation occurred, the valve was maintained closed. A ventilator was used to modify transpiration/evaporation rate with respect to the one naturally occurring in the laboratory.

Table 5.1:Column dimension and instrument location

Column dimension	
Inner diameter [mm]	295
Inner height [mm]	250
Wall thickness [mm]	9
Drain height [mm]	10
Instruments location (from top)	
Level 'HIGH' (1 TDR- 1 HCT) [mm]	40
Level 'MEDIUM' (1 TDR – 1 HCT) [mm]	125
level 'LOW'(1 TDR – 1 HCT) [mm]	210

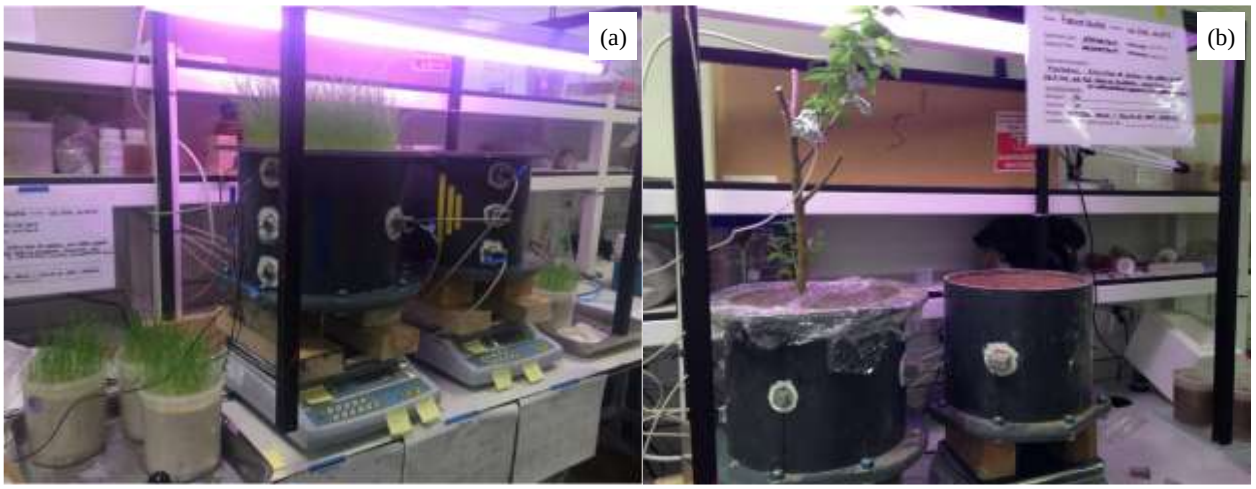

Figure 5.1:Infiltration column, vegetated and bare soil; (a) Herbaceous species*: Lollium Perenne*; (b) Shrub: *Salix Cinerea*

5.2.2 Soil, plant species, and sample preparation

5.2.2.1 Test Lollium Perenne (grass)

The final soil was obtained mixing 4 different 'ingredient' soils of known grain size distribution, in order to obtain a well-graded material. The result of the mixing was a silty sand (Soil A in Figure 5.2), which was expected to be characterised by an air-entry value of few kPa and a gradual transition from saturated to residual state. The soil was initially mixed dry, sprayed with water to reach 9.6 % water content, mixed again and compacted to 100 kPa vertical stress. Both columns were then connected to the external reservoir to saturate the sample. The column was then isolated from the water reservoir and the samples were let dry for 7 days. This allowed reaching a final bulk density of $\rho_d = 1.85\ {}^{g}/_{cm^3}$.The surface of one of the columns was then seeded with the herbaceous species *Lolium Perenne* (family of *Poaceae)*. The plant is commonly used in Europe for surface protection, shallow reinforcement and erosion control (Coppin & Richards, 1990). The herbaceous species was chosen because of its fast growth as it typically germinates within 4-5 days from sowing. In order to obtain an evenly distributed root density, 3 seeds were inserted in 1-cm deep-holes located horizontally on a grid of 1 cm spacing. After seeding, the soil was kept moist to allow for grass growth. Irrigation was achieved by connecting the column to an external water reservoir maintained level with the bottom of the column. The two columns were disconnected from the water reservoir after 15 days from sowing and the water was let to freely drain from the bottom. The grass was let grow for 28 days before the beginning of the test, while the soil was kept moist by imposing a water table at the middle height of the column.

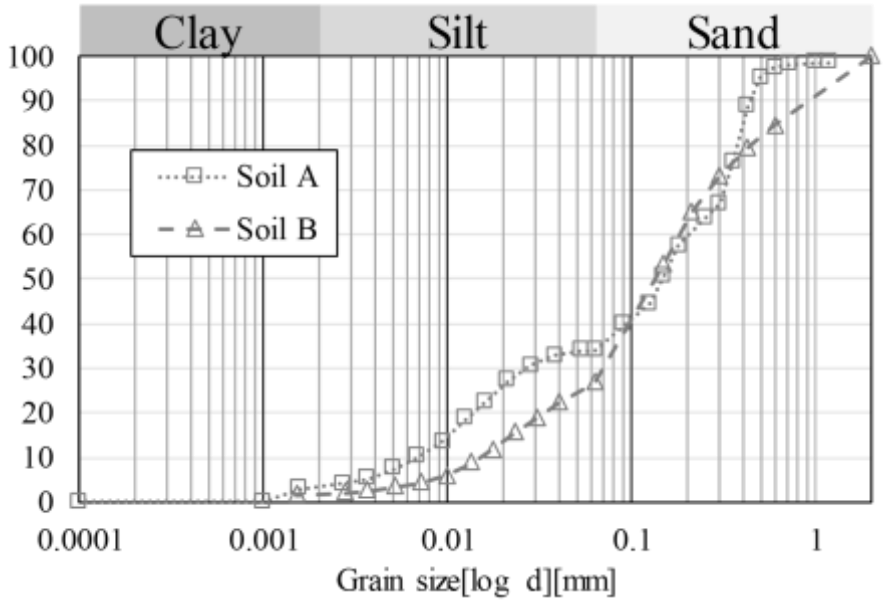

Figure 5.2: Grain size distribution

5.2.1.1 Test Salix Cinerea (shrub)

The soil used in this test was a silty sand taken from 'Rest and Be Thankful' site (Scotland, UK). The soil was dried in the lab and sieved to 2 mm. The grain size distribution is reported in Figure 5.2 (Soil B).

The 'bare' sample was created by water pluviation. The column was filled with water, the soil was added gradually from the water surface and let sediment until the column was filled up to 10 mm from the top edge of the column. Water was then allowed to drain from the bottom of the column for 2 days with the sample surface undergoing some settlements. The valve at the bottom of the column was then closed, the column was filled again with water, and additional soil added by deposition. The valve was opened again to allow water to drain and the additional top layer to settle. At the end of this procedure, the sample surface was located at about 10 mm below the column top edge.

To prepare the vegetated sample, a willow (*Salix Cinerea*) was selected. This plant is well adapted to both moist and dry conditions and it is commonly used as riparian vegetation, especially for erosion control, shallow and deeper reinforcement and

moisture depletion (phreatophytes) (Coppin & Richards, 1990). The shrub initially developed in loose organic soil, and was then transplanted into the column before the test. Before transplanting, the root system was removed from its original pot and submerged in water for 48 h, in order to remove all the original organic soil. The plant was then suspended into the column with the root network positioned at the middle height of the column (see Table 5.2 for the final root dry mass distribution). The column was then filled with water and the soil was added gradually by deposition using the same procedure illustrated above for the 'bare' sample. Water deposition allowed the soil particles to penetrate into the root network. During the transplanting, the willow was kept under complete darkness to prevent transpiration and avoid plant water stress.

The profile distribution of the root dry density in the two columns is reported in Table 5.2. Roots were separated from soil at the end of the test and let dry in the oven at 60°C for approximately 2 weeks.

The final dry density of the two samples was $\rho_d = 1.47\ g/cm^3$ for the bare soil and $\rho_d = 1.57\ g/cm^3$ for the vegetated column. After the formation of the samples, soil water was let evaporate from the surface for 15 days in both columns. Afterwards, the columns were connected to an external reservoir with its water level positioned at mid height of the column in order to ensure moist conditions required for the shrub to grow. The shrub was let to grow into the newly formed soil for almost 2 months before the beginning of the test. Both columns were subjected to the same boundary conditions for the whole period preceding the test.

Table 5.2: Distribution of root biomass for *Lollium perenne* and *Salix cinerea*

Test	Depth (from the top border of the soil specimen) [cm]	Roots dry mass [g]
Test 1 *Lollium perenne*	12-23	5.53
	0-12	0.83
Test 2 *Salix cinerea*	16-23	8.63

7-16	36.34
0-7	4.2

5.3 Experimental procedures

5.3.1 HCT calibration and conditioning

The High-Capacity Tensiometers (Tarantino & Mongioví 2003) were calibrated in the positive range 0-1500 kPa and the standard deviation of the error was found to be no greater than 4 kPa. The HCTs were then let to cavitate by positioning them on a very dry soil sample and subsequently pressurised at 4 MPa for 48 h before the beginning of the test. This procedure maximises the maximum sustainable suction and the measurement duration (Tarantino, 2004). The HCTs were removed from the saturation chamber and placed into free water, to let the instrument to equilibrate to atmospheric pressure and allow for zeroing. The HCTs were then installed through the lateral wall of the column. A saturated paste –prepared at approximately the liquid limit—was applied on top of the tensiometer porous ceramic filter to ensure hydraulic continuity between the soil sample and the instrument. The contact paste for the *Lollium Perenne* test was prepared with kaolin clay as 5% of kaolin clay was present in the soil mixture (Soil A). The contact paste for the *Salix Cinerea* test was prepared using the fraction of Soil B passing through the 53 μm sieve. In this way, the paste was made similar to the soil to which the HCTs were put in contact (Marinho, et al., 2008). The presence of the saturated soil paste requires some time –usually a few hours—to achieve hydraulic equilibrium between the instrument, the paste, and the soil.

5.2.1 TDR calibration

The TDR system consisted of the Campbell Scientific TDR100 unit and 75mm long 3-rod probes. The electrical length of the TDR probe and the time at which the electromagnetic step pulse enters rods were calibrated for each TDR probe by

performing measurement in air and demineralized water (Tarantino, et al., 2008). The apparent dieletric permittivity K_a inferred from the velocity of propagation of the electromagnetic wave through the probe was then related to the soil volumetric water content through the equation suggested by Ledieu, et al.(1986):

$$\theta = 0.1138 \cdot \sqrt{K_a} - 0.1758 \quad [1]$$

5.2.2 Test *Lollium Perenne* (grass)

Following the grass growth period, the valve at the bottom of the column was closed and the test commenced. The test lasted 29 days, with continuous monitoring of the evapo-transpiration rate and the evolution of the suction and water content profiles. The system was subjected to the atmospheric boundary conditions described in Table 5.3; it was exposed to natural ventilation from day 1 to day 19 and to forced ventilation imposed at the surface of the two columns from day 19 to 29. The forced ventilation was imposed in order to increase the evaporation rate and possibly bring the specimens into the water-limited regime. Day/night cycles were imposed using a growth lamp.

5.2.3 Test *Salix Cinerea* (shrub)

The water level of the reservoir was raised up to the top surface of the specimens for 24 h prior to the start of the test to impose a condition of complete saturation before the beginning of the test. Water was then let to drain overnight (~12h) from the bottom of the column and the valve was then closed. During the whole duration of the test, the bare surface of the vegetated sample was covered with a plastic film to prevent evaporation and allow the monitoring of the sole transpiration.

The test lasted for 88 days, the atmospheric boundary conditions imposed are summarised in Table 5.3. The columns were subjected to day/night cycles (using a growth lamp) and forced ventilation (fan), in order to increase the transpiration rate. Two HCTs were applied on the trunk of the willow, in order to monitor continuously the negative water pressure in the tree, and a Pressure Chamber was used for

discontinuous reading of the negative water pressure in the leaves (see Chapter 3 for the complete description of the setup and experimental results).

Table 5.3: 'Atmospheric' Boundary Conditions during the test

Stage	BC1	BC2
First test: *Lollium Perenne*		
Time interval (days)	0-18	19-24
Forced ventilation (fan)	No	Yes
Second test: *Salix Cinerea*		
Time interval (days)		0-88
Forced ventilation (fan)		Yes
Daily cycle:		
Growth lamp (h)	14	14
Darkness (h)	10	10
Environmental conditions:		
Temperature (°C)	20°C	20°C
Relative humidity (%)	~45 %	~45 %

5.3 Results

The measurement of the average volumetric water content and the outward water flux were derived from the change in weight over time recorded continuously by the balances. The average volumetric water content $\bar{\theta}$ was calculated as:

$$\bar{\theta} = \frac{V_w}{V_{tot}} = \bar{\theta}_{ref} \pm \frac{\Delta m / \rho_w}{V_{tot}} \qquad [2]$$

where V_w is the volume of water in the sample, V_{tot} is the total volume of the sample, Δm is the cumulative change in mass with respect to the reference time, ρ_w is the density of water, $\bar{\theta}_{ref}$ is the average volumetric water content of the column of soil at the reference time corresponding to end of test for the *Lollium Perenne* (grass) test and to the beginning of the test for the *Salix Cinerea* (shrub) test. The reference volumetric water content was calculated based on the total mass and total volume of the sample respectively and its gravimetric water content (the sign on the right-hand side of Eq. [2] depends on the reference time considered).

Figure 5.3.a show the variation in average volumetric water content over time for the bare sample and the sample vegetated with grass respectively. Natural ventilation (BC 1) was imposed until day 19 and forced ventilation (BC2) was imposed using a fan from day 19 to day 29. When the bare and vegetated soil are compared in terms of average volumetric water content, no significant differences are appreciated. However, significant differences emerge when the evaporation and evapotranspiration rates for the bare and vegetated samples are compared in Figure 5.3.c (evaporation and evapotranspiration rates were calculated assuming an evaporative surface equal to the surface of column). Evaporation from bare soil and evapotranspiration from vegetated soil are similar for the case of natural ventilation (BC1) whereas they diverge significantly under forced ventilation (BC2). In addition, there is a time interval where the evaporation/evapotranspiration remains constant (with its value shifting upward when the fan was switched on) and a time interval where the evaporation/evapotranspiration starts to decay. The decay occurs earlier for the bare soil.

Figure 5.3.b and Figure 5.3.d report the average volumetric water content and the evaporation/transpiration rates for the bare sample and the sample vegetated with the shrub. Again, an evaporative surface equal to the surface of the column was considered to calculate the evaporation/transpiration rates. In this test, only forced ventilation was imposed (BC2). Differences in average volumetric water content are significant, with the bare sample drying at a faster rate than the vegetated one. Similarly to the experiment involving the sample vegetated with grass, there is a time interval where the evaporation/transpiration remains constant and a time interval where the evaporation/transpiration starts to decay. Again, the decay occurs earlier for the bare soil.

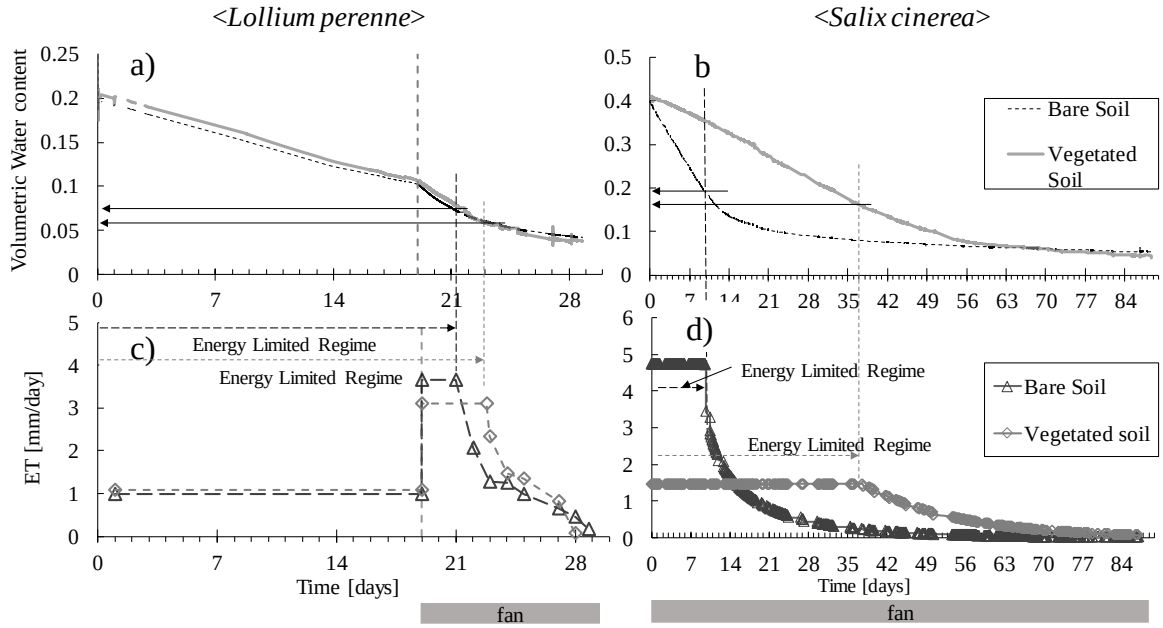

Figure 5.3: *Lollium perenne* test (grass): (a) volumetric water content over time and (c) evaporation/evapotranspiration rate for bare and vegetated soil. Salix cinerea test (shrub): (b) Volumetric Water Content over time and (d) evaporation/transpiration rate for bare and vegetated soil.

The process of water extraction occurring at the surface for the bare soil and distributed along the rooting zone for the vegetated soil can be further investigated by inspecting the measurement of pore-water pressure and volumetric water content profiles derived from HCTs and the TDR probes respectively (Figure 5.4).

Figure 5.4.a and Figure 5.4.c compare the pore-water pressure and the water content profiles for the bare soil and the soil vegetated with grass. Up to day 19, the profiles are essentially coincident, which is consistent with the similar average water content and evaporation/evapotranspiration rate observed until day 19 (Figure 5.3.a,c). When the evaporation/evapotranspiration rate increases because the fan is switched on (day 19 to day 21), the increased rate is accommodated differently by the bare and vegetated soils. Higher pore-water pressure gradients develop in the bare soil close to the surface, which is intuitive because water extraction is concentrated at the surface. On the other hand, pore-water pressure gradients are smoother in the vegetated soil which is also intuitive because water extraction is distributed across the entire sample depth. The gradients in the vegetated soil, higher at the top and slightly lower at the bottom are consistent with the root density that decreases with the depth.

This pattern consisting of high pore-water pressure gradients close to the surface in the bare soil and moderate gradients evenly distributed in the vegetated soil is even more pronounced at the end of the test (day 29) when the evaporation/evapotranspiration rate had reduced significantly. It is worth noticing that, in the bare soil, gradients in water content are less noticeable than gradients in pore-water pressure from day 19 to day 29. This is because the soil is approaching the residual state where water content changes slightly despite large variations in pore-water pressure.

Figure 5.4.b and Figure 5.4.d compare the pore-water pressure and the water content profiles for the bare soil and the soil vegetated with shrub. On day 0, pore-water pressures are close to zero and the water contents are close to the saturated ones. Water availability therefore allows evaporation and transpiration to occur at their maximum. On day 17, the pore-water pressure and the water content in the vegetated sample have decreased only slightly. In the bare soil, pore-water pressure and the water content have decreased significantly and, at the same time, high gradients developed close to the surface. Pore-water pressure in the top layer had become so negative (possibly around -2000 kPa) that the measurement became unstable and eventually the tensiometer closer to the surface cavitated. This is the reason why the measurement of the uppermost tensiometer in the bare soil is missing from day 17 onward. It is interesting to observe that the maximum depletion in pore-water pressure and water content occurs at the centre of the sample were the concentration of roots was higher according to the post-mortem measurements (Table 5.2). It is often observed that water uptake is proportional to active root density (Salisbury & Ross, 1992).

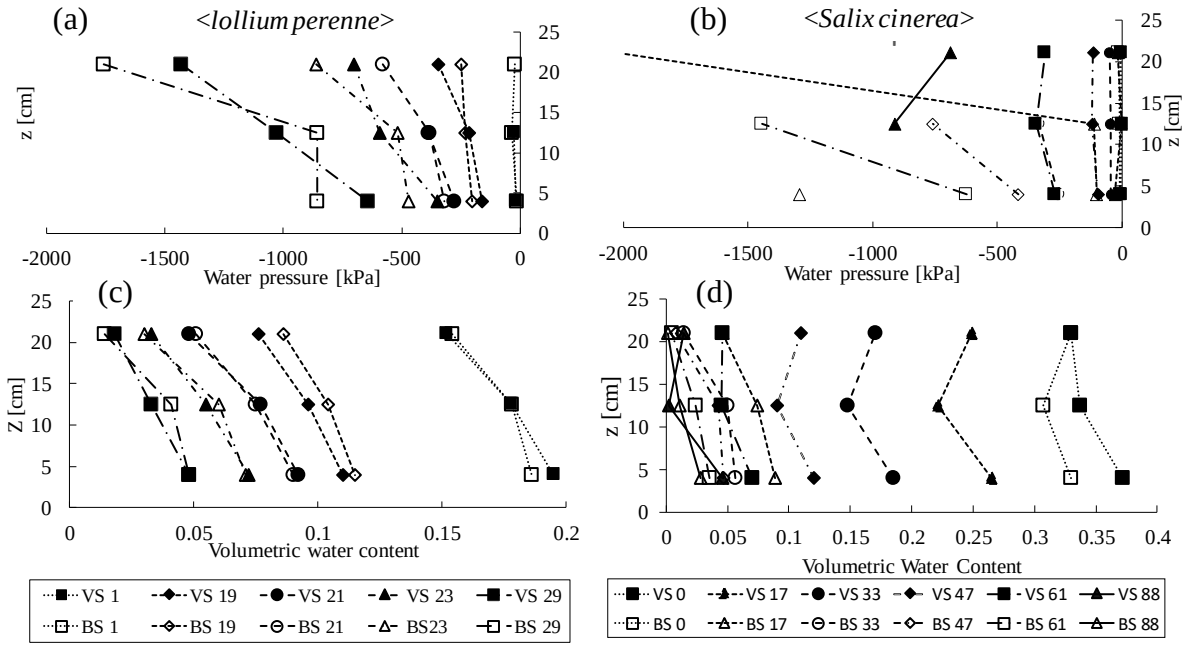

Figure 5.4:*Lollium perenne* test (grass): (a) suction profiles and (c) volumetric water content profiles over time for bare (open symbols) and vegetated soil (solid symbols);. *Salix cinerea* test: (b) suction profiles and (d) volumetric water content profiles over time for bare (open symbols) and vegetated soil (solid symbols).

Figure 5.5.a compares the (negative) water-pressure measured in the willow xylem with the (negative) pore-water pressure measured in the soil at three different depths. The measurement by HCTs on the xylem shows daily oscillations in phase with the daily cycles imposed by the growth lamp. Xylem water fluctuated between -180 and -330 kPa around an almost constant value in the first 35 days, and started decreasing at a faster rate after day 42.

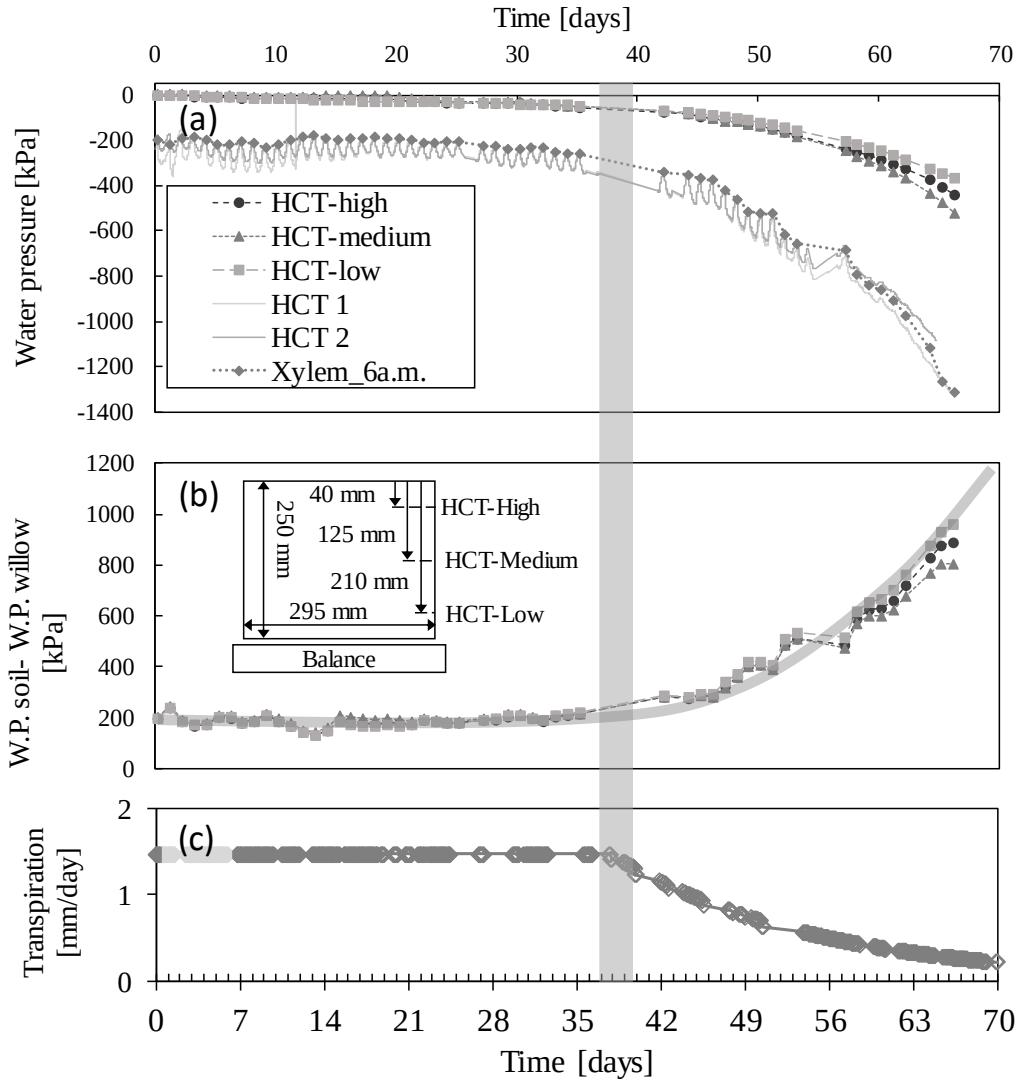

Figure 5.5:(a) Measurement of xylem water pressure and soil water pressure. The points represent the measurement taken at 6am, at the end of the night cycle. (b) Difference between the measurement of water pressure in the xylem and in the soil at 6 am. (c) transpiration rate over time.

The measurements taken at 6am are highlighted with dots. The xylem water pressure at 6am is associated with the maximum daily value and can be considered equivalent to a pre-dawn measurement. If the plant is not under water stress, the plant can be considered to be in equilibrium with the soil (Sellin, 1999).The difference between the value of water pressure in the xylem and on the soil at 6am is reported in Figure 5.5.b. It can be observed that the difference remains essentially constant until day 38 and is observed to increase almost exponentially after day 38. The most striking aspect is that

the increase in the pressure differential occurs at the same time transpiration start decaying from its maximum value as shown in Figure 5.5.c.

5.4 A conceptual framework for vegetation-driven hydrological 'reinforcement'

The results presented in the previous section are specific to the soils, plant species, and atmospheric and hydraulic boundary conditions imposed in the experiments. In addition, the laboratory scale is inevitably not truly representative of the field scale. The challenge in this work is to identify some of fundamental mechanisms of water extraction that can be extrapolated to the field scale.

In the two experiments presented above, regardless of whether water was removed by evaporation from bare soil, evapotranspiration from the soil covered with grass, and transpiration from the sample with the transplanted shrub, two regimes have been clearly identified:

1) *Energy-limited regime* – The hydraulic system (soil or soil plus plant) can supply the water demanded by the atmosphere. Loosely speaking, this occurs when the soil is sufficiently wet or the soil hydraulic conductivity is relatively high. If the atmospheric conditions remain constant, the rate of water uptake remains constant. On the other hand, any change in the atmospheric conditions modifies the water uptake (e.g. the wind speed as in the 'grass' experiment). If the hydraulic system made of soil or soil plus plant can accommodate the evaporative demand of the atmosphere, water uptake takes place at its maximum rate (potential evaporation/evapotranspiration/transpiration).
2) *Water-limited regime* – The hydraulic system can reach a condition where it can no longer supply the water demanded by the atmosphere. Loosely speaking, this occurs when the soil is relatively dry and/or the soil hydraulic conductivity becomes relatively low. Water uptake is therefore dictated by the soil and its hydraulic interaction with the root network. Water uptake occurs at a rate that is lower than the maximum.

These two regimes of evaporation/transpiration are well known and were clearly observed in Figure 5.3.c and Figure 5.3.d. The efficiency of transpiration in removing water from vegetated ground in comparison with the water removed by evaporation from the bare ground is discussed separately for these two regimes.

5.4.1 Energy-limited regime

The water uptake in the energy-limited regime (potential evapotranspiration) can be conveniently represented by the Penman-Monteith equation (Monteith, 1965). For the case negligible solar net radiation R_n, this equation becomes:

$$PET = \frac{1}{\lambda}\frac{\rho_a \cdot c_p \cdot p_{v0}(z) \cdot [1 - RH(z)]}{\Delta \cdot r_a + \gamma \cdot (r_a + r_c)} \quad [3]$$

where *PET* is the potential evapotranspiration rate, λ is the latent heat of vaporisation of water at the air temperature *T*(z), Δ is the slope of the saturation vapour pressure curve at the air temperature *T*(z), γ is the psychrometric constant at the air temperature *T*(z), ρ_a is the air density, c_p is the specific heat of air, p_{v0} is the saturation vapour pressure at the air temperature *T* at the elevation *z*, *RH* is the relative humidity at the elevation *z*, r_a is the resistance term for the aerial transport of water vapour from the canopy, and r_c is the canopy resistance (resistance at the leaf level of the transpiring crop).

Upon evaporation, water molecules tend to saturate the first layer above the evaporative surface, reducing therefore the vapour pressure gradient regulating the evaporation process. The rate of evaporation depends on how efficient this saturated layer is swept away and replaced with relatively dry fresh air. This depends on the turbulence the overlaying atmosphere, which is in turn controlled by the wind velocity and the roughness of the evaporative surface. The higher the wind velocity and the surface roughness, the lower is therefore the aerodynamic resistance r_a, The canopy resistance r_c takes into account the additional resistance associated with the water flowing from the soil to the xylem through the roots and the resistance due to water

vapour flowing through the leaf stomata (Canny, 1977). The canopy resistance is plant dependent.

Differences in potential evapotranspiration between the bare and vegetated soils subjected to the same atmospheric conditions lie on the differences between r_a and r_c. The canopy resistance r_c is obviously zero for the bare soil and greater than zero for the vegetated soil. The aerodynamic resistance tends to be relatively high for the bare soil because the evaporative surface is relatively smooth. On the other hand, r_a tends to decrease when moving from short vegetation (grass) to tall vegetation (trees) because of the increase of air turbulence associated with the wind flowing over a wavy canopy surface. This effect could not be captured in these laboratory experiments because only a single 'tree' was tested. In the laboratory, it would be reasonable to assume that r_a is very similar for the bare and vegetated soils.

Eq. [3] can be used to explain the differences in potential evapotranspiration observed in the experiments. For the test where the bare soil was compared with the sample vegetated with grass, the transition from natural to forced ventilation was accompanied by a decrease in the aerodynamic resistance r_a , in turn resulting in an increase in the rate of water uptake, both in the bare and vegetated soil (day 19 in Figure 5.3.c).

When natural ventilation was imposed, energy-limited evapotranspiration between bare and vegetated soil was very similar (days 0 to 19 in Figure 5.3.c) and became higher in the bare soil when forced ventilation was imposed (days 19 to 21 in Figure 5.3.c). This is because the aerodynamic resistance was very high for the case of natural ventilation and, as a result, the canopy resistance had a relatively little weight in the denominator of Eq. [3]. When forced ventilation was imposed, the aerodynamic resistance dropped and the canopy resistance in the vegetated grass started playing a role, causing the evapotranspiration from vegetated sample to be lower than the one from bare soil.

This effect was more pronounced in the experiment involving the willow tree, where potential evaporation from bare soil was significantly higher than potential transpiration through the shrub is (days 0 -10 Figure 5.3.d). In this case, water was removed from the vegetated sample solely by transpiration (the soil surface was

covered), and this amplified the difference with respect to the one observed in the sample vegetated with grass, where water uptake was a blend of transpiration and evaporation.

In conclusion, the competition between potential evaporation from bar soil and evapotranspiration from vegetated soil depends on the competition between the aerodynamic resistance and the canopy resistance. In these laboratory experiments, differences were only generated by the canopy resistance, which made the bare soil outperforming compared to the vegetate ground. However, in the real world, the lower aerodynamic resistance of the vegetated ground can reverse such a competition in favour of the vegetated ground.

5.5.1 Water- limited regime

Difference between bare and vegetated soil in the water limited regime can be summarised as follows (Figure 5.3.c,d):

1) The transition from energy-limited to water-limited regime occurred earlier in the bare soil.
2) Once entered the water-limited regime, the decay of water uptake rate was relatively sharp in the bare soil compared to the vegetated one.
3) Once entered the water-limited regime, the pore-water pressure profile in the bare soil presented very high gradients close to the surface in contrast with the vegetated soil where pore-water pressure gradients are much lower.

These effects were more pronounced in the experiment with the shrub as water was removed only by transpiration in contrast with the experiment with grass were water was removed by a combination of evaporation and transpiration. The mechanisms behind these responses, which all appear to be in favour of vegetation can be summarised as follows.

Since water in the bare soil is extracted at the surface, high gradients need to develop at the surface and this is achieved at the expenses of a very large decrease in pore-

water pressure in the top layers (Figure 5.6). In turn, this is accompanied by a significant decrease in degree of saturation in the top layers, which tend to act as an impermeable barrier preventing water in the bottom layers to be removed. On the other hand, water extraction in the vegetated ground is well distributed across the sample depth and can therefore take place at much lower gradients. Pore-water pressure and water content remain relatively high and so does the hydraulic conductivity. The soil-plant system can therefore accommodate the relatively high evaporative demand of the atmosphere for longer time (energy-limited regime) and ensure higher flux even in the water-limited regime (Figure 5.3.d).

The more efficient mode of extraction of roots is also reflected in the average volumetric water content recorded at the transition from the energy limited to the water-limited regime. As shown in Figure 5.3.a and Figure 5.3.b, the average volumetric water content at the point of transition is higher in the bare soil than in the vegetated ground.

In conclusion, transpiration through vegetation appears to be always more efficient than evaporation from bare soil in the water-limited regime.

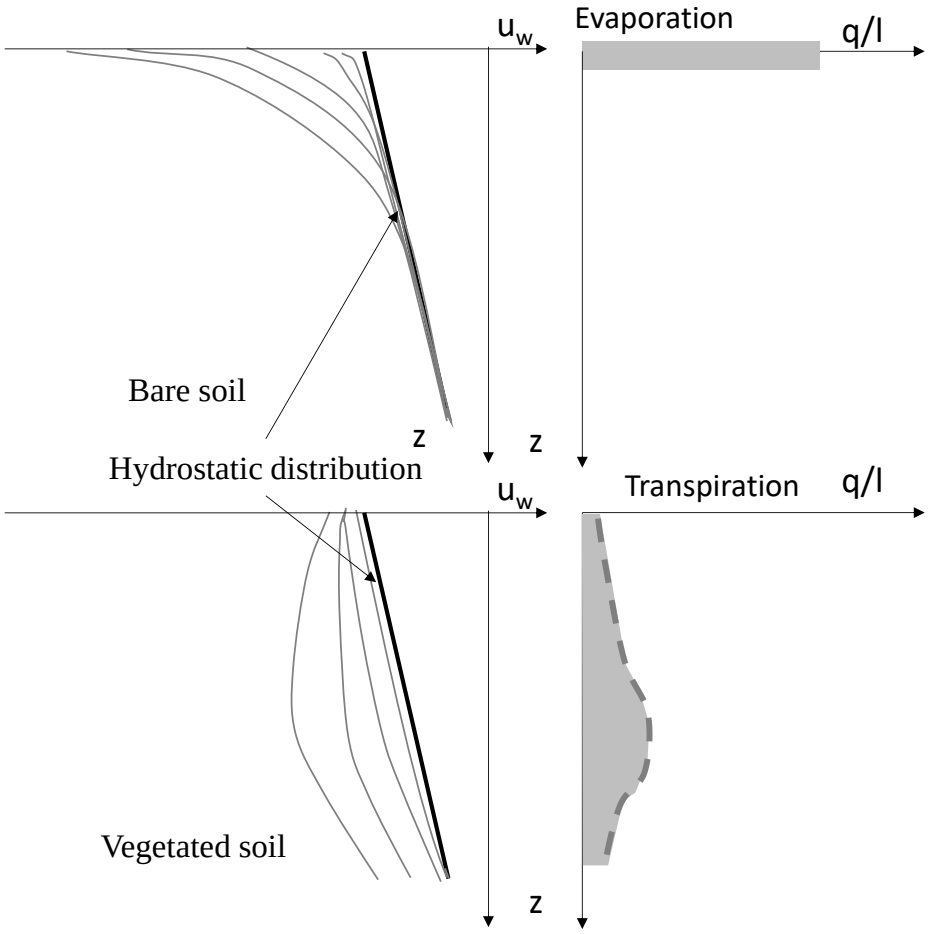

Figure 5.6: Effect of the different mode of extraction in bare and vegetated soil on pore-water pressure profile (initial and boundary conditions analogues to the column under study)

5.6. Numerical investigation into the mode of root water extraction

In the water limited regime, water uptake is controlled by the soil or soil plus plant hydraulic system and the key difference between the bare soil and the vegetated one is the different spatial mode of extraction. To investigate this aspect further, a numerical model for root water uptake was developed.

The flow of water due to evaporation and transpiration was modelled using Darcy's law, extended to the case of unsaturated soils:

$$\vec{v} = -\boldsymbol{K}\, grad(\Psi) = -\boldsymbol{K} grad\left(z + \frac{u_w}{\gamma_w}\right) \quad [4]$$

where $\vec{v}$ is the flow velocity vector, ψ the hydraulic head, K is the hydraulic conductivity, u_w is the pore-water pressure; γ_w the unit weight of water, and z is the vertical coordinate increasing upward. The hydraulic conductivity is a function of the pore-water pressure.

The mass balance equation can be written as follows for an incompressible fluid [5]:

$$\text{div}\, \vec{v} + \frac{\partial \theta}{\partial t} = 0 \quad [5]$$

Richard's equation in terms of hydraulic head can be obtained substituting equation [5] into equation [4]:

$$C \frac{\partial \Psi}{\partial t} = div[\boldsymbol{K} grad(\Psi)] \quad [6]$$

where $C = \gamma_w \, {}^{\partial \theta}/_{\partial u_w}$ is the water storage capacity of the soil. The volumetric water content θ is given by:

$$\theta = n' \cdot S_r \quad [7]$$

where n' is the porosity of the soil and S_r the degree of saturation. The porosity is usually dependent on the pore-water pressure and the definition of the variation of θ would therefore require the coupling of a hydraulic and mechanical model. However, the only deformations were observed in the specimen in the first few weeks of evaporation after the creation of the fully saturated samples, while no visible deformation observed during the evaporation test. The soil skeleton was therefore assumed to be incompressible, i.e. the porosity was assumed to independent of pore-water pressure. The problem of flow within the unsaturated soil could be uncoupled and assessed independently through equation [6]. The problem of water flow was solved numerically via the FEM using the module SEEP/W of the commercial software Geostudio.

5.6.1 Water retention characterisation

The water retention curve was derived from the measurements of pore-water pressure via HCTs and soil water content via TDRs at three different depths as shown in Figure 5.7. Figure 5.8.a reports the curves obtained for the bare soil, Figure 5.8.b the curves for the vegetated soil. Each data point is associated with HCT and TDR measurements at the same depth. The curve so defined was intended to be a dynamic water retention curve, coherently to the dynamic process of soil water removal by evaporation: the static definition (at equilibrium) of the soil parameters results in fact in a lower amount of water hold within the grains for the same suction (Schultze & Durner, 1999). The anomalous points encircled in the vegetated soil graph are related to the atypical trend shown by the central HCT, probably due to a slow process of cavitation occurring within the instrument.

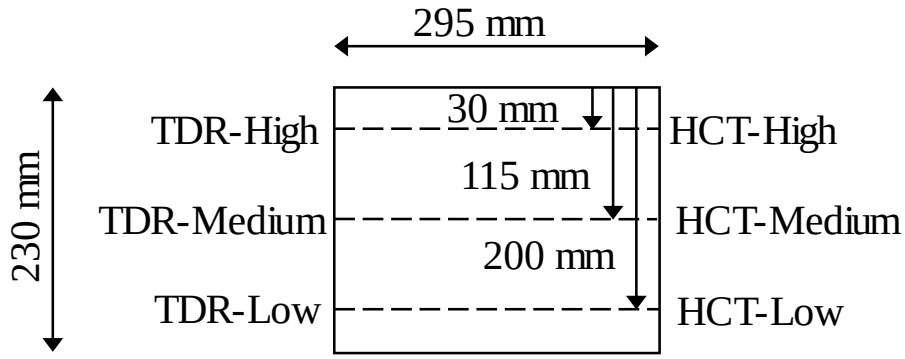

Figure 5.7: Geometry of the soil specimen and position of the instruments in each column

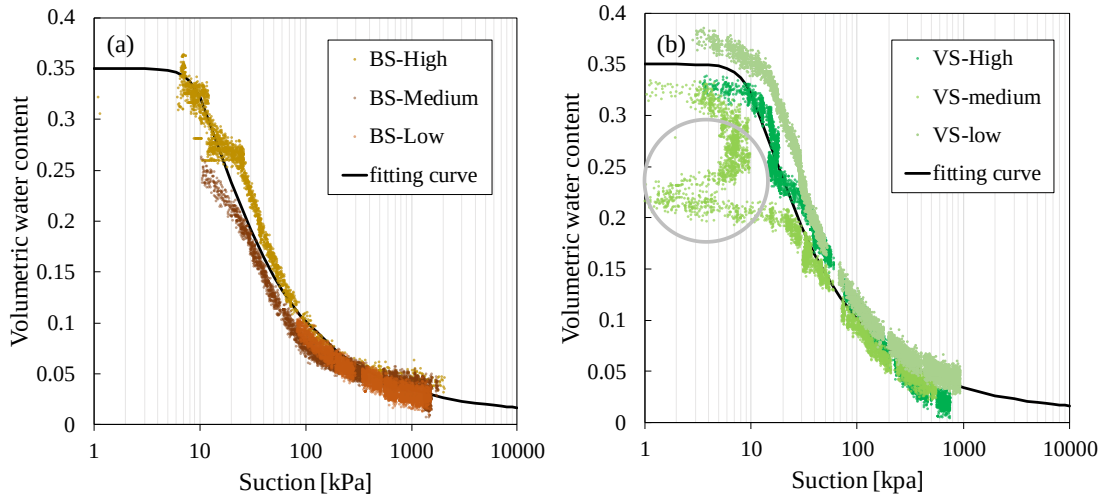

Figure 5.8: water retention curve from experimental data a) on bare soil and b) on vegetated soil.

Data for the two columns have not been represented on the same graph for clarity of presentation. However, these trace the same water retention curve and a single function was used to fit the experimental data, as reported in Figure 5.8.a and in Figure 5.8.b. Water retention data were fitted via the van Genuchten's equation (Van Genuchten, 1980):

$$\theta = \theta_r + \frac{(\theta_S - \theta_r)}{\left[1 + \left(\alpha \cdot (-u_w)\right)^n\right]^m} \qquad [8]$$

where θ is the volumetric water content, θ_r and θ_S are the residual and saturated volumetric water content respectively, u_w is the pore-water pressure of the soil and α, n, m are fitting parameters. The parameters used to fit the experimental data are reported in Table 5.4.

Table 5.4: Parameters of the van Genucthen fitting curve

θ_S	θ_r	α [kPa^{-1}]	n	m
0.35	0.01	0.1	4.559014	0.115

5.6.2 Hydraulic conductivity characterisation

The equation used to characterise the unsaturated hydraulic conductivity was assumed to be a power function of the degree of saturation according to Brooks and Corey (1964):

$$K(u_w) = K_{sat} \cdot {S_{re}}^{\lambda} \quad [9]$$

where $K(u_w)$ is the unsaturated hydraulic conductivity dependent on the pore-water pressure, K_{sat} is the hydraulic conductivity of the soil at saturation, S_{re} is the effective degree of saturation , and λ is a fitting parameter.

The parameters K_{sat} and λ of the hydraulic conductivity function were derived by inverse analysis of the water flow in the bare soil. The effective degree of saturation was derived from the van Genuchten's function:

$$S_{re}(u_w) = \frac{\theta - \theta_r}{\theta_S - \theta_r} = \frac{1}{[1 + (\alpha \cdot (-u_w))^n]^m} \quad [10]$$

To capture the order of magnitude of the saturated hydraulic conductivity and generate an initial value of the hydraulic conductivity for the inverse analysis, a constant-head hydraulic conductivity test was carried out on a specimen of Soil B prepared using the same procedure used to prepare the sample in the column. However, this specimen was much smaller than the sample in the column (diameter of 80 mm equal to the diameter of the oedometer cell used for the hydraulic conductivity test) and was not considered to be truly representative of the sample in the column due to scale effects. The value derived from this test on a specimen of reduced size was $K_{sat} = 5 \cdot 10^{-6} m/s$.

5.6.2.1. Geometry and boundary conditions for inverse modelling

The column of bare soil has been studied assuming a 'one dimensional' water flow. The water flow region was then represented by a column a 1 cm-wide and 23 cm high as shown in Figure 5.9 (height corresponded to the height of the real column). The lateral walls and bottom side of the column were assumed to be impermeable (light

blue lines) and a flux was imposed at the top surface (upward arrows). The flux imposed was derived from the bare soil experimental data (Figure 5.3.d). The initial (hydrostatic) condition was generated by assuming zero pore-water pressure at the base of the column to mimic the condition achieved in the soil column after saturation and subsequent drainage at the bottom of the column.

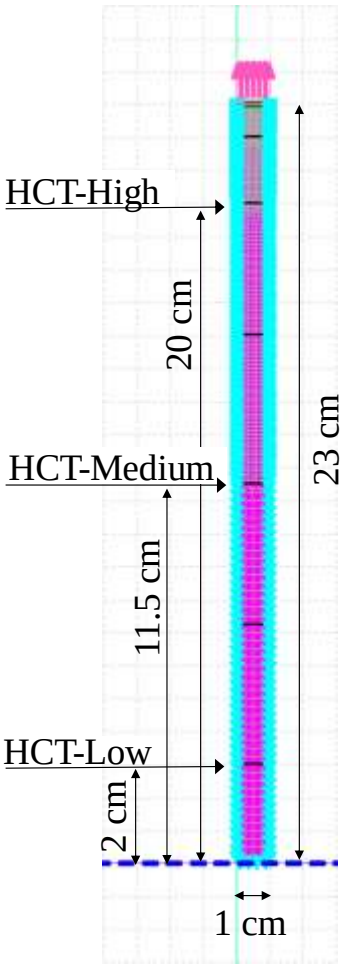

Figure 5.9:Geometry and boundary conditions for the study of the mono-dimensional flow in the column of bare soil.

5.6.2.2. Relative hydraulic conductivity inferred from inverse modelling

The parameters K_{sat} and λ were elected to return the best match between simulated and measured pore-water pressure as shown in Figure 5.10. The thin curves represent the

readings of the pore-water pressure by HCTs at three different depths. The abrupt interruption of the readings before the end of the test is due to cavitation experienced by the HCT-High and HCT-Medium. The thick curves represent the pore-water pressure simulated numerically. The values of λ and K_{sat} derived from the inverse analysis are reported in Table 5.5.

Table 5.5: Parameters of the hydraulic conductivity function

λ	K_{sat}
6	$4.76 \cdot 10^{-7}$

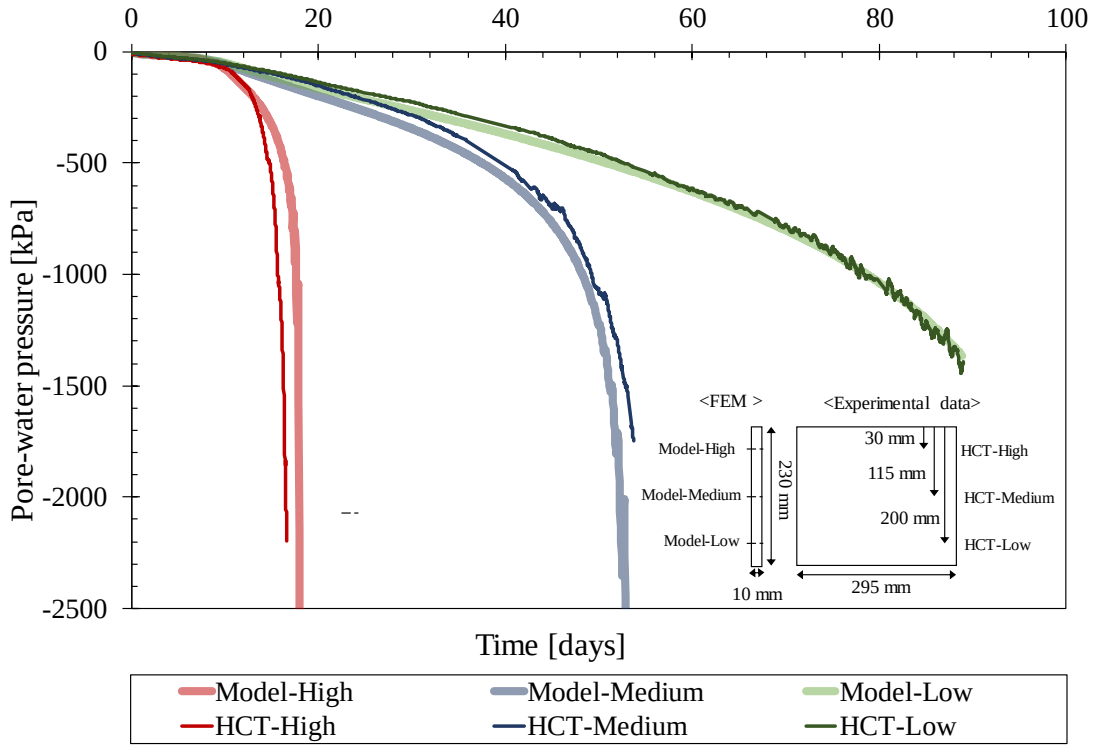

Figure 5.10:Comparison between the pore water pressure over time measured by HCTs and modelled via FEM, with parameters of the hydraulic conductivity function as reported in Table 5.5.

5.6.3 Modelling root water uptake

Once the soil characterised hydraulically, water flow in the sample vegetated with willow could be simulated. As a first approach the flow was considered to be 'one-dimensional' and the presence of roots was simulated imposing a distributed outward

water flow (Neumann condition), equivalent to the use of a 'sink term' in the water flow equation widely used in geotechnical and hydrological applications (Feddes, 1982) (Nyambayo & Potts, 2010). The second approach consisted in imposing a known suction (Dirichlet condition) at a number of discrete locations in the soil sample, to mimic a process of water uptake by a distributed root network regulated by the water pressure in the plant.

5.6.3.1 Imposing root water uptake (flux)

Similarly to the simulation of the bare soil, a column of 1cm wide and 23 cm high was used to simulate one-dimensional water flow (Figure 5.11.a). As for the bare soil, zero pore-water pressure was imposed at the base of the column as initial condition. All boundaries were assumed to be impermeable (light blue lines in Figure 5.11.b).

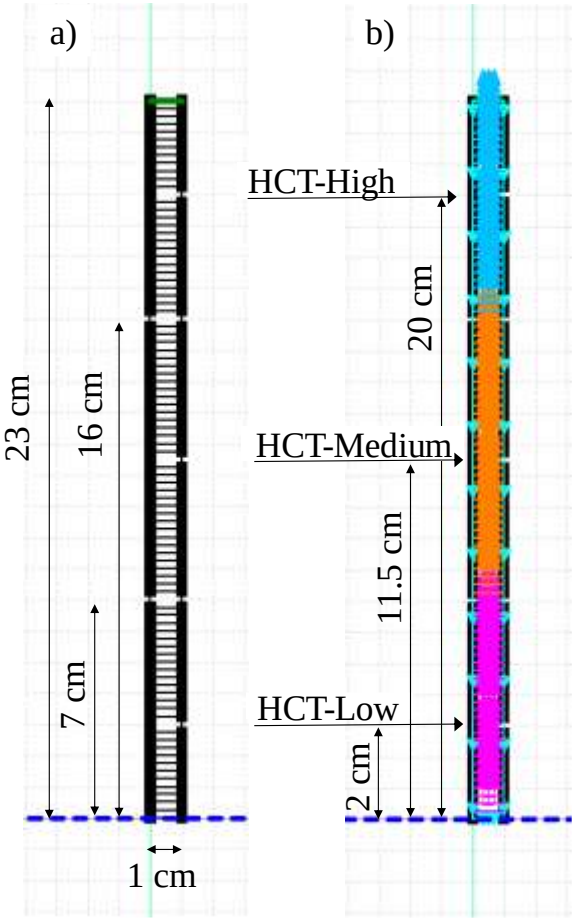

Figure 5.11: a) Geometry and b) boundary conditions for the study of the one-dimensional flow in the soil column with a shrub of *Salix cinerea*.

The outward water flow associated with plant transpiration was introduced by imposing 'extraction lines' within the soil (horizontal lines in Figure 5.11).

The flux imposed at each line was considered to be dependent on the density of root tips, indicator of the younger and more absorptive part of the roots (Salisbury & Ross, 1992; Sanderson, 1983). The number of root tips for three different levels within the column is reported in *Figure* 5.12.a. The outward water flux imposed at each extraction line was assumed to be proportional to the amount of root tips measured. It was the imposed that the cumulative water flux equalled the measured transpiration rate T:

$$\sum_{0}^{7\ cm} q_{i,0-7} + \sum_{7\ cm}^{16\ cm} q_{i,7-16} + \sum_{16\ cm}^{23\ cm} q_{i,16-23} = T \qquad [11]$$

where q_i is the water flux of water applied to a single extraction line. The outer water flux imposed during the first 38 days at each layer (potential transpiration) is reported in Figure 5.12.b. After 38 days the cumulative outward water flow was imposed to decrease according to the experimental data (see Figure 5.3). Details about the imposed water fluxes are reported in Table 5.6.

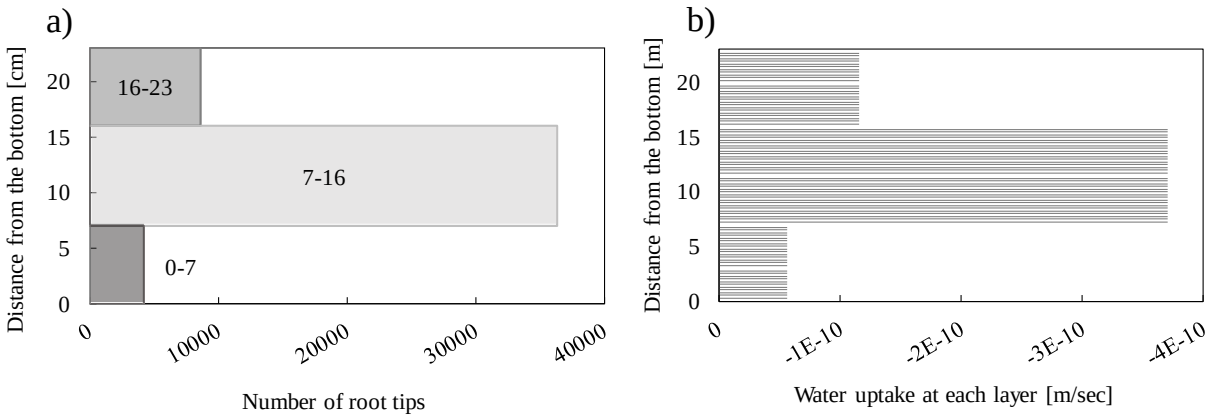

Figure 5.12: a) number of root tips for three specimen sections. b) flux of water imposed at each layer.

Table 5.6: Geometry of the extraction lines

Depth [cm]	No. extraction lines	Extraction line spacing	PT Flux
0-7	26	2.5 mm	$-5./6 \cdot 10^{-11} m/s$
7-16	34	2.5 mm	$-3.7 \cdot 10^{-10}\ m/s$
16-23	26	2.5 mm	$-1.15 \cdot 10^{-10}\ m/s$

The comparison between the pore-water pressure measured (thin curves) and the pore-water pressure simulated numerically (thick curves) is presented in Figure 5.13. As expected, the simulated pore-water pressure in the central part of the column, were most of the roots are concentrated, decreases more rapidly that the pore-water pressure in the top and bottom part. It must be noted that, even if the response at 30 mm and 200 mm depth appears to coincide, the flux imposed in the top and bottom section is different (as reported in Figure 5.12.b). Overall, the simulated pore-water pressure tends to decrease much more rapidly than the measured one. This indicates that the soil is not capable of supplying the water demanded by the flux imposed as boundary condition. Pore-water pressure at the point of extraction is then depleted by the model in the attempt to generate hydraulic gradients capable of accommodating the imposed flux. This suggests that the mechanism of water extraction is not associated with a constant water flux pattern. This is the well-known mechanism of root compensation (e.g. Yadav et al. 2009) whereby roots initially active are 'switched off' when the surrounding soil becomes excessively dry in favour of roots in wetter regions that become active.

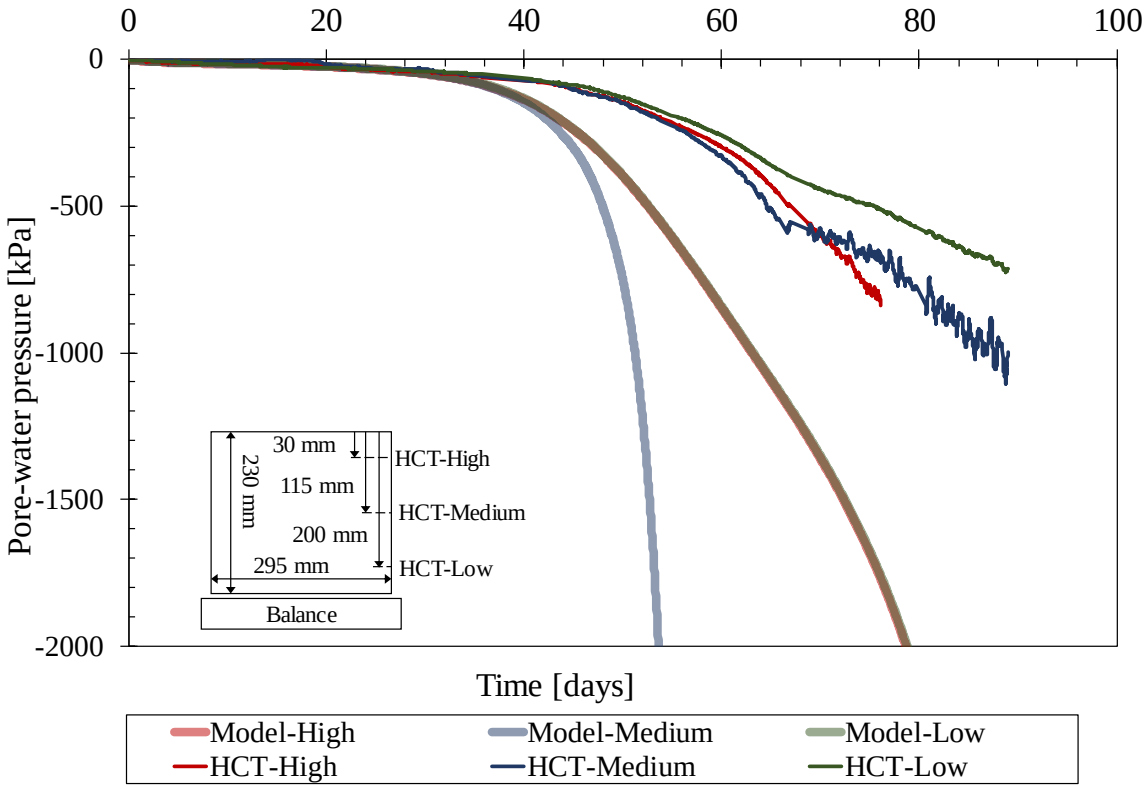

Figure 5.13:Comparison between the pore water pressure over time measured by HCTs and modelled via FEM for imposed flux.

5.6.3.2 Imposing root xylem pressure

The difficulty to model root water uptake with an imposed flux distributed along a given pattern suggests a different mechanism of root water extraction.

Water in the soil moves into the plant because of hydraulic gradients, i.e. water flows from regions at higher water potential (soil) to regions at lower water potential (root> xylem> leaf> atmosphere) (Gardner, 1960). When the water potential in the soil reduces, the water potential in the root must reduce as well in order to sustain the water uptake. The driver of transpiration is therefore the water potential gradient between the soil and the root. The water flux through the plant is therefore the result of such a gradient and not its cause. In this sense, the use of a sink term in the water flow equation to simulate transpiration does not appear to be conceptually correct.

The problem of transpiration through the shrub of willow was modelled by imposing the same water potential (water pressure) in a number of discrete points in the rooting zone to mimic the water potential common to all adsorbing roots. The water pressure was imposed according to the values measured in the xylem. An additional 'resistance' was created around the extraction points to mimic the high-resistance of the soil-root interface (Weatherley, 1979).

A bi-dimensional model was generated to study the water flow in the vegetated column. Again, the boundaries were assumed to be impermeable and zero-pore water pressure was imposed at the base of the sample to generate the initial condition. To simulate the resistance of the soil-root interface, each extraction point was surrounded by an additional 'material' characterised by a lower hydraulic conductivity than the surrounding soil under saturated conditions. The length of each extraction point was fixed to 2.5 mm and the thickness of the interface material was fixed to 7.5 mm (Figure 5.14). The density of extraction points reflected approximately the distribution of root tips at different depths. The 'interface material' was assumed to be saturated and characterised by constant hydraulic conductivity (independent of the water pressure).

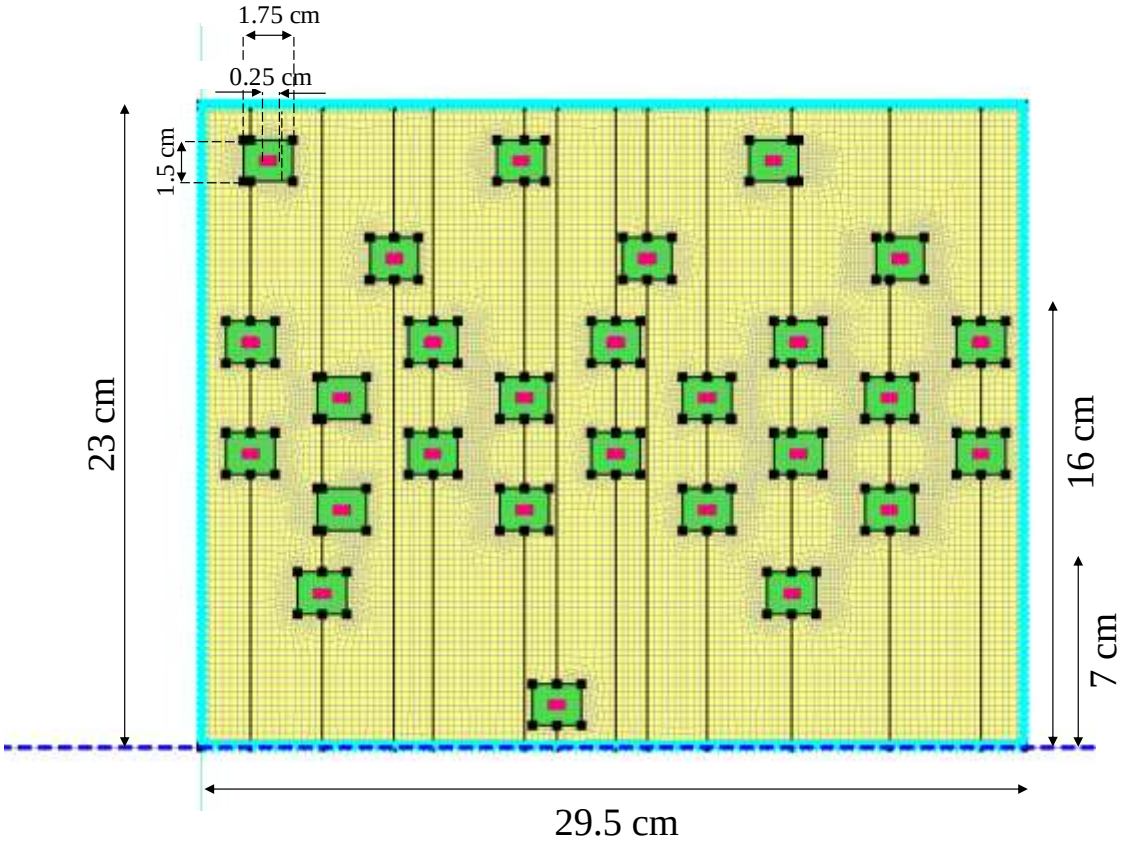

Figure 5.14: Geometry and boundary conditions for the study of the two-dimensional flow in the vegetated column.

The water pressure imposed at the extraction points was derived from the xylem water pressure measurements. A simplified water pressure pattern was considered as shown by the dashed line in the inset of Figure 5.15. This pattern took into account the daily fluctuations of xylem water pressure. After day 65 both HCTs installed on the stem cavitated and it was no longer possible to monitor the evolution of the xylem water pressure. The value imposed at day 88 was arbitrarily fixed at -230 kPa. However, it was verified that the results were not very sensitive to this arbitrary value of water pressure as water pressure of -230+(-100÷+300) kPa returned variations in the final cumulative water loss of less than 1.6%.

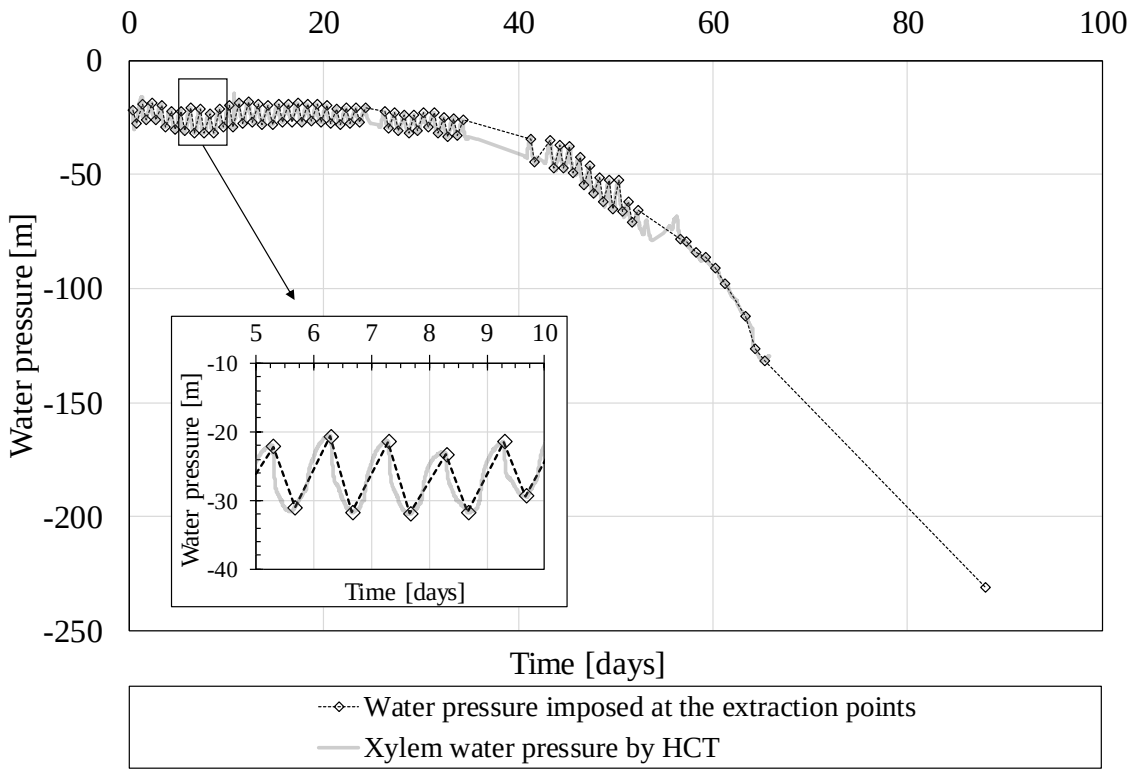

Figure 5.15: Xylem water pressure measured by HCTs on the stem and water pressure imposed at the extraction points.

The hydraulic conductivity of the soil-root interface, $K_{sat,interface}$ was determined by inverse analysis of the cumulative water loss measured experimentally by the balance. Figure 5.16 presents the comparison between the experimental cumulative water loss and the one simulated on the basis of the optimised $K_{sat,interface}$ (Table 5.7) . A correction factor was introduced to take into account the lack of water loss from the volume of the 'resistant elements', whose material was imposed to be saturated at all conditions.

Table 5.7: Characteristics of the soil-root interface

Thickness element	$K_{sat,interface}$ [m/s]
7.5 mm	$3 \cdot 10^{-12}$

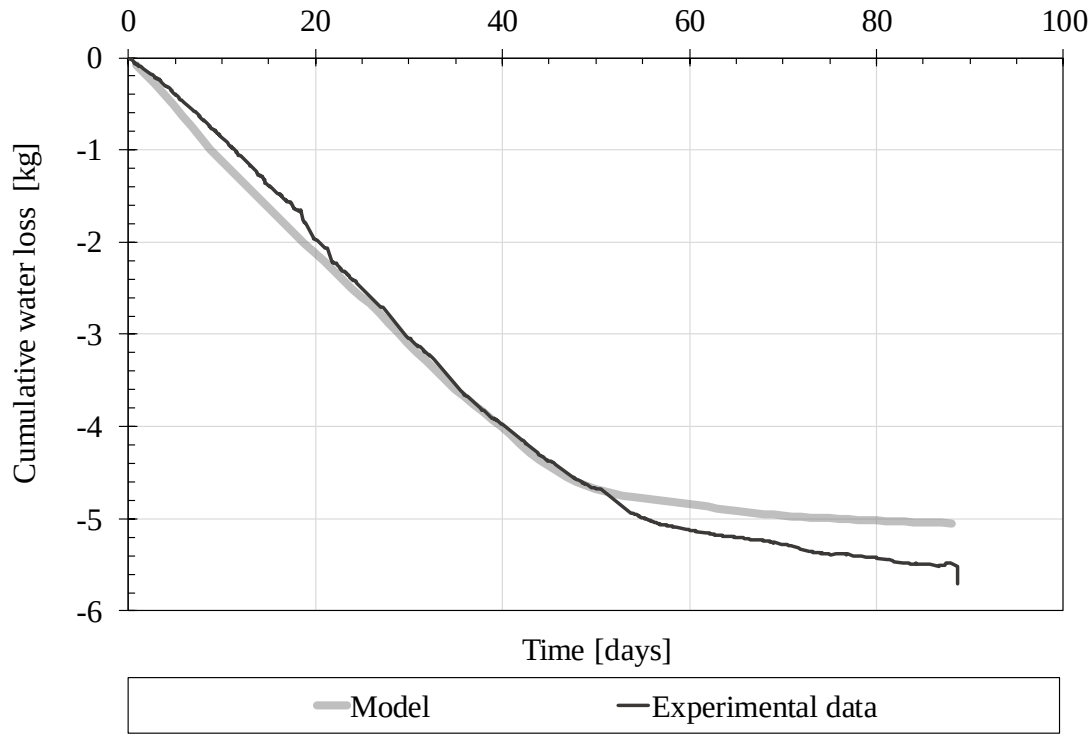

Figure 5.16:Comparison between the cumulative water loss of the system measured via the balance and the cumulative water loss obtained by the FEM model for the vegetated column.

The comparison between the pore-water pressure measured by the HCTs and the pore-water pressure at the corresponding depth simulated numerically is presented in Figure 5.17. The water pressure imposed at the extraction points is represented by a grey line. The model does not capture quantitatively the pore-water pressure once the system enters the water-limited regime at day 38 although the trend of the simulated pore-water pressure now appears to be consistent with the pore-water pressure measured experimentally. The numerical simulation should be further refined by increasing the number of extraction points and/or moving the tensiometer measurement point away from the extraction points (to avoid that tensiometer measurement point is affected excessively by the local gradients around the extraction points). Nonetheless, the approach based on water-pressure extraction points surrounded by a soil-root interface appears to be very promising.

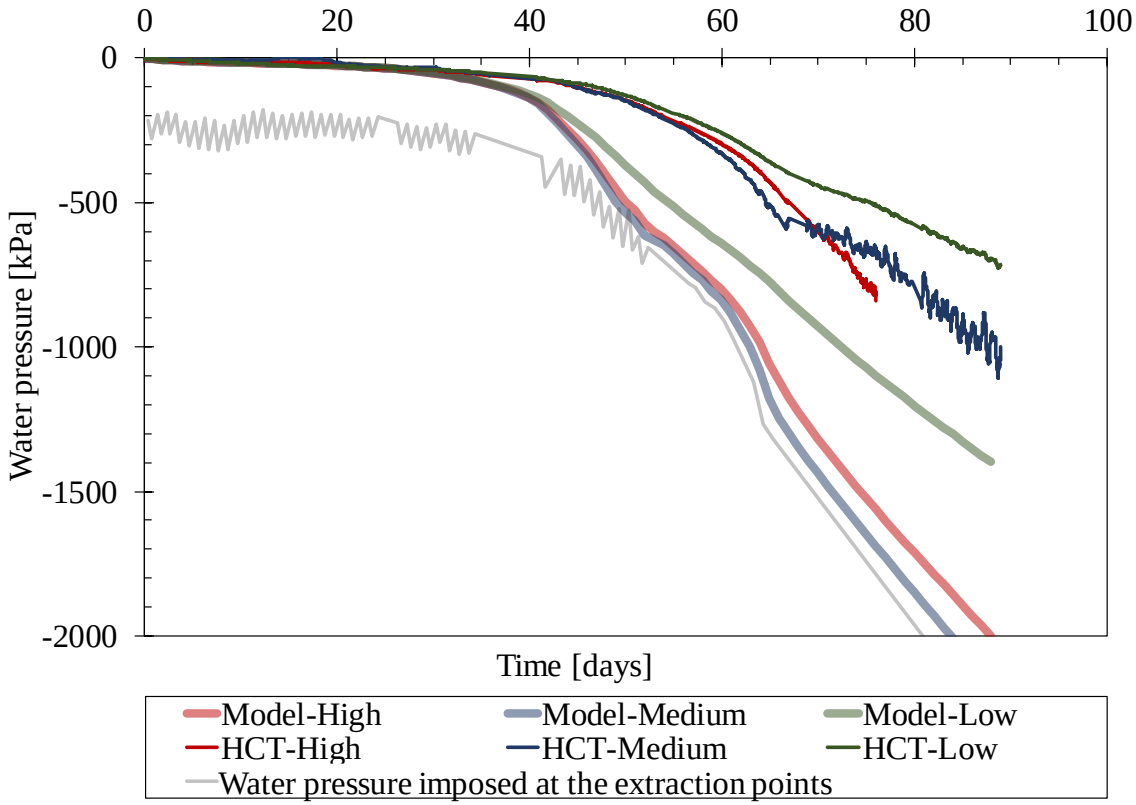

Figure 5.17:Comparison between the pore water pressure over time measured by HCTs and modelled via FEM for extraction points at imposed suction.

5.7 Conclusions

This paper has presented an experimental programme to investigate the efficiency of vegetation in generating suction with respect to the bare soil (under the same atmospheric conditions). Two different experiments have been presented. Evaporation from bare soil was compared with either evapo-transpiration from a sample vegetated with grass (*Lollium perenne*) or transpiration from a sample with transplanted shrub of willow. Comparison could be made in the energy-limited regime (potential evaporation/transpiration) and the water-limited regime.

Under forced ventilation in the energy-limited regime, potential evaporation from bare soil was greater than evapotranspiration from the sample vegetated with grass and transpiration from the sample vegetated with the willow tree. Experimental data therefore showed that vegetation may not always be the most efficient way to deplete

the soil water moisture, if compared with the water extracted from bare soil under the same atmospheric conditions. Competition between bare and vegetated ground in the energy-limited regime is controlled by the competition between aerodynamic resistance and the canopy resistance appearing in the Monteith's equation. In the laboratory, the zero canopy resistance in the bare ground prevailed. In the field, aerodynamic resistance of a canopy may reduce significantly with respect to the aerodynamic resistance of the bare soil, possibly generating higher potential transpiration rates in the vegetated ground.

Water-limited regime was entered much later in the vegetated soil and transpiration rate was maintained higher in the vegetated soil than the bare soil in the water-limited regime. The evolution of the profiles of pore-water pressure measured by the HCTs showed that pore-water pressure gradients in the water-limited regime were very high close to the ground surface for the bare soil whereas gradients are more evenly distributed in the vegetated samples.

The very high gradients in the bare soil close to the evaporating surface are achieved at the expenses of a very large decrease in pore-water pressure in the top layers. In turn, this is accompanied by a significant decrease in degree of saturation in the top layers, which tend to act as an impermeable barrier preventing water in the bottom layers to be removed. In contrast, water uptake is more evenly distributed in the rooting zone in a vegetated ground and this makes water extraction in the water-limited regime much more efficient in presence of vegetation.

The numerical analyses highlighted that the use of a sink term in the water flow equation may not be the most appropriate way to simulate the root water uptake. On the other hand, modelling water uptake by imposing the same water pressure in a discrete number of extraction points surrounded by a soil-root interface is closer to the actual mechanisms of water uptake and has the potential to reproduce the phenomenon of root compensation in a natural way.

The laboratory setup has clear limitations as it could not mimic the natural recharge from the water table generally and could not analyse the interaction between the rooting zone and the underlying non-vegetated layers. Nonetheless, it allowed developing a conceptual framework for vegetation-driven hydrological 'reinforcement' that can be extended to field conditions.

References

Anon., 2018. *2016 UK greenhouse gas emissions, final figures,* s.l.: Department for businness, energy & industrial strategy.

Anon., n.d. *http://www.ictinternational.com/casestudies/physiology-of-water-absorption-and-transpiration/.* [Online].

Anon., n.d. *https://www.legislation.gov.uk/ukpga/2008/27/contents.* [Online].

Balzano, B., Amabile, A., Caruso, M. & Tarantino, A., 2014. *A numerical study of hydrological effects of vegetation on slope stability.* s.l., s.n.

Biddle, P., 1983. Patterns of soil drying and and moisture deficit in the vicinity of trees on clay soils. *Geotechnique,* Volume 33, pp. 107-126.

Biddle, P., 1998. *Patterns of Soil Drying in the proximity of trees on clay soils.* Wantage (UK): Willowmead Publishing Ltd..

Canny, 1977. *Flow and Transport in Plants.* s.l.:s.n.

Coppin, N. & Richards, I., 1990. *Use of Vegetation in Civil Engineering.* s.l.:CIRIA.

Dainese, R. & Tarantino, A., 2019. Measurement of plant xylem water pressure using High-Capacity Tensiometers. *Geotechnique.*

De Baets, S. et al., 2008. *Root tensile strength and root distribution of typical Mediterranean plant species and their contribution to soil shear strength.* s.l., Springer.

Endo, T. & Tsuruta, T., 1969. On the effect of roots upon the shearing strength of soil.. *Annual report of Hokkaido Branch,* pp. 167-183.

Feddes, R., 1982. Simulation of field water use and crop yield. In: *Simulation of Plant growth and crop production.* Wageningen: Pudoc, pp. 194-209.

Fredlund, D. & Raharjo, H., 1993. *Soil Mechanics for unsaturated soils.* s.l.:John Wiley & Sons.

Gardner, W., 1960. Dynamic aspects of water availability to plants. *Soil Science,* Volume 89, pp. 63-73.

Gray, D., 1978. *Role of woody vegetation in reinforcing soils and stabilising slopes.*. Sidney, Australia, s.n.

Gray, D. & Leiser, A., 1982. *Biotechnical slope protection and erosion control.* New York: Van Nostrand Reinhold.

Greenway, D., 1987. Vegetation and slope stability. In: M. Anderson & K. Richards, eds. *Slope stability.* s.l.:John Wiley & Sons Ltd., pp. 187-230.

Guthrie, R., 2002. The efefcts of logging on frequency and distribution of landslides in three watersheds of Vancouvver Island, British Columbia.. *Geomorphology,* Volume 43, pp. 273-292.

Jackson, R. et al., 1996. A global analysis of rot distributions for terrestrial biomes. *Oecologia,* Volume 108, pp. 389-411.

Jarvis, P. & McNaughton, K., 1986. Stomatal control of transpiration: scaling up from leaf to region. *Advances in Ecological research,* Volume 15.

Ledieu, J., De Ridder, P., De Clerck, P. & Dautrebande, S., 1986. A method of measuring soil moisture by time-domain reflectometry. *Journal of Hydrology,* Volume 88(3-4), pp. 319-328.

Marinho, F. A. M., Take, W. A. & Tarantino, A., 2008. Measurement of matric suction using tensiometric and axis translation techniques. *Geotechnical and Geological Engineering,* Volume 26(6), pp. 615-631.

Monteith, J., 1965. *Evaporation and environment. The state and movement of water in living organisms.*. s.l., Cambridge University Press.

Nyambayo, V. & Potts, D., 2010. NUmerical simulation of evapotranspirationusing a root water uptake model. *Computers and geotechnics,* Volume 37, pp. 175-186.

Pollen-Bankhead, N. & Simon, A., 2010. Hydrologic and hydraulic effects of riparian root networks on streambank stability:Is mechanical root reinforcement the whole story?. *Geomorphology,* Volume 116, pp. 353-362.

Riestenberg, M., 1994. *Anchoring of thin colluvium by roots of Sugar Maple and White Ash on hillslopes in Cincinnati,* s.l.: U.S. Geological Survey Bulletin.

Saito, H., Murakami, W., Daimaru, H. & Oguchi, T., 2017. Effect of clear-cutting on landslides occurrences: Analysis of rainfall thresholds at Mt. Ichifusa, Japan.. *Geomorphology,* Volume 276, pp. 1-7.

Salisbury, F. & Ross, C., 1992. *Plant Physiology.* s.l.:Wadsworth.

Sanderson, J., 1983. Water uptake by different regiorn of barley root. Pathways of radial flow in relation to development of the endodermis.. *Journal of experimental botany*, Volume 34, pp. 240-253.

Sellin, A., 1999. Does pre-dawn water potential reflect conditions of equilibrium in plant and soil water status?. *Acta Oecologica*, Volume 20, pp. 51-59.

Sinha, R., 2004. *Modern Plant Physiology.* s.l.:CRC Press.

Tarantino, A., 2004. Panel lecture: direct measurement of soil water tension. pp. 1005-1017.

Tarantino, A., Ridley, A. & Toll, D., 2008. Field measurement of suction, water content, and water permeability. *Geotechnical and Geological Engineering*, Volume 26(6), pp. 751-782.

Tarantino, A. & Tombolato, S., 2005. Coupling of hydraulic and mechanical behaviour in unsaturated compacted clay. *Geotechnique*, pp. 307-317.

Tsukamoto, Y. & Kusakabe, O., 1984. *Vegetative influences on debris slide occurrences on steep slopes in Japan.* Honolulu, Hawaii, Environment and Policy Institute.

Van Asch, W., Buma, J. & Van Beek, L., 1999. A view on some hydrological triggering systems in landslides. *Geomorphology*, 30(1-2), pp. 25-32.

Van Genuchten, M. T., 1980. A closed-form equation for predicting the hydraulic conductivity of unsaturated soils. *Soil science society of America journal*, Volume 44, pp. 892-898.

Weatherley, P., 1979. The hydraulic resistance of the soil-root interface-A cause of water stress in plant. In: *The Soil-Root Interface*. s.l.:Academic Press, pp. 275-286.

Wu, T., McKinnell, W. & Swanston, D., 1979. strength of tree roots and landslides on Prince of Wales island, Alaska. *Canadian Geotechnical Journal*, Volume 16, pp. 19-33.

Ziemer, R., 1978. *Logging effects on soil moisture losses,* s.l.: Colorado State University.

Ziemer, R., 1981. *The role of vegetation in the stability of forested slopes.* Kyoto, s.n.

Chapter 6 Accessible approach for the selection of candidate vegetation species for hydraulic groundwater remediation

Abstract

The stability of slopes and geotechnical structures is related to the shear strength the soil can develop at the failure surface. In the case of landslides within the vadose zone, the failure can occur in unsaturated conditions, where the shear strength of the soil is related to the negative pore-water pressure. The natural source of water extraction from the soil is the interaction with the atmosphere, occurring through evaporation (bare soil) or transpiration (plants). The water depletion from the deeper layers of soil by roots may increase the negative pore-water pressure and hence help to stabilize the slope.

This paper presents a simplified setup for a preliminary assessment of the effectiveness in terms of groundwater removal of different plant species on different soils. The test includes the preparation of at least three soil specimens to be vegetated with the selected grass species and two to be left bare and daily monitoring of the water content. The test was able to detect a different evaporative behavior between the bare soil and the vegetated specimens. In general, bare soil had a higher potential evaporation when in the energy-limited regime, but the vegetated specimens could delay the system entering the water limited regime. The most evident effect of the presence of vegetation in terms of evapotranspiration rate was found for fine natural soil. This work presents an accessible way to select Figure *6.1*: more promising plant species for soil moisture depletion for a given soil, with the objective of investigate them further in an up-scale experimental setup.

6.1 Introduction

The stability of geotechnical structures depends on the shear strength the soil can develop at the failure surface. In the case of partially saturated soils, the water removal is associated with an increase in the shear strength of the soil, as documented experimentally (Tarantino & El Mountassir, 2013). The water uptake by roots from the deeper layers of the soil can decrease the negative pore-water pressure and enhance the shear strength of the soil. Experimental results by Boldrin, et al.(2018) and Biddle (1983) reported cases of negative pore-water pressure below the shallow layer of soil that was maintained throughout 'wet' periods. The hydrological contribution of the water depletion by plants on slope stability was assessed by Pollen-Bankhead & Simon (2010) and Kim, et al. (2017).

The definition of a boundary condition associated to the presence of vegetation and a model to forecast the evolution of the suction profile within the soil is an important step towards the 'design' of vegetation to enhance groundwater removal.

The phenomena of evapo-transpiration refer to the contemporary contribution of transpiration (from the plant) and evaporation (from bare soil). Both evaporation and transpiration are driven by the evaporative demand of the atmosphere: for the transpiration process, the water is removed by the atmosphere through the plant, therefore if the plant was not present, water loss via evaporation from the bare soil would occur anyway. Consequently, the problem of the effectiveness of groundwater removal by vegetation should be studied with respect to the bare soil.

The phenomena of water loss from a system can occur under two different regimes: the energy limited regime and the water limited regime. In the first case the system is able to accommodate the evaporative demand of the atmosphere. Evapotranspiration occurs at its maximum rate and it is referred to as Potential Evapotranspiration (PET). The PET can be described by the Penman-Monteith equation (Monteith, 1965):

$$PET = \frac{1}{\lambda[T(z)]}\left[\frac{\Delta \cdot R_n + \rho_a c_p p_{v0}(z)[1 - RH\ ]/r_a}{\left[\Delta + \gamma\ \left(\frac{r_a + r_c}{r_a}\right)\right]}\right] \quad [1]$$

where λ [J kg^{-1}] is the latent heat of vaporisation of water at the air temperature T(z), PET [kg m^{-2} s^{-1}] the potential evapotranspiration rate, Δ [Pa °C^{-1}] the slope of the saturation vapour pressure curve at the air temperature T(z), γ [Pa °C^{-1}] the psychrometric constant at the air temperature T(z), R_n [W m^{-2}] the rate of net radiation, ρ_a the air density [kg m^{-3}], c_p [J kg^{-1} °C^{-1}] the specific heat of air, p_{v0} [Pa] the saturation vapour pressure at the air temperature T at the elevation z, RH the relative humidity at the elevation z, r_a [s m^{-1}] the resistance term for the aerial transport of water vapour from the canopy and it is a function of the wind velocity and surface roughness, r_c [s m^{-1}] the canopy resistance (resistance at the leaf level of the transpiring crop).

In the water limited regime the soil-plant hydraulic system is not able anymore to accommodate the evaporative demand of the atmosphere. The outward water flux is in this case lower than the PET and it is referred to as Actual Evapotranspiration (AET<PET).

The continuity of the hydraulic system formed by the soil-plant-atmosphere implies a coupled effect of soil and vegetation on the outward water flux. The characterisation of the boundary condition requires therefore the observation of the interplay between variables.

This work presents an accessible way to select promising plant species for a given soil, with the objective of investigate them further in an up-scale experimental setup. The simplified experiment includes the preparation of at least three specimens of vegetated soil and two specimens of bare soil (Figure 6.1). The specimens are subjected to identical environmental and initial conditions. The water loss over time of each soil specimen is

monitored at least daily by a balance. The limited resources required for the test make it a useful tool for the pre-assessment of soil-plant interaction.

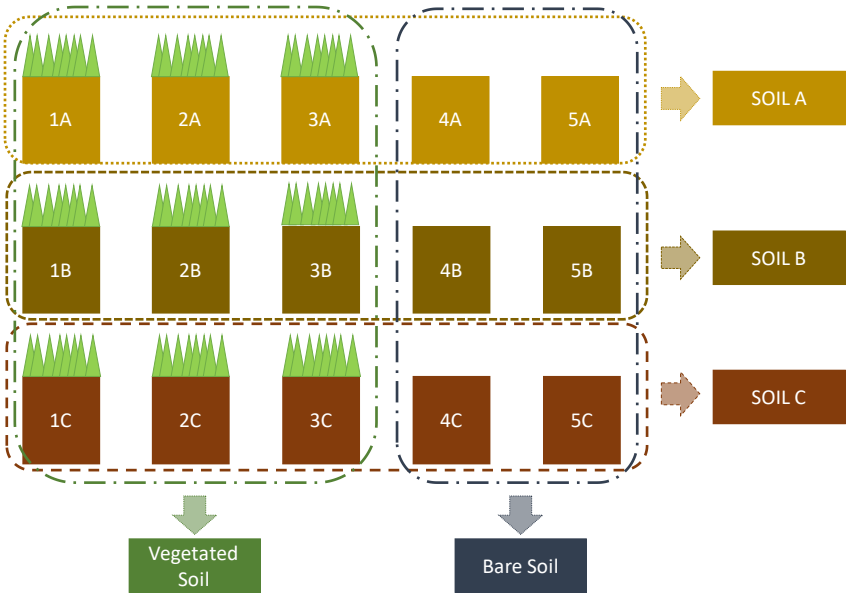

Figure 6.1: Schematic representation of the specimens tested, for three different kind of soil and one grass species.

6.2 Materials

The test included the use of 3 different kinds of soils and 2 different grass species. For each soil, a series of 5 pots was prepared, 3 of which were sown and 2 were left bare (Figure 6.1). The first series of 9 pots out of 15 was vegetated with L*ollium perenne* for Test 1, the second series of 9 pots was vegetated with *Medicago sativa* for Test 2. The grass was let grow before the beginning of the test. During the test the pots were let dry under imposed conditions, with daily measurements of the change in mass over time.

6.2.1 Containers

Plastic 1.4 L pots were used to accommodate the soil specimen. The base was drilled and a filter of coarse material was installed at the bottom of each pot. The filter was composed

of a metallic mesh, to guarantee stiffness and avoid differential settlements during compaction, 2 layers of geotextile (Figure 6.2.1), a layer of coarse sand approximately 1 cm thick (Figure 6.2.2), and two additional layers of geotextile (Figure 6.2.3). The presence of a high-permeability filter had the goal of re-distributing homogeneously along the surface any upward water flow and allow drainage from the bottom.

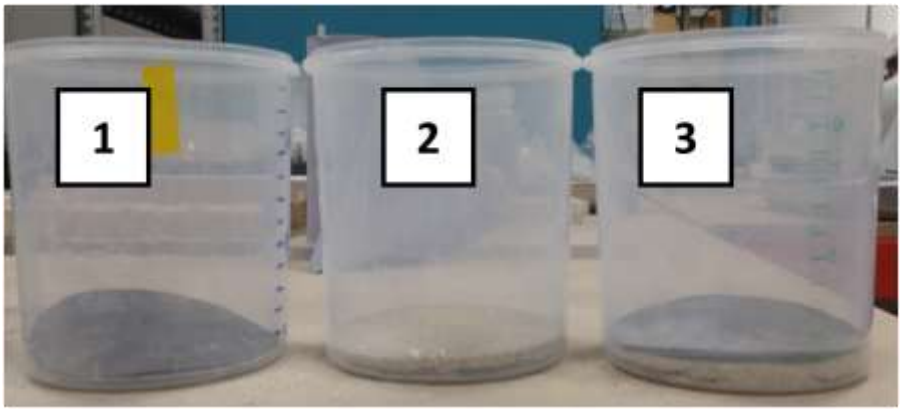

Figure 6.2:Pots and bottom filter

6.2.2 Soil

Three different soils were selected for the test: a silty sand mixed in the lab (soil A), a natural silty sand (soil B) and a clayey sand (Soil C).The grain size distribution of the tree soils is reported in Figure 6.3, while the main soil properties of the specimens are reported in Table 6.1.

Soil A was obtained by mixing 4 soils with different granulometric characteristics, in order to obtain a well-graded silty sand. The soil was mixed dry and moistened spraying the surface with an amount of water equal to the 25% in weight of the amount of fine particles of the soil. The soil was then gently mixed, in order to obtain aggregates with a diameter <1.5 cm. The soil was compacted in each pot at 100 kPa using a loading frame. The compaction was done in 3 stages, in order to obtain a more homogeneous compaction along the depth. Each pot was then fully saturated by partial immersion in a tank of water, with the water accessing the pot from the bottom filter. The water was enriched with fertilized, to provide nutrients for the grass to grow (15 mL of Miracle growth© every 10

L of water). Each pot was kept in water for 1 hour, until complete saturation. The pot was then removed and the excess water was let drain from the bottom and by evaporation from the surface for two days, before seeding.

Soil B was a silty sand originally coming from 'Rest and Be Thankful' site (Scotland, UK), air dried in the lab and sieved at 2 mm. The specimens were prepared by sedimentation: each pot was partially immersed in water, the soil was poured from the top and let settle at the bottom of the pot. When the target amount of soil had been added, the pot was removed from the tank and the excess water was let dry for two days, before seeding. The water used was enriched with fertilizer, as for Soil A.

Soil C was a clayey sand obtained mixing 90% of coarse sand with 10% of kaolin clay. The clay was added to the sand to enhance the cohesion between the particles. The soil preparation and compaction was analogous to the one used for Soil A. Each pot was then partially immersed in water enriched with fertilizer. The hydraulic conductivity of soil C was higher than Soil A and Soil C, therefore a shorter time was necessary to wet the soil. The soil was removed from the tank as soon as free water appeared on the surface. The pots were then removed and let dry for two days, before seeding.

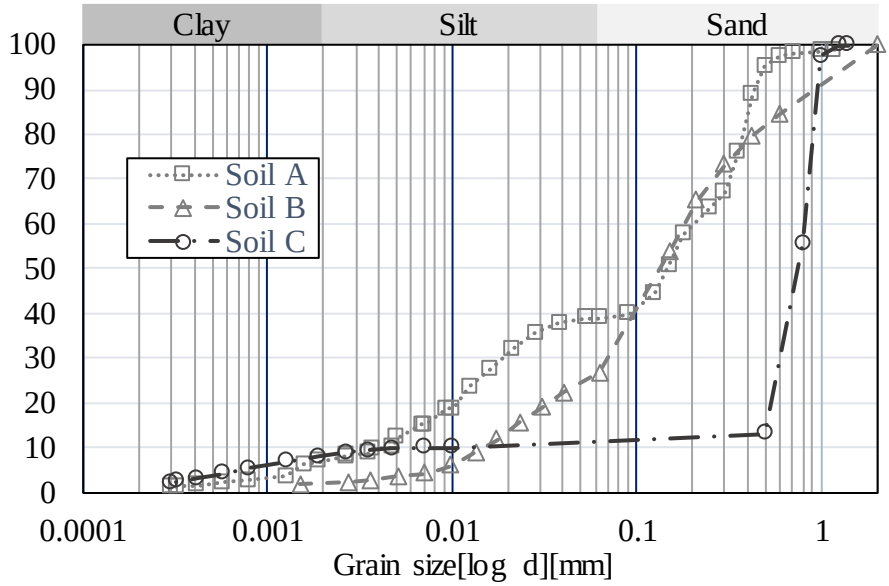

Figure 6.3:grain size distribution for soils used during the test. Classification by particle size based on BS 1377:1990

The average volume of soil of each pot and the bulk density, calculated from the known value of dry soil used for each sample, are reported in Table 6.1. Soil A is slightly denser, with a bulk density of around 1.78 g/cm3, while Soil B and Soil C have respectively a bulk density of 1.55 g/cm3 and 1.66 g/cm3.

The saturated hydraulic conductivity was measured by a permeability test at constant head. The soil specimen has been prepared with the same procedure as the soil specimens in the pots, wet and let dry for few days. The soil has then been sampled with a cutting ring and placed within an oedometer for the permeability test. It has not been possible to obtain reliable results for Soil C, due to its very high permeability.

Table 6.1: Soil specimens characteristics

	Dry soil [g]	V soil [cm3]	Bulk density [g/cm3]	K_sat [m/sec]
Soil A	1700	952±17	1.78±0.3	$2.15 \cdot 10^{-5}$
Soil B	1550	998±18	1.55±0.3	$2.55 \cdot 10^{-5}$
Soil C	1500	903±16	1.66±0.3	$> 10^{-5}$

6.2.3 Vegetation

Two different grass species were selected to vegetate the pots. The grass species selected for Test 1 was *Lollium perenne,* a perennial ryegrass. This grass is commonly used for surface protection, it is a quick-growing and wear tolerant species (Coppin & Richards, 1990). *Lollium perenne* has a fibrous root system that develops a thick network of shallow roots, when the plant is fully developed (Weaver & Darland, 1949).

Medicago sativa was selected for Test 2. This species is commonly used for surface protection, deeper reinforcement and for the removal of soil water (Coppin & Richards, 1990). *Medicago sativa* is commonly known as alfalfa and develops a tap rooting system: a single thick root grows straight into the ground and can penetrate deep into the soil.

Two days after the sample preparation, the selected pots were seeded. Holes approximately 10 mm deep were dig on the surface of the soil, at a distance of 1 cm in the two directions. 3 seeds were inserted in each hole, to increase the germination success. The pots were placed on a tray with 1 cm of water, and the surface was sprayed daily, in order to keep the soil moistened. A growth lamp was switched on from 6am to 8 pm, mimicking the daily light.

The grass growth was monitored daily: the rate of germination was evaluated by the operator: it was an esteem of the percentage of germinated seeds with respect to the total amount of seeds placed on the surface(Table 6.2); the density of seeds placed on the surface was 3 seeds/cm2.The average growth of the grass was assessed by measuring the

average height of the stems for the single pot (Figure 6.4). It was not possible to grow *Medicago sativa* in soil A for the second test.

The evaporation test started 14 days after seeding, when the grass had almost reached its maximum growth (Figure 6.4).

Table 6.2: Germination rate (germinated seeds with respect to the total amount of seeds placed on the surface of each pot) of Lollium perenne and Medicago sativa in the vegetated pots

		Seed germination [%]			
		Test 1: *Lollium perenne*		Test 2: *Medicago sativa*	
		Pots	average	Pots	average
Soil A	Veg 1	20			
	Veg 2	20	20		
	Veg 3	20			
Soil B	Veg 1	85		75	
	Veg 2	70	72	20	40
	Veg 3	60		25	
Soil C	Veg 1	90		70	
	Veg 2	85	88	45	42
	Veg 3	90		15	

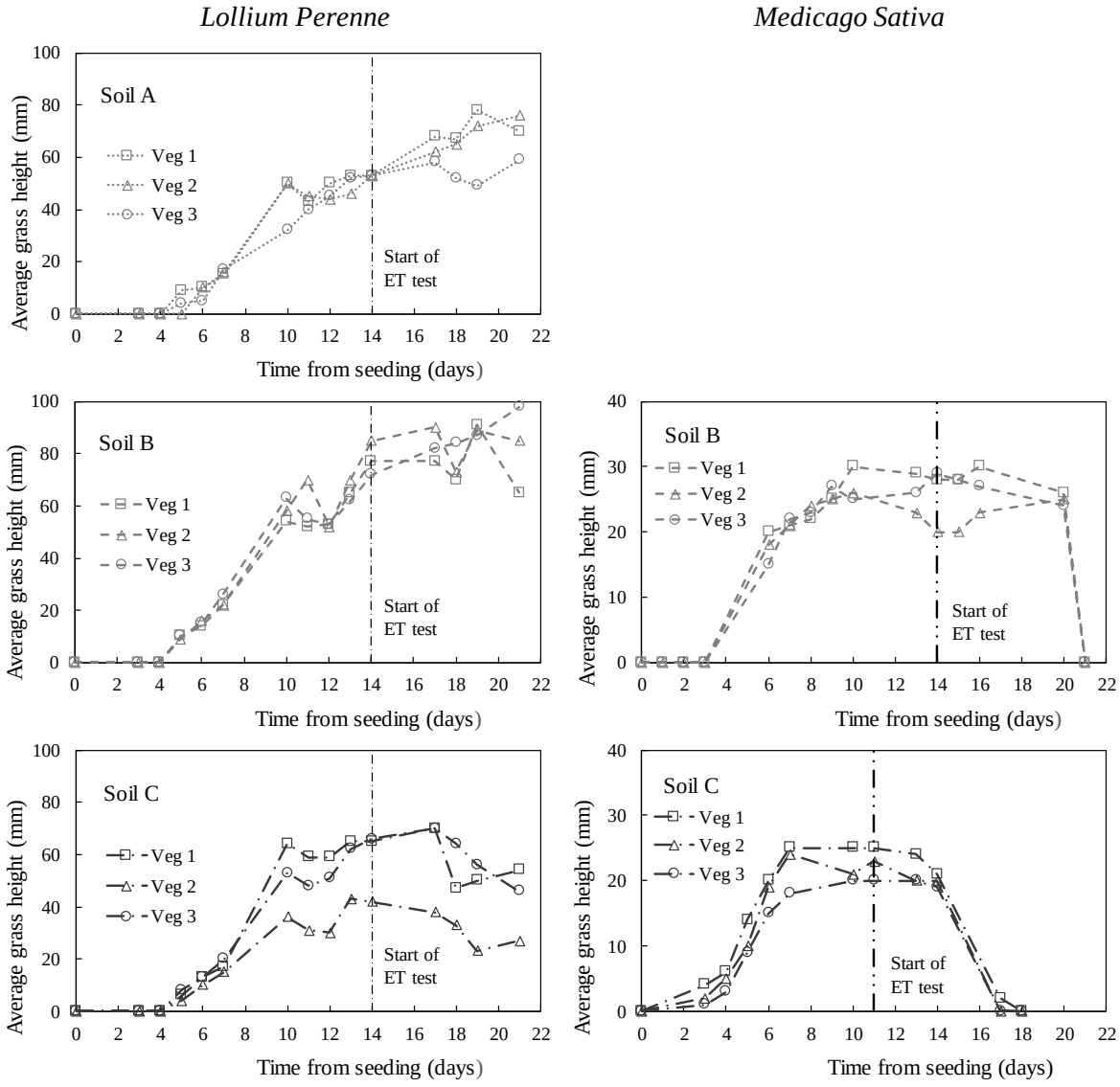

Figure 6.4:Grass growth: Test 1_*Lollium perenne* and Test 2_*Medicago sativa*

6.2.4 Evaporation test: Setup

The evaporation test started 14 days after seeding, when the vegetation almost reached its maximum growth (Figure 6.4). The water pots were kept moist before the test, to allow grass growth. The pots were removed from the tray with imposed water table and placed

on a bench in the lab. During the evaporation test, the pots were weighted daily using an electronic balance to measure the change in weight over time.

The pots were positioned randomly, approximately at the same distance from a central fan, as shown in Figure 6.5. The pots were subjected to the environmental conditions of the lab (Temperature 20°C, RH 45%), daily cycles of 14 h were imposed using a growth lamp and forced ventilation was added to the system via a fan to accelerate the water loss. Pots of water were placed among the specimens, in order to have a reference for the demand of the conditions imposed in the different points of the setup. The disposition of the pots for the two tests is shown in Figure 6.6. The evaporation from the pots of water among the specimen and the relative distance from the fan is reported in Table 6.3.

a)

Lollium perenne

b)

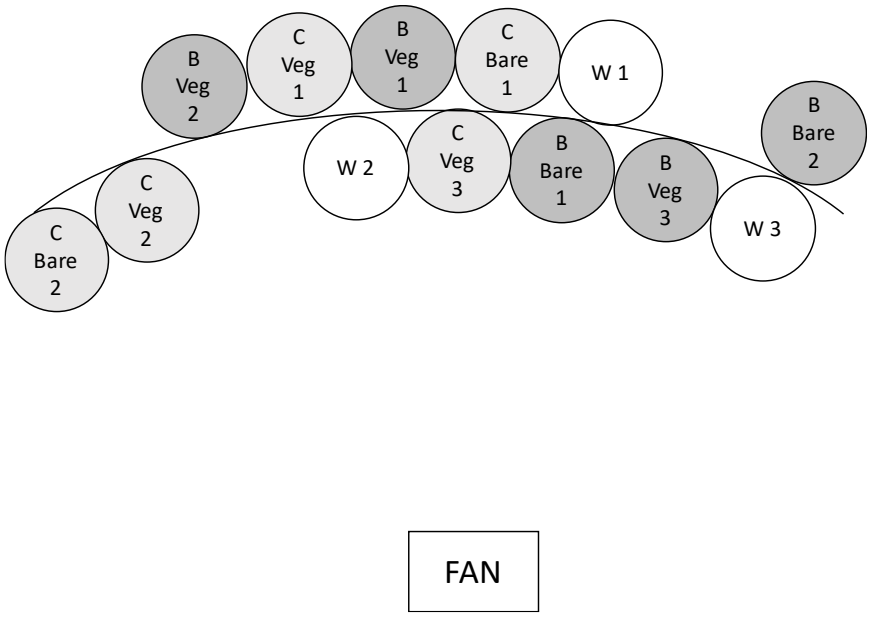

Medicago sativa

Figure 6.5: Random disposition of the pots in proximity to the fan for: a)Test 1_*Lollium perenne* and b) Test 2_*Medicago sativa*

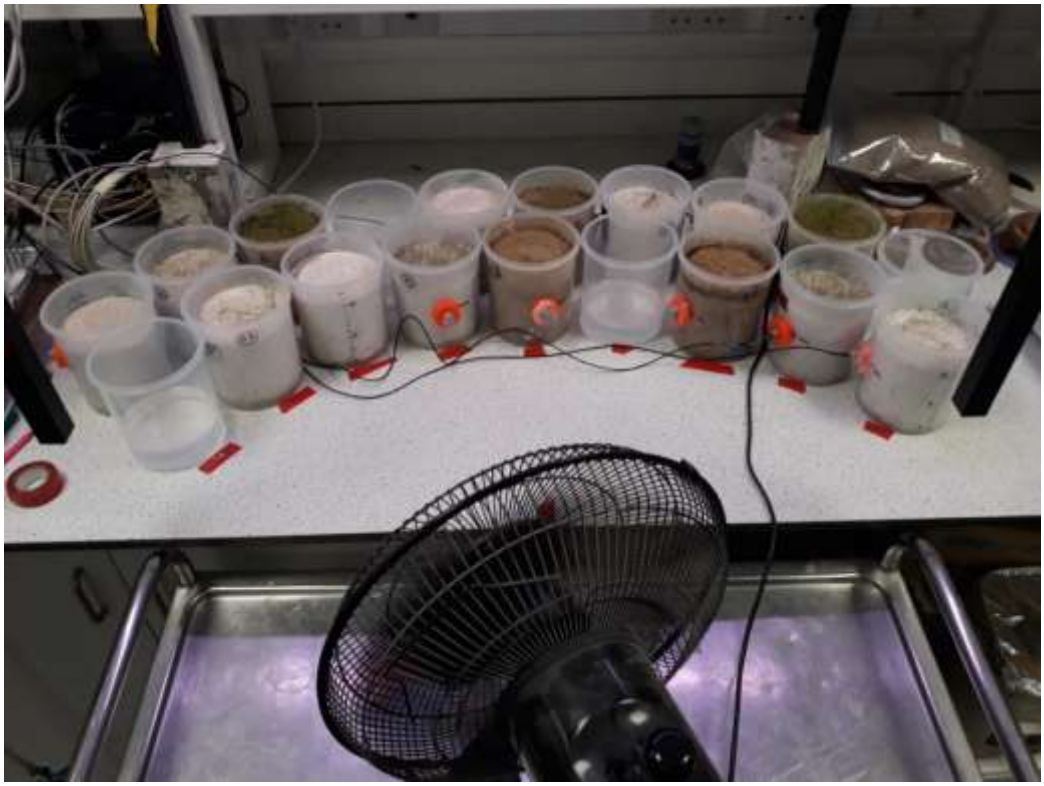

Figure 6.6: Disposition of the pots for Test 1_*Lollium perenne*

Table 6.3: Evaporation from pots of water

	Test 1		**Test 2**	
	ET [g/day/cm2]	Distance from fan [cm]	ET [g/day/cm2]	Distance from fan [cm]
WATER 1	-0.53	63	-0.71	63
WATER 2	-0.71	64	-0.89	52
WATER 3	-0.89	52	-0.67	52
WATER 4	-0.82	50		

6.3 Results and discussion

Results of the evaporation test are reported in Figure 6.7 for Test 1 on Lollium perenne and in Figure 6.8 for Test 2 on Medicago sativa. Results are reported in terms of loss of water from the system over time (top row of each figure) and evaporation rate or evapo-transpiration rate for each pot (bottom row). The first day of readings has been omitted from the results presented: the non-linearity of the initial part of the curve was assumed to be due to the desaturation of the bottom layer of coarse sand; during the rest of the test, the change of mass over time is assumed to be attributable to the water loss from the soil specimen only.

The total water loss over time, referred to the initial weight of the system, is reported in the two figures. The continuous lines refer to vegetated pots, while the dotted lines refer to the bare specimens. Data of water loss over time are plotted as evaporation and evapo-transpiration rate in the second row of Figure 6.7 and Figure 6.8, in respect with the surface of each pot. The curves show a common trend: each pot has an initial water loss over time that appears to be constant (linear trend of the curve of water loss, constant ET): the system is in energy limited regime and can accommodate the evaporative demand of the atmosphere. When the water availability decreases, the outward water flow from the system reduces (water limited regime). The moment of transition between the energy limited regime and the water limited regime is clearly identified in the graphs of evapo-transpiration over time by the end of the constant trait at maximum outward water flux. The latter identifies by definition the potential evapo-transpiration of each specimen.

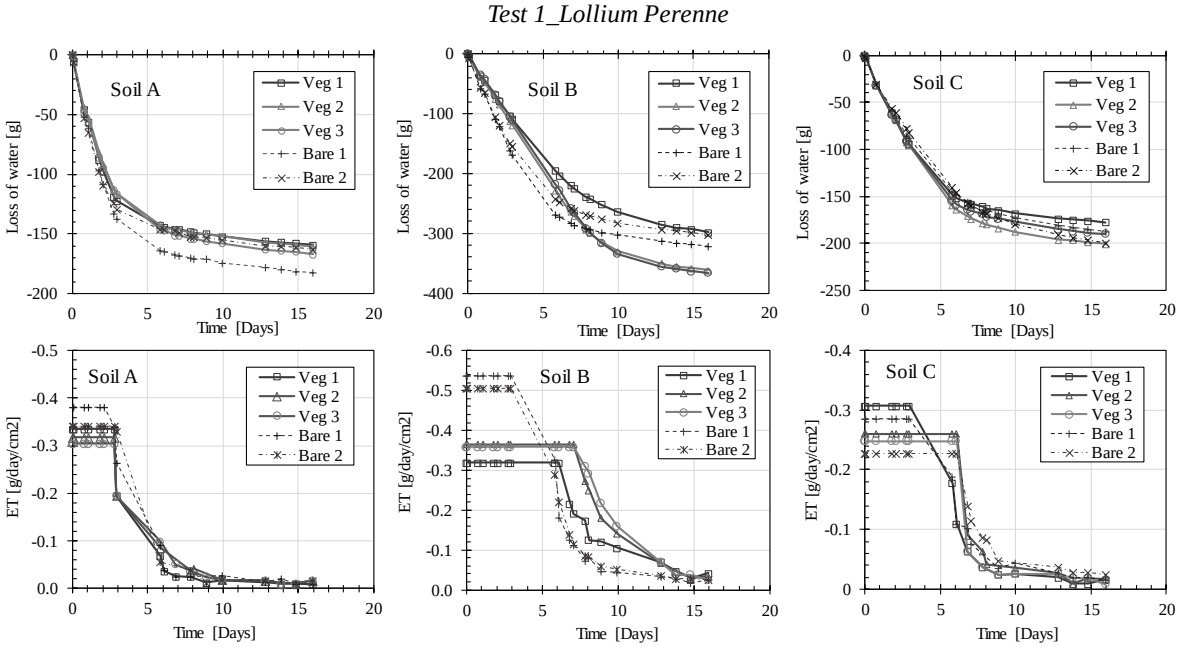

Figure 6.7:Water loss over time (top line) and evaporation/evapo-transpiration rate over time (bottom line) for Test 1_*lollium perenne*.

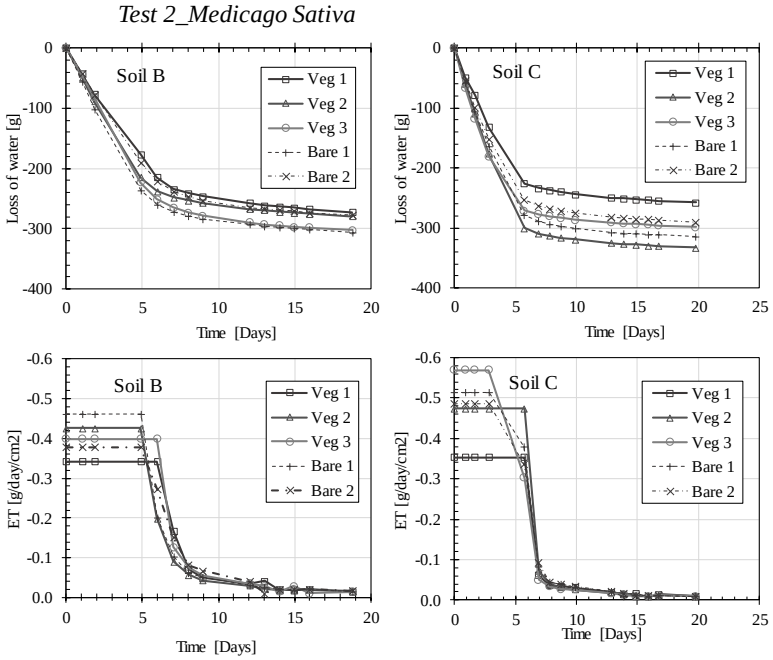

Figure 6.8:Water loss over time (top line) and evaporation/evapo-transpiration rate over time (bottom line) for Test 2_*Medicago sativa*.

In order to be able to compare the different systems, the potential evapo-transpiration of each pot and the moment of transition between the energy limited and water limited regime are reported in Figure 6.9, as average of the results on the vegetated and bare specimens for each soil type, for the two different tests.

In general, when in the energy limited regime, the bare soil shows a higher rate of evaporation. The only exception is for soil C vegetated with *Lollium perenne*, where the difference is however still within the repeatability of the measurement. This result is coherent with the additional aerodynamic resistance introduced by the increased surface roughness related to the presence of the grass (Trombetti & Tagliazucca, 1984), and by the stomata resistance component (Monteith, 1965). The transition from the energy-limited regime to the water-limited regime is usually delayed for the vegetated soil in comparison to the bare soil. This is particularly evident in the case of Soil B vegetated with *Lollium perenne* and Soil C vegetated with *Medicago sativa*. The difference disappears in the case of Soil A during Test 1.

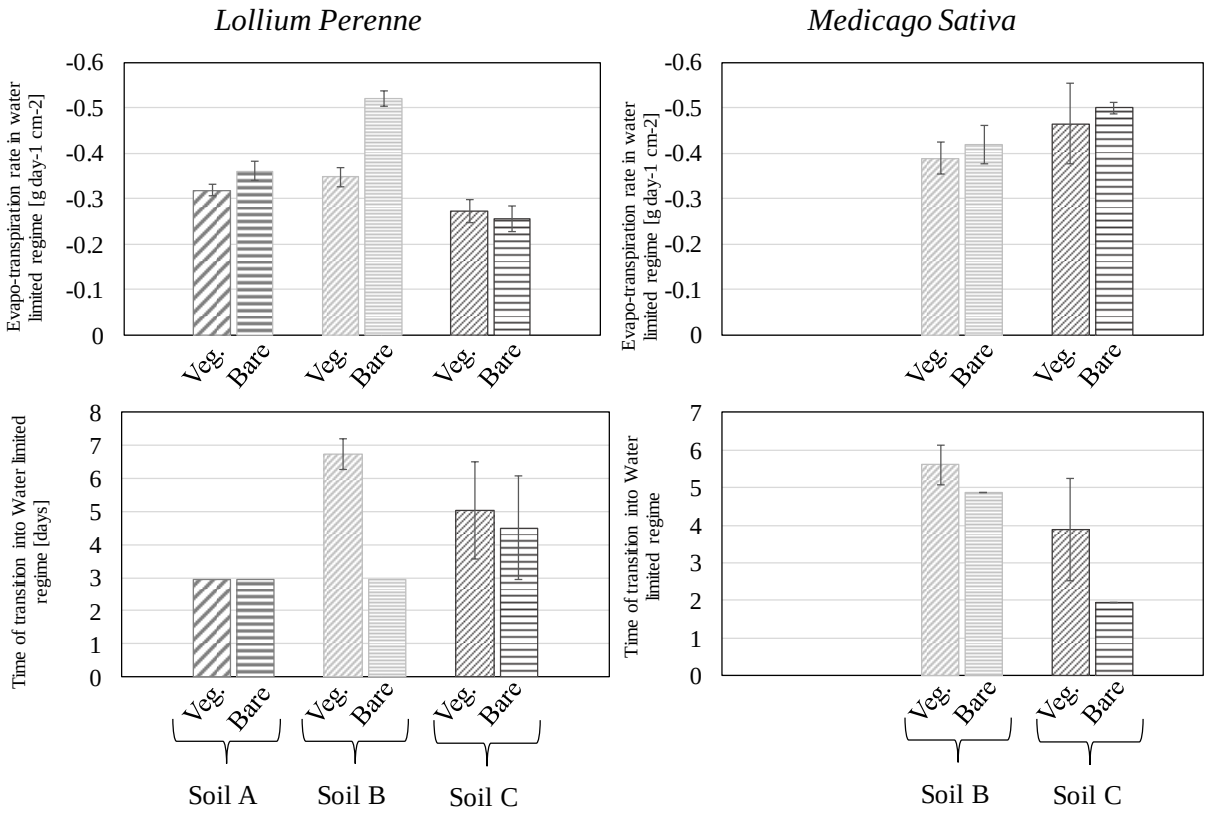

Figure 6.9:Water loss over time in the energy limited regime and moment of transition between the energy limited and the water limited regime for Test 1:*Lollium perenne* and Test 2_*Medicago sativa*. The error on the measurement taken on different samples is indicated by the error bars.

The preliminary assessment of the evaporative demand done on the pots of water gives a relevant difference (Table 6.3) between pots placed in the first or in the second row (Figure 6.5). However, comparing the behaviour of the vegetated and bare pots, when other conditions (i.e. vegetated or bare, rate of germination) are similar and all the specimens are in close proximity, the average evaporative behaviour does not result to be particularly affected by the distance from the fan.

To understand whether the different behaviour of specimens of different soil is due to the interaction plant-soil or to the mere unequal plant coverage, the potential evapo-transpiration and the transition time are represented together with the germination rate of each pot in Figure 6.10. The evapo-transpiration rate in the energy-limited regime and the

moment of transition to the water limited regime are reported for each vegetated pot. The width of the column and the label refer to the germination rate of the individual pot: this is used as a reference of the density of the vegetative cover. The fourth column, named Bare_av., indicates the average value for the two pots of bare soil.

Soil A had an almost negligible difference in behaviour with the bare soil, both in terms of water loss over time and for the transition into the water limited regime. The specimens had a very low germination rate for Test 1_*Lollium perenne* and the germination failed completely during Test 2_*Medicago sativa*. To the very low germination rate corresponds an almost negligible effect of vegetation on the mechanism of water extraction.

Soil B had a relevant difference in behaviour between the vegetated and the bare soil during Test 1_*Lollium perenne*, while the behaviour became more similar during the second test (Figure 6.9). The coverage is quite good for the first test while it reduced considerably in two pots out of three during the second test (Figure 6.10). However, it seems not to be possible to relate the effect of vegetation only to the germination factor: during the second test the most relevant differences in terms of water loss over time are in fact found in pots with less vegetation.

Soil C had a good grass density during the first test, and a germination rate comparable to Soil B for the second test. There is a considerable difference in behaviour with the bare soil in terms of delay of the water limited conditions, but the rate of water loss over time is quite similar.

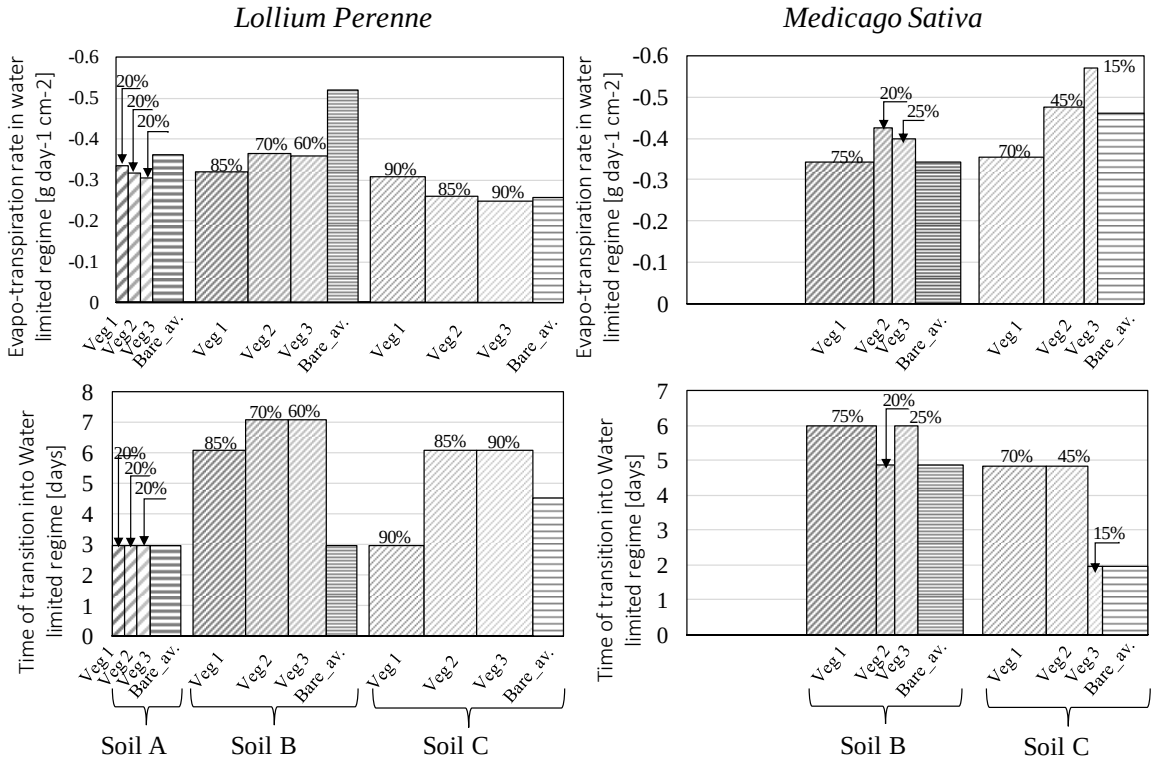

Figure 6.10:Water loss over time in the energy limited regime and moment of transition between the energy limited and the water limited regime for Test 1_*Lollium perenne* and Test 2_*Medicago sativa*. The width of each column refers to the germination rate of the single pot.

The effect of vegetation in delaying the system entering the water-limited regime has been discussed in Figure 6.9 and in Figure 6.10. However, the critical time of the system gives only a partial information, given the different outward water flow from each specimen. In order to untangle the result from the factor of time, the evaporation/evapo-transpiration rate of the specimens are reported Figure 6.11 in terms of change in volumetric water content over time. The volumetric water content has been calculated considering the incremental change in water lost from each pot, in respect to a known condition of the system:

$$\theta = \frac{V_w}{V_{tot}} = \theta_{initial} + \frac{\Delta m / \rho_w}{V_{tot}} \quad [1]$$

Where θ is the mean volumetric water content of the pot, V_w is the volume of water, V_{tot} is the total volume of the system, $\theta_{initial}$ the volumetric water content at the beginning of the test, Δm is the cumulative change in mass of water evaporated (negative value) and ρ_w is the density of water. $\theta_{initial}$ was calculated from the first valid measurement of volumetric water content (day 1) and the known value of dry soil in each specimen, and referred to the volume of soil reported in Table 6.1.

The continuous lines in Figure 6.11 represent the vegetated samples, while the dotted lines represent the bare soil. During the first test, the majority of the vegetated pots moved into the water limited regime for lower water contents than the pots of bare soil. During the second test, the difference in volumetric water content for the transition is quite relevant in the case of the coarse soil C, while it is less consistent in the case of soil B. Results presented in terms of volumetric water content confirm, or enhance in the case of Soil A, the results reported in Figure 6.8.

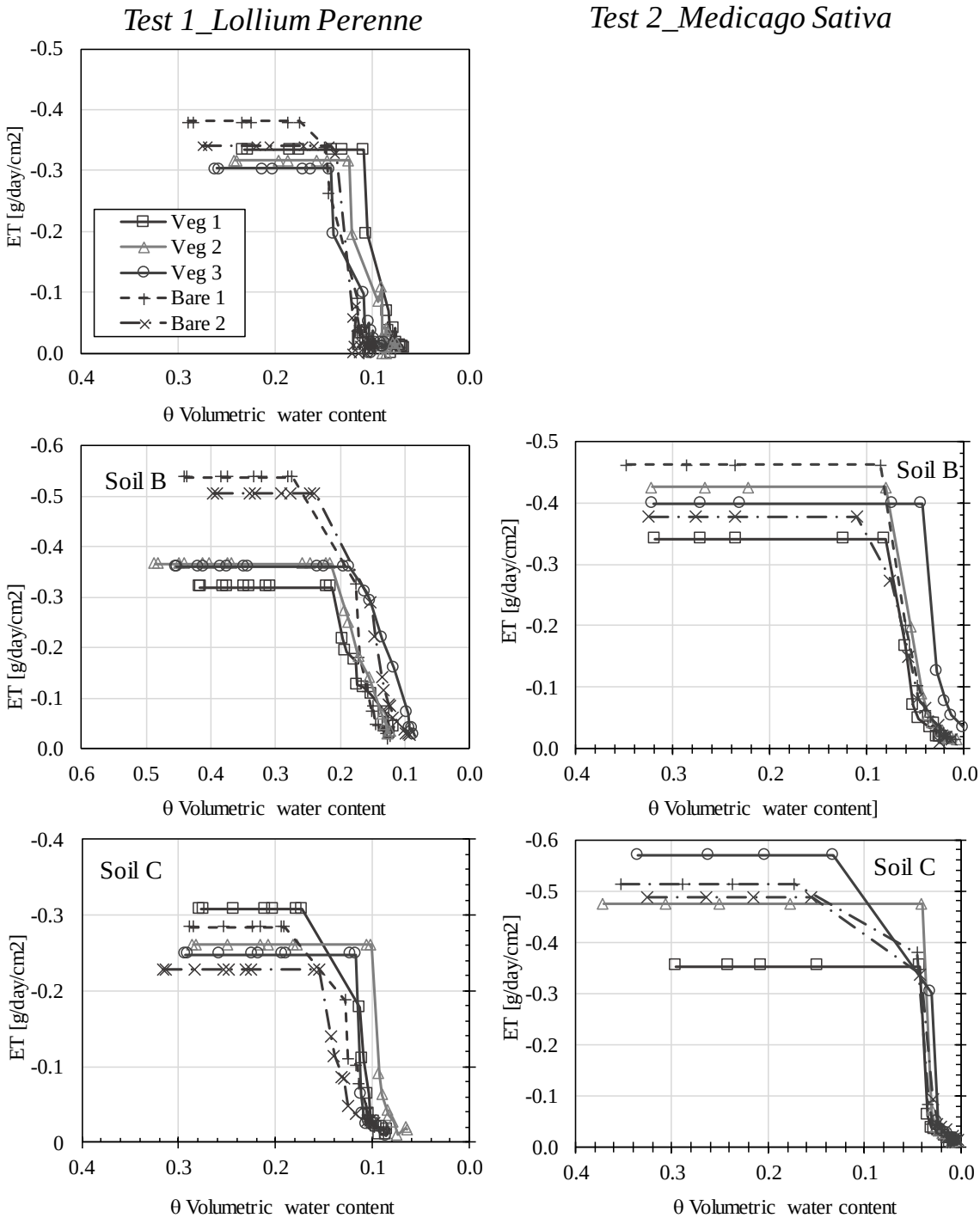

Figure 6.11:Potential evaporation/evapo-transpiration rate over the volumetric water content of the each specimen, for Test 1_Lollium perenne (left column) and Test 2_Medicago sativa (right column).

6.4 Conclusion

The paper has presented an accessible way to investigate the interaction between the soil and the vegetation under constant evaporative conditions. Results have shown how the presence of vegetation affects the maximum water loss over time the system can allocate under imposed environmental conditions, coherently with the Penman-Monteith equation, and the time required for the system to move into the water limited regime. In general, the presence of vegetation decreases the evapo-transpiration rate in the energy-limited regime, but delays the entrance of the system into a condition of water-limited regime. Those effects are more pronounced when the vegetative cover is sufficiently developed and the transpiration plays a relevant role in the process of water loss. In this regard, the results given by Soil A cannot possibly be trusted, given the insufficient germination of the seeds.

The effect of vegetation on the hydraulic behaviour of the system seems to be more pronounced in the case of a fine soil (Soil B) vegetated with *Lollium perenne*. The mean evapo-transpiration rate is considerably lower in the vegetated soil than in the bare, and the transition into the water limited regime of the vegetated soil is delayed of several days. However, the same behaviour is not so evident for the *Medicago sativa*. The difference may lay in the different interaction between the soil and the plant species.

A coarse soil like Soil C, on the other hand, shows a considerable delay of the transition moment during the second test, while the difference was on average less than one day during the first test. The potential evapo-transpiration for the vegetated soil C is very similar to the bare soil for both grass species.

The general output from the preliminary results hereby presented shows a higher effect of the vegetation on fine grains soils. However, it is difficult to extrapolate a general rule from the preliminary results presented in this chapter, especially for the reduced dimension of the specimens and the unrealistic low density of the vegetation. Furthermore, the possibility of taking only one measurement per day makes the accuracy of the measurement of the evaporation phenomena liable to interpretation errors. The possibility

of improving the vegetation cover and increasing the frequency of the mass of the system would strengthen the observations done in this work.

However, in view of selecting few possible species to be investigated further, the procedure proposed has the great advantage of being easily implemented and replicated to investigate the hydraulic relation between different soil types and vegetation species. The selected plants may then be further studied via a more complete monitoring system.

References

Biddle, P., 1983. Patterns of soil drying and and moisture deficit in the vicinity of trees on clay soils. *Geotechnique,* Volume 33, pp. 107-126.

Boldrin, D., Leung, A. & Bengough, A., 2018. Hydrologic reinforcement induced by contrasting woody. *Plant soil,* Volume 427, pp. 369-390.

Coppin, N. & Richards, I., 1990. *Use of Vegetation in Civil Engineering.* s.l.:CIRIA.

Fredlund, D. & Rahardjo, H., 1993. *Soil mechanics for unsaturated soils.* New york: John Wiley and Sons.

Kim, J. et al., 2017. Vegetation as a driver of temporal variations in slope stability: The impact of hydrological processes. *Geophysical research letters,* Volume 44, pp. 4897-4907.

Marinho, F. A. M., Take, W. A. & Tarantino, A., 2008. Measurement of matric suction using tensiometric and axis translation techniques. *Geotechnical and Geological Engineering,* Volume 26(6), pp. 615-631.

Monteith, J., 1965. Evaporation and environment. In: *Symposia of the society for experimental biology.* Cambridge: Cambridge University Press (CUP), pp. 205-234.

Monteith, J., 1965. *Evaporation and environment. The state and movement of water in living organisms.*. s.l., Cambridge University Press.

Pollen-Bankhead, N. & Simon, A., 2010. Hydrologic and hydraulic effects of riparian root networks on streambank stability:Is mechanical root reinforcement the whole story?. *Geomorphology,* Volume 116, pp. 353-362.

Tarantino, A. & El Mountassir, G., 2013. Tarantino, Alessandro, and Gráinne El Mountassir. "Making unsaturated soil mechanics accessible for engineers: Preliminary hydraulic–mechanical characterisation & stability assessment.. *Engineering geology,* Volume 165, pp. 89-104.

Tarantino, A. & Mongiovi', L., 2001. Experimental procedures and cavitation mechanisms in tensiometer measurements. *Geotech Geol Eng,* pp. 189-210.

Trombetti, F. & Tagliazucca, M., 1984. *Characteristic scales of atmospheric surface layer.,* Bologna, Italy: Istituto FISBAT-C.N.R..

Weaver, J. & Darland, R., 1949. Quantitative study of root system in different soil types.. *Science,* pp. 164-165.

Chapter 7 Field monitoring of water content in ground vegetated with poplars and grass: lessons learned for the design of transpiration boundary condition in geotechnical applications

Abstract

The stability of geotechnical structures depends on the shear strength the soil can mobilise along the failure surface. In the vadose zone, the shear strength depends on the negative pore-water pressure and the degree of saturation of the soil, which are in turn controlled by the natural interaction with the atmosphere (precipitation and evapotranspiration). The process of plant transpiration depletes water content in the ground and this generates an increase in shear strength. 'Engineering' vegetation to increase water content depletion therefore represents an approach to enhance stability of natural and man-made slopes. The aim of this work is to investigate the process of water content depletion by vegetation with deep rooting system by comparison with the response of a nearby field where trees were absent Volumetric water content was monitored in a poplar forestry plot and in an adjacent field newly vegetated with grass by means of the instrument 'Drill&Drop' (Sentek). The experimental site is located at the Domaine de Restinclieres, France. The water content profiles and the weather conditions were recorded from July to October 2018. Interpretation of the water content monitoring data could reveal that the shallow and the deep rooting systems operate independently and that the water uptake by the tree deeper roots is two-dimensional. It is therefore shown that volumetric water content data can be interpreted to derive site-specific parameters of the Penman-Monteith potential evapo-transpiration model.

7.1. Introduction

The stability of geotechnical structures depends on the shear strength the soil can mobilise along the failure surface. In the vadose zone, the shear strength is controlled by the negative pore-water pressure and the degree of saturation of soil (Vanapalli et al. 1996). A decrease in degree of saturation associated with water removal is generally associated with an increase in soil suction and, hence, shear strength

The natural interaction with the atmosphere, through the processes of evaporation from the bare soil and transpiration through the plants, is the main source of water removal from the soil (Garg, Coo, Wang, & Ng, 2015; Li, Yue, Tham, Lee, & Law, 2005). If vegetation is 'engineered' to enhance this process, vegetation can be potentially used as a hydrological remedial measure. A first step towards this goal is the qualitative and quantitative understanding of the mechanism of water removal by vegetation.

The evaporation and transpiration process, from now on called evapo-transpiration to refer to a cumulative effect of the two occurring in proximity of the ground surface, can occur under two different regimes, the energy limited and the water limited regimes. In the energy-limited regime the outward water flow is driven by the evaporative demand of the atmosphere and it is not restricted by the water availability in the system. Evapotranspiration occurs at its maximum rate and is referred to as Potential Evapotranspiration (PET). In the water-limited regime the water extraction is limited by the water availability within the system. The actual evapo-transpiration (AET) is lower than the flux driven by the evaporative demand of the atmosphere (AET<PET).

The most common way to model the water uptake by plants in geotechnical applications is to consider the actual evapo-transpiration as a product of the potential evapo-transpiration and a reduction function (Nyambayo & Potts, 2010). The water flow related to transpiration is then applied to the volume of soil through a sink term, to simulate the different distribution of root water uptake in the soil.

The potential evapo-transpiration rate of a system is usually calculated through the Penman-Monteith equation (Monteith, 1965):

$$PET = \frac{1}{\lambda}\frac{\Delta \cdot R_n + \rho_a \cdot c_p \cdot p_{v0}(z) \cdot {}^{[1-RH(z)]}/_{r_a}}{\Delta + \gamma \cdot [{}^{(r_a + r_c)}/_{r_a}]} \quad [1]$$

where λ is the latent heat of vaporisation of water at the air temperature T(z), Δ is the slope of the saturation vapour pressure curve at the air temperature T(z), γ is the psychrometric constant at the air temperature T(z), R_n is the net solar radiation, ρ_a is the density of the air, c_p is the specific heat of air, p_{v0} is the saturation vapour pressure at the air temperature T at the elevation z, p_v is the actual air vapour pressure at the elevation z, RH is the relative humidity at the elevation z, r_a is the aerodynamic resistance and r_c is the surface resistance of the transpiring vegetation. The limitation of the Penman-Monteith equation is the difficulty in assessing the values of aerodynamic and canopy resistance. Several empirical models are available for the assessment of the aerodynamic resistance as a function of the wind speed, but they require uniform conditions on the area under study, and usually refers to conditions of open field (Penman, 1956; Allen, et al., 1998). The definition of the canopy resistance is widely documented in the case of crops, while less information is available about systems of trees. This calls for an approach to determine site-specific potential evapotranspiration parameters in geotechnical applications. .

A widely used reduction function was suggested by Feddes and relates the reduction factor to the pore-water pressure in the soil (Feddes & Zaradny, 1978). Although very convenient for the implementation into geotechnical models, the Feddes function is commonly adopted using standard parameters of the function, usually referring to crop species in loosely compacted organic soils, and neglecting the coupled effect of the soil-vegetation interaction (Briggs, 2016; Tsiampousi et al., 2017). Again, this calls for an approach to determine site-specific reduction function for geotechnical applications. .

It is important to note that both the evaporation and the transpiration process are regulated by the evaporative demand of the atmosphere: the water is extracted **through** the plant, as a side effect of the acquisition of CO2 for the photosynthetic process. Less

than 10% of the water uptake by the roots is in fact used for physiological processes (photosynthesis and growth) (Sinha, 2004), hence a plant could live in a nearly-saturated environment with very little transpiration (Hillel, 1980). The assessment of the effect of a given vegetation species on soil water depletion should therefore be ideally studied in comparison with the same soil in the absence of that vegetation species under the same driving atmosphere conditions.

The aim of the work is to study the different mechanism of soil water removal within a forestry plot vegetated with 20-years old poplars by comparison in an open field, only vegetated with shallow and newly developed plants. Furthermore, this work aims to define an accessible approach for the determination of the site-specific potential evapotranspiration Penman-Monteith parameters based on field measurement .

Volumetric water content in the forestry plot and in the newly vegetated adjacent field was monitored by means of the commercial instrument 'Drill&Drop' (Sentek). from July to October 2018 at the experimental site located at the Domaine de Restinclieres, France.

7.2.Site overview

The selected area is part of the 'Domaine de Restinclieres' (Prades-le-lez, France. Latitude 43.7160448, longitude 3.85919764), belonging to the Hérault department. The estate is divided in numerous agroforestry plots (Figure 7.1), used for agricultural studies. The Lez, a stream of water, partially runs along one side of the area.

The measurement of soil water content over time were taken in the area named B17 (Figure 7.1), a forestry plot vegetated with poplars. All the plants were 20 years old, coming from the same clone. Trees were evenly spaced, 5 m apart one from each other in two orthogonal directions, in lines of 15 trees. The lines of trees were parallel to the stream running along the plot on the S-W side. A schematic representation of the forestry plot is reported in Figure 7.2. The orientation of the plot with respect Figure 7.1is given by the red arrow reported in both images.

A field dedicated to the cultivation of crop is located on the west side of the forestry plot. Before the test started, the field had not been cultivated for several years, growing spontaneous shallow vegetation. At the beginning of the test the field was ploughed, exposing the bare soil underneath the surface. Spontaneous shallow vegetation grew during the duration of the test.

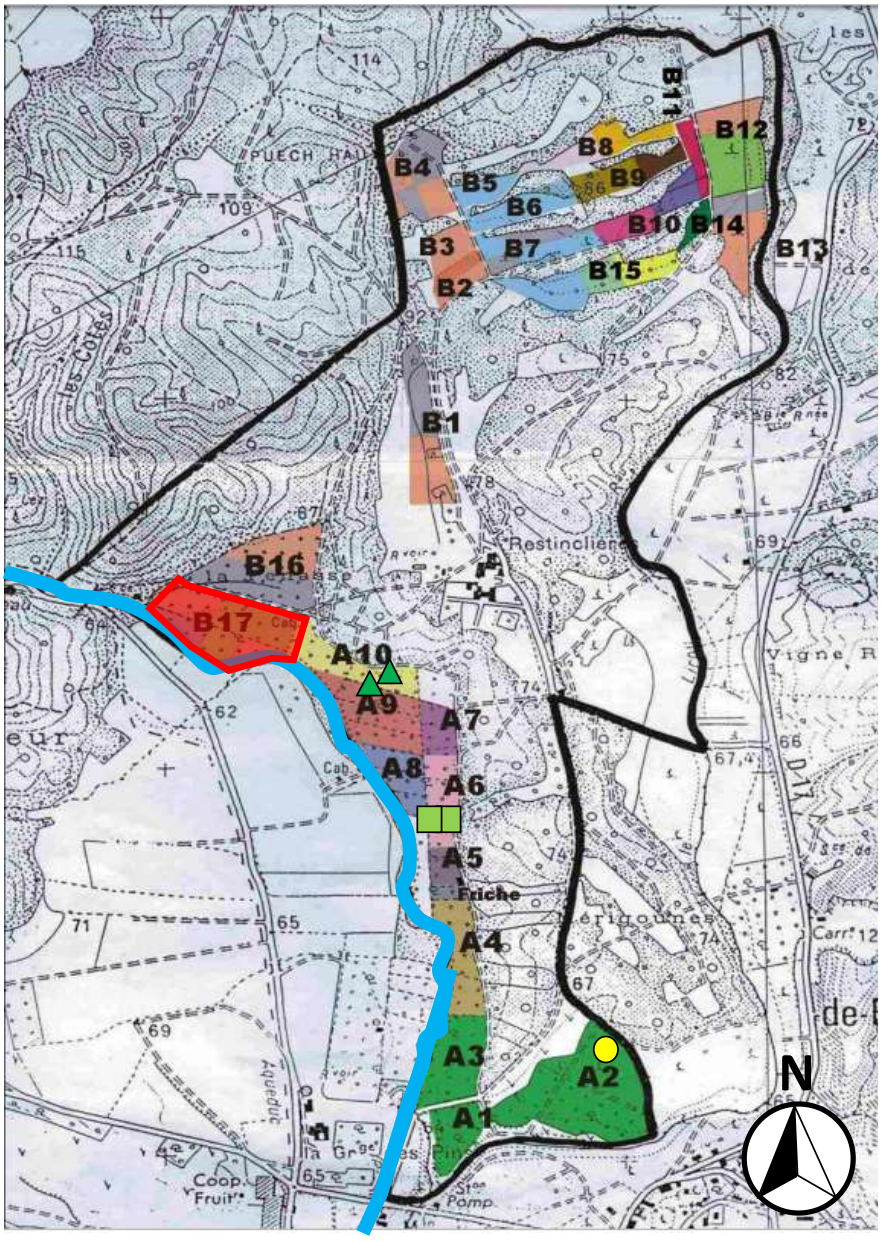

Figure 7.1: Domaine de Restinclieres, France. The black line marks the borders of the domain, the blue line identifies the presence of the water stream 'Lez'. The alphanumeric code identifies several plots, characterised by different cultivations and/or logistic agreements (e.g.

concessions). The position of the selected field test and instruments is identified in the figure : B 17) Experimental field Weather station; A2) Weather station ◯ ; A10) Piezometer Δ; A6) Piezometer □

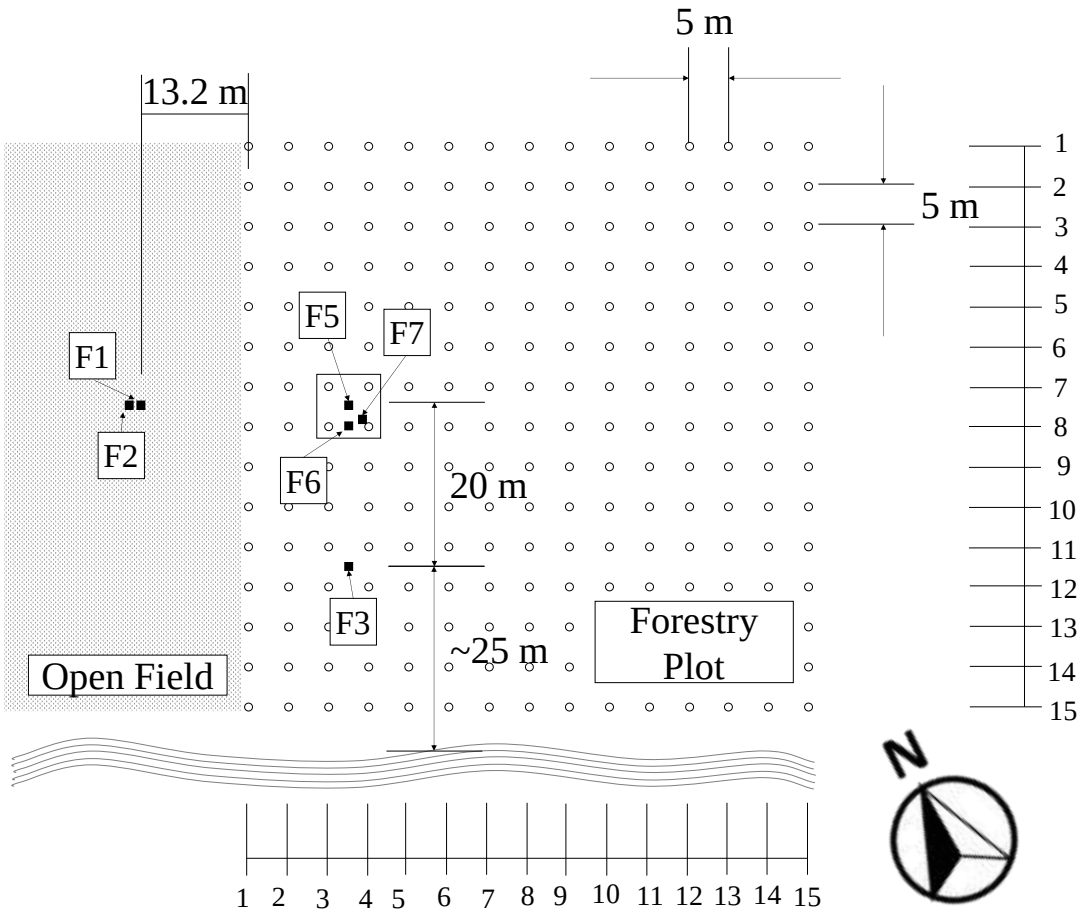

Figure 7.2: simplified representation of the experimental site. The open circles represent the poplar trees; the filled squares illustrate the position of the bore holes. The curve lines symbolise the position of the water stream 'Lez'.

Previous investigations on the site by CIRAD characterised the soil as an alluvial deposit of silty clay. The grain size distribution of the soil is reported in Figure 7.3. The specimens were taken at different depth on two different cores of soil, as reported in the labels (Figure 7.3); . The position of the two bore holes is indicated in Figure 7.2: the first was drilled in the forestry plot, between line 7 and 8 (F5), the second was drilled at the same distance from the river in the open field (F2).

The profile of bulk density of the soil with depth was measured for all bore holes (position reported in Figure 7.2), approximately every 20÷30 cm. The profiles obtained are reported in Figure 7.4.

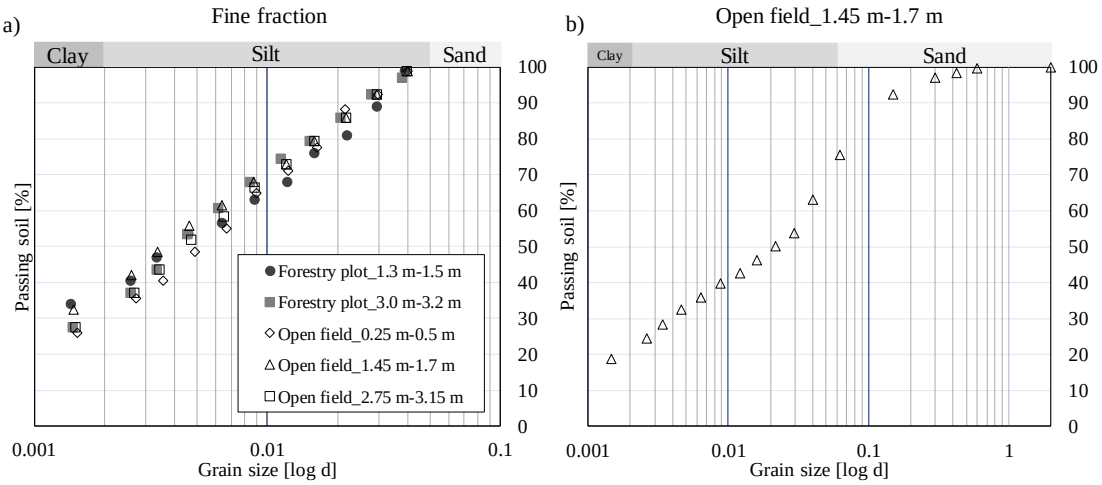

Figure 7.3: Grain size distribution in the open field (F2) and in the forestry plot (F5). a) grain size distribution for s34; b) grain size distribution of the fine part for all specimens.

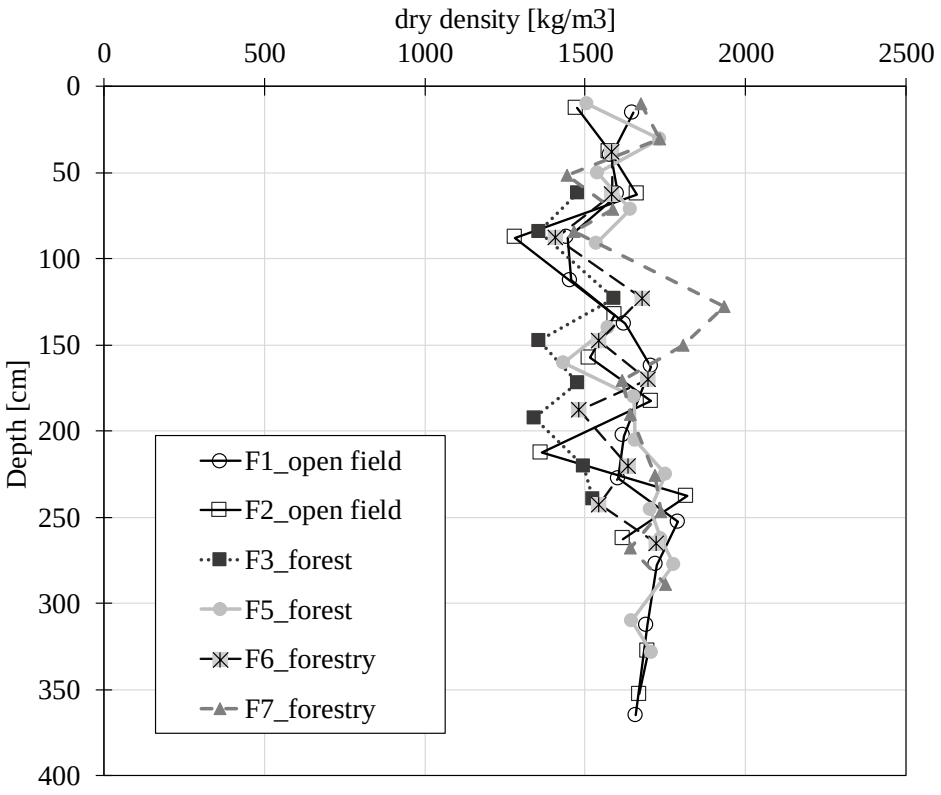

Figure 7.4:Bulk density calculated on cores from the open field and from the forestry plot (Figure 7.2)

7.3.Monitoring system

The evolution of the soil water content was monitored from July 2018 to October 2018 in the forestry plot and in the adjacent field. The period was initially selected with the aim of monitoring a dry summer period and a wet autumn period. Weather conditions were recorded during the whole duration of the measurements by a weather station installed in plot A2 (see Figure 7.1). Bore holes were drilled on the 12th of October 2018, to assess the soil characteristics and the root distribution. The position of the bore holes is reported in Figure 7.2.

The water status of the soil in the field was monitored via capacitance probes. The method is based on the soil working as a capacitor, where the electric field aligns the permanent water dipoles in the dielectric medium, which become polarized. The dielectric constant is given by the measurement of the capacitance, and it is used to infer the water content of the soil(Paltineanu & Starr, 1997). The relative permittivity of air is 1, it ranges between 3 and 5 for most soils and it is approximately 80 for water at 20°. the measurement of the instrument is therefore strongly influenced by the permittivity of water present in the sampling volume (Tarantino, et al., 2008).

The first version of portable capacitance instruments used a fixed case installed in the soil, and a removable probe that could be inserted within the casing. This solution allowed the repetition of the measurement in different locations using only one probe. However, the instrument interests quite a small volume of soil around the tube (~3 cm distance from the pipe), making the measurement sensitive to changes in water content and bulk density near the access tube; therefore, the readings suffer from any possible soil disturbance during installation (i.e. air gap) (Evett, Tolk, & Howell, 2006). A different kind of probe, based on the same working principle, has been developed in recent years for quick-installations. The idea is not to use a fixed casing and to avoid the use of a slurry to fill the gaps, that may generate preferential water paths along the probe (Anon., n.d.). The measurements of volumetric water content were taken in the superficial 120 cm using the 'Drill and drop sensor' (Sentek). Each probe is 120 cm long and contains 12 sensors, spaced at 10 cm interval along the instrument. The first sensor is centred at 5 cm from the top. Probes were installed following the procedure suggested by the manufacturer (Anon., n.d.): a hole was drilled in the ground using a adequately shaped auger; the drill&drop probe was the inserted within the hole, without using any slurry. The instrument has a slightly conical shape, to facilitate the insertion and reduce the possible presence of air gaps.

The position of the 'Drill and Drop' probes is reported in Figure 7.5 and Figure 7.6. Two probes were installed in the forestry plot more than 10 m away from the open field and more than 30 m apart from the water stream. Probe 2 was installed in the proximity of the geometrical centre of the reference 4-trees stand (the reference plot is

highlighted by a black profile in Figure 7.2), while Probe 3 was positioned along one of the diagonals, 1 m apart from the tree. The probes were installed between line 3 and line 4 of the trees, with respect to the open field; positions nearer to the open field were avoided, considered to be liable of border effects related to the uneven tree distribution. Probe 4 was installed at the same distance from the river, at approximately 13 m from the last line of trees.

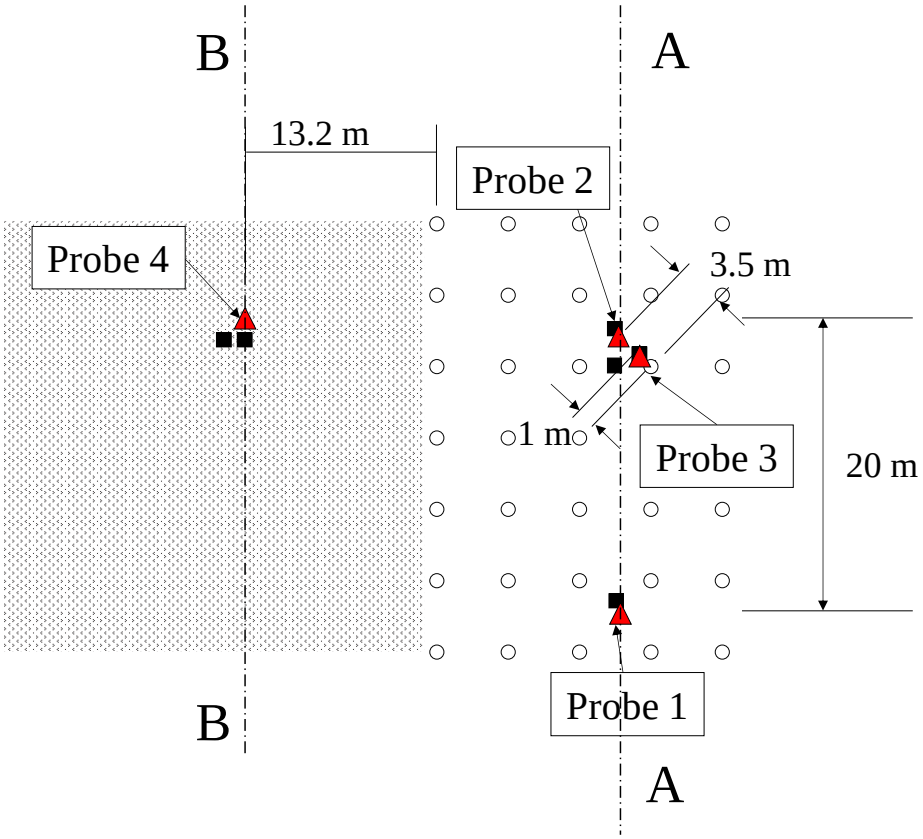

Figure 7.5:Position of the 'Drill & Drop' probes

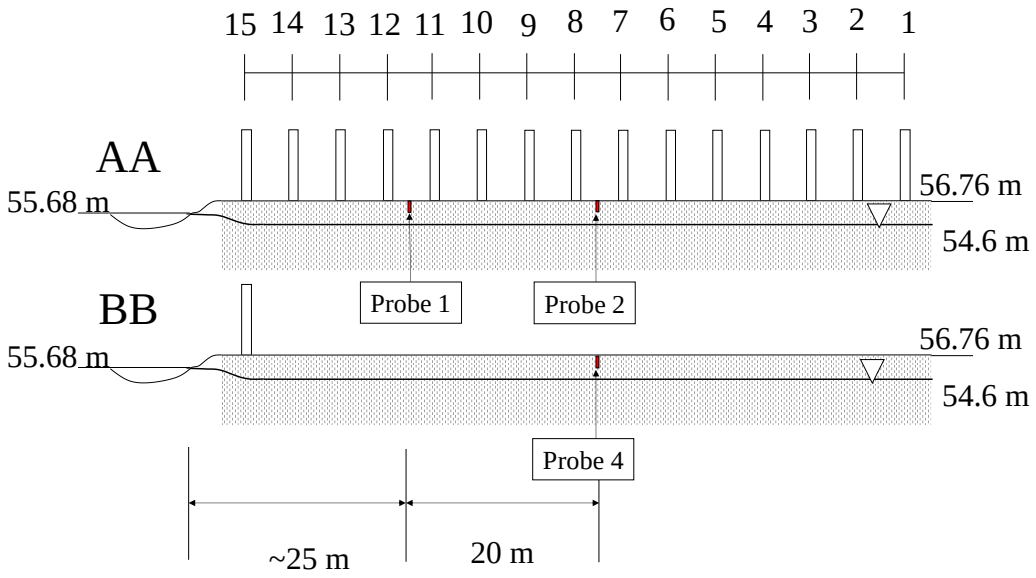

Figure 7.6: Position 'Drill & Drop' probes, section. AA) Forestry plot; BB) Open field. Position of the ground water table based on measurements by piezometers located in Plot.

The two probes installed in the forestry plot and the probe installed in the open field were used as a reference to compare the changes in the soil water content profiles over time. Given the similar characteristics of the soil (Figure 7.3), altitude and distance from the stream of water, the selected positions were considered to be appropriate for the comparison of the evapo-transpiration effects of a highly vegetated plot and a field vegetated with newly established shallow vegetation.

An additional probe was installed in an intermediate position between the line of the other three probes and the stream of water. Probe 1 was installed between line 3 and line 4 of trees, with respect to the open field, 20 m far from Probe 2 and approximately 25 m far from the stream.

Data about the weather conditions during the monitoring period were collected by a weather station previously installed in Plot A2 (Figure 7.1). The recorded precipitations, Relative humidity and temperature of the air, net solar radiation and wind speed are reported in Figure 7.7. Seasonal data about the water table were made available by CIRAD (Figure 7.8); the measurements come from piezometers located in Plot A6 and Plot A10 (Figure 7.1).

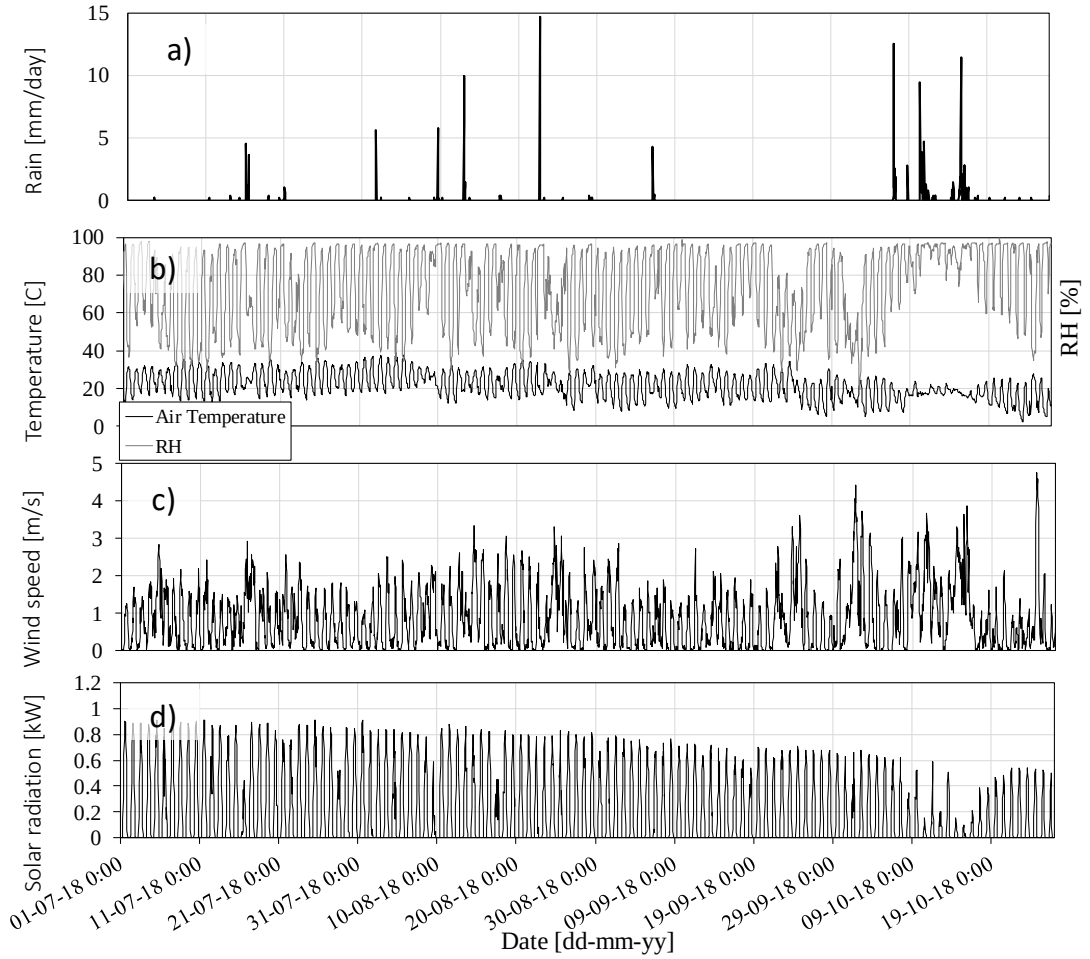

Figure 7.7: data by weather station (A2); a)rain; b)Air Temperature and Relative Humidity; c)Wind speed; d) net Solar radiation

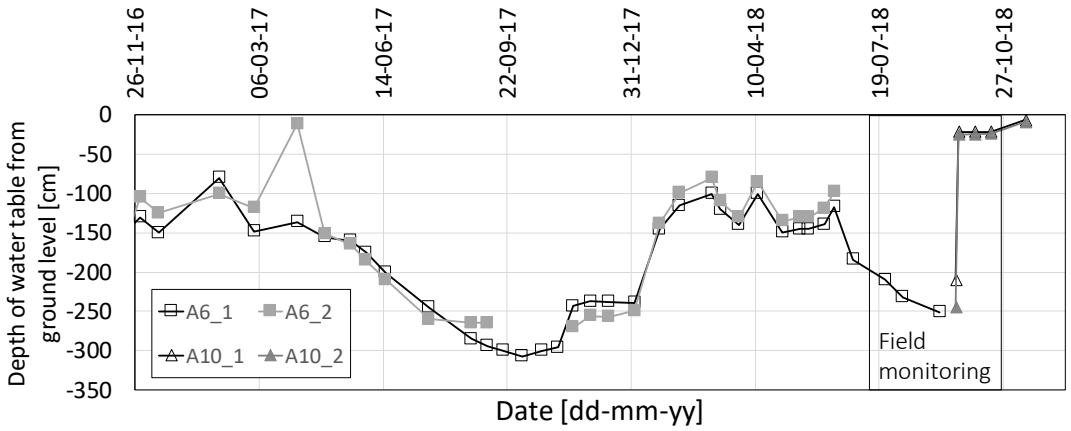

Figure 7.8: Seasonal data from Piezometers, located in Plot A6 and in plot A10

7.4.Results

7.4.1. Data quality assessment

The measurements of volumetric water content over time is presented in Figure 7.9 and Figure 7.10 for Probe 2 and Probe 3, in the reference stand of trees, and in Figure 7.11 for Probe 4 in the open field. Figure 7.12 reports the measurements done by Probe 1, nearer to the stream of water. The trend registered by each sensor along the depth of each probe is displayed separately. A sketch of the reference probe is represented on the left side of the graphs, to individuate the location of the sensor the single graph refers to. The horizontal line indicates the ground level: the first sensor from the top, located at 5 cm depth, was not interred within the soil, its measurement is therefore omitted in the graphs.

There are two effects detected by the probe: a long-term effect, where the water content changes gradually over time and a short-term effect, related to impulsive rainy events, that result in abrupt changes of water content (peaks in the measurement).

The long term effects are particularly visible in the deeper layers of soil, especially below the 95-cm sensor. In most cases there is a gradual decrease in the soil water content concentrated during the month of July 2018. An exception is the continuous decrease in water content observed by Probe 2 in the deeper layers throughout the whole summer season, and the increase in water content detected by Probe 1, located in the proximity of the river, starting from the 20/07/2018.

Comparing the graph reporting the atmospheric precipitations and the trend of the volumetric water content over time for each probe, it is possible to notice that the rainy events are clearly identified by a peak in readings of the probes, representing a sudden increase in the measure of water content. There are two different reactions to the rainy event:

Probe 3 and Probe 1 show high peaks on the surface, at the 15-cm sensor (position at approximately 7 cm below the ground surface, as average); sensor 25-cm and 35-cm

detect the peak, but the intensity decreases with depth. The sensors positioned at lower levels do not detect any sudden change connected to rainy events.

Probe 2 and Probe 4 show high peaks on the surface, that reduces slightly in the lower layers, but remain present for the whole depth of the probe. The time delay between the peak shown at the surface and the peaks registered by the deeper sensors is less than 10 min (time resolution of the readings). Probe 4 registers peaks due to rainy events down to the 105-cm sensor, with an intensity decreasing with depth. Probe 2 registers peaks along the whole length of the probe, with non-negligible intensity of the peak at all depths.

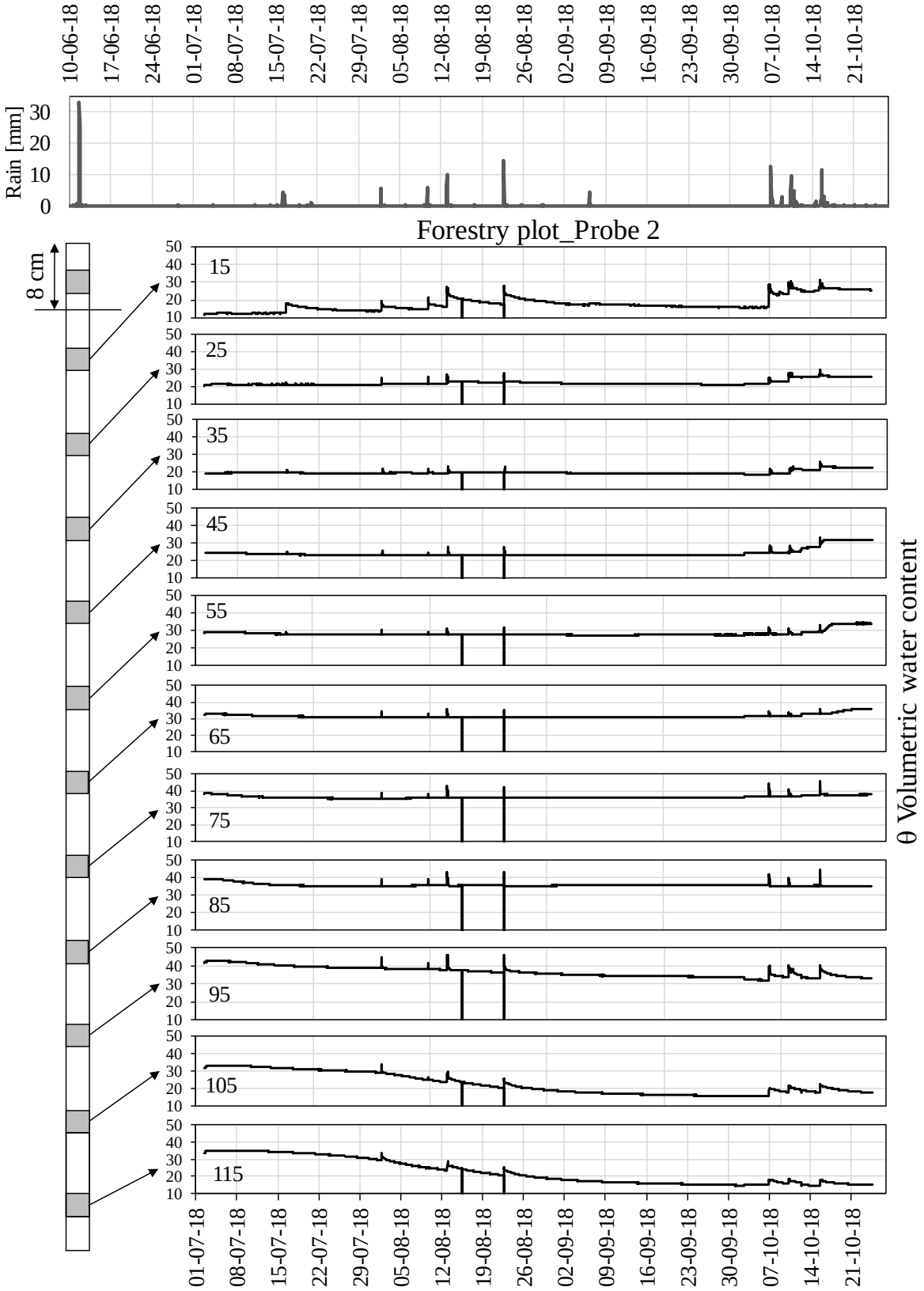

Figure 7.9:Probe 2: volumetric water content over time, along the depth of the probe

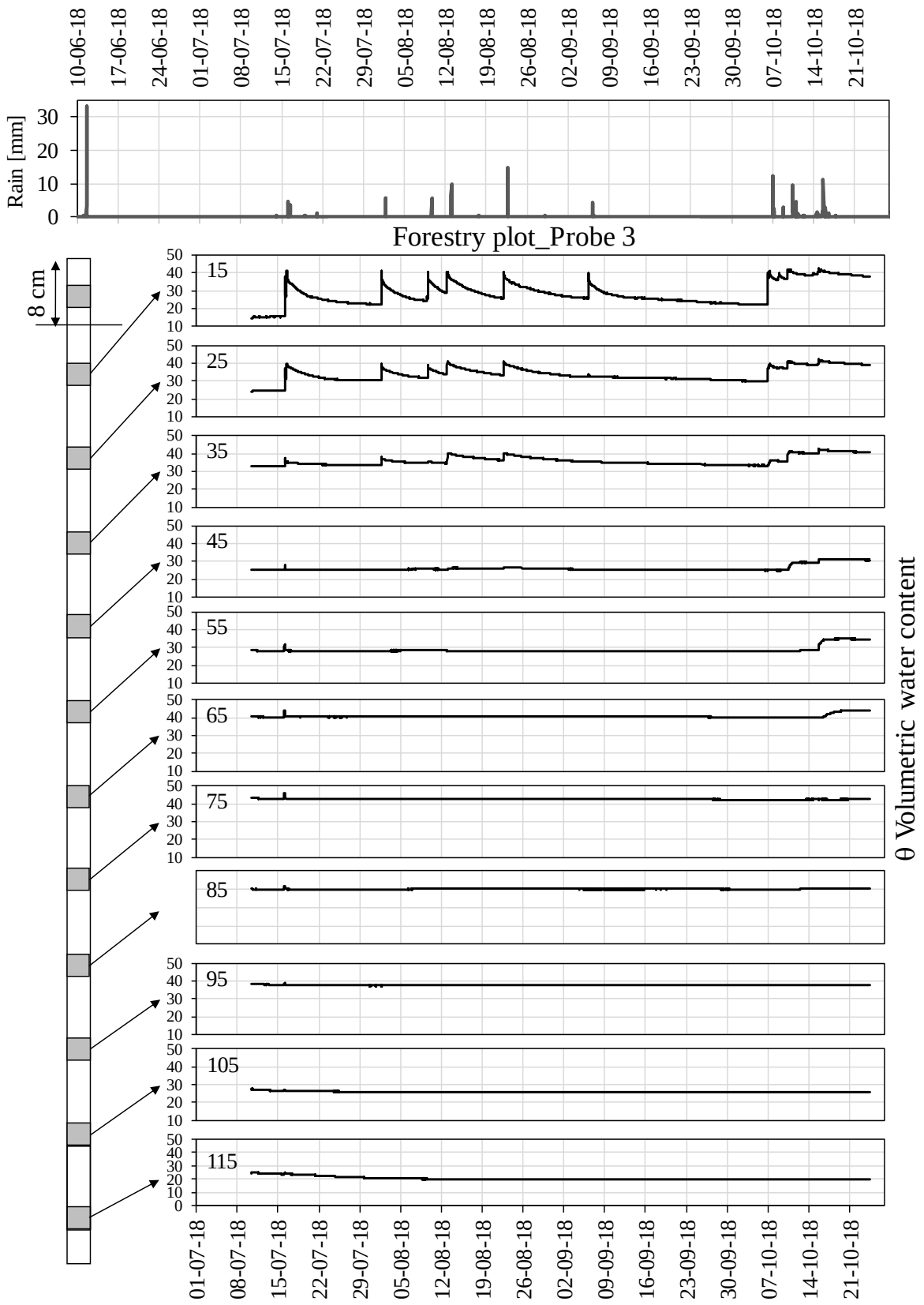

Figure 7.10:Probe 3: volumetric water content over time, along the depth of the probe

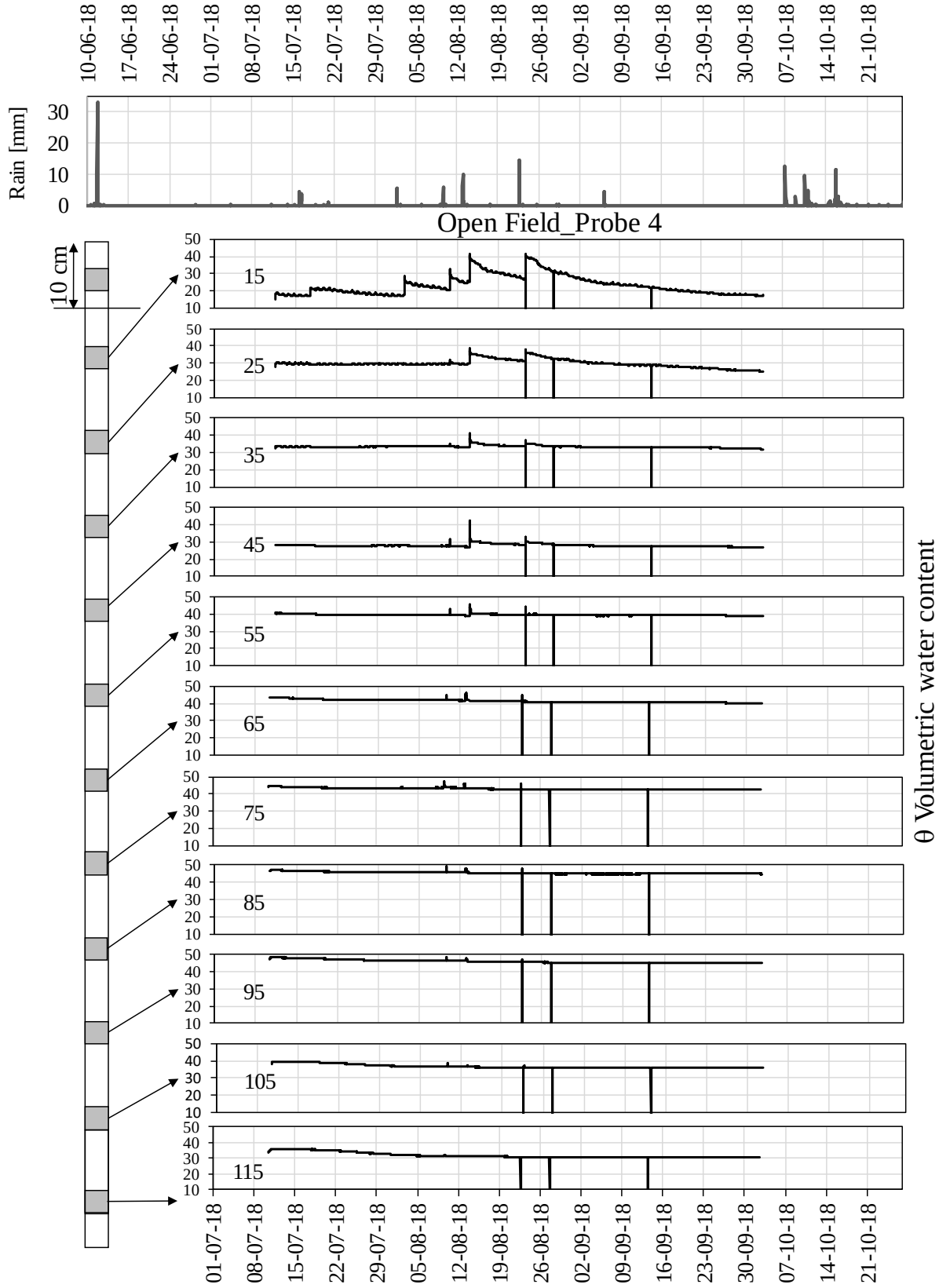

Figure 7.11:Probe 4: volumetric water content over time, along the depth of the probe

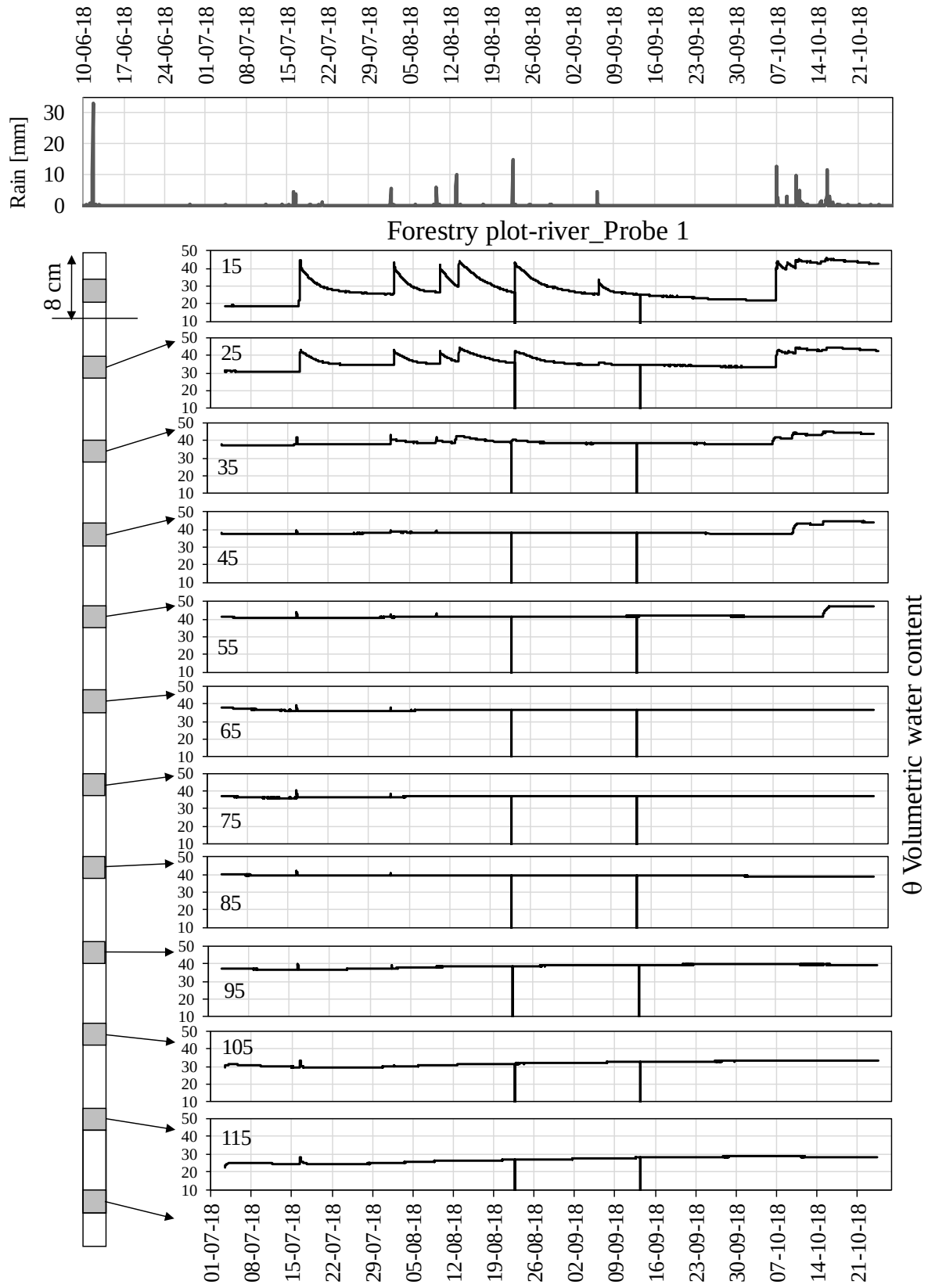

Figure 7.12:Probe 1: volumetric water content over time, along the depth of the probe

Sensors along Probe 1 and Probe 3 detect the changes in water content after a rainy event with a time delay related to the depth of the single sensor, coherently with the infiltration process. The anomalous behaviour of Probe 2 and 4 suggests a spurious effect due to the presence of an air gap around the probe, with water entering directly in contact with the probe during the rainy events.

The qualitative effect of the presence of an air gap around the probe is presented qualitatively in Figure 7.13, in a) long-term conditions, b) during and c) after a rainy event. The dimension of the air gap is magnified in the figure for clarity of presentation.

The measurement of the 'Drill and drop' probe is based on the assessment of the average relative permittivity of the sampling volume. The high difference in relative permittivity between air (1) and water (80) allow the measurement of changes in water content over time. However, the presence of a gap around the probe influences the measurement of the real soil volumetric water content with a dependency of the spurious effect on the ratio between the air gap and the sampling volume of the probe. The effect of the presence of an air gap on the measurement of soil water content is conceptually described in (Figure 7.13). The presence of a layer of air, at a lower permittivity in comparison to the soil and water, within the sampling volume, reduces the overall resistivity, resulting in an underestimation (a*) of the soil water content.

When a rainy event occurs, in case of perfect contact between the probe and the soil the increase in water content will be detected by the various sensors in the probe with a delay related to the depth, and the intensity of the signal will reduce for the deeper layers of soil, coherently with the infiltration process. When an air gap is present, the water will run along the probe and reach all the sensors with virtually no delay. Hence, a flawed installation results in the presence of synchronous peaks at all depth of the probe in the case of a rainy event (Figure 7.13.b), with a correlated overestimation of the soil volumetric water content (h*), due to the high resistivity of water. After few hours from the end of the precipitation, the excess of water around the probe will reach an equilibrium with the soil in the surroundings, shown by a new registered stable value (Figure 7.13.c). The latter value, due to the damping effect of the air layer in the

gap, will tend to underestimate the real water content of the soil, as for the case of Figure 7.13.a.

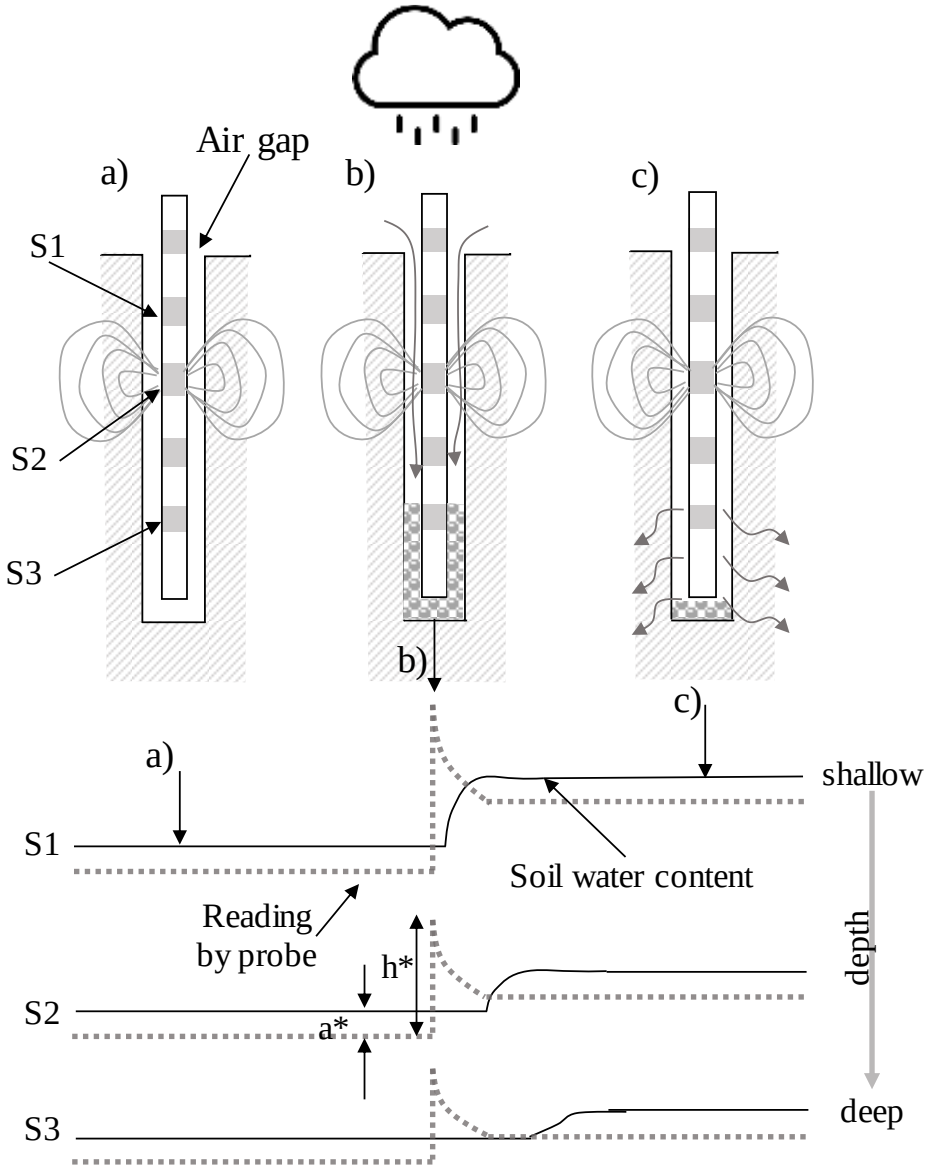

Figure 7.13:effect of an air gap on the measurement of soil water content

7.4.2. Estimation of measurement accuracy

The qualitative assumptions described in Figure 7.13 can be verified quantitatively for the case of a specific rainy event. The selected event is a rainfall occurring in date 22/08/2018.

The profiles of volumetric water content before and after the rainy event are shown in Figure 7.14 for each probe. The continuous dark line refers to the profile observed before the rainfall, at 16:10. The continuous light line shows the profile of maximum water content registered by the probe. The dotted lines refer to a reference moment approximately 3 h after the rainy event, when the excess water infiltrated in the gap of the instrument was assumed, by the trend of the sensors over time, to have equilibrated with the soil in the surroundings.

The volume of water infiltrated is calculated through integration of the change in water content over depth in the hours after rainfall. The obtained value refers to a normalized surface, it is therefore possible to compare the calculated water infiltrated to the intensity of the rainy event measured by the weather station.

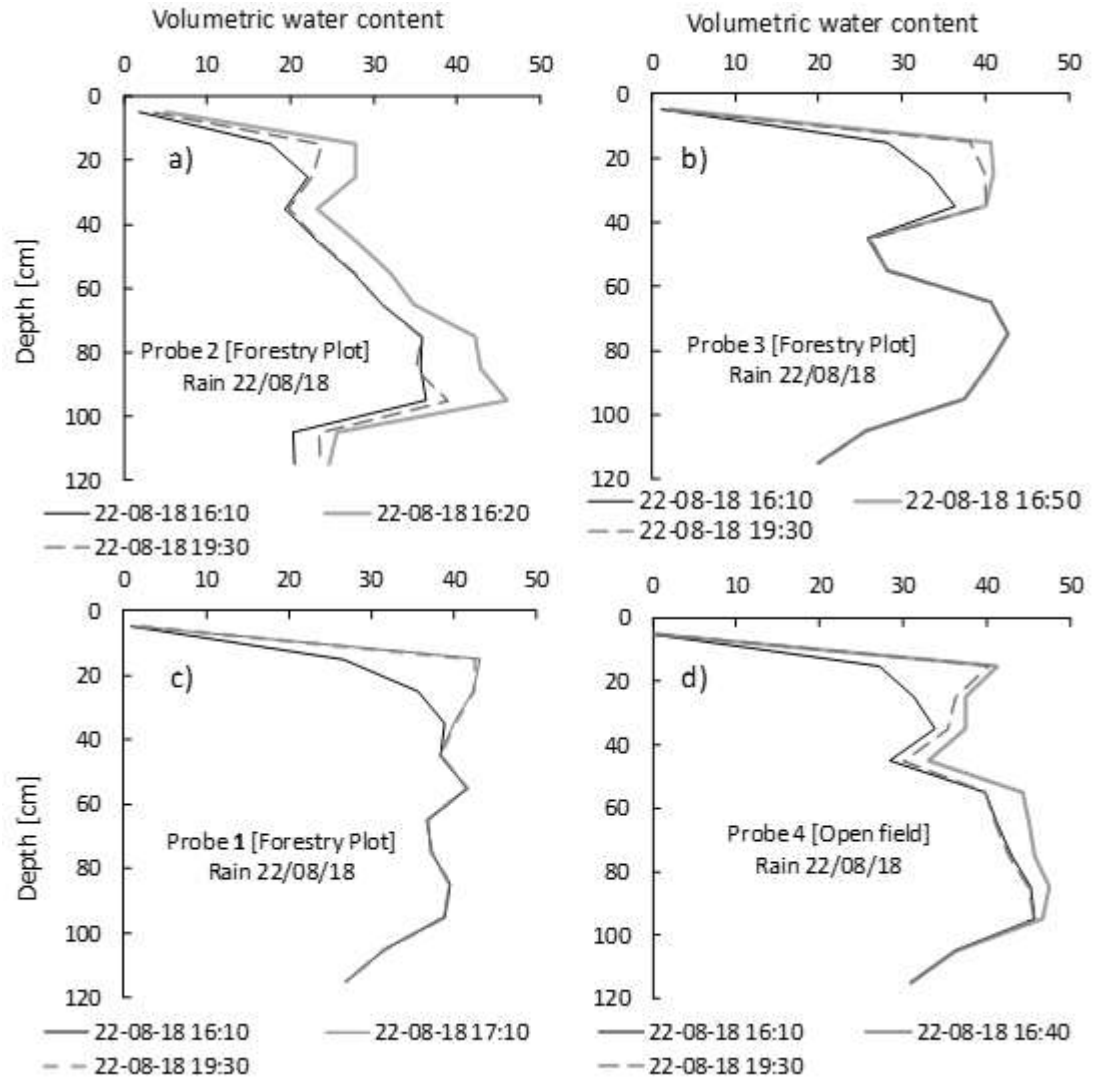

Figure 7.14:Profiles of volumetric water content before and after the rainfall registered in date 22/08/2018

The rainy event registered by the weather station had an intensity of 14.66 mm and it was concentrated between 16:00 and 17:00 (the time resolution of the weather station is 60 min). The values of water infiltration calculated from the profiles at the peak are reported in Table 7.1. Probe 1 and Probe 3 gave an outcome comparable to the experimental value; however, Probe 2 and Probe 4 overestimate the precipitation by a factor of 4 and 2 respectively. This result is coherent with the qualitative discussion represented in Figure 7.13 and confirms the presence of an air gap around the two probes.

It is possible to calculate the amount of water infiltrated when the system reaches an equilibrium (Figure 7.9.c) and the excess of water around the probe re-equilibrates with the soil in the surroundings. The profiles taken into account correspond to the measurement at 19:30 (dotted lines in Figure 7.14), when the peaks of the individual sensors have reached a stable condition (the change in water content in a time frame of 1 hour is negligible). The water infiltrated in the soil is calculated with respect to the reference moment before rainfall, the values are reported in Table 7.1.

In the case of Probe 1 and Probe 3, the measurement of water infiltration after approximately 3 hours is comparable to the measurement at the peak, indicating a negligible air gap. Probe 2 and Probe 4 show a significant reduction of the calculated water infiltration, if compared to the result obtained at the peak. The result is in accordance with the process of water infiltration from the gap into the surrounding soil. The measurement of water infiltrated for Probe 2 and Probe 4 after around 3 h from the rainy event are comparable with the measured intensity of the rainfall, but they tend to underestimate the event.

The error of the estimation of water infiltrated in the soil is calculated in respect to the measured intensity of the precipitation (Table 7.1). It should be noted that this estimation of the error is does not take into account the uneven distribution of the precipitation on the forestry plot, due to canopy interception.

In conclusion, the presence of an air gap effects the measurement, leading to an underestimation of the real soil water content in drying condition and a high overestimation during and immediately after a rainy event. However, if the values at non-equilibrium are omitted, the readings of long-term events are still valid, with the consideration that the absolute value of water content will be an underestimation of the water content in the soil. Any change in water content detected by the probe in the soil in the presence of the air layer in the sampling volume will underestimate the water content change in the field. In addition, fluctuations over diurnal cycles will be dampened.

Table 7.1: Rainy event in date 22/08/2018. Water infiltrated calculated by 'Drill and drop' probes and intensity of the precipitation

	water infiltrated		
	Calculated at the peak [mm]	Calculated after 3 h [mm]	Error at ~3 h
Probe 1	15.9	16	+9%
Probe 2	58	10.9	-25%
Probe 3	17.5	16.8	+14 %
Probe 4	36.2	13.9	-5%
Intensity rainy event (by weather station)		**14.66 mm**	

7.4.3. Response at the seasonal-scale

The profiles of volumetric water content by the two probes in the forestry plot and by the probe in the open field are plotted in Figure 7.15. The selected probes are located at the same distance from the river. The plotted profiles are selected at approximately 1-week interval, during a ‘wet’ and a ‘dry period’; the chronologic sequence of the profile is indicated by the black arrow (The intensity of the line colour decreases with time: lighter lines correspond to profiles taken at a later time throughout the test). The ‘wet’ period goes from the 12/07/2018 to the 22/08/2018 and it is characterized by almost weekly rainfall events. The ‘dry’ period goes from the 30/08/2018 to the 04/10/2018, it was selected for the prolonged absence of precipitations (only one significant rainy event was detected in date 06/07/2018). The period after the 07/10/2018, characterized by very intense precipitations, was considered to be unsuitable for the comparison of the profiles in different location: the frequent rainfalls did not allow the abatement of the spurious effect related to the presence of the gap. Due to logistic constraints, it was not possible to have any probe installed in the open field for the period following the beginning of October.

The soil water content profiles were taken, as far as possible, at equilibrium between the probe and the surrounding soil, in moments not affected by the spurious effect arising during rainfall related to the presence of air gaps.

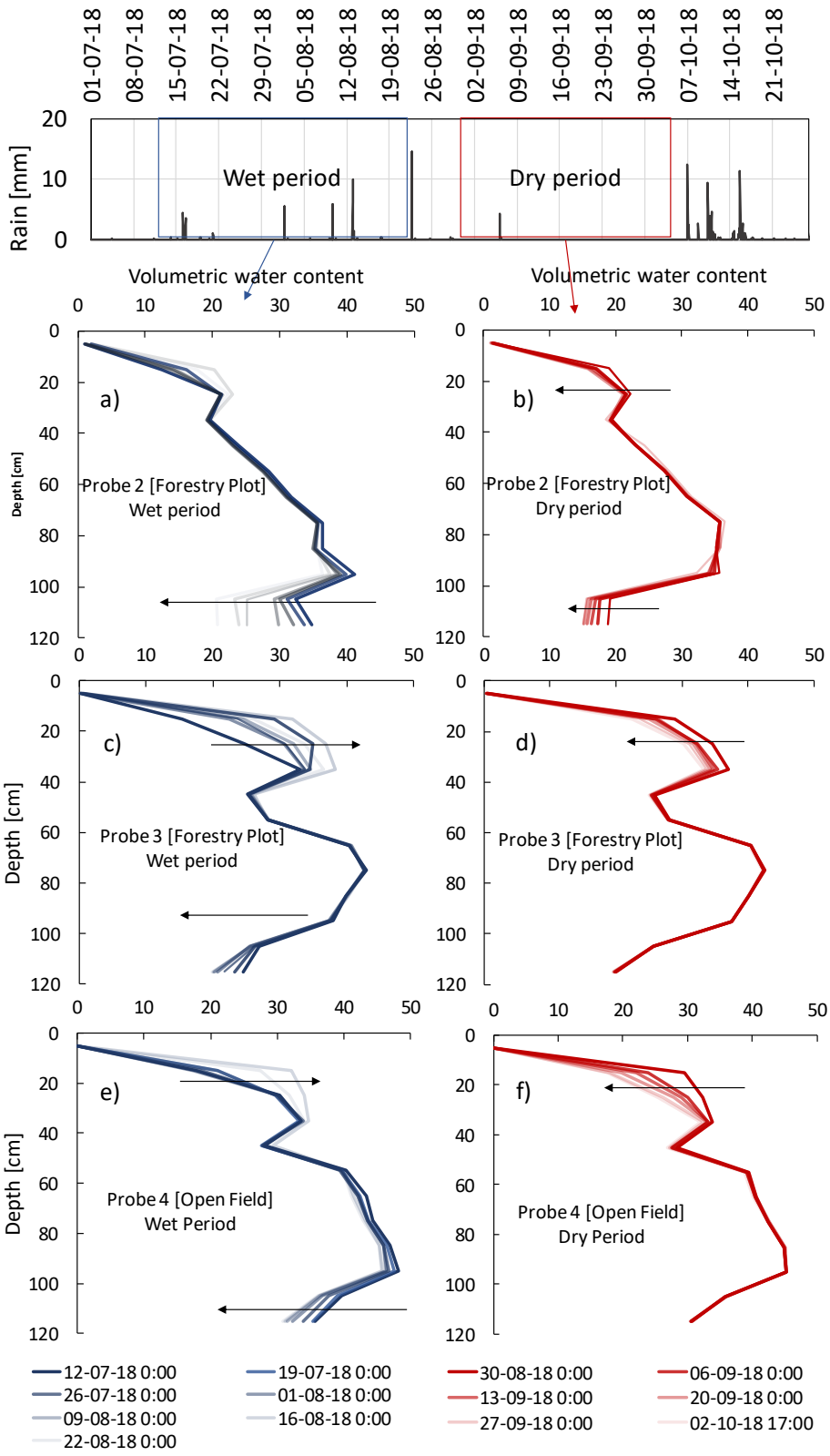

Figure 7.15:Change in water content profile for a wet [12/07/2018-09/08/2018] and a dry period [30/08/2018-04/10/2018]

The results presented in Figure 7.15 show three different zones in each profile: a shallow zone, approximately in the first 40 cm, characterized by relevant changes of soil water content over time; a central zone, approximately between 40cm and 70÷80 cm deep, where the soil water content remains stable over time; a deeper zone, below 70÷80 cm, where changes of water content profile can be observed only for certain probes.

The presence of an intermediate zone with a stable value of soil water content over time implies the presence of a steady state within the layer. Given the non-linearity of the infiltration process (Touma & Vauclin, 1986) and the general absence of a response in the hours after a rainy event by the sensors placed between 45 and 75 cm depth, the central layer is by hypothesis not effected by infiltration in the case of the rainy events observed during the summer period. This suggests a mainly independent behaviour between the shallow zone and the deep zone. This hypothesis is not valid in the case of very intense and frequent rainfalls that effect the water table, where the water infiltration is detected by the sensor at 55 cm and 65 cm in Probe 3 and 1 respectively. (Figure 7.8, see Figure 7.9, Figure 7.10, Figure 7.11 with respect to the period following the 07/10/2018.)

7.4.3.1. *Water removal from the shallow layer*

Figure 7.15 shows how the first 40 cm are subjected to an increase in water content during the ‘wet period’, when the rainfalls result in an infiltration and accumulation of water in the shallow layers. The higher water accumulation is more evident in the forestry plot for Probe 3, placed at 1-m distance from a tree, and less for Probe 2, situated at the centre of the same stand of trees. The change in water content in the shallow layer observed by Probe 4 in the open field shows an intermediate behaviour between the two probes among trees.

In the ‘dry period’ the trend of the profiles in the upper zone of the soil shows a decrease over time of the soil water content. The water loss seems to be more relevant for Probe 4 and Probe 3. It must be noted that the smaller changes of water content

within the soil detected by Probe 2 can be partially due to the presence of the air gap previously discussed.

The shallow zone within the first 40 cm of soil seems to be effected by processes of evapo-transpiration and infiltration, occurring both in the open field and in the forestry plot. Both phenomena seems to be localized within the shallow zone, for the time scale captured by Figure 7.15

7.4.3.2. Water removal from the deep layers

The water extraction from the deeper layer is particularly noticeable for Probe 2, in the forestry plot, where the volumetric water content (θ) in the 115-cm sensor reduces of $\Delta\theta$=14% in 6 weeks during the 'wet period' and $\Delta\theta$=3.8% during the 'dry period'. At the same depth Probe 3 in the forestry plot and Probe 4 in the open field observe a reduction of soil volumetric water content of $\Delta\theta$=4.5% and $\Delta\theta$=4.8% respectively in the 'wet period' and a negligible difference during the 'dry period'. From the comparison between Probe 2 and Probe 4 it can be noticed how the process of water uptake from the deeper layers is more significant at the centre of the stand of trees, in both intervals.

The behaviour of Probe 3 (close to the tree) and Probe 2 (in the middle of the stand) is very different in terms of water uptake from the deep layers. The change in water content over time detected by Probe 3 can be related more to the behaviour observed by Probe 4 in the open field. However, it is necessary to relate the change in of volumetric water content to the absolute water content of the soil, in order to discriminate the possible causes of the lack of water uptake. Figure 7.16 shows the measured water content of the soil for sensors located at 95 cm, 105 cm and 115 cm within the probe. The continuous grey lines represent the measurements of Probe 2 and Probe 3 in the forestry plot, while the dotted line represents the readings by Probe 4 in the open field.

The values of absolute water content represented in Figure 7.16 show how the measurement in the deeper layers of the open field and in the forestry plot remains almost constant throughout the test for Probe 3 and Probe 4. The decrease in water

content detected in the first few weeks of the test is consistent for the three probes at the depths taken into account. The locations of the three probes are different, two of them are placed in the forestry plot, where trees uptake water from the deep layers, and one of them is in the open field, where water is supposed to be extracted only from the shallow layers. The similar trend of change in water content for different local conditions of water depletion suggests the influence of an external factor. The change over time is coherent with the measurement by piezometers on the nearby plots, the trend of decreasing water pressure was therefore assumed to be related to changes in the water table (Figure 7.8).

With respect to Figure 7.16, the water content observed in the open field is consistently higher than the water content observed in the forestry plot. The conditions of water extraction in the deeper layers of soil observed by Probe 3 and Probe 4 results therefore not to be comparable, even if the water extracted is comparable.

The probes in the forestry plot show a similar trend for all sensors considered: at the beginning of the observation, the water content observed by Probe 3 near the tree is consistently lower than the water content measured in the middle of the stand of trees by Probe 2. The water content measured by Probe 3 remains almost constant during the test, while the water content measured by Probe 2 decreases considerably over time, ending in a water content lower than the one measured nearby the tree.

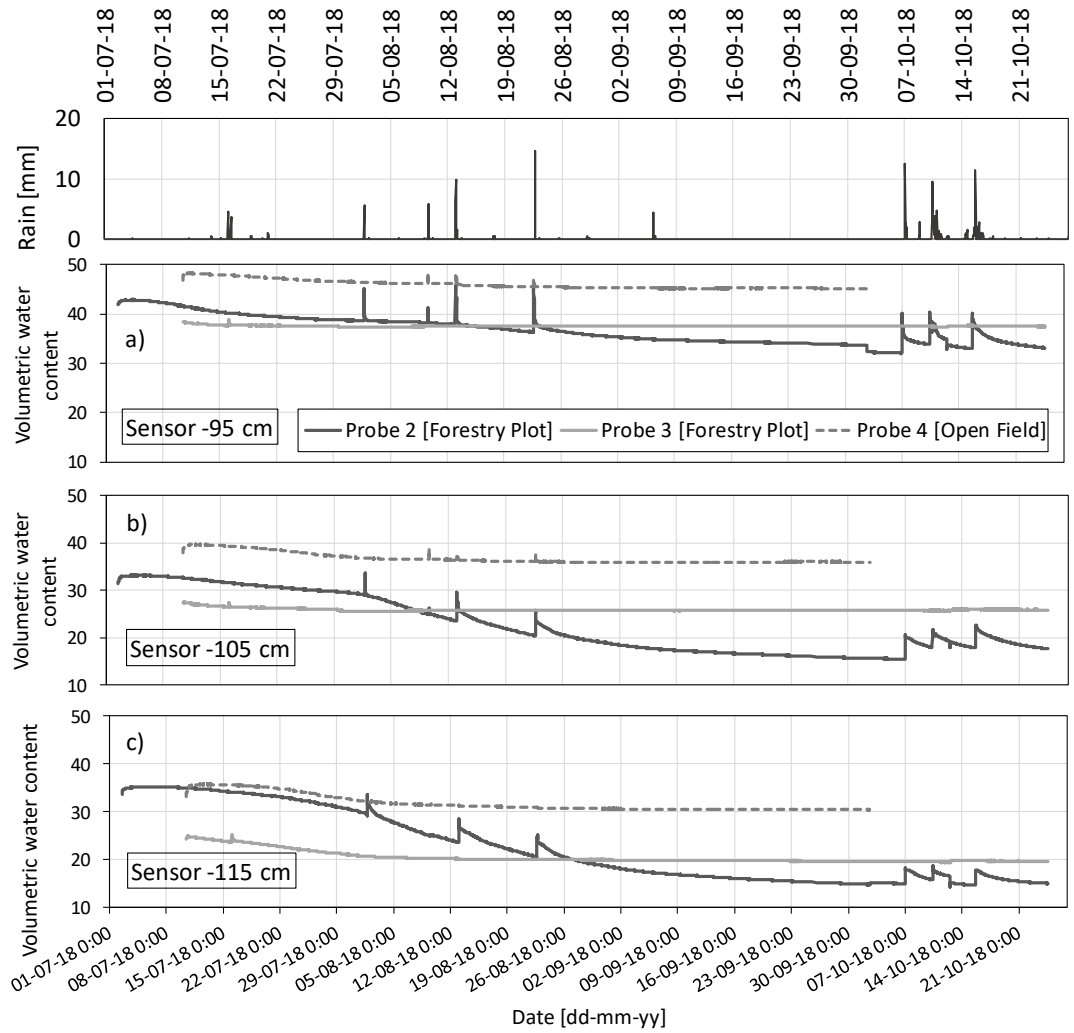

Figure 7.16:Comparison of volumetric water content over time in the deeper layers of soil by Probe 2, Probe 3 (forestry plot) and Probe 4 (open field)

The comparison between the measurement by Probe 2 (in the middle of the stand) and Probe 3 (at the centre of the stand) suggests an uneven distribution of the water uptake.

The difference can be preliminary explained by conceptually idealising the influence of root water uptake on the surrounding soil as a spherical body at constant suction placed between the water table and an impermeable border (the latter assumed to be a representation of the constant-θ zone between 40 and 70 cm depth). The flow net generated by the boundary conditions so defined is reported in Figure 7.17. In this case, the equipotential lines expand with the distance from the point of water uptake.

Therefore, the volume of soil next to the idealised body will have a lower pore-water pressure with respect to the regions further away. Returning to the real case of the rooting system of the tree, it can be assumed that areas where roots are denser are subjected to more intense rates of water uptake; the water depletion concentrated in a narrow volume may lead to a local condition of drought/water limited regime.

The water flow from the soil into the roots is regulated by a gradient in water potential generated by the plant to replace the water lost by transpiration at the level of the leaves (Tyree, 1997). With respect to the conceptual model represented in Figure 7.17, the roots will tend to extract water in areas of soil at higher pore-water pressure, at a further distance from the tree. The hypothesis of redistribution of the water uptake by the roots to face conditions of local drought is coherent with what observed by Mary, et al.(2019), monitoring the root water uptake from a citrus tree by means the Electrical Resistivity Tomography (ERT). The mechanism is usually referred to as 'compensation mechanism' and allows the plant to enhance the water uptake from root in wetter regions when only a limited amount of water can be absorbed by roots in water-scarce portions of soil (Brijesh, et al., 2009).

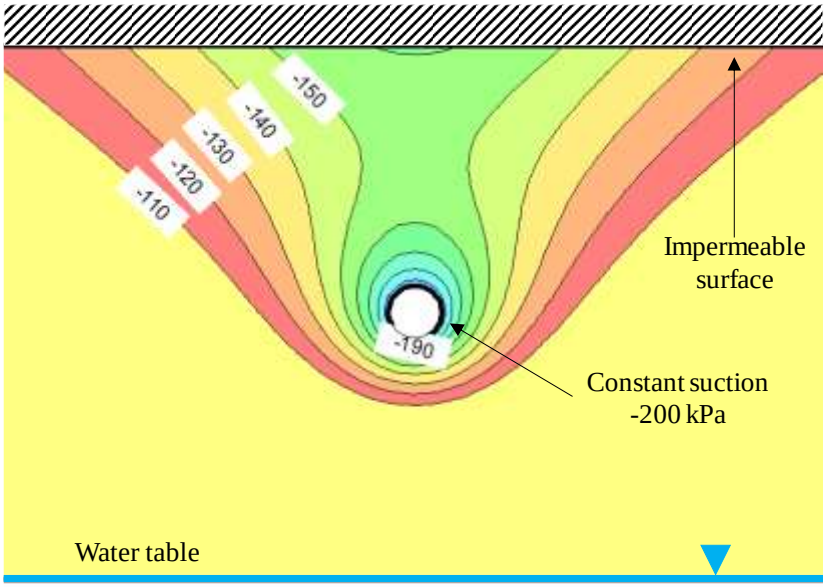

Figure 7.17: Pore water pressure distribution for a body at constant suction above water table and below an impermeable surface

The conceptual model of the flow net generated by a body at negative pore water pressure is corroborated by the distribution of the fine roots (ϕ<1mm) within the soil (Figure 7.18). The roots samples were taken from the boreholes, located as shown in Figure 7.2 and dried at 60°C for approximately two weeks. The dry biomass reported is normalized with respect to the calculated volume of the original section of core. The portion of fine roots –with a diameter below 1 mm –was taken into account, as representative of the younger roots, usually characterised by the physiological function of absorption of water and nutrients (Salisbury & Ross, 1992; Stokes, et al., 2009). The root density distribution in Figure 7.18 shows a higher density between 150 and 250 cm depth. The water table is at around 150 cm depth for most of the time and oscillates between 50cm and 300 cm during the year (see Figure 7.8). The presence of an unusual root density of poplar trees within the capillary fringe was observed by (Hall, 2011).

The majority of fine roots is concentrated in the shallow 40 cm and approximately between 1 and 2.5 m of depth, in the case of the forestry plot. The mass of roots for the open field is reported for comparison (F1, F2, dotted lines). The profile of root biomass on a core taken at 1m from the tree (F7) shows higher concentrations with respect to the profiles of F5 and F6, located at approximately 2.5÷3 m from the tree, partially confirming the idea of the soil near the tree being associated to a higher water uptake and entering the water limited regime (and therefore restricting further water extraction) before the soil in the centre of the stand. It must be noted that the profiles of root density reported in Figure 7.18 can only give an approximate idea of the trend of the fine roots distribution, but they are not indicative of the real root distribution, given the limited amount of sampled soil volume.

Although Probe 2 tended to underestimate water content due to the presence of an air gap, this does not invalidate the observation of the trend of the seasonal variability of soil water content: the presence of the air gap tends to dampen the measurement of changes, the real variation could be more relevant. The underestimation of the absolute value of volumetric water content by Probe 2 may partially justify the decrease of

water content in the centre of the stand below the values observed near the tree, that was assumed to be in conditions of water-limited regime.

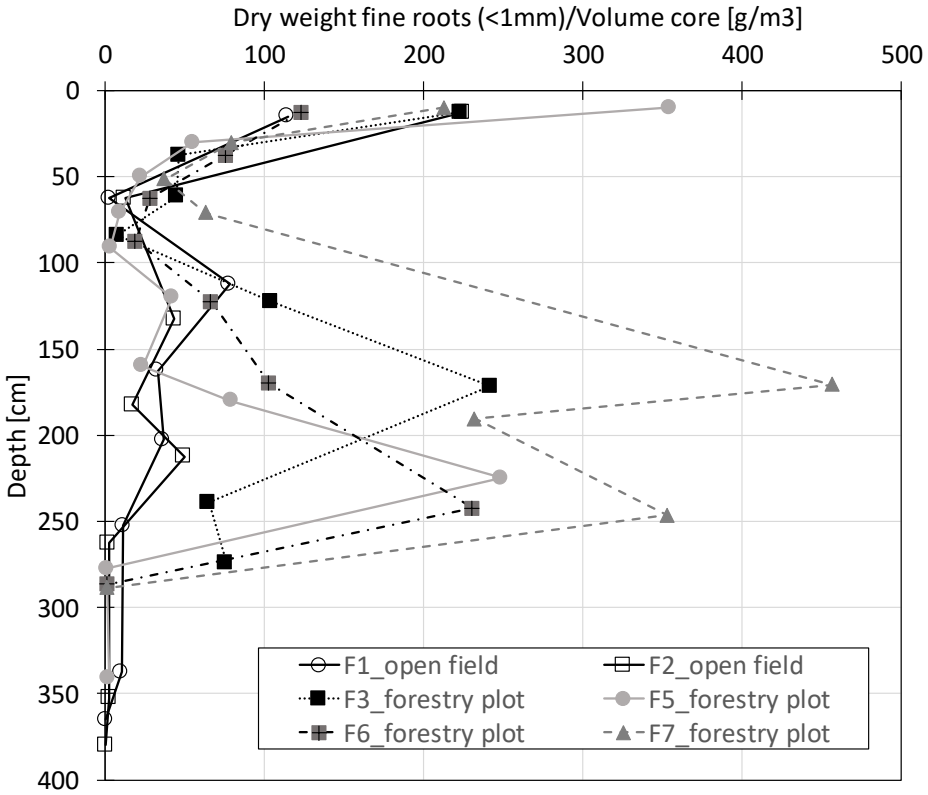

Figure 7.18:Distribution of fine roots biomass over depth.

7.5.An Approach to calibrate evapotranspiration model parameters from field measurement of water content

The amount of water infiltrated in the soil calculated from the profiles of Probe 1 and Probe 3 in date 22/08/2018 was comparable to the intensity of the rainy event registered by the weather station (Table 7.1). Furthermore, the error due to the presence of an air gap for Probe 4 in the open field resulted to be acceptable, if the spurious effect of the accumulation of water immediately after the rainfall was not taken into account in the water balance analysis (Table 7.1).

The trend of the cumulative water loss over time, for a time period following the 22/08/2018, is reported in Figure 7.19. It is calculated by integration of the change in volumetric water content over the shallow 40 cm, for Probe 4 in the open field, and for Probe 3 and Probe 1 in the forestry plot. The reference profile was assumed to be the peak of water content related to the rainy event in date 22/08/2018. The three probes show a common trend in the period following the rainy event: the water content in the soil decreases non linearly for approximately 1 day, it decreases linearly in the following few days, after when it starts reducing the rate of water loss over time. The atmospheric conditions were quite stable within the period taken into account (Figure 7.7).

The first day is assumed to be associated to the non-linear process of infiltration of the residual water accumulated in the gap around the probe into the surrounding soil. The non-linearity is in fact more relevant for Probe 4, assumed to have a wider air gap.

Given the preliminary hypothesis of independent hydrological behaviour of the shallow layer of soil within the period taken into account, the cumulative loss of water from the soil can be associated to the interaction with the atmosphere and to the evapo-transpiration process. The linear part of the curve, highlighted in the graph by a straight line, is typical of a system in energy-limited conditions, where the outward water flux can accommodate the evaporative demand of the atmosphere. The decrease in the rate of water loss over time occurring after approximately 3-4 days, is associated to a progressive limitation of the water availability. In other words, the system is entering a condition of water-limited regime.

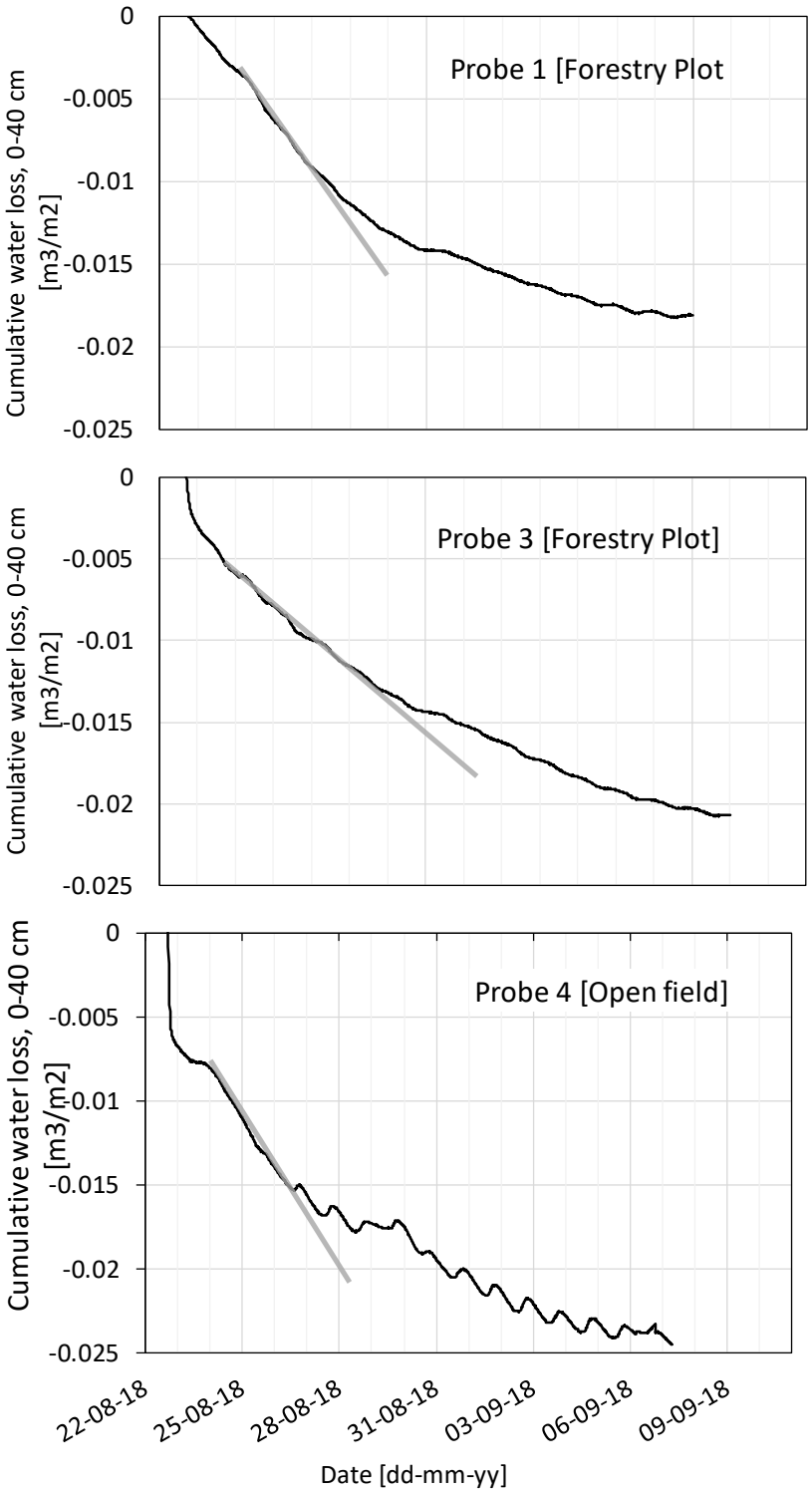

Figure 7.19:cumulative water loss over time in the shallow 40 cm, period [22/08/18-07/09/2018]

The local potential evapo-transpiration rate can be calculated as the rate of change in water content over time in the shallow 40 cm while the system is in the energy limited regime. The rate of water extraction so calculated is reported in

Table 7.2. The reference time interval for the calculation is between 24/08/2018 and 26/08/2018.

Results show a higher rate of water loss for the open field in comparison to the forestry plot, with a reduction of approximately 30% for Probe 3 and 10% for Probe 1, with respect to the value measured by Probe 4 in the open field.

Table 7.2: rate of water loss from the shallow 40 cm during the period between 24/08/2018 and 26/08/2018

	Open field_Probe 4	Forestry plot_Probe 3	Forestry plot_Probe 1
Rate of water loss [mm/day]	3.03	1.9	2.7

The potential evapo-transpiration rate of a system is calculated by eq. [1]. The aerodynamic resistance is calculated according to the model suggested by (Allen, et al., 1998):

$$r_a = \frac{ln\left[\frac{z_m - d}{z_{om}}\right] ln\left[\frac{z_h - d}{z_{oh}}\right]}{k^2 u_z} = \frac{ln\left[\frac{z - d}{z_{om}}\right]^2}{k^2 u_z} \quad [2]$$

Where z_m and z_h are the heights where wind and humidity measurements are respectively taken, d is the zero plane displacement height, z_{om} is roughness length governing momentum transfer, z_{oh} roughness length governing transfer of heat and vapour, k is the von Karman's constant, 0.41 and u_z is the wind speed at height z . In the weather station positioned in plot A2 (Figure 7.1), the wind speed and the relative humidity sensors are placed approximately in the same position, at 2 m above the ground surface. The roughness length governing momentum transfer and the

roughness length governing transfer of heath and vapour are assumed to be identical (Brutsaert, 1982).

Given the proximity of the plots and the similar height of vegetation in the open field in plot A2, where the weather station is located, and in plot B17, where Probe 4 is installed, the weather data about the wind speed and the solar radiation are assumed to be valid for the calculation of the potential evapo-transpiration in the plot under study. The vegetation is comparable to a long grass or a crop and it was around 60 cm high during the period taken into account. The value of z_{om} suggested by Trombetti and Tagliazucca (1984) for the kind of vegetation present in the open field is 0.05m.

The canopy resistance of the vegetation in the open field was inferred by imposing as a potential evapo-transpiration the rate of water loss in the shallow 40 cm of soil in the energy limited regime, calculated for Probe 4. The parameters of eq. [2] imposed to capture the measurement of the probe are reported in Table 7.3. The value of canopy resistance of 340 s/m is comparable to experimental values reported by Monteith(1965) for low vegetation.

Table 7.3: values for the calculation of PET in the open field and reference value of PET by Probe 4

h [m]	z_{om} [m]	r_c [s/m]	PET measured via Probe 4
0.6	0.05	340.37	3.03

The evapo-transpiration registered by the probes in the forestry plot is lower than for the open field, coherently with a screening effect of the trees. The effect of the different conditions for the two probes in the forestry plot was taken into account by imposing a ‘shading factor’ to the solar radiation. The wind speed resulted to be less relevant than the solar radiation in the determination of the potential evapo-transpiration, for the periods taken into account. Hence, the wind speed within the forestry plot was assumed to be equal to the wind speed measured in the open field. The aerodynamic and canopy resistance were assumed to be comparable with the resistances in the open field.

The shading factor for Probe 1 and Probe 3 was assessed independently, given the different position among the trees and the uneven coverage of the canopy. The 'shading factor' was calculated with reference to the climatic conditions and the rate of water loss over time in the period between 24/08/2018 and 26/08/2018. The values so-assessed where then applied to forecast the potential evapo-transpiration for Probe 1 and Probe 3 in the period between 17/07/2018 and 19/07/2018, where the system could be assumed to be in the energy limited regime. The measured and calculated evapo-transpiration are reported in Table 7.4, with the imposed 'shading factor'.

Table 7.4: PET calculated and measured for Probe 1 and Probe 3

		Probe 1	Probe 3
Shading factor		1.49	6.85
PET measured by the probe [24-26/08/2018]	[mm/day]	2.7	1.9
PET by eq. [2] [24-26/08/2018]	[mm/day]	2.7	1.9
PET measured by the probe [17-19/07/2018]	[mm/day]	3.35	2.41
PET by eq. [2] [24-26/08/2018]	[mm/day]	3.86	2.5

The potential evapo-transpiration calculated introducing a 'shading factor' as reported in Table 7.4 gives an error of 15% for Probe 1 and 4% on Probe 3 on the forecast of the PET.

7.7.1. Evaluation of deep transpiration

The approach used for the estimation of the potential evapo-transpiration in the shallow layers of soil has been applied to the evaluation of transpiration from the deeper zones reached by Probe 2.

The trend of the cumulative water loss over time, for a time period following the 01/08/2018, is reported in Figure 7.20; it is calculated by integration of the change in

volumetric water content between 80 cm and 110 cm depth for Probe 2 in the forestry plot. The reference profile was assumed to be the peak of water content related to the rainy event in date 01/08/2018. The trend of the curve shows an initial non-linear trait, coherently with the behaviour at the shallow layers of the other probes and it is associated with the presence of a gap around the probe. After approximately 24 h from the rainy event, the trend of the curve becomes linear (linear trend highlighted by a straight line in the graph), if the natural daily fluctuations are not taken into account. In contrast to the behaviour in the shallow layer, the rate of water extracted over time remains constant for the time interval of 6 days taken into account.

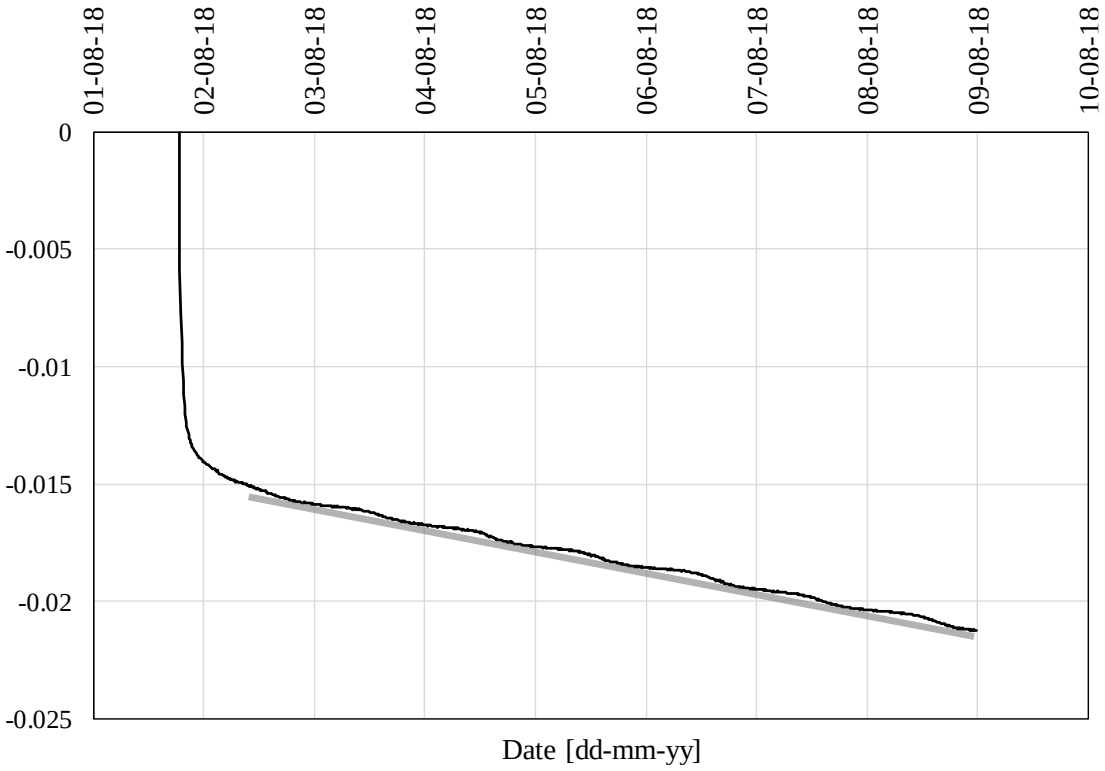

Figure 7.20:cumulative water loss over time in the deep layers of the forestry plot, based on measurements by Probe 2

The daily rate of water loss, calculated with respect to the linear part of the curve in Figure 7.19, is 0.9 mm/day. The Potential evapo-transpiration for the open field in the same period, calculated imposing the parameters defined in Table 7.3, is reported in

Table 7.5. The value of transpiration for the 6m-high trees in the forestry plot is roughly estimated by imposing the value of the tree height and assuming a $z_{om} = 0.4$ m (Trombetti & Tagliazucca, 1984).

Table 7.5: Potential transpiration for the period [03/08/2018-09/08/2018]

Deep transpiration measured by Probe 2 [mm/day]	Evapo-transpiration calculated via eq [1] for open field [mm/day]	Transpiration calculated via eq [1] for forest of 6m-high trees [mm/day]
0.9	4.04	3.46

It is clearly noticeable how the value of transpiration calculated from the measurements of water content by Probe 2 is severely underestimating the (roughly calculated) potential transpiration. The error in the evaluation of the transpiration has two main reasons:

- As already discussed, the measurement of Probe 2 tends to underestimate the values of θ and its variations.
- The area of soil monitored by the probe does not capture the whole depth interested by the root water uptake. Ideally, the total transpiration for a given period is given by the envelope of the change in water content evaluated on the total volume of soil effected by the plant. The envelope represented in Figure 7.21 refers to a single vertical. As visible in the figure, the probe captures only a limited part of the envelope, resulting in an underestimation of the potential transpiration rate.

The evaluation of the transpiration from the plant should be assessed ensuring the perfect installation of the probe and providing a probe able to capture the whole extension along depth of the effect of water depletion.

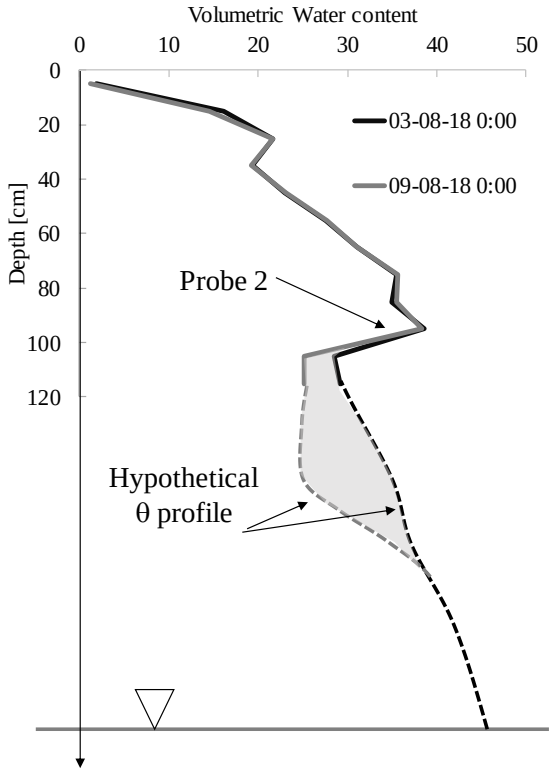

Figure 7.21:measurement of volumetric water content by Probe 2 and hypothetical envelope of water removal by transpiration between 03/08/2018 and 09/08/2018

7.6 Conclusions

The work presented the results of the monitoring of soil water content profile from July to October 2018, by means of the instrument 'Drill&Drop' by Sentek.

The monitoring data allowed identifying two different zones of water uptake, a shallow zone (approximately the first 40 cm of soil) where water is removed by evapo-transpiration, and a deep zone at depths below 80 cm where water uptake is controlled by tree transpiration. The behaviour of the shallow layer and of the deep layer were observed to be independent at least in the period of observation between 02/07/2018 and 04/10/2018.

The analysis of the water balance in the shallow layer allowed to discriminate periods where the system was locally in the energy-limited regime or in the water limited regime. The behaviour observed in the shallow layer in the forestry plot and in the open field was comparable. However, the water content in the deep layers of the open

field was significantly higher, confirming the capability of plants of removing water while the bare soil enters the water limited regime.

The evaluation of the potential evapo-transpiration rate based on the measurements by the 'Drill&Drop' was used to infer some of the parameters of the Penman-Monteith equation, and to forecast the PET for a different period of time. The outcomes are promising based on the prediction achieved. However, complete a validation of the approach to inform eq. [1] will need further study under different conditions and with independent assessment of the various parameters appearing in the potential evapotranspiration equation.

An attempt was made to calculate the deep transpiration in the forestry plot, but the values significantly underestimated the order of magnitude of potential transpiration through the plant. This was due to a probe that was not extended enough to cover the entire depth affected by tree water removal.

A possible approach for the estimation of the root water uptake from the deeper layers in the field would consist in coupling Electrical Resistivity Tomography technology (ERT) and the Drill&Drop probes. The ERT is a useful tool to detect changes in water content at on a volume of soil. The preliminary definition of the area interested by the root water uptake would define the length of the probe required to capture the process of water uptake. Results from the Drill&Drop would be necessary to calibrate the results of the ERT in terms of electrical resistivity against water content. A similar approach was suggested by Mary, et al. (2019), coupling the ERT technology to Mise-a-la-masse (MALM) technology.

The interpretation of data from the 'Drill&Drop' sensors allowed the quantification of the potential evapo-transpiration and the detection of the transition between the energy-limited regime and the water limited regime of the system. The 'Drill&Drop' data could therefore be potentially used to characterise the parameters for potential evapotranspiration model and site-specific reduction function to be implemented as boundary condition in geotechnical applications.

References

Allen, M., Pereira, R. G., Raes, D. & Smith, L., 1998. Crop evapotranspiration: Guidelines for computing crop waterrequirements. *FAO Irrigation and Drainage Paper,* Volume 56.

Anon., n.d. *https://sentektechnologies.com/product-range/soil-data-probes/drill-and-drop/.* [Online].

Briggs, K., Smethurst, J., Powrie, W. & O'Brien, A., 2016. The influence of tree root water uptake on the long termhydrology of a clay fill railway embankment.. *Transportation Geotechnics,* Volume 9, pp. 31-48.

Brijesh, K., Shashi, M. & Maarten, ,. A., 2009. Soil Moisture Dynamics modelling considering the root compensation mechanism for water uptake by plants.. *Journal of hydrological engineering,* 14(9), pp. 913-922.

Brutsaert, W., 1982. *Evaporation into the atmosphere.* s.l.:Dordrecht: Kluwer Academic Publisher.

Feddes, R. & Zaradny, H., 1978. Model for simulating soil-water content considering evapotranspiration-comments. *Journal of hydrology,* Volume 37, pp. 393-397.

Fredlund, D. & Rahardjo, H., 1993. *Soil mechanics for unsaturated soils.* New york: John Wiley and Sons.

Garg, A., Coo, J. & Ng, C., 2015. *Field study of indluence of root characteristics on soil suction distribution in slopes vegetated with Cynodon dactylon and Schefflera heptaphylla,* s.l.: Earth surface process and landforms.

Hillel, D., 1980. *Fundamentals of soil physics.* s.l.:Academic press.

Li, A. et al., 2005. Field-monitoring variations of soil moisture and matric suction in a saprolite slope. *Canadian Geotechnical Journal,* Volume 42, pp. 13-26.

Li, K., De Jong, R. & Boisvert, J., 2001. An exponential root-water-uptake model with water stress compensation. *Journal of Hydrology,* Volume 252, pp. 189-204.

Mary, B., Vanella, D., Consoli, S. & Cassiani, C., 2019. Assessing the extent of citrus trees root apparatus under deficit irrigation via multi-methos geo-electrical imaging. *Scientific reports,* Volume 9, p. 9913.

Monteith, J., 1965. Evaporation and environment. In: *Symposia of the society for experimental biology.* Cambridge: Cambridge University Press (CUP), pp. 205-234.

Nyambayo, V. & Potts, D., 2010. NUmerical simulation of evapotranspirationusing a root water uptake model. *Computers and geotechnics,* Volume 37, pp. 175-186.

Penman, H., 1956. Estimating evaporation. *Eos, transactions american geophysical union,* Volume 37, pp. 43-50.

Salisbury, F. & Ross, C., 1992. *Plant Physiology.* s.l.:Wadsworth.

Sanderson, J., 1983. Water uptake by different regiorn of barley root. Pathways of radial flow in relation to development of the endodermis.. *Journal of experimental botany,* Volume 34, pp. 240-253.

Sinha, R., 2004. *Modern Plant Physiology.* s.l.:CRC Press.

Stokes, A. et al., 2009. Desiderable plant root traits for protecting natural and engineered slopes against landslides. *Plant and soil,* 324(1-2), pp. 1-30.

Tarantino, A., Ridley, A. & Toll, D., 2008. Field measurement of suction, water content, and water permeability. *Geotechnical and Geological Engineering,* Volume 26(6), pp. 751-782.

Touma, J. & Vauclin, M., 1986. Experimental and numerical analysis of two-phase infiltration in a partially saturated soil. *Transport in porous media,* Volume 1, pp. 27-55.

Trombetti, F. & Tagliazucca, M., 1984. *Characteristic scales of atmospheric surface layer.,* Bologna, Italy: Istituto FISBAT-C.N.R..

Tsiampousi, A., Zdravkovic, L. & Potts, D., 2016. *Soil-atmosphere interaction in unsaturated cut slopes.* Paris, s.n.

Tyree, M., 1997. The cohesion-tension theory of sap ascent: current controversies. *Journal of experiemntal botany,* 48(315), pp. 1753-1765.

Chapter 8 Conclusions and Future work

The work developed in this thesis has focused on the study of the hydraulic response of the soil-plant-atmosphere continuum. The first problem tackled by this work was the development of a measurement technique to measure the (negative) water pressure both in the soil and the plant. The second part has investigated experimentally the process of water extraction driven by the interaction of the ground with the atmosphere, by comparing the cases where such an interaction occurs in bare ground (evaporation) or is mediated by vegetation (transpiration). A conceptual framework was put forward for the quantitative evaluation of the hydrological effects of vegetation based on laboratory experimental observations and it was adopted in a second stage for the interpretation of field measurements.

In order to monitor the water pressure in the soil-plant hydraulic system, a novel application of the HCT for the measurement of xylem water pressure was developed. The technique was validated by comparison with the pressure chamber and the thermocouple psychrometer. The comparison showed a good agreement between the pressure chamber and the HCT. Observations made with the thermocouple psychrometer and the HCT showed a comparable prompt response time and an excellent agreement for negative water pressure below -500÷ -700 kPa. The novel procedure for the use of HCTs allows for the use of a single instrument to monitor the negative water pressure in the whole soil-plant continuum.

The transpiration process was first investigated under laboratory conditions by benchmarking against to the process of evaporation. Two columns were set up, one including a vegetated sample and the other one including a bare sample. The two columns were subjected to the same environmental conditions.

The results highlighted that the presence of vegetation may not be always beneficial to soil water removal. Two evaporation/transpiration regimes can be distinguished, the

energy-limited (potential) and the water limited-regimes respectively. In the energy limited regime, the potential transpiration is controlled by the aerodynamic and canopy resistance whereas the evaporation is only controlled by the aerodynamic resistance (the canopy resistance is obviously nil). Because the aerodynamic resistance is generally lower for vegetated soil than bare soil, the combination of the aerodynamic and canopy resistances can play either in favour of the bare or the vegetated soils depending on the vegetation type. In the water-limited regime, the effect of vegetation is always beneficial due to the different mode of water extraction (concentred at the ground surface for the bare soil and distributed along the rooting zone for the vegetated soil). This was reflected in the time at which the transpiration entered the water limited regime (i.e. the transpiration starts reducing from the potential values), which was definitely longer in the vegetated soil than the bare one. This result was more evident for the well-developed rooting systems, as the plant could access more easily the deeper soil layers. Numerical simulations were able to capture the process of soil water extraction by the roots. In the preliminary study presented, the modelling of water extraction via a sink term (Nyambayo & Potts, 2010) related to the root distribution appeared to be not appropriate to represent root water uptake. The root water uptake was indeed modelled by imposing the suction measured in the xylem over a number of extraction points. This boundary condition is coherent with the physiological process of root water uptake driven by a water pressure gradient between the soil and the xylem in the root (Tyree, 1997). Though highly dependent on the geometry imposed for the case presented, this approach based on this mode of water extraction could better capture the time evolution of the transpiration process from the vegetated system.

These tests also allowed suggesting an innovative approach to model transpiration in geotechnical applications. This is usually achieved via the Feddes reduction function, a simplified method to model transpiration in the water-limited regime. In the case under study, the comparison between the water pressure in the soil and the plant xylem water pressure allowed for a more accurate estimation of the reduction function parameters in contrast to the current geotechnical practice, where parameters are

borrowed from the agricultural literature for crop species and often loosely compacted organic soils.

The repeatability of the results obtained from the two columns was tested on a simplified setup, to compare the difference between the mechanism of evaporation and transpiration on for different species. The results corroborated the findings obtained from the fully instrumented column, including that the effect of vegetation on soil water extraction is not always beneficial in comparison with bare soil. In general, the bare soil could accommodate a higher water flux while in energy-limited regime, ensuring faster water depletion. At the same time, the vegetated system enters the water limited regime much later than the bare soil. The most relevant differences between the vegetated and the bare soil could be appreciated in the fine grain natural soil.

The experimental investigation carried out in the laboratory was up scaled to the field, to overcome the limitations of the laboratory setup. The test was carried out in a forestry plot, vegetated with 20 years old poplar trees, and the adjacent open field, where shallow vegetation grew during the test. The area was located in the Domaine of Restinclieres, France. The change of soil water content in the forestry plot and in the field was monitored between July 2018 and October 2018 by means of Drill&Drop probes. The results showed two almost independent ongoing processes along the soil profile: evapo-transpiration from the shallow layers (above 40 cm of depth) and transpiration from the deeper layers (below 80 cm of depth). During the period where water content was monitored, the intermediate zone seemed not to be affected by the changes in volumetric water content, for the rainfall intensity recorded between July 2018 and September 2018. The behaviour in the shallow layers of soil in the open field and in the forestry plot appeared to be comparable. The behaviour in the deeper layers of the forestry plot and of the open field, where only newly established shallow vegetation was present, was considerably different. Changes in water content associated with transpiration were relevant in the forestry plot in comparison to the open field. In addition, the water content recorded in the deeper layers of the open field was consistently higher than the water content observed by the two probes in the

forestry plot, confirming in this case the positive effect of deep root vegetation on soil moisture depletion, in comparison to shallow vegetative cover. The difference observed by the two probes in the forestry plot was assumed to be related to a redistribution of root water uptake due to a local condition of drought (Mary, et al., 2019).

The conceptual framework developed on the basis of laboratory results experience was adopted for the interpretation of the monitoring data in the field. It was possible to identify a condition of energy limited regime for the shallow part of the soil after a rainy event, and the transition to the water limited regime after few days. The potential evapo-transpiration calculated from the change in water content profile along the first 40 cm resulted to be higher in the open field than in the forestry plot, for the time intervals considered. The potential evapotranspiration rate, calculated from measurement of volumetric water content by 'Drill&Drop' while the system was locally in the energy limited regime, were used to characterise as a first approximation some of the parameters of the Penman-Monteith equation for evapotranspiration.

It was possible to identify a period where water extraction occurred in the energy limited regime in the deeper layers of the forestry plot. No reduction of the rate of water extraction over time was observed. Over the period of observation, the deeper soil remained in a condition of energy limited regime. These results were consistent with the observations made during laboratory experiments consisting in an increased capacity of water depletion when the pressure gradients are redistributed along the rooting depth. Unfortunately, it was not possible to compare the transition time from Energy-limited regime to Water-limited regime for the transpiration from the deep layers in the forestry plot and the evapo-transpiration from the shallow layers. The condition of energy-limited regime seemed to be achieved only after main rainfall events (i.e. 22/08/2018).

An attempt was made to evaluate water uptake associated with to the process of transpiration in the deeper layers of soil. However, the water uptake inferred from the water content profile probes significantly underestimated the potential transpiration of

the tree, the error was related to the fact that the probe length was to short compared to the depths where roots were extracting water.

In conclusion, the conceptual framework defined through laboratory experiments allowed the interpretation of data in the field. The assessment of the effect of vegetation through comparison with the bare soil, the discrimination between conditions of energy-limited and water limited regimes, the competing effect of canopy resistance and aerodynamic resistance for the evaluation of the potential evapo-transpiration, and the redistribution of the gradients according to the different mechanisms of water extraction, are identified to be key points when assessing potential beneficial hydrological effects of vegetation.

The lesson learned from field monitoring included the need of characterising water uptake by evapo-transpiration in shallow layers and by transpiration in the deeper layers. In addition, water uptake in the deeper layers appears to be a 2D process, which is intuitive. The observation of the soil water regime in the field seemed to confirm the dependency of root water uptake to the local water availability in the soil, as corroborated by the numerical simulation of laboratory experiments. The outcome is consistent with the observation of compensative mechanisms of root-water uptake (Lai & Katul, 2000) (Li, et al., 2001).

The next steps towards the ‘engineering’ of vegetation as hydrological remedial measurement includes the development of a model for the soil-plant-atmosphere continuum where characteristics of the soil and vegetation can be taken into account quantitatively. Vegetation may or may not be beneficial in increasing shear strength depending on a number of competitive factors, including the possible adverse effects on the soil hydraulic characteristics related to phenomena of water infiltration (Ghestem, et al., 2011). However, this dissertation has contributed to lay down a framework to investigate experimentally the effect of the vegetation on the soil moisture depletion within the soil.

The experimental setup and the data interpretation presented, with a focus on the measurement by HCT in both on the plant and the soil, is a step forward towards the achievement of an ‘open field laboratory’, where the water uptake is characterised directly in the field.

Future work

Improvements to the work presented

The work presented in this thesis aimed to develop tools for monitoring water flow in the soil-plant continuum and to develop a framework to guide the investigation of the hydrological effects of vegetation in the field. However, several other steps would be required before to achieve the goal of ‘engineering’ vegetation to enhance soil water uptake.

The validation of the HCT should be extended to more plant species with a variety of weather conditions, both in the field and in the laboratory. Furthermore, measurements of xylem water pressure by the HCT and the Thermocouple Psychrometer should be replicated under field conditions, to assess the impact of temperature gradients between plant, instrument, and surrounding air.

Additional information on the soil used during the study should be added, especially for the soil of Restinclieres, possibly defining the water retention curve for the soil and hydraulic conductivity. Tests presented in Chapter 5 might have been complemented by conventional ‘static’ water retention data possibly to investigate whether ‘static’ water retention data are appropriate to investigate and model a dynamic process (water retention data were properly assessed ‘dynamically’ in the infiltration column tests).

The experiments did not take into account the evolution of the plant effects over time and the dependencies related to the plant growth. Especially for the case of experiments undertaken in the laboratory on newly vegetated soils, the results were probably influenced by the limited plant growth. This was intentional, to prevent

changes in soil bulk properties along the experiment; nonetheless growth effects should be taken into account.

The main limitation of the numerical model developed to capture transpiration and evaporation from the columns via resistive extraction points is associated with the discretional distribution if extraction points selected, which affects both the back-calculated resistance at the soil-root interface and the pore-water pressure simulation. The effect of the geometry should be studied further and results regarding the back-calculated soil-root interface resistance should be compared with experimental data. Given the limitations of the commercial software Geostudio in defining a geometry able to capture the phenomena investigated at the root scale, other options should be explored. Furthermore, given the geometry of the specimen, it would be more appropriate to simulate the experimental data under axisymmetric rather than 2D conditions.

With regard to the 'accessible' method for the selection of vegetation for groundwater removal, tests should be repeated with other species and soil types in order to build a relatively large database. The use of grass species is particularly appropriate for the vegetative cover of geotechnical structures like river banks and flood embankments considering that the presence of large and deep roots may create preferential paths when water penetrates the soil from the submerged slope during floods (Coppin & Richards, 1990). Furthermore, the test should be repeated ensuring the complete coverage of the soil with grass blades, in order to differentiate transpiration from evaporation.

The conceptual framework for the interpretation of the results in the field allowed the identification of periods of energy-limited regime and water-limited regime for the shallow layer of soil. However, several simplifications were taken into account. The assumption of independent hydraulic behaviour from the deeper layers of soil and from the shallow part should be further explored through the analysis of the soil properties and of the root distribution. The hypothesis was considered to be valid between July and beginning of October. However, intense precipitations at the end of October lead

to visible phenomena of infiltration within the first 65 cm. The assumption that shallow and deep layers behave independently should be further explored in relation with the weather conditions.

The comparison of the mechanisms of deep root extraction and shallow evapo-transpiration requires the comparison of the cumulative outward water flow over time. Unfortunately, it was not possible to compare the extraction of water from the two different layers within the time period observed, to observe the transition from energy-limited to water limited regime. The potential transpiration from the deeper layers could not be compared with the evapo-transpiration in the shallow layers due the limited depth sampled by the 'Drill&Drop' probes. A possible solution to overcome this limitation would be coupling Drill&Drop measurement with Electrical Resistivity Tomography to assess water uptake over larger and deeper volumes.

The method to assess locally the parameters for the potential evapo-transpiration should be further explored and tested against established methods, under different climatic and vegetation conditions.

Future work to 'engineer' vegetation as hydrological remedial measure

The goal of this work was to lay down a conceptual framework to understand and assess in a quantitative way the effect of vegetation on the extraction of water from the soil (in comparison with the bare soil). The next step would be to develop a simplified soil-plant-atmosphere model where soil and vegetation characteristics can be taken into account. The model could then be used to identify the vegetation requirements to be used in the design of remedial measures for soil stabilisation.

The study of the optimal characteristics of vegetation for soil water removal should then be assessed in terms of impact on the stabilisation of slopes and geotechnical structures. The same type of vegetation should be applied in trials involving different sites, in order to estimate the critical conditions in terms of slope and water infiltration. Furthermore, it would be important to compare the stabilising effect of water depletion

by transpiration with respect to the mechanical effects due to the presence of the roots and the adverse hydrological effects related to the increased permeability of the shallow layers of soil.

References

Angers, D. & Caron, J., 1998. Plant induced changes in soil structures: processes and feedbacks. *Biogeochemistry,* Volume 42, pp. 55-72.

Aubertin, G., 1971. Nature and extent of macropores on forest soils and their influence on subfarce water movement. *U.S.D.A. FOREST SERVICE RESEARCH PAPER* .

Coppin, N. & Richards, I., 1990. *Use of Vegetation in Civil Engineering.* s.l.:CIRIA.

Ghestem, M., Sidle, R. & Stokes, A., 2011. The influence of plant root systems on subfarce flow: inmplications for slope stability. *Bioscience,* 61(11), pp. 869-879.

Lai, C.-T. & Katul, G., 2000. The dynamic role of root-water uptake in coupling potential to actual transpiration. *Advances in water resources,* Volume 23, pp. 427-439.

Li, K., De Jong, R. & Boisvert, J., 2001. An exponential root-water-uptake model with water stress compensation. *Journal of Hydrology,* 252(1-4), pp. 189-204.

Mary, B., Vanella, D., Consoli, S. & Cassiani, C., 2019. Assessing the extent of citrus trees root apparatus under deficit irrigation via multi-methos geo-electrical imaging. *Scientific reports,* Volume 9, p. 9913.

Nyambayo, V. & Potts, D., 2010. NUmerical simulation of evapotranspirationusing a root water uptake model. *Computers and geotechnics,* Volume 37, pp. 175-186.

Tyree, M., 1997. The cohesion-tension theory of sap ascent: current controversies. *Journal of experiemntal botany,* 48(315), pp. 1753-1765.

Appendix A

Plant growth conditions

Plant species

The table reports the plants species used for the experiments reported in this thesis, with the growth conditions and the provenience of the plants. The soil type is better defined in section "Soil Type".

Experiment reported in:	Plant species	Main characteristics	Provenience	Growth conditions	Soil Type
Chapter 3	Chestnut tree *Castanea sativa mill.*	Tree, angiosperm	~15 years old orchard	In situ conditions-Campania-Italy	S1
	Pear tree *Pyrus communis*	Shrub, angiosperm	Nursery, ~2 years old	Lab. Conditions*	L1
	Salix tree *Salix cinerea*	Shrub, angiosperm	Nursery, ~1 years old	Lab. Conditions*	S2
Chapter 4	Cherry tree *Bigarreau burlat*	Shrub, angiosperm	Nursery, ~2-3 years old	Lab. Conditions*	L1
	Oak tree *Quercus rubra*	Shrub, angiosperm	Nursery, ~2-3 years old	Lab. Conditions*	L1
Chapter 5	*Lollium perenne*	Herbaceous species	From seeds	Lab. Conditions*	L2

	Willow tree *Salix cinerea*	Shrub, angiosperm	Nursery, ~1 years old	Lab. Conditions*	S2
Chapter 6	*Lollium perenne*	Herbaceous species	From seeds		S2, L2
	Medicago sativa	Herbaceous species	From seeds		S2, L2
Chapter 7	Poplar tree	Tree, angiosperm	20 years old orchard	In situ conditions-Montpellier-France	S3

Soil Type

Code	Name	Provenience	Main characteristics
S1	Pyroclastic soil	Penisola Sorrentina, Naples, Italy, at about 850 m above sea level.	Pyroclastic soil, presenting a shallow layer of organic matter, a layer of cinerite and angular pumices with a thickness varying from a few millimetres to a few centimetres and an underlying layer of 3÷4 cm angular pumices at least 1 m thick (Rodrigues Afonso Dias, 2019)
S2	Silty sand	Rest&BeThankful, Scotland, UK (56.21, -4.83)	73% sand, 23% silt, 4% clay (See chapter 5 for the grain size distribution and main hydraulic properties)
S3	Clayey silt	Demain de restinclieres (43.71, 3.85)	24% sand, 50% silt, 26% clay (See chapter 7 for the grain size distribution)

L1	Organic soil	highly organic and lose soil (92 % organic matter, 8% sandy silt (68% silt, 32% sand))
L2	'Synthetic' silty sand	65% sand, 30% silt, 5% clay (See chapter 5 for the grain size distribution)

Growth conditions

Trees *in situ* were subjected to natural conditions before and after the test, it was not within the scope of the study to change the given conditions.

*Lab conditions: the laboratory has a climatic system that allows to maintain an almost stable temperature and relative humidity throughout the year, during day and night time. The temperature is approximately 20±1°C, and the RH is 40±5; a continuous record of RH and air temperature in standard laboratory conditions is reported in Figure 0.1.

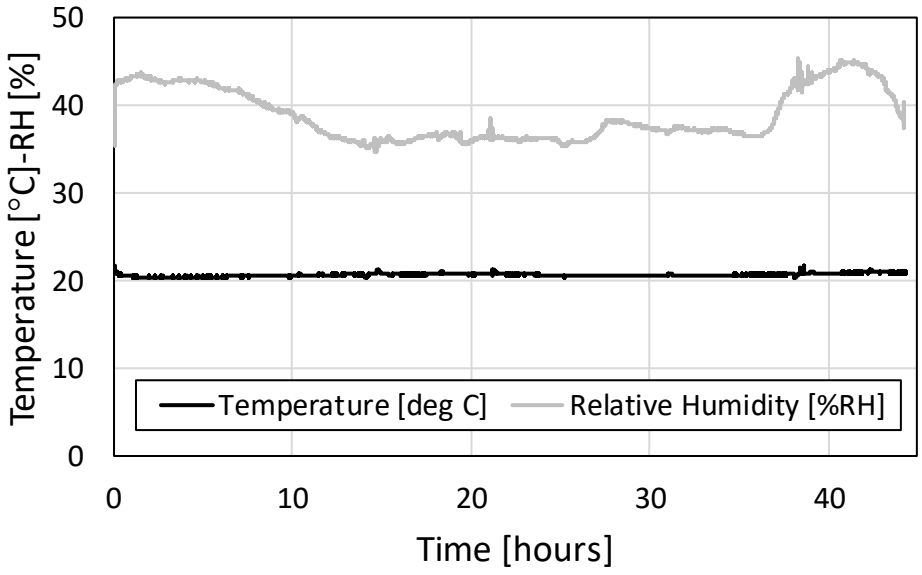

Figure 0.1: Record of relative humidity and air temperature in standard laboratory conditions, measured by Sensirion RH sensors. The measurement was done in early December 2019 and lasted almost 45 hours.

Solar radiation was mimicked by a 36 W growth lam produced by Sylvania. The model was F36/GRO and it was 120 cm long. The lamp was switched on for 14 h (6 a.m.-8 p.m.) and off for the remaining 10 h (8 p.m.-6 a.m.), to simulate natural day/night cycles. Ventilation, when provided, was added using a normal fan placed at about 1 m from the work bench. The wind velocity, measured with a hot wire thermos anemometer, was about 2.0÷4.5 m/sec, depending on the position of the measurement site in relation to the fan central axis (i.d. the air flow on the sides is weaker than the central flow)

Bushes were taken from specialize nurseries, while the grass cover was seeded directly on the soil surface. Before the beginning of each test, the vegetation was let grow, or let develop new leaves and shoots, in the case of young trees. This “pre-conditioning” was done in the controlled conditions of the lab, mimicking the day/night cycles using the growth lamp and supplying an adequate amount of water for plant to develop (i.d. watering occurred twice a week for bushes, while the soil surface was wet daily for grass cover).

Appendix B

Effect of temporal and spatial discretization on the modelling water extraction via evaporation from bare soil

The solution presented in Chapter 5 for the evaporation from bare soil was calculated imposing a spatial discretization of 2.5 mm and temporal discretization of approximately 2 min. In order to exclude the possibility of a local point of instability of the solution, the numerical model was executed refining the temporal and spatial discretization of respectively 33% and 20%. Results of the analysis in terms of trend of the pore-water pressure over time at three different height of the specimen are reported in Figure 2.

A summary of the discretization imposed for each case and related results is reported in Table 6.

Table 6:Spatial and temporal discrimination imposed for each model and related cumulated water loss

	Presented model	Refined Spatial discretization	Refined Spatial discretization
Mesh dimension	0.0025 m	0.002 m	0.0025
Total duration simulation	10+78 days	10+78 days	10+78 days
Number of time steps (WL)	92160	92160	113760

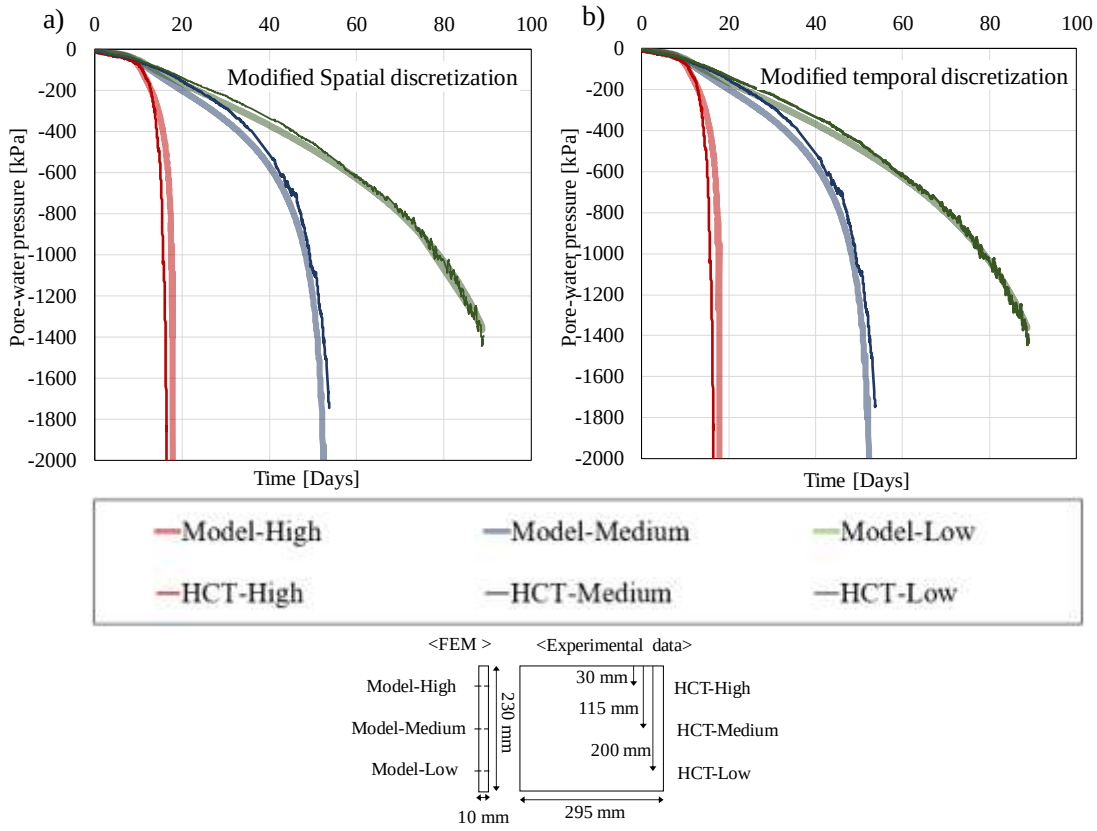

Figure 2: Pore water pressure measured by HCTs and modelled via FEM, for a a) modified spatial discretization and for a b)modified temporal discretization

Appendix C

Imposition of different water pressure at the extraction points

It was not possible to impose a known xylem water pressure at the extraction points for the last 23 days, due to cavitation of both HCTs on the willow. The pressure was assumed to increase linearly to a final value of -231 kPa, discretionally chosen. The final water extraction from the system related to the function of water pressure over time so-defined is reported in Table 7. The case of different final water pressures was taken into account, imposing the functions of the evolution of water pressure over time reported in Figure 3.a and Figure 4.b. The resulting evolution of water loss over time and the final water loss from the system are reported in Figure 3, Figure 4 and Table 7.

Table 7:Final water pressure imposed and relative final water loss.

Final water pressure [kPa]	Final water loss [kg]	Relative error
-231	-5.05	
-132	-4.97	-1.58%
-531	-5.11	1.18 %

- **Final Water pressure: -133 kPa**

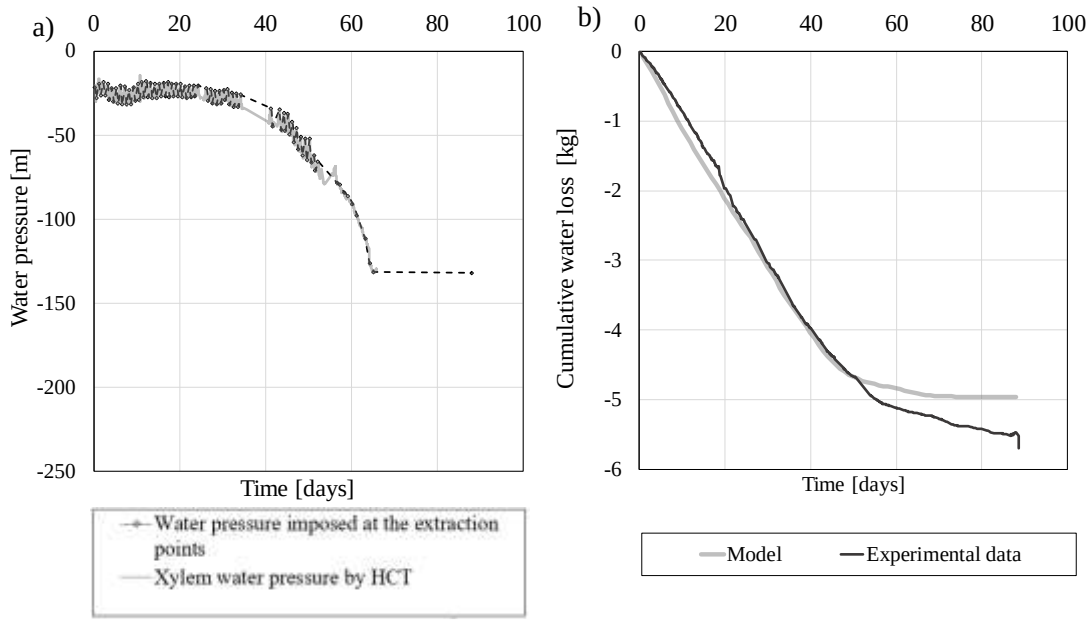

Figure 3: Final Water pressure: -132 kPa. a) water pressure imposed at the extraction points and xylem water pressure measured by the HCTs on stem; b) cumulative water loss over time

- **Final Water pressure: -531 kPa**

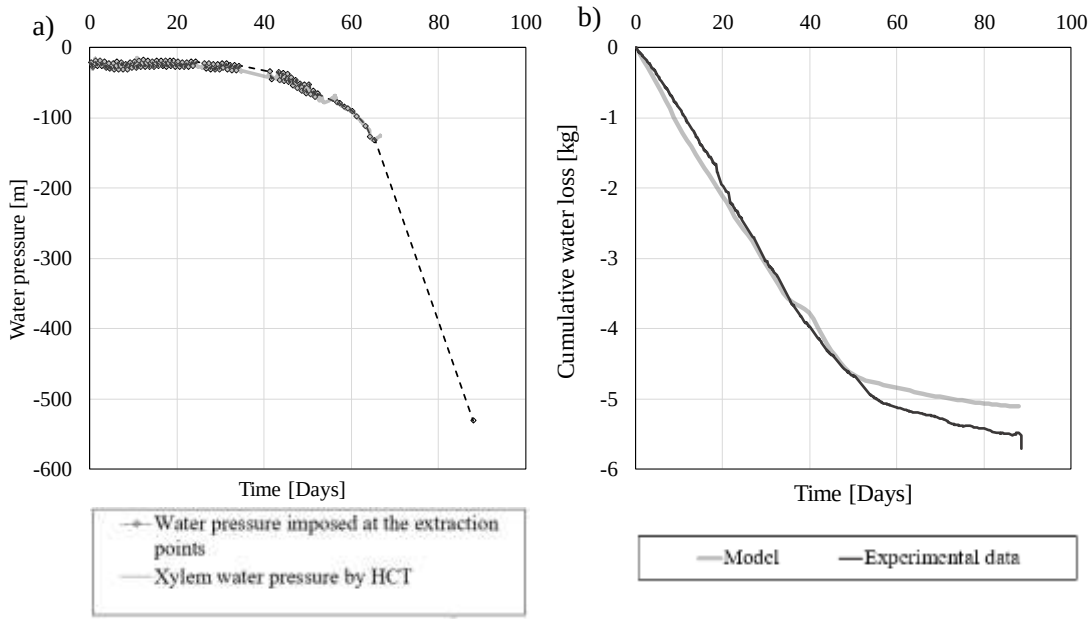

Figure 4: Final Water pressure: -531 kPa. a) water pressure imposed at the extraction points and xylem water pressure measured by the HCTs on stem; b) cumulative water loss over tim

Appendix D

Imposition of different water root water extraction function

Different root extraction functions were tested, based on the root dry density and the number of root tips in the column. The distribution reported is a function of the root tips distribution, shaped in order to have a smoother transition between layers. On the right it is presented the outcome of the FEM.

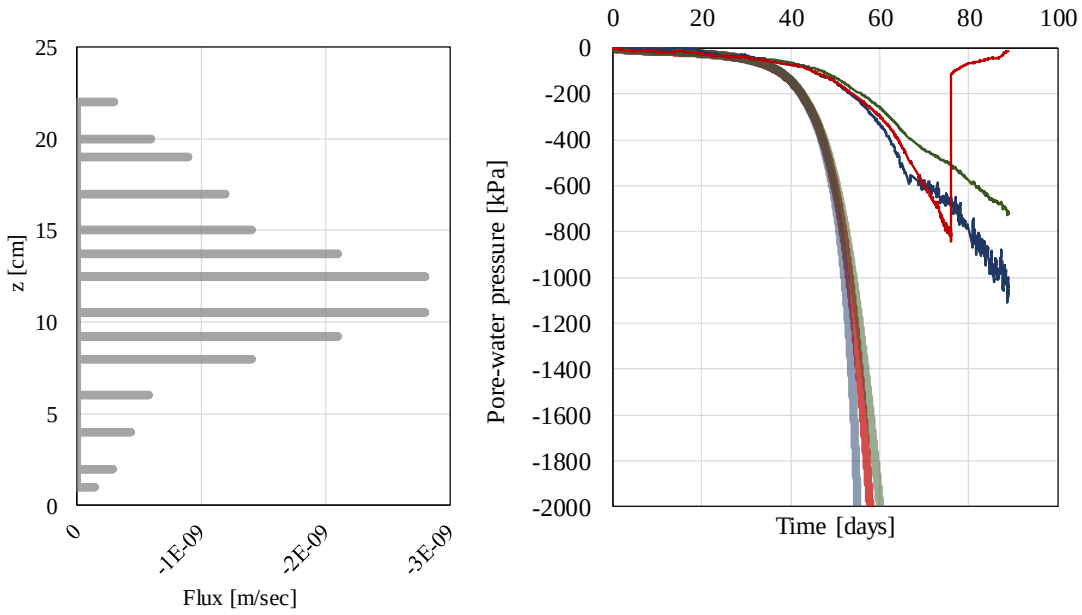

Appendix E

Effect of temporal and spatial discretization on the modelling water extraction via evaporation from bare soil

The solution presented in Chapter 5 was calculated imposing a spatial discretization of 2.5 mm and temporal discretization of approximately 2 min. In order to exclude the possibility of a local point of instability of the solution, the numerical model was executed refining the temporal and spatial discretization of respectively 33% and 20%. Results of the analysis in terms of cumulative water loss are reported in Figure 5. A summary of the discretization imposed for each case and related results is reported in Table 6.

Table 8:Spatial and temporal discrimination imposed for each model and related cumulated water loss

	Presented model	Refined Spatial discretization	Refined Spatial discretization
Mesh dimension	0.0025 m	0.002 m	0.0025
Total duration simulation	88 days	88 days	88 days
Number of time steps	36000	36000	48000
Final cumulative water loss		-5.05 Kg	-5.05 kg
Difference		0	0

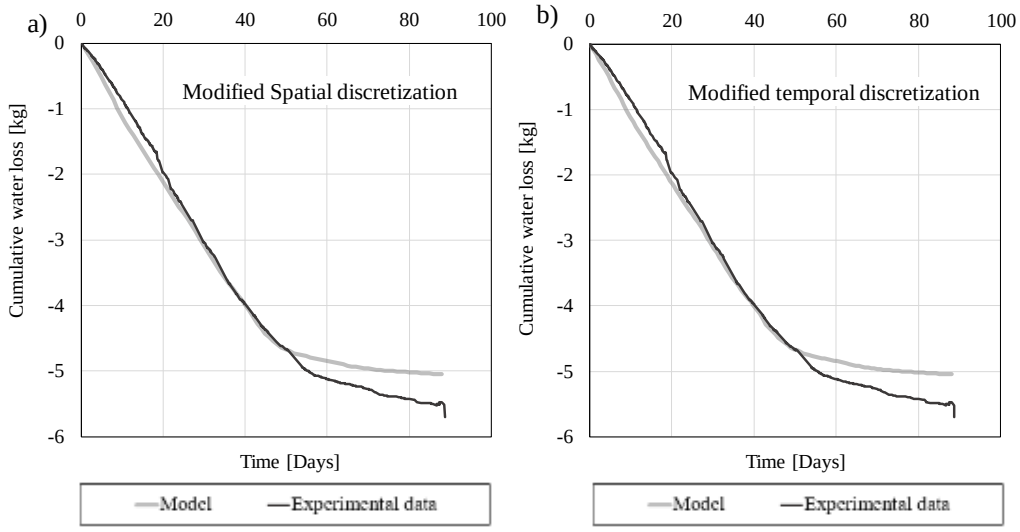

Figure 5: Cumulative water moss over time for a) different spatial discretization; b) different temporal discretization

L'utilisation du tensiomètre de grande capacité dans le cadre d'un système intégré de surveillance du continuum sol-plante pour les applications géotechniques

Résumé

La stabilité des pentes, des berges et des structures de terre est déterminée par la force de résistance au cisaillement que le sol peut mobiliser. La portion supérieure du profil du sol (zone vadose) ainsi que les structures de terre sont généralement partiellement saturées et la force de cisaillement est affectée par la pression de l'eau interstitielle (négative) et le degré de saturation. Quand la quantité d'eau dans le sol diminue, la pression d'eau interstitielle est réduite, ce qui augmente la force de cisaillement. L'extraction d'eau du sol peut ainsi être vue comme une technique permettant de renforcer le sol et d'en améliorer sa stabilité.

Une approche naturelle pour extraire l'eau du sol, à bas coût et à faibles émissions de carbone, consiste à exploiter la demande évaporative de l'atmosphère. Celle-ci peut advenir par deux procédés principaux : l'évaporation et la transpiration. L'amélioration de la stabilité pourrait ainsi être obtenue par un flux d'eau vers l'atmosphère. L'évaporation de sol nu a fait l'objet de nombreuses études approfondies. Cependant, il est difficile de mettre en place ce procédé en pratique pour améliorer l'extraction d'eau du sol. Le problème de la transpiration des plantes est plus complexe, car il dépend d'un couplage entre le sol, les plantes et l'atmosphère. Cependant, il présente une opportunité de contrôler activement le procédé d'extraction d'eau par la sélection adéquate d'espèces couvrant la surface du sol. Il en résulte que la végétation peut potentiellement être 'conçue' pour stabiliser les structures géotechniques. On ne peut étudier l'usage de la végétation pour la stabilisation de ces structures sans préciser que durant le processus de transpiration, l'eau est extraite par l'atmosphère (par le biais de la plante) et non pas par la plante elle-même. En d'autres termes, l'efficacité de la végétation à extraire l'eau du sol peut seulement être évaluée en comparant la transpiration d'un sol végétal avec l'évaporation d'un sol vu sous conditions atmosphériques équivalentes.

Ce travail propose un cadre expérimental pour l'investigation de l'efficacité de la végétation à extraire l'eau du sol par transpiration dont la méthodologie générale se base sur la comparaison entre la transpiration (depuis un sol végétal) et l'évaporation (depuis un sol nu), tant en laboratoire que dans le milieu naturel. L'étude s'intéresse essentiellement aux plantes ligneuses (arbres, arbustes) pour lesquelles les flux de sève peuvent être mesurés sur le tronc et les branches. La transpiration implique un flux d'eau du sol à travers le xylème jusqu'au feuilles. L'étude expérimentale du processus de transpiration requiert ainsi le suivi continue des flux d'eau sol-plante-atmosphère. En l'occurrence, le suivi de la pression d'eau du xylème (négative) continue de poser de nombreux défis, pour lesquels une solution est premièrement proposée dans cette dissertation.

Une nouvelle méthode a été développée pour suivre la pression d'eau du xylème. Le tensiomètre à haute-capacité (HCT) (Figure 6.a) développé par les chercheurs en géotechnique pour mesurer la pression de l'eau interstitielle négative dans des sols non-saturés a été adapté pour mesurer la pression d'eau dans les arbres (Figure 6.b). Le fonctionnement de l'HCT se base sur l'équilibre d'une phase liquide entre l'eau dans l'instrument et l'eau dans le sol/xylème. La présence d'une interface céramique poreuse permet à l'instrument de suivre la pression d'eau (négative) jusqu'à une valeur de -1.5/-2.0 MPa. Cette méthode a été validée en comparaison avec les méthodes usuelles utilisées en science des plantes, c.à.d la chambre de pression et le psychromètre thermocouple. Les mesures effectuées avec l'HCT se révèlent consistantes avec celles réalisées par ces deux méthodes, avec un temps de réponse équivalent. Cette nouvelle technique pour la mesure de la pression négative d'eau dans le xylème est un changement majeur dans l'étude des flux continus d'un système sol-plante, surtout dans le domaine géotechnique. Elle permet l'utilisation d'un unique instrument pour suivre la totalité de la continuité sol-plante.

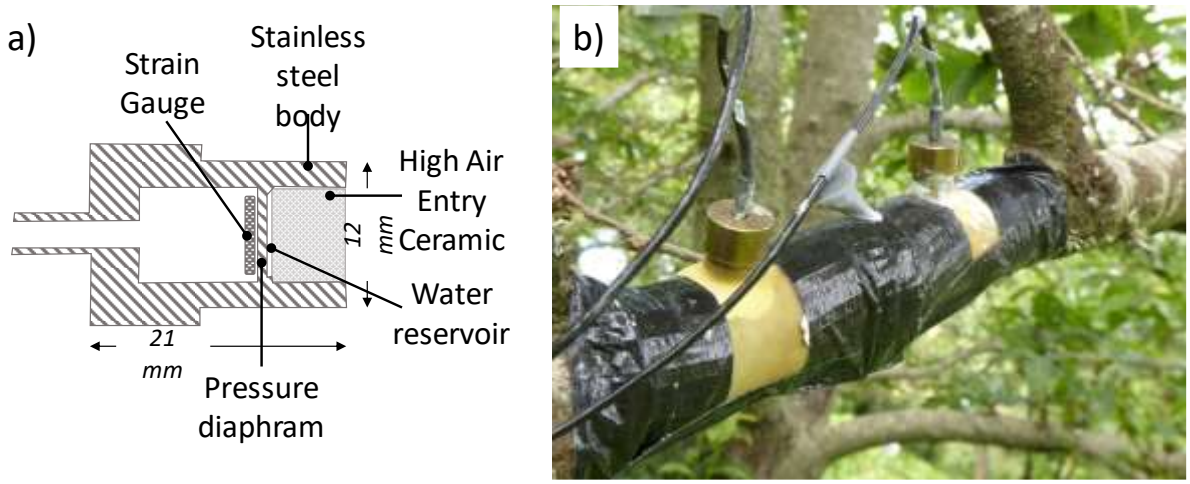

Figure 6:structure du tensiomètre à haute-capacité et b) exemple d'installation

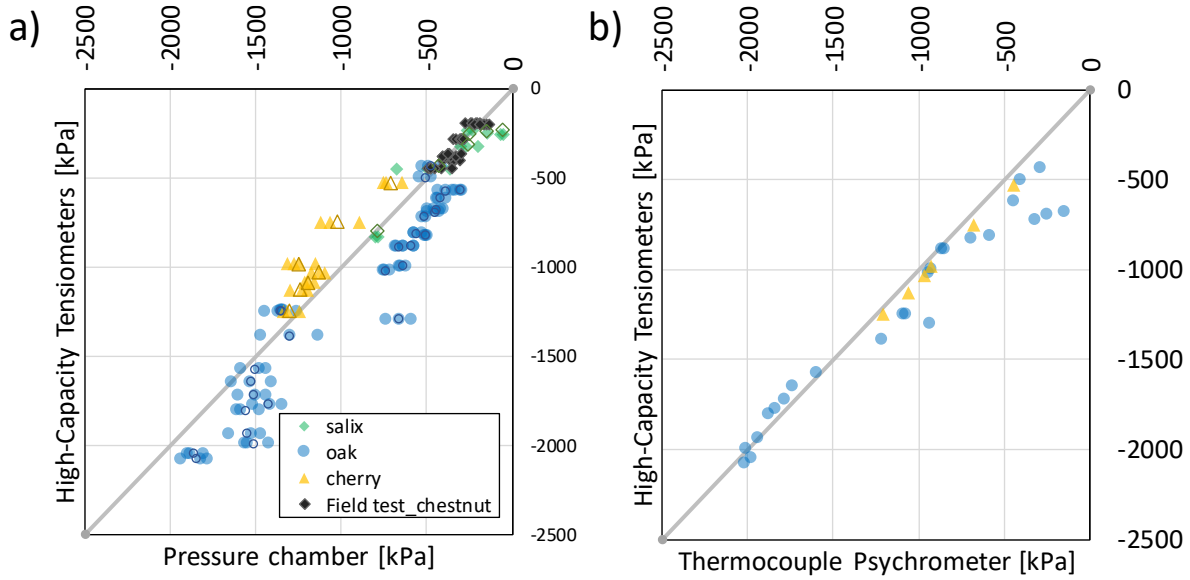

Figure 7: validation de la technique de tensiomètre à haute-capacité en comparaison avec les méthodes a) de la chambre de pression et b) du psychromètre thermocouple.

L'émission de vapeur d'eau dans l'atmosphère a tout d'abord été étudiée en laboratoire. Deux colonnes de sol ont été considérées, une avec végétation et l'autre avec un sol nu de référence pour comparaison de la transpiration et de l'évaporation sous conditions atmosphériques équivalentes. Les colonnes (Figure 8) étaient instrumentées avec i) des sondes TDR et des HCT pour suivre respectivement la quantité d'eau et la pression négative d'eau interstitielle, ii) des HCT pour suivre la pression d'eau du xylème, et iii) des balances pour mesurer la perte d'eau du sol et ainsi le taux de transpiration.

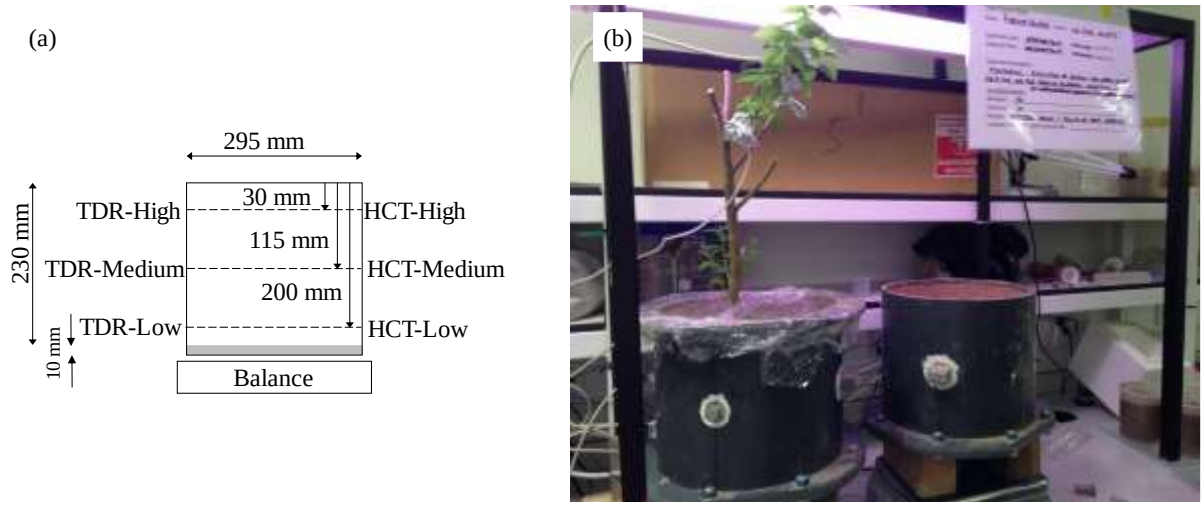

Figure 8: a)instrumentation de la colonne et b) photo des deux colonnes utilisées pour l'expérience avec Salix cinerea

Le résultat principal de ces tests en laboratoire est que la végétation n'a pas toujours un effet bénéfique (Figure 9). Deux régimes d'évaporation/transpiration peuvent être distingués : le régime d'énergie-limitée (potentielle) et celui d'eau-limité. Dans le régime d'énergie limitée, la transpiration potentielle est contrôlée par la résistance aérodynamique. Puisque la résistance aérodynamique est généralement plus faible pour des sols avec végétation que des sols nus, la combinaison de la résistance aérodynamique et de la résistance de la canopée peut avoir une influence en faveur du sol nu ou végétal en fonction du type de végétation. Ceci a été démontré par les expériences en laboratoire. Dans le régime limité en eau, l'effet de la végétation est toujours bénéfique car le mode d'extraction d'eau est différent (concentré à la surface du sol pour le sol nu, et distribué le long des racines pour le sol végétal). Ceci est mis en évidence par le fait que le temps que met le processus de transpiration à entrer en régime d'eau-limitée (c.à.d quand la transpiration commence à diminuer depuis sa valeur potentielle) est plus long dans un sol végétal que dans un sol nu. Ce résultat est encore plus apparent dans un système aux racines bien développées, car la plante peut accéder plus aisément à des strates de sol plus profondes. Des simulations numériques du flux d'eau dans les colonnes végétales et nues permettent de corroborer ces conclusions.

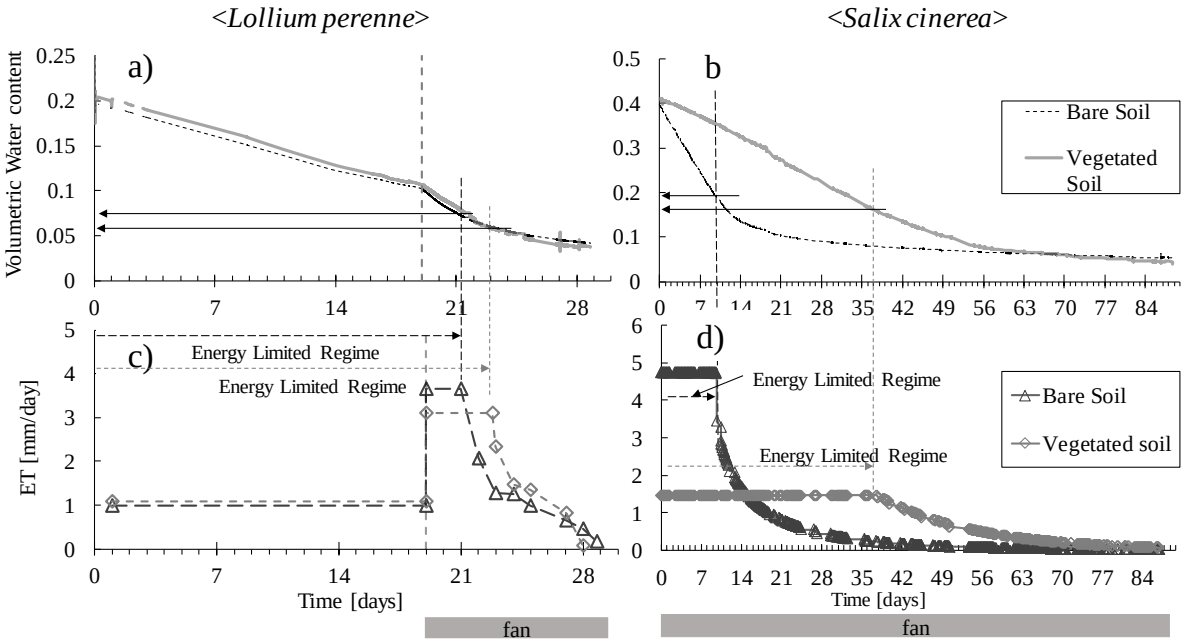

Figure 9: résultats expérimentaux avec *Lollium perenne* (a et c) et *Salix cinerea* (b et d)

Ces expériences permettent de suggérer une approche innovante pour modéliser la transpiration dans des applications géotechniques. La modélisation de la transpiration se base généralement sur la fonction de réduction proposée par Feddes. Il s'agit d'un modèle simplifié de la transpiration dans le régime d'eau-limitée. Nous avons démontré que la méthode proposée (comparaison entre la pression d'eau dans le sol et dans le xylème de la plante) permet une estimation plus précise des paramètres de la fonction de réduction par rapport aux pratiques géotechniques actuelles, où ces paramètres sont inférés depuis la littérature agricole pour chaque espèce et souvent dans des sols organiques peut compactés.

Les effets hydrauliques de la végétation ont finalement été étudiés in situ dans une plantation de peupliers à Montpellier, France. Le profil de contenu en eau a été suivi pendant toute la saison sèche et la période de pluie suivante dans une zone plantée de peupliers ainsi que dans le champ voisin labouré (sol nu de référence). Le cadre conceptuel développé sur la base d'expériences en laboratoire a été ainsi fondamental pour permettre l'interprétation des résultats obtenus en milieu naturel, et montrer dans quel régime la végétation a un effet bénéfique dans ces conditions.

Pour conclure, cette dissertation a permis de développer une nouvelles méthodes simple permettant de mesurer de façon comparative les effets de l'évaporation du sol et de la

transpiration des plantes dans l'extraction d'eau du sol dans un contexte forestier. Cette technique a fait l'objet d'une validation croisée avec d'autres méthodes utilisées pour mesurer les flux et pressions hydriques dans les arbres. Pouvant être indifféremment utilisée pour des mesures de pression d'eau dans le sol et dans le xylème des arbres, elle permettra d'évaluer, sur la base de mesures quantitatives, la stabilité des pentes et des structures terrestres végétalisées. La capacité de la végétation à augmenter ou diminuer la résistance au cisaillement du sol dépend d'un certain nombre de facteurs en compétition. La méthode expérimentale proposée permettra d'en évaluer leurs effets et fournira aux géotechniciens des outils pour optimiser la gestions de sites à risque de glissement de terrain via des pratiques de végétalisation adaptées.